# Number statistics in random matrices and applications to quantum systems

Ricardo Marino

**NNT :** 2015SACLS045

# THÈSE DE DOCTORAT
## DE
## L'UNIVERSITÉ PARIS-SACLAY
## PRÉPARÉE À
## L'UNIVERSITÉ PARIS-SUD

ECOLE DOCTORALE N° 564
Physique en Île de France

Spécialité de doctorat : Physique

Par

**M. Ricardo Marino**

# Number statistics in random matrices and applications to quantum systems

**Thèse présentée et soutenue à Orsay, le 16 octobre 2015.**

**Composition du Jury :**

| | | |
|---|---|---|
| M. Hilhorst, Hendrik-Jan | Professeur Paris-Saclay | Président |
| M. Burda, Zdzislaw | Professeur AGH UST | Rapporteur |
| M. Eisler, Viktor | Chercheur TU Graz | Rapporteur |
| M. Le Doussal, Pierre | Directeur de recherche LPTENS | Examinateur |
| M. Majumdar, Satya N. | Directeur de recherche LPTMS | Directeur de thèse |
| M. Vivo, Pierpaolo | Chercheur King's College London | Co-directeur de thèse |

*A physics model is like an Austrian timetable. Austrian trains are always late. A Prussian visitor asks the Austrian conductor why they bother to print timetables. The conductor replies: "If we didn't, how would we know how late the trains are?"*

V. F. WEISSKOPF

# Acknowledgments

First and foremost, I would like to thank my advisors Satya N. Majumdar and Pierpaolo Vivo. Satya and Pier taught me much more than scaling eigenvalues and orthogonal polynomials, they showed me what a physicist is, what a physicist should be and they showed me, with example, what is the kind of physicist I want to become. Satya's uncanny intuition and clarity of ideas, allied with Pier's attention to detail and unmatched patience, form the pillars that hold this thesis together. I owe them more than I can ever repay.

Second, I thank the referees Zdzislaw Burda and Viktor Eisler for accepting the task of going through these pages and evaluating my work. I also thank Hendrik Hilhorst and Pierre Le Doussal for accepting the invitation to be part of my jury. There are very few people more qualified than them to evaluate and judge the work I did in the last three years, and ever fewer would be able to fully understand the motivations and implications of my work.

Finally, I thank my partner in science, apartment and life Laís for the impressive ability to bear with me during the final moments of this thesis. I also thank my friends Mazanti, Levi, Lucas, Chico, George and Natal for listening to so many random matrices ramblings and conjectures, probably many more than they deserved. I thank my friend Antoine for helping me so many times that, ultimately, I am not sure this thesis would be possible without him.

The LPTMS has been a second home to me during these last three years, and I would like to specially thank Grégory Schehr for his mentoring and friendship. I also thank Olivier Giraud and Christophe Texier for bearing with my swarm of questions and my share of visits into their offices. Their patience should be rewarded. This thesis would certainly not be possible without the incredibly efficient work of Claudine, Géraldine and Vincent, the administrative branch of the LPTMS. My friends Pierre-Élie, Yasar, Pierre, Thibault and Stéfano are special part of this family, and your friendship was for me a discovery much more relevant than any other presented in this thesis.

# Contents

# — 1 —
# Synthèse en français

Il y a eu une intense activité dans le domaine des atomes froids dans les deux dernières décennies [16, 116]. Depuis les premières réalisations de condensation de Bose-Einstein [6, 18, 34], des nouveaux développements expérimentaux impliquant le refroidissement et le confinement des particules dans des pièges optiques ont conduit à un nouveau chapitre dans le domaine des systèmes quantiques à plusieurs corps, où les statistiques des particules est a le rôle central, plutôt que des atomes individuels.

Après la réalisation de refroidissement des fermions piégés au point où la statistique de Fermi devient dominante [95], les expériences ont été en mesure d'explorer les propriétés remarquables de gaz de Fermi [60]. Fermions sans interactions présentent des effets quantiques non-triviaux, découlant du principe d'exclusion de Pauli. Alors que les bosons confinés peuvent s'effondrer au plus bas niveau de la trappe, les fermions sont contraints à diluer et à se comporter comme un système fortement corrélé, indépendamment de leur interaction originale. Ceci induit un mouvement de Fermi des particules, qui est un phénomène purement quantique et est le principal facteur pour cette dilution, en supprimant le rôle des interactions individuelles parmi les fermions, qui peut être, dans de nombreux cas, négligés ou traités comme une petite perturbation [116]. Cela transforme le gaz parfait de Fermi dans la première étape naturelle pour discuter des propriétés des gaz de Fermi.

Nous considérons le cas du gaz de Fermi à une dimension de $N$ particules confiné par un potentiel harmonique $V_Q(x) = \frac{1}{2}m\omega^2 x^2$. Pour plus de simplicité, nous avons posé $m = \omega = \hbar = 1$. L'état fondamentale de la fonction d'onde à plusieurs corps de ce système est donnée par le déterminant de Slater $\Psi(\vec{x}) = \det[\phi_i(x_j)]/\sqrt{N!}$, Où $\phi_i(x_j)$ est la fonction d'onde d'un seul oscillateur harmonique $\phi_n(x) \propto \mathrm{e}^{-x^2/2}H_n(x)$ et $H_n(x)$ sont les polynômes d'Hermite. En manipulant le déterminant, on peut écrire la densité de probabilité de l'état fondamental

$$|\Psi(\vec{x})|^2 = \frac{1}{Z_N}\mathrm{e}^{-\sum_{i=1}^{N} x_i^2}\prod_{j<k}(x_k - x_j)^2, \tag{1.1}$$

où $Z_N$ est la constante de normalisation. Rédigé sous cette forme, nous remarquons que la fonction de densité de probabilité conjointe de la position de ces fermions sur leur état fondamental est équivalente à la distribution des valeurs propres de la $N \times N$ matrice gaussienne hermitienne [100]. Dans ce travail, nous utilisons ce lien remarquable entre fermions froides et théorie des matrices aléatoires pour explorer les fluctuations quantiques

du gaz de Fermi à une dimension harmonique confiné, élargir les résultats annoncés dans [97].

L'un des principaux observables dans la théorie des matrices aléatoires et beaucoup physique quantique du corps est la densité, qui est définie comme

$$\rho_N(x) = \frac{1}{N}\sum_{i=1}^{N}\delta(x - x_i), \tag{1.2}$$

où $\{x_i\}$ sont les positions de valeurs propres ou fermions sur la ligne. Il est connu que la densité moyenne des valeurs propres d'une matrice aléatoire gaussienne converge vers la loi du demi-cercle de Wigner [149, 100] dans la limite de grand $N$:

$$\langle\rho_N(x)\rangle \xrightarrow{N\gg 1} \frac{1}{N\beta\pi}\rho_{sc}\left(\frac{x}{\sqrt{N\beta}}\right), \qquad \rho_{sc}(x) = \frac{\sqrt{2-x^2}}{\pi}, \tag{1.3}$$

où $\beta$ est l'indice Dyson, dont la valeur est donnée par $beta = 1, 2$ ou 4 si la matrice gaussienne est symétrique réelle, complexe hermitienne ou quaternionique self-dual, respectivement. La correspondance avec les fermions froids est valable pour le cas $\beta = 2$. Il y a une échelle claire sur les valeurs propres gaussiennes avec $\sqrt{N}$, et il est commode de les redimensionner pour obtenir des valeurs propres de l'ordre de l'unité. Ceci est équivalent à ajuster la variance des éléments de la matrice de Gauss d'un facteur $\sqrt{N\beta}$, et correspond au problème de fermions froids pour des distances mises à l'échelle comme $\sqrt{2N}$.

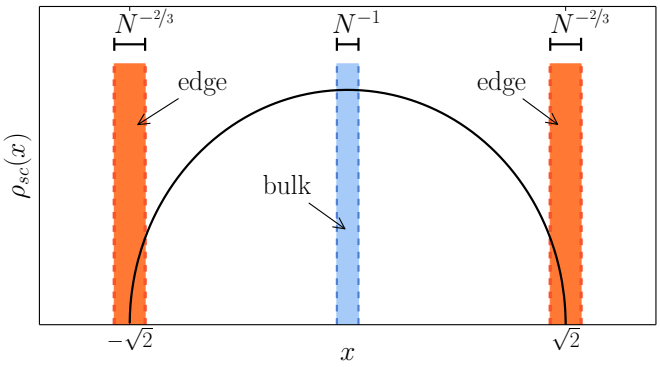


**Figure 1.1** — Densité moyenne des valeurs propres gaussiennes avec la représentation des régimes bulk et edge.

Cette mise à l'échelle donne une densité moyenne indépendante de $N$ dans la limite de large $N$, donnée par $\rho_{sc}(x)$ dans l'équation (1.3). Cette densité a deux régimes très importants, ou zones de redimensionnement, nommés *régime bulk* et *régime edge*, représentés dans la figure 1.1. Le bulk est un intervalle dont la taille est de l'ordre de la distance interparticulaire, qui dans le cas à l'échelle est $1/N$, et représente un " Zoom " dans une partie du spectre. Dans ce régime, le confinement harmonique des fermions peut être négligé, et le comportement des particules à cette échelle est dominé par les effets du

principe d'exclusion de Pauli. Le bord, qui pour le cas gaussien est placé à $x = \pm\sqrt{2}$, est un point singulier pour la densité moyenne. Plusieurs observables changent radicalement leur comportement lorsqu'ils sont étudiés autour du bord [115]. Statistiques de la plus grande valeur propre d'une matrice aléatoire gaussienne, dont la valeur moyenne est $\sqrt{2}$, sont décrits par la distribution de Tracy-Widom [134, 135]. Ces fluctuations typiques sont de l'ordre $O(N^{-2/3})$ autour du bord, et ils représentent la largeur du régime edge.

Cette densité fait allusion à un comportement très riche des fluctuations quantiques de fermions froides. Une façon d'explorer ce phénomène est d'analyser les *statistiques de numéro*, ou des statistiques complètes de comptage, de fermions piégés. Cela représente compter le nombre $N_{\mathcal{I}}$ de fermions à l'intérieur d'un intervalle $\mathcal{I}$ autour du minimum de la trappe et d'étudier comment ce nombre évolue lorsque l'intervalle croît en taille. Pour le cas de bosons idéal à température nulle, toutes les particules sont concentrées sur l'état fondamentale, centré sur le minimum du piège. Elles ne sont pas corrélées et la statistique de leur nombre peut être facilement déterminée. Le cas fermionique, cependant, présente la question naturelle de déterminer la statistique de la variable aléatoire $N_{\mathcal{I}}$, le nombre de fermions, ou valeurs propres, qui tombent à l'intervalle $\mathcal{I}$.

Étonnamment, l'observable $N_{\mathcal{I}}$ a une dépendance riche et très non triviale sur la taille de l'intervalle. Alors que sa moyenne est facilement obtenue en intégrant $\rho_{sc}(x)$ sur l'intervalle $\mathcal{I}$, ses autres moments ne sont pas évidents. Calculer le statistique complète de $N_{\mathcal{I}}$ est une tâche très difficile que nous avons récemment résolu pour une symétrique intervalle $\mathcal{I}$ autour de l'origine en utilisant la connexion entre les statistiques d'un gaz de Fermi dimensions et les valeurs propres de la gaussienne unitaire ensemble de matrices aléatoires [97]. Dans ce travail, nous obtenons la pleine j.p.d.f. de $N_{\mathcal{I}}$ dans la limite de grand $N$ pour tout intervalle $\mathcal{I}$, nous présentons une étude détaillée de sa variance des fluctuations typiques et nous appliquons cette étude à deux autres ensembles de la matrice aléatoire: l'ensemble de Wishart et l'ensemble de Cauchy.

La densité spectrale moyenne de $\rho(x)$ de l'ensemble est la distribution marginale de la joint probability density function:

$$\rho(x) = \left\langle \frac{1}{N}\sum_{i=1}^{N}\delta(x-x_i)\right\rangle = \int \mathrm{d}x_2\cdots\mathrm{d}x_N P(x,x_2\ldots,x_N)\ . \tag{1.4}$$

Ici, nous étudions trois différentes classes d'ensembles avec des potentiels différents.

*Ensemble gaussien:* $V(x) = x^2/2$. L'ensemble le plus largement étudié, ayant la propriété remarquable (et unique) d'avoir entrées indépendantes et d'être en même temps invariant par rotation [100]. L'ensemble est composé des matrices du type symétrique réelle $\beta = 1$, complexe hermitienne $\beta = 2$ ou quaternion auto-dual $\beta = 4$ matrices dont les entrées sont variables gaussiennes telles que la probabilité d'obtenir la matrice $X$ est donné par $P(X) \propto e^{-\mathrm{Tr}X^2/2}$. La densité spectrale moyenne pour grande $N$ et pour tout $\beta > 0$ converge vers la célèbre loi semi-circulaire de Wigner.

$$\rho_{sc}(x) = \frac{1}{\pi}\sqrt{2-x^2}\ . \tag{1.5}$$

*Ensemble Wishart:* $V(x) = \frac{x}{2} - \alpha\ln x$, où $\alpha$ est une constante. Pour $\beta = 1, 2, 4$, ce potentiel de confinement peut être concrètement réalisé de la façon suivante. Soit $X$

une matrice $M \times N$ dont les entrées sont i.i.d. variables aléatoires gaussiennes (réel, complexes ou quaternions). Nous définissons une matrice Wishart $W$ comme $N \times N$ matrice de covariance $W = X^\dagger X$ de la matrice de données gaussiens $X$. La constante $\alpha$ est $\alpha = \beta(1 + MN)/2N - 1/N$. Cet ensemble est également connu comme l'ensemble Laguerre, en raison de la classe des polynômes orthogonaux qui lui sont associés. Matrices de Wishart sont semi-définie positives et symétriques. Cet ensemble a été introduit par Wishart en 1928 [152] et largement étudié par les statisticiens [66, 53] longtemps avant la naissance officielle de RMT en physique.

La densité spectrale moyenne dans la limite de $N, M$ larges (avec $N/M = c \leq 1$ fixe) pour les matrices de Wishart a été obtenu par Marčenko et Pastur [98] (voir figure 1.2a. pour le cas $N = M$) et donné par

$$\rho_{mp}(x) = \frac{1}{2\pi x}\sqrt{(x - x_-)(x_+ - x)}, \tag{1.6}$$

où $x_\pm = (1 \pm 1/\sqrt{c})^2$.

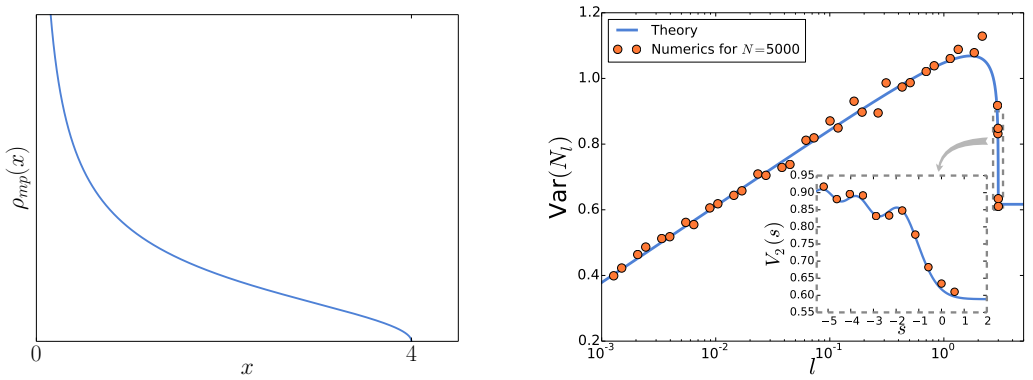


**(a)** **(b)**

**Figure 1.2** — (a) Densité moyenne des valeurs propres de la matrice de Wishart dans le cas $N = M$ et (b) Résultat pour la variance du nombre de valeurs propre dans l'intervalle $\mathcal{I} = [1, 1 + l]$.

*Ensemble de Cauchy*

Nous considérons $N \times N$ matrices qui pourraient être symétriques ($\beta = 1$), hermitienne ($\beta = 2$) ou auto-dual ($\beta = 4$) tirées de la distribution

$$P(\mathbf{H}) \propto \left[\det\left(\mathbb{1}_N + \mathbf{H}^2\right)\right]^{-\beta(N-1)/2-1}, \tag{1.7}$$

où $\mathbb{1}_N$ est la matrice identité $N \times N$.

Initialement conçu comme un remplacement convenable pour l'ensemble gaussien dans le contexte de transports quantique [22], l'ensemble de Cauchy est aussi trouvé dans le contexte de probabilités libres [23, 24, 59]. La j.p.d.f. de ces valeurs propres est donnée

par

$$P(\lambda_1, \cdots, \lambda_N) = \frac{1}{Z_N} \prod_{j=1}^{N} \frac{1}{(1+\lambda_j^2)^{\beta(N-1)/2+1}} \prod_{i<k} |\lambda_i - \lambda_k|^\beta \,. \tag{1.8}$$

L'ensemble de Cauchy est aussi un des rares ensembles exactement solubles dont la densité spectrale moyenne a queues épaisses s'étendant sur l'axe réel complète, et donné par (voir Fig. 3.2c)

$$\rho_N(\lambda) = \frac{1}{\pi} \frac{1}{1+\lambda^2}. \tag{1.9}$$

Notamment, la densité moyenne ne dépend pas de $N$.

La principale caractéristique qui nous amènent à considérer cet ensemble est la "fat tail" dans la densité moyenne. Plusieurs quantités calculées d'un ensemble changent radicalement une fois qu'un " bord " est atteint, une fois l'intervalle considéré pour le comptage de valeurs propres traverse le bord de la densité moyenne si cette densité a un support compact. En l'absence d'un support compact, nous nous attendons à obtenir un comportement différent, et nous avons pu le comparer avec les résultats des autres ensembles. Les matrices de Wigner avec "fat tails" ont été étudiés par [15] et l'ensemble de Cauchy représente un équivalent intéressante dans le domaine invariant.

Dans ce qui suit, nous allons décrire la principale méthode appliquée pour résoudre les problèmes traités dans cette thèse. Cette procédure est appelée la méthode de Coulomb-gaz. Elle a été introduite par Dyson et Mehta sur les documents fondateurs du sujet [43, 45], et des nombreuses applications ont été trouvées depuis son origine, telles que l'étude d'analyse en composante principale (PCA) dans des ensembles aléatoires de données [94], l'évaluation des résistance, conductance et la puissance de bruit dans des cavités mésoscopiques chaotiques [61, 140, 142], l'étude de l'information mutuelle et la transmission de données en sortie multiple à entrées multiples (MIMO) de réseaux [78], l'intrication quantique bipartite des systèmes quantiques [28, 51, 108, 109], sur la plus grande valeur propre de gaussiennes et Wishart matrices [91, 37] et beaucoup d'autres.

Nous allons explorer cette méthode dans un cadre très général. Tous les ensembles présentés ci-dessus possèdent la même forme (équation (3.7)) pour le j.p.d.f. de leurs valeurs propres, de sorte que la méthode applique pour tout potentiel confinant $V(x)$.

Prenons un ensemble de matrices aléatoires dont la j.p.d.f. des valeurs propres est donnée par

$$P(\boldsymbol{x}) = \frac{1}{Z_{N,\beta}} e^{-\beta N \sum_{i=1}^{N} V(x_i)} \prod_{j<k} |x_k - x_j|^\beta. \tag{1.10}$$

Nous pouvons réécrire cette expression de la façon suivante

$$P(\boldsymbol{x}) = \frac{1}{Z_{N,\beta}} e^{-\beta N \sum_{i=1}^{N} V(x_i) + \beta \sum_{k<j} \log|x_k - x_j|}. \tag{1.11}$$

Cette probabilité peut être interprété comme le poids de Boltzmann d'un système électrostatique associé. Soient $N$ charges dans un gaz 2 dimensions limité à une ligne et soumis à un potentiel $NV(x)$. La répulsion électrostatique 2-D est logarithmique, et la

probabilité de trouver des charges à des positions $\boldsymbol{x} = (x_1, \ldots, x_n)$ sera donnée par

$$P(\boldsymbol{x}) = \frac{1}{Z_{N,\beta}} e^{-\beta E[\boldsymbol{x}]} \qquad E[\boldsymbol{x}] = N \sum_{i=1}^{N} V(x_i) - \sum_{j<k} \log|x_j - x_k|. \tag{1.12}$$

Écrit comme cela, cette statistique est équivalente au poids de Boltzmann d'un système physique de charges placées dans des positions $\boldsymbol{x}$ dont l'énergie est $E[\boldsymbol{x}]$ et $Z_{N,\beta}$ est la fonction de partition du système. Cette correspondance fondamentale entre les particules chargées et les valeurs propres au hasard nous permet d'importer de nombreuses techniques de la mécanique statistique pour traiter ce problème. Un système décrit par l'énergie $E[\boldsymbol{x}]$ est appelé un gaz de Coulomb, ou log-gaz.

Prenons le cas Gaussien, où $V(x) = x^2/2$. Nous introduisons la densité à deux points:

$$\rho_2(x, x') = \frac{1}{N(N-1)} \sum_{i \neq j} \delta(x - x_i)\delta(x' - x_j) \ . \tag{1.13}$$

Et on peut écrire

$$\sum_i f(x_i) = N \int \mathrm{d}x \rho(x) f(x) \ , \tag{1.14}$$

$$\sum_{i<j} f(|x_i - x_j|) = \frac{N(N-1)}{2} \iint \mathrm{d}x \mathrm{d}x' \rho_2(x, x') f(|x - x'|) \ . \tag{1.15}$$

Pour l'énergie $E[\boldsymbol{x}, \mu, N_{\mathcal{I}}]$ on obtient

$$E[\boldsymbol{x}, \mu, N_{\mathcal{I}}] = N^2 \int_{-\infty}^{+\infty} \rho(x) \frac{x^2}{2} \mathrm{d}x - \frac{N(N-1)}{2} \iint_{-\infty}^{+\infty} \mathrm{d}x \mathrm{d}x' \rho_2(x, x') \ln|x - x'| + \eta \left( N \int_{-\infty}^{+\infty} \rho(x) \mathrm{d}x - N \right),$$

Où un multiplicateur de Lagrange supplémentaire $\eta$ a été introduit pour assurer la normalisation de la densité. À la limite de grand $N$, la densité à deux points peut être remplacée par le produit de deux densité à un point et on obtient

$$E[\boldsymbol{x}, \mu, N_{\mathcal{I}}] \overset{N \gg 1}{\approx} N^2 S^{(G)}[\rho, \mu], \tag{1.16}$$

où

$$\begin{aligned} S^{(G)}[\rho, \mu] = &\int_{-\infty}^{+\infty} \rho(x) \frac{x^2}{2} \mathrm{d}x - \frac{1}{2} \iint_{-\infty}^{+\infty} \mathrm{d}x \mathrm{d}x' \rho(x)\rho(x') \ln|x - x'| \\ &+ \mu \left( \int_a^b \rho(x) \mathrm{d}x - k_{\mathcal{I}} \right) + \eta \left( \int_{-\infty}^{+\infty} \rho(x) \mathrm{d}x - 1 \right) \end{aligned} \tag{1.17}$$

est appelée "l'action" du système.

L'introduction de la densité $\rho(x)$ convertit cet intégrale dans une intégrale fonctionnelle sur toutes les densités normalisées possibles. Le jacobien de cette transformation est d'ordre $\mathcal{O}(N)$, qui est donc sous-dominant pour grande $N$. Par conséquent, nous pouvons écrire

$$\mathcal{P}_\beta^{(G)}(N_{\mathcal{I}} = k_{\mathcal{I}} N) = \frac{1}{Z_{N,\beta}} \int \mathcal{D}[\rho] \mathrm{d}\eta \, \mathrm{e}^{-\beta N^2 S^{(G)}[\rho] + \mathcal{O}(N)} \ , \tag{1.18}$$

qui peut être évaluée par la méthode du colle.

$$\mathcal{P}_\beta^{(G)}(N_\mathcal{I} = k_\mathcal{I} N) = \frac{1}{Z_{N,\beta}} \int \mathcal{D}[\rho] \mathrm{d}\mu \mathrm{d}\eta \, \mathrm{e}^{-\beta N^2 S^{(G)}[\rho]} \approx \mathrm{e}^{-\beta N^2 \left( S^{(G)}[\rho^\star] - S^{(G)}[\rho_{sc}] \right)} = \mathrm{e}^{-\beta N^2 \psi^{(G)}(k_\mathcal{I})} \, . \tag{1.19}$$

Nous obtenons la densité d'équilibre de la façon suivante.

$$\left. \frac{\delta S^{(G)}}{\delta \rho} \right|_{\rho^\star} = 0 = \frac{x^2}{2} - \int \mathrm{d}x' \rho^\star(x') \ln |x - x'| + \eta, \quad x \in \text{supp } \rho^\star. \tag{1.20}$$

Dériver cette équation encore une fois par rapport à $x$ nous permet d'obtenir l'équation qui définit la densité d'équilibre $\rho^\star(x)$.

$$x = \mathrm{PV} \int \frac{\rho^\star(x')}{x - x'} \mathrm{d}x', \quad x \in \text{supp } \rho^\star, \tag{1.21}$$

Pour résoudre cette équation, on applique la méthode de la résolvante. Soit $G(z)$ une fonction complexe, appelée la résolvante, définit par

$$G(z) = \int \frac{\rho^\star(x)}{z - x} \mathrm{d}x, \quad z \in \mathbb{C} \setminus \text{supp } \rho^\star. \tag{1.22}$$

La normalisation de $\rho^\star$ à 1 implique que $G(z)$ se comporte comme $1/z$ lorsque $|z|$ est grand. On utilise l'identité suivante

$$\lim_{\epsilon \to 0^+} G(x + \mathrm{i}\epsilon) = \lim_{\epsilon \to 0^+} \int \frac{\rho^\star(y)}{x + \mathrm{i}\epsilon - y} \mathrm{d}y = \lim_{\epsilon \to 0^+} \int \frac{\rho^\star(y)(x - y - \mathrm{i}\epsilon)}{(x + \mathrm{i}\epsilon - y)(x - y - \mathrm{i}\epsilon)} \mathrm{d}y \tag{1.23}$$

$$\lim_{\epsilon \to 0^+} \left[ \int \frac{\rho^\star(y)(x - y)}{(x - y)^2 + \epsilon^2} \mathrm{d}y - \mathrm{i} \int \frac{\rho^\star(y)\epsilon}{(x - y)^2 + \epsilon^2} \mathrm{d}y \right] = \mathrm{PV} \int \frac{\rho^\star(y)}{x - y} \mathrm{d}y - \mathrm{i}\pi\rho^\star(x), \tag{1.24}$$

où $\delta(x) = \lim_{\epsilon \to 0^+} (1/\pi)\epsilon/(x^2 + \epsilon^2)$, la $\rho^\star(x)$ peut être obtenu de la partie imaginaire de la resolvente

$$-\frac{1}{\pi} \lim_{\epsilon \to 0^+} \mathrm{Im} G(x + \mathrm{i}\epsilon) = \rho^\star(x) \, . \tag{1.25}$$

Avec quelques manipulations, cette technique nous permet d'obtenir plusieurs résultats et informations sur les ensembles considérés, et est particulièrement adaptée pour obtenir des information sur la statistique de comptage du nombre de valeurs propres dans une intervalle $\mathcal{I} = [a, b]$, cela étant le résultat principal de cette thèse. On attaque ce problème, d'abord en considérant un cas plus simple. Soit $\mathcal{I} = [0, \infty)$, donc le comptage de valeurs propres est en effet le comptage des valeurs propres positives de l'ensemble de matrice. Prenons d'abord le cas de l'ensemble Gaussien $V(x) = \frac{x^2}{2}$.

L'importance de l'indice a été noté d'abord par May [99], dans le domaine de l'écologie théorique. Dans son travail, May a étudié un système complexe de la forme $\frac{\mathrm{d}\boldsymbol{x}}{\mathrm{d}t} = A\boldsymbol{x}$ où le éléments $a_{ij}$ de la matrice $A$ $N \times N$ ont été pris à partir d'une distribution aléatoire de variance $\alpha$ et moyenne nulle. Il a déterminé que le système était presque sûrement stable si $\alpha < N^{-1/2}$ et presque sûrement instable si $\alpha > N^{-1/2}$, la transition entre

les deux régime étant forte, sa mise à l'échelle de largeur $N^{-2/3}$. Lorsque la variance est maintenue fixe, le système sera presque certainement instable, la probabilité d'avoir toutes les valeurs propres négatives décroît très vite lorsque la taille du système augmente. Bien que ce régime de transition obtenu par May préfigure une évolution beaucoup plus profond dans la théorie des matrices aléatoires, la question de savoir comment exactement cette probabilité diminue avec $N$ est restée sans réponse jusqu'à 2006 [37].

Nous voulons calculer la densité de probabilité complète de l'index d'une matrice aléatoire gaussienne de taille $N \times N$. Nous rappelons que la j.p.d.f. des valeurs propres est donnée par

$$P(\mathbf{x}) = \frac{1}{Z_{N,\beta}} \mathrm{e}^{-\frac{\beta N}{2}\sum_{i=1}^{N} x_i^2} \prod_{j<k} |x_k - x_j|^\beta. \tag{1.26}$$

La variable $N_+$ possède la p.d.f. suivante

$$P(N_+ = kN) = \frac{1}{Z_{N,\beta}} \int \prod_i \mathrm{d}x_i P(\mathbf{x}) \delta\left(\sum_i \mathbb{1}_{[0,\infty)}(x_i) - kN\right). \tag{1.27}$$

Comme présenté auparavant, nous appliquons la méthode de gaz Coulomb pour obtenir la fonction de grandes déviations pour la variable $N_+$. L'idée est d'écrire la p.d.f. (1.27) comme le poids Gibbs-Boltzmann d'un système physique associé, utiliser la hypothèse de large-$N$, appliquer une méthode du col et d'en tirer la fonction de grandes déviations pour $N_+$. Nous commençons en utilisant la représentation exponentielle du delta pour écrire

$$P(N_+ = kN) = \frac{1}{Z_{N,\beta}} \int \prod_i \mathrm{d}x_i \int \mathrm{d}\mu \mathrm{e}^{-\frac{\beta N}{2}\sum_i x_i^2 + \beta \sum_{k>j} \log|x_k - x_j| + \beta\mu\left(\sum_i \mathbb{1}_{[0,\infty)}(x_i) - kN\right)} \tag{1.28}$$

$$= \frac{1}{Z_{N,\beta}} \int \prod_i \mathrm{d}x_i \int \mathrm{d}\mu \mathrm{e}^{-\beta E(\mathbf{x},\mu)}, \tag{1.29}$$

où

$$E(\mathbf{x},\mu) = N\sum_{i=1}^{N} \frac{x_i^2}{2} - \frac{1}{2}\sum_{i\neq j} \log|x_i - x_j| + \mu\left(\sum_{i=1}^{N} \mathbb{1}_{[0,\infty)}(x_i) - kN\right) \tag{1.30}$$

est dite l'énergie de la configuration $\{x_i\}$. Dans la section précédente nous l'avons mentionné l'analogie entre la p.d.f. des valeurs propres de l'ensemble gaussien et un système deux dimensionnel de charges confinées à une ligne soumise à un potentiel harmonique. Ce résultat est toujours exigé dans le cas de l'indice, la p.d.f. (1.29) est aussi le poids Gibbs-Boltzmann du même système électrostatique, avec un petit changement dans le potentiel, un saut d'une hauteur $\mu$ (voir figure 1.3). Le multiplicateur de Lagrange $\mu$ a comme rôle d'assurer la condition $N_+ = kN$. Dans l'analogie électrostatique, ce changement dans le potentiel veillera à ce que la fraction des valeurs propres positives est en effet $k$. Cette quantité sera comparée à la fraction moyenne de valeurs propres positives, $k^\star = 1/2$, et nous nous attendons à un changement brusque dans le comportement du système lorsque $k$ va de $< 1/2$ à $> 1/2$.

Pour analyser la fonction de probabilité (1.29), nous allons transformer l'approche discrète de la position des valeurs propres à une intégrale fonctionnelle de continuum sur

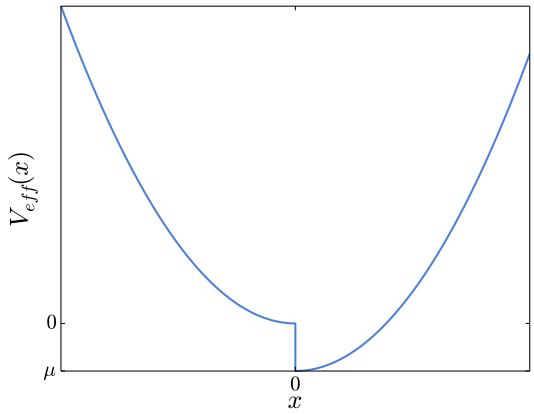


**Figure 1.3** — Croquis du potentiel harmonique à laquelle le système de l'équation associée (6.5) est soumise, pour le cas $\mu < 0$.

la densité $\rho$, comme décrit précédemment. Remise à l'échelle $\mu \to N^2\mu$ on trouve

$$E[\mathbf{x}, \mu] \xrightarrow{N \text{ large}} N^2 S[\rho], \tag{1.31}$$

où

$$\begin{aligned} S[\rho] = &\int \frac{x^2}{2}\rho(x)\mathrm{d}x - \frac{1}{2}\iint \rho(x)\rho(x')\log|x-x'|\mathrm{d}x\mathrm{d}x' \\ &+ \mu\left(\int_0^\infty \rho(x)\mathrm{d}x - k\right) + \eta\left(\int_{-\infty}^\infty \rho(x)\mathrm{d}x - 1\right) \end{aligned} \tag{1.32}$$

est l'action.

Comme dans l'exemple précédent, nous avons ajouté un multiplicateur de Lagrange supplémentaire $\eta$ pour renforcer la normalisation de la densité moyenne de valeur propres. En utilisant l'hypothèse de large-$N$, on applique la méthode du col pour obtenir une approximation de la fonction de probabilité (1.29).

$$\frac{1}{Z_{N,\beta}}\int \prod_i \mathrm{d}x_i \int \mathrm{d}\mu \mathrm{e}^{-\beta N^2 S[\rho]} = \frac{1}{Z_{N,\beta}}\mathrm{e}^{-\beta N^2 S[\rho^\star]}, \tag{1.33}$$

où $\rho^\star$ minimise le fonctionnel $S[\rho]$.

Pour l'obtenir, on dérive (1.32) fonctionnellement par rapport à $\rho$.

$$\left.\frac{\delta S}{\delta \rho}\right|_{\rho^\star} = 0 = \frac{x^2}{2} - \int \rho^\star(x')\log|x-x'|\mathrm{d}x' + \mu \mathbb{1}_{[0,\infty)} + \eta, \quad x \in \mathrm{supp}(\rho^\star). \tag{1.34}$$

Et encore une fois par rapport à $x$ pour obtenir

$$x + \mu\delta(x) = \fint \frac{\rho^\star(x')}{x-x'}\mathrm{d}x', \quad x \in \mathrm{supp}(\rho^\star), \tag{1.35}$$

où $⨍$ représente la partie principale de l'intégrale.

L'équation intégrale (1.35) est très similaire à l'équation résolue précédemment, la seule différence étant le facteur delta supplémentaire. Nous avons mentionné que l'équation (1.34) est un bilan de l'énergie pour le problème de gaz Coulomb, veillant à ce que la répulsion et le potentiel sont équilibrés dans tous les points du support de la densité moyenne. Le calcul de l'indice ajoute le multiplicateur de Lagrange $\mu$, qui peut être interprété comme un potentiel chimique ajouté à l'intervalle $[0, \infty)$.

Cette interprétation est important pour estimer la forme de la distribution de densité moyenne qui émergera de l'équation (1.35). Dans le cas $k > \frac{1}{2}$, nous forçons plus de valeurs propres à être positives par rapport à la valeur moyenne. Ceci est équivalent à ajouter un potentiel chimique négative. La discontinuité de ce potentiel va créer une divergence de charge de zéro. Les charges sur le côté positif seront empiler à l'origine, tandis que les frais sur le côté négatif seront repoussés par cet empilement. Cela est en effet l'image que nous observons dans la résolution de l'équation (1.35), comme nous le verrons.

Par cette description, il est clair que nous nous attendons au support d'avoir des pièces compacts disjoints multiples. Cela transforme le théorème de Tricomi dans une option pas très favorable. Bien que ce soit la méthode utilisée pour d'abord calculer cette quantité dans [89], nous préférons utiliser l'option résolvant la fois pour la commodité et l'uniformité avec le reste de calculs dans cette thèse. Certains résultats de cette thèse impliquent un support à trois coupes, Tricomi théorème exigerait vaste calcul qui peut être plus facilement réalisée avec la méthode résolutive.

On rappelle l'équation de la résolvante

$$G(z) = \int \frac{\rho^\star(x)}{z-x} \mathrm{d}x. \tag{1.36}$$

À la suite de la recette prévue dans 1.22, on multiplie les deux côtés de l'équation par $\frac{\rho^\star(x)}{z-x}$ et nous intégrons plus de $x$. Notre but est d'écrire l'équation (1.35) comme une équation algébrique sur la résolvante, obtenir le résolutive et utiliser relation entre la résolvante et la densité pour obtenir la densité moyenne $\rho^\star(x)$, ce qui est la densité moyenne soumis à la contrainte d'avoir une fraction $k$ de valeurs propres sur le côté positif.

$$\int x \frac{\rho^\star(x)}{z-x} \mathrm{d}x + \mu \int \delta(x) \frac{\rho^\star(x)}{z-x} \mathrm{d}x = \iint \frac{\rho^\star(x')}{x-x'} \frac{\rho^\star(x)}{z-x} \mathrm{d}x' \mathrm{d}x, \quad x \in \mathrm{supp}(\rho^\star), \tag{1.37}$$

On intègre équation (1.35), en répétant les mêmes étapes décrites auparavant, on obtient

$$-1 + G(z) + \frac{A}{z} = \frac{1}{2} G(z)^2, \tag{1.38}$$

dont la solution est immediate

$$G(z) = z \pm \sqrt{\frac{2A - 2z + z^3}{z}} = z \pm \sqrt{\frac{(z-b_1)(z-b_2)(z-a)}{z}}. \tag{1.39}$$

Bien que $G$ n'a qu'un seul paramètre à être calculée en utilisant la fraction $k$, il est commode d'écrire la résolvante en termes de racines du polynôme sur le numérateur de

la racine carrée, tel que présenté dans l'équation (1.39). Ces racines peuvent être obtenus en mettant en équation le coefficient de deux polynômes.

$$a + b_1 + b_2 = 0 \tag{1.40}$$
$$ab_1 + ab_2 + b_1 b_2 = -2 \tag{1.41}$$

Et à la dernière variable nous déterminons en utilisant directement la condition $\int_0^\infty \rho^\star(x)\mathrm{d}x = k$. En utilisant l'identité suivante, nous calculons la densité moyenne contraint à la condition d'avoir une fraction $k$ de valeurs propres positives.

$$-\frac{1}{\pi}\mathrm{Im}\left[\lim_{\varepsilon\to 0^+} G(x+i\varepsilon)\right] = \frac{1}{\pi}\sqrt{\frac{(b_1-x)(x-b_2)(x-a)}{x}} = \rho^\star(x). \tag{1.42}$$

Nous remarquons comment les racines du polynôme deviennent les bords de la densité moyenne, dont le support est $[b_1, 0[\cup[a, b_2]$ pour le cas $k < \frac{1}{2}$ et $[b_1, a]\cup]0, b_2]$ pour le cas $k > \frac{1}{2}$. Nous traçons ces deux cas de cette densité, quand $a > 0$ et quand $a < 0$. Il y a un changement radical dans le comportement sur le point $a = 0$, ce qui correspond à $k = \frac{1}{2}$, sa valeur moyenne. Naturellement, lorsque la fraction des valeurs propres positives est sa valeur moyenne, on obtient la densité moyenne sans contraintes, le demi-cercle de Wigner. Cela peut être vu clairement dans la figure 1.4.

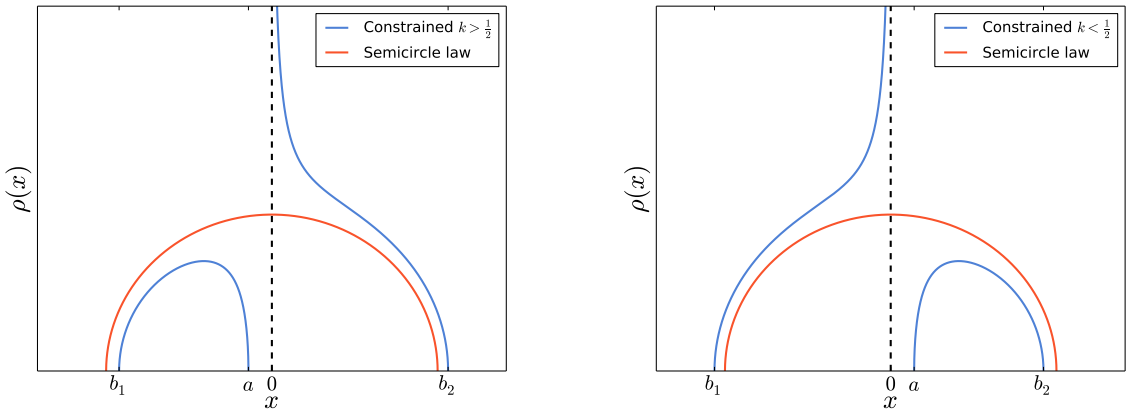


**(a)** **(b)**

**Figure 1.4** — Densité moyenne contrainte (bleu) et la comparaison avec le demi-cercle de Wigner (orange) pour l'index de l'ensemble gaussien dans les cas (a) $k > \frac{1}{2}$ et (b) $k < \frac{1}{2}$ (équation (1.42)).

Armé de la densité moyenne $\rho^\star(x)$, nous calculons la fonction totale, nommée rate function. La p.d.f. de $N_+$ est donné par l'équation (1.33). La fonction de partition $Z_{N,\beta}$ peut être facilement calculée en utilisant la méthode du col

$$Z_{N,\beta} = \int P(\boldsymbol{x})\mathrm{d}\boldsymbol{x} = \int \mathcal{D}\rho e^{-\beta N^2 S[\rho]} \approx e^{-\beta N^2 S[\rho_{sc}]} \tag{1.43}$$

Comme $\rho_{sc}$ est la densité qui minimise le fonctionnel $S$ sans contraintes, elle est en fait le demi-cercle de Wigner. La p.d.f. de $N_+$ devient

$$P(N_+ = kN) = \frac{1}{Z_{N,\beta}} e^{-\beta N^2 S[\rho^\star]} = e^{-\beta N^2 \psi(k)}, \tag{1.44}$$

où $\psi(k) = S[\rho^\star] - S[\rho_{sc}]$ est la *rate function*. Pars définition, $\psi(k)$ atteint son minimum lorsque $k = \frac{1}{2}$.

On rappelle que l'action $S$ évaluée à $\rho^\star$ est donnée par l'équation (1.32)

$$S[\rho^\star] = \int \frac{x^2}{2}\rho^\star(x)\mathrm{d}x - \frac{1}{2}\iint \rho^\star(x)\rho^\star(x')\log|x-x'|\mathrm{d}x\mathrm{d}x' \tag{1.45}$$

$$+ \mu \underbrace{\left(\int_0^\infty \rho^\star(x)\mathrm{d}x - k\right)}_{=0} + \eta \underbrace{\left(\int_{-\infty}^\infty \rho^\star(x)\mathrm{d}x - 1\right)}_{=0}, \tag{1.46}$$

où l'on note les termes nuls, vu que $\rho^\star$ satisfait les deux conditions par définition. Les autres termes sont une seule intégrale sur le potentiel quadratique et une intégrale double d'un terme logarithmique. Cette intégrale double est problématique, et on peut la remplacer par d'autres plus faciles à calculer. Nous faisons usage de l'équation du bilan d'énergie (1.34) appliquée à $\rho^\star$ en le multipliant par $\rho^\star(x)$ et en l'intégrant en $x$. Cela donne

$$\int \rho^\star(x)\frac{x^2}{2}\mathrm{d}x - \iint \rho^\star(x)\rho^\star(x')\log|x-x'|\mathrm{d}x\mathrm{d}x' + \eta \underbrace{\int \rho^\star(x)\mathrm{d}x}_{=1} + \mu \underbrace{\int_0^\infty \rho^\star(x)\mathrm{d}x}_{=k} = 0, \tag{1.47}$$

qui peut s'écrire comme

$$\iint \rho^\star(x)\rho^\star(x')\log|x-x'|\mathrm{d}x\mathrm{d}x' = \int \rho^\star(x)\frac{x^2}{2}\mathrm{d}x - \eta - \mu k. \tag{1.48}$$

Cela montre que, pour le cas de $\rho^\star$, l'équation du bilan d'énergie nous permet d'échanger l'intégrale double par une intégrale simple, il suffit de calculer les multiplicateurs de Lagrange. La forme finale de l'action $S$ calculée pour $\rho^\star$ devient

$$S[\rho^\star] = \frac{1}{4}\int \rho^\star(x)x^2\mathrm{d}x - \frac{\mu k}{2} - \frac{\eta}{2}. \tag{1.49}$$

Le calcul de la Lagrange multiplicateurs $\mu$ et $\eta$ est encore nécessaire. Pour l'accomplir, nous explorons une fois de plus l'équation du bilan d'énergie (1.34). Cette équation est valable en tout point dans le support, de sorte que nous calculons sur les points $a$ et 0. Ce sont des bords du support, et nous prenons la limite dans la bonne direction pour obtenir ces équation, tout en restant à l'intérieur du support de $\rho^\star$. Pour plus de simplicité, nous prenons le cas où $k < \frac{1}{2}$, ce qui implique $a > 0$. Cela implique

$$\frac{a^2}{2} - H(a) + \mu + \eta = 0 \tag{1.50}$$

$$-H(0)+\eta=0, \tag{1.51}$$

où on a définit la fonction $H(x)=\int\rho(x')\log|x-x'|\mathrm{d}x'$.

De (1.51), on obtient $\eta=H(0)$. Alors que $H(0)$ peut être traitée directement, nous voulons éviter de traiter avec l'intégrale de $\rho(x')\log|x-x'|$. Au lieu de cela, nous le remplaçons dans la première équation telle qu'elle est, et l'on obtient la valeur de $\mu$.

$$\mu=H(a)-H(0)-\frac{a^2}{2}. \tag{1.52}$$

Remarquablement, vu que $H$ est la primitive de $G$, la différence $H(a)-H(0)$ peut être écrit que $\int_0^a G(x)\mathrm{d}x$. La formule finale pour le premier multiplicateur de Lagrange est

$$\mu=\int_0^a G(x)\mathrm{d}x-\frac{a^2}{2}. \tag{1.53}$$

Intégrales de la résolvante sont beaucoup plus faciles à calculer que la valeur de $H$ dans un point, donc on effectue une petite manipulation pour obtenir $\eta$ comme une intégrale de $G$. On développe $\log|b_1-x|$ en $x$ et on obtient

$$\int\rho^\star(x)\log|b_1-x|\mathrm{d}x=\log|b_1|-\int\sum_{n=1}^{\infty}\frac{x^n}{b_1^n}\rho^\star(x)\mathrm{d}x=\log|b_1|-\int_{b_1}^{-\infty}\left(G(x)-\frac{1}{x}\right)\mathrm{d}x. \tag{1.54}$$

En utilisant cette rélation et muni de l'équation (1.34) appliquée à $b_1$ on obtient

$$\eta=\log|b_1|-\frac{b_1^2}{2}-\int_{b_1}^{-\infty}\left(G(x)-\frac{1}{x}\right)\mathrm{d}x. \tag{1.55}$$

Et la formule finale de l'áction devient

$$\begin{aligned}S[\rho^\star]=&\frac{1}{4}\int\rho^\star(x)x^2\mathrm{d}x-\frac{1}{2}\left(\int_0^a G(x)\mathrm{d}x-\frac{a^2}{2}\right)k\\&-\frac{1}{2}\left(\log|b_1|-\frac{b_1^2}{2}-\int_{b_1}^{-\infty}\left(G(x)-\frac{1}{x}\right)\mathrm{d}x\right).\end{aligned} \tag{1.56}$$

La valeur de l'action calculée dans le demi-cercle peut être facilement réalisée. Les bords du support sont $b_1=-\sqrt{2}$, $b_2=\sqrt{2}$ et $a=0$ pour le demi-cercle, de sorte que la résolvante prend la forme $G(z)=z\pm\sqrt{z^2-2}$. Nous obtenons $\mu=0$ et les intégrales restantes sont simples. Elles donnent

$$S[\rho_{sc}]=\frac{1}{4\pi}\int x^2\sqrt{2-x^2}\mathrm{d}x-\frac{\log 2}{4}+\frac{1}{2}+\frac{1}{2}\int_{-\sqrt{2}}^{-\infty}\left(x+\sqrt{x^2-2}-\frac{1}{x}\right)\mathrm{d}x=\frac{3}{8}+\frac{\log 2}{4}. \tag{1.57}$$

Une dernière simplification digne de mention est l'intégrale $\int x^2\rho^\star(x)\mathrm{d}x$. Ceci est le calcul du deuxième moment de la densité moyenne, qui peut aussi être donnée par l'expansion de la résolvante des commandes de $z$

$$G(z)=\int\frac{\rho^\star(x)}{z-x}\mathrm{d}x=\frac{1}{z}+\frac{1}{z^2}\int x\rho^\star(x)\mathrm{d}x+\frac{1}{z^3}\int x^2\rho^\star(x)\mathrm{d}x+\mathcal{O}(z^{-4}). \tag{1.58}$$

Développent la résolvante (1.39) et appliquant les conditions de normalisation(1.40) et (1.41) donne

$$G(z) = \frac{1}{z} + \frac{a(a^2-2)}{2z^2} + \frac{1}{2z^3} + \mathcal{O}(z^{-4}). \tag{1.59}$$

Qui implique la valeur

$$\frac{1}{4}\int x^2 \rho^\star(x)\mathrm{d}x = \frac{1}{8}. \tag{1.60}$$

La formule finale de la rate function est, donc,

$$\psi(k) = -\frac{1}{2}\left(\int_0^a G(x)\mathrm{d}x - \frac{a^2}{2}\right)k - \frac{1}{2}\left(\log|b_1| - \frac{b_1^2}{2} - \int_{b_1}^{-\infty}\left(G(x) - \frac{1}{x}\right)\mathrm{d}x\right) - \frac{1}{4} - \frac{\log 2}{4}. \tag{1.61}$$

La formule finale de l'action implique intégrales qui sont analytiquement compliquées, mais ne représentent aucun défi numérique. Nous traçons les résultats numériques de cette formule de la figure 1.5. En effet, nous observons le minimum à $k^\star = 1/2$ et la symétrie, conséquence de l'invariance de réflexion du problème.

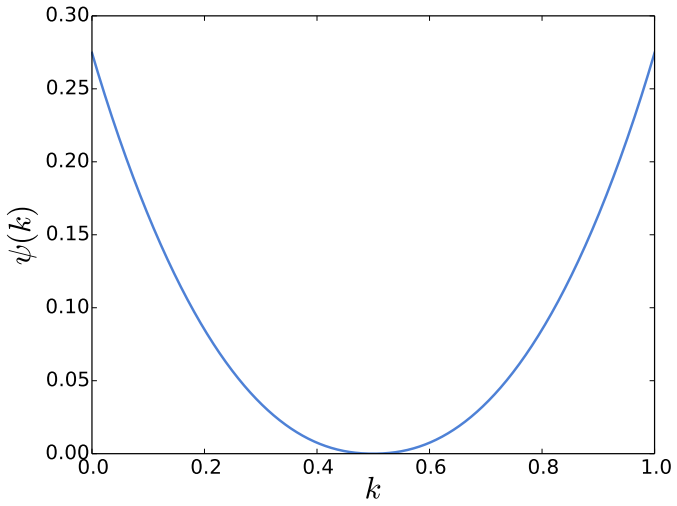


**Figure 1.5** — Rate function $\psi(k)$ de l'index de l'ensemble gaussien (équation (1.61)).

La rate function, quand tracée par rapport à $k$, présente un minimum symétrique claire autour $k = 1/2$. Cela nous invite à étudier les fluctuations typiques de $k$ autour de sa moyenne, et d'explorer la variance de la variable $N_+$. Notre objectif est développer $\psi(k)$ environ $k = \frac{1}{2} + \delta$ pour les principaux termes dans petite $\delta$. Cette expansion est pas simple, et on procède de la manière suivante.

On sait que quand $k = k^\star = 1/2$, les bords $a$, $b_1$ et $b_2$ collapsent à 0, $-\sqrt{2}$ et $\sqrt{2}$ respectivement. On perturbe les bords par un petit paramètre

$$a = \epsilon, \qquad b_1 = -\sqrt{2} - \epsilon_2, \qquad b_2 = \sqrt{2} - \epsilon_3. \tag{1.62}$$

La condition de normalisation implique les équations (1.40) et (1.41), cela implique une relation entre les perturbations

$$\epsilon - \epsilon_2 - \epsilon_3 = 0 \tag{1.63}$$
$$\epsilon_2 - \epsilon_3 = 0 \tag{1.64}$$

Qui implique $\epsilon = 2\epsilon_2 = 2\epsilon_3$. La relation entre $\epsilon$ et $\delta$ sera donnée par la condition finale $\int_0^\infty \rho^\star(x)\mathrm{d}x = k = \frac{1}{2}+\delta$. On remplace les bords par les valeurs perturbées et on développe la résolvante en petites valeurs de $\epsilon$. Vu que les cas $k > \frac{1}{2}$ et $k < \frac{1}{2}$ sont symétriques, on prend, sans perdre de généralité, le deuxième cas, qui implique $\epsilon > 0$.

On rappelle la formule de $\mu$ et on y remplace les bords perturbés

$$\mu = \int_0^a G(x)\mathrm{d}x - \frac{a^2}{2} = \int_0^\epsilon \sqrt{\frac{(x-\sqrt{2}+2\epsilon)(x+\sqrt{2}+2\epsilon)(x-\epsilon)}{x}}\mathrm{d}x. \tag{1.65}$$

Nous répétons ce genre d'intégration à plusieurs reprises dans cette thèse, et la technique est la même. Vu que l'intervalle d'intégration est très petit, nous avons partagé l'intégrale dans le produit d'une fonction que varie rapidement et une fonction qui varie lentement. Les parties de variation lente peuvent simplement être évaluées en prenant $x = 0$, tandis que le la partie de variation rapide est intégré. La procédure est la suivante

$$\mu = \int_0^\epsilon \sqrt{\frac{(x-\sqrt{2}+\epsilon/2)(x+\sqrt{2}+\epsilon/2)(x-\epsilon)}{x}}\mathrm{d}x = \sqrt{2}\int_0^\epsilon \sqrt{\frac{\epsilon-x}{x}}\mathrm{d}x + o(\epsilon) = \frac{\pi}{\sqrt{2}}\epsilon + o(\epsilon). \tag{1.66}$$

D'abord, on calcule l'intégrale $I = \int_{b_1}^{-\infty}\left(G(x) - \frac{1}{x}\right)\mathrm{d}x$ en partageant le domaine d'intégration en deux parties:

$$I = \underbrace{\int_{b_1}^{-\sqrt{2}}\left(G(x) - \frac{1}{x}\right)\mathrm{d}x}_{I_1} + \underbrace{\int_{-\sqrt{2}}^{-\infty}\left(G(x) - \frac{1}{x}\right)\mathrm{d}x}_{I_2}. \tag{1.67}$$

Pour $I_1$, nous répétons la procédure de (1.66).

$$I_1 = \int_{b_1}^{-\sqrt{2}}\left(x - \frac{1}{x}\right)\mathrm{d}x + \int_{b_1}^{-\sqrt{2}}\sqrt{\frac{(x-\sqrt{2}+\epsilon/2)(x+\sqrt{2}+\epsilon/2)(x-\epsilon)}{x}}\mathrm{d}x \tag{1.68}$$
$$= -\frac{\epsilon}{2\sqrt{2}} + 2^{\frac{3}{4}}\int_{b_1}^{-\sqrt{2}}\sqrt{x+\sqrt{2}+\frac{\epsilon}{2}}\mathrm{d}x + o(\epsilon) \tag{1.69}$$
$$= -\frac{\epsilon}{2\sqrt{2}} + o(\epsilon). \tag{1.70}$$

Pour $I_2$, on développe l'intégrande en puissances de $\epsilon$ et on intègre terme à terme de $-\sqrt{2}$ à $-\infty$. Le partage du domaine est important pour préserver la convergence de cette procédure.

$$I_2 = \int_{-\sqrt{2}}^{-\infty}\left(x + \sqrt{x^2-2} - \frac{1}{x}\right)\mathrm{d}x + \int_{-\sqrt{2}}^{-\infty}\frac{\epsilon}{x\sqrt{x^2-2}}\mathrm{d}x + o(\epsilon) \tag{1.71}$$

$$= -\frac{1}{2} + \log 2 + \frac{\pi\epsilon}{2\sqrt{2}}. \tag{1.72}$$

On ajoute le développement de $\log|b_1| - b_1^2/2$ pour obtenir la formule finale de $\eta$

$$\eta = -\frac{1}{2} - \frac{\log 2}{2} - \frac{\pi\epsilon}{2\sqrt{2}}. \tag{1.73}$$

Pour calculer $k$, on développe la densité moyenne en puissances de $\epsilon$

$$\rho^\star(x) = \frac{1}{\pi}\sqrt{\frac{(x-\sqrt{2}+\epsilon/2)(x+\sqrt{2}+\epsilon/2)(x-\epsilon)}{x}} = \frac{1}{\pi}\sqrt{2-x^2} - \frac{\epsilon}{\pi x\sqrt{2-x^2}} + o(\epsilon). \tag{1.74}$$

La valeur de $k$ peut être facilement calculé. Nous concentrons notre attention sur le cas $k < \frac{1}{2}$ et $\epsilon > 0$. Comme ils sont symétriques, nous allons simplement calculons ce cas. La valeur de $k$ est l'intégrale entre $a$ et $b_2$, et on calcule chaque terme de l'RHS de l'équation (1.74).

$$\int_a^{b_2} \frac{\sqrt{2-x^2}}{\pi}\mathrm{d}x = \frac{1}{2} - \frac{\sqrt{2}}{\pi}\epsilon + o(\epsilon), \tag{1.75}$$

$$\int_a^{b_2} \frac{\epsilon}{\pi x\sqrt{2-x^2}}\mathrm{d}x = \frac{3\log 2}{2\sqrt{2}\pi}\epsilon - \frac{1}{\pi\sqrt{2}}\epsilon\log\epsilon + o(\epsilon). \tag{1.76}$$

On garge les deux premier termes dominants, donc on écrit

$$k = \frac{1}{2} + \frac{1}{\pi\sqrt{2}}\epsilon\log\epsilon + o(\epsilon\log\epsilon). \tag{1.77}$$

Où nous pouvons facilement reconnaître la relation entre $\epsilon$, la perturbation dans les bords, et $\delta$, la perturbation dans la fraction de valeurs propres à l'intérieur de $\mathcal{I}$

$$\delta = \frac{1}{\pi\sqrt{2}}\epsilon\log\epsilon. \tag{1.78}$$

On ajoute les contributions calculées auparavant et, après une impressionnante suite de simplifications, nous obtenons

$$\psi\left(\frac{1}{2}+\delta\right) = -\frac{\mu k}{2} - \frac{\eta}{2} - \frac{1}{4} - \frac{\log 2}{4} = -\frac{\pi}{2\sqrt{2}}\epsilon\delta + o(\epsilon\delta). \tag{1.79}$$

Comme prévu, le terme constant a été compensé par la constante de normalisation $S[\rho_{sc}]$ et le terme linéaire disparu lors de l'expansion dans le minimum. Le terme résiduelle est d'ordre quadratique, mais il reste à exprimer $\epsilon$ en termes de $\delta$ pour être en mesure de lire la variance de lui. Nous utilisons l'équation (1.78). L'inverse ne peut être exprimée par des fonctions simples, mais nous pouvons utiliser le fait que les deux $\epsilon$ et $\delta$ sont petits pour fournir le ansatz suivant, valable à l'ordre dominant dans $\epsilon$ et $\delta$

$$\epsilon = \pi\sqrt{2}\frac{\delta}{\log\delta}. \tag{1.80}$$

Cette relation peut être vérifiée en l'insérant dans (1.78) et vérifiant qu'elle elle correcte en ordre dominant de *delta*. La rate function devient

$$\psi\left(\frac{1}{2}+\delta\right) = -\frac{\pi^2}{2}\frac{\delta^2}{\log\delta} + o\left(\frac{\delta^2}{\log\delta}\right). \tag{1.81}$$

Nous sommes intéressés aux fluctuations typiques de $N_+$ autour de sa moyenne $N/2$, on prend $N_+ - N/2 \ll N$. Le résultat précedent nous permet d'écrire

$$\log\delta = \log\left(\frac{N_+ - \frac{N}{2}}{N}\right) \approx -\log N. \tag{1.82}$$

La rate function de fluctuations typiques de l'index de l'ensemble Gaussien devient

$$\psi(N_+) \approx \frac{\pi^2}{2N^2}\frac{(N_+ - \frac{N}{2})^2}{\log N}. \tag{1.83}$$

La p.d.f. des fluctuations typiques de $N_+$ est,donc

$$P(N_+) = e^{-\beta N^2\psi(N_+)} \approx e^{-\beta\frac{\pi^2}{2}\frac{(N_+-\frac{N}{2})^2}{\log N}}, \tag{1.84}$$

ce qui nous permet d'écrire la comportement de large $N$ de la variance des fluctuations typiques du nombre positif de valeurs propres

$$\operatorname{Var} N_+ = \frac{1}{\beta\pi^2}\log N + \text{cte} + o(1). \tag{1.85}$$

Ce qui est en accord avec les résultats en [32] pour $\beta = 1$ et avec le résultat présenté en [89, 90]. Le terme constant est très difficile de déterminer avec la méthode du gaz de Coulomb, et il a été trouvé en [90] pour $\beta = 2$ et donné par cte $= \frac{\gamma+1+3\log 2}{2\pi^2} \approx 0.1852....$

On compare l'inclination de la formule (1.85) et des simulations numériques pour les valeurs propres de GOE ($\beta = 1$) à la figure1.6.

La méthode décrite ci-dessus est la base des résultats de cette thèse, mais sa compréhension générale est possible par cet exemple de l'index de l'ensemble Gaussien. Je laisse au texte complet en anglais pour les détails de l'application de cette méthode dans le contexte de l'intervalle général et l'application dans d'autres ensembles des matrices. Dans ce que suit, je résume les résultats de cette thèse.

Cette thèse met ensemble trois années de travail dans la théorie des matrices aléatoires, et il se concentre sur un aspect particulier de celui-ci: le comptage des valeurs propres à l'intérieur d'un intervalle donné. Bien que ce problème a été traité dans le passé en de nombreuses occasions [43, 128, 54, 33], il y avait très peu de résultats pour les statistiques du nombre en dehors des régimes de bulk et de edge classiques.

Le début de mon travail était pas sur ce sujet précis. Je commence à travailler dans les applications de la théorie des matrices aléatoires au transport quantique, qui est décrit dans le chapitre 9. Nous avons pu montrer que les effets des impuretés dans les canaux d'un point quantique peuvent être obtenus en termes de quantités calculées dans le cas

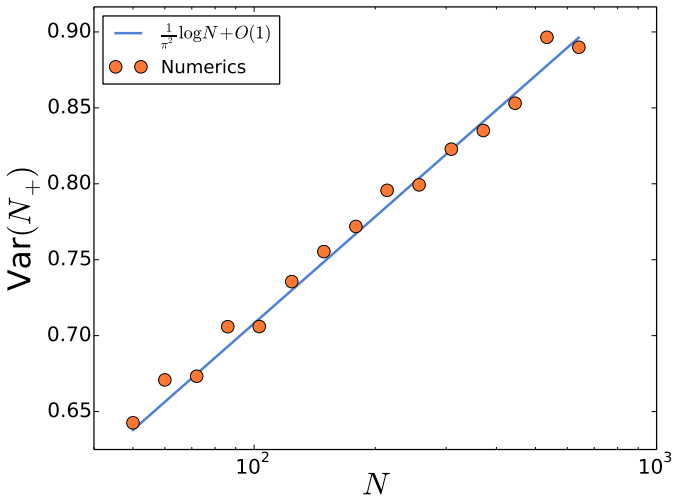


**Figure 1.6** — Comparaison entre le comportement à large $N$ de la variance et de simulations numériques pour GOE ($\beta = 1$).

idéal, et nous avons fourni les outils nécessaires pour effectuer ce calcul. Le cas général complet, mais pas trivial, a été obtenu en termes de polynômes de Schur, un cadre naturel pour les variables symétriques telles que les valeurs propres de transmission d'un transport quantique.

De cet intérêt nous sommes passés à des considérations plus générales sur l'ensemble de Cauchy, une classe de matrices qui se dégage naturellement de transport quantique dont la densité moyenne des valeurs propres a la propriété remarquable d'être pris en charge sur toute la ligne réelle. Les statistiques sur le nombre de valeurs propres positives d'une matrice de Gauss ont été obtenues dans [89, 90], et nous voulions savoir si la même technique pourrait être appliquée à un cas différent, l'ensemble de Cauchy, où la densité moyenne des valeurs propres ne présente pas de bord. A notre grande surprise, les fluctuations des valeurs propres positives de l'ensemble Cauchy étaient précisément deux fois la taille des fluctuations de l'ensemble de Gauss, comme le montre la figure 1.7. De la variance de l'indice de l'ensemble de Cauchy nous trouvons

$$\mathrm{Var}(N_+^C) = \frac{2}{\beta\pi^2}\log N + O(1), \tag{1.86}$$

Ce résultat nous conduit à examiner le rôle de l'arête des fluctuations. résultats précédents pour fluctuations de valeurs propres gaussiennes [43, 100] a montré que, pour les petits intervalles, le nombre variance croît de façon logarithmique avec la taille de l'intervalle. Prendre un symétrique intervalle $[-L, L]$, il est clair que cet écart devrait aller à zéro si l'intervalle contient l'ensemble du support de la répartition moyenne, que de façon exponentielle quelques valeurs propres tomberait dehors de l'intervalle et les fluctuations ne serait pas produite . De la croissance logarithmique à zéro une fonction d'adaptation est nécessaire, et ce changement de comportement se passerait dans l'échelle

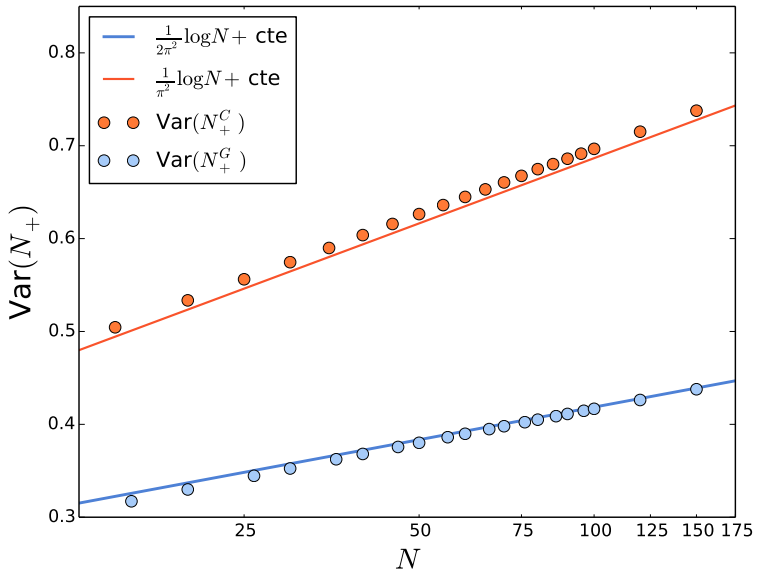


**Figure 1.7** — Évaluation numérique de la variance de l'index avec $\beta = 2$ pour l'ensemble unitaire de Cauchy (noté $N_+^C$, ligne supérieure) et de l'ensemble Gaussien unitaire (noté $N_+^G$, ligne inférieure). Voir [96].

mésoscopique.

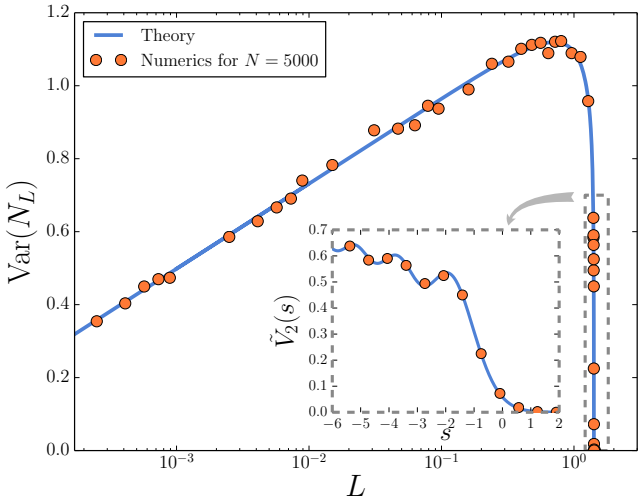


**Figure 1.8** — Résultats pour la variance de $N_\mathcal{I}$ pour l'ensemble Gaussien lorsque $\mathcal{I} = [-L, L]$ et $L < \sqrt{2}$. Voir [97].

Information sur les échelles mésoscopiques, lorsque l'intervalle considéré était de l'ordre de la taille du système, étaient presque inexistants, et en collaboration avec Majumdar,

Schehr et Vivo nous avons obtenu, pour la première fois, la fonction complète des statistiques de nombre de GUE [97], comme nous avons discuté dans le chapitre 7. Les résultats pour le nombre variance correspondent simulations numériques remarquablement bien, comme le montre la figure 1.8.

La méthode pour obtenir ce résultat, la méthode de gaz Coulomb, se sont avérés très générale et donne des résultats pour une large classe de matrices aléatoires, ceux dont la distribution des valeurs propres peut être écrit que l'équation (4.1). Nous avons exploré cela entraîne pour les matrices de Wishart et matrices de Cauchy dans le chapitre 8, mais la même étude peut être appliqué pour l'ensemble circulaire ou l'ensemble Jacobi, car ils partagent la même structure pour la distribution des valeurs propres.

L'application de cette méthode à d'autres ensembles montré des similitudes intéressantes pour ces types très différents de matrices. En particulier, la structure de la variance du nombre pour le régime dite masse prolongée est similaire. Nous trouvons, pour les grandes valeurs de $N$,

$$\mathrm{Var}(N_{\mathcal{I}}) \approx \begin{cases} \frac{2}{\beta\pi^2} \log\left(NL(2-L^2)^{\frac{3}{2}}\right), & \text{Gaussian and } \mathcal{I} = [-L, L] \\ \frac{2}{\beta\pi^2} \log\left(Nl(3-l)^{\frac{3}{4}}\right), & \text{Wishart and } \mathcal{I} = [1, 1+l] \\ \frac{2}{\beta\pi^2} \log\left(\frac{NL}{1+L^2}\right), & \text{Cauchy and } \mathcal{I} = [-L, L] \end{cases} \tag{1.87}$$

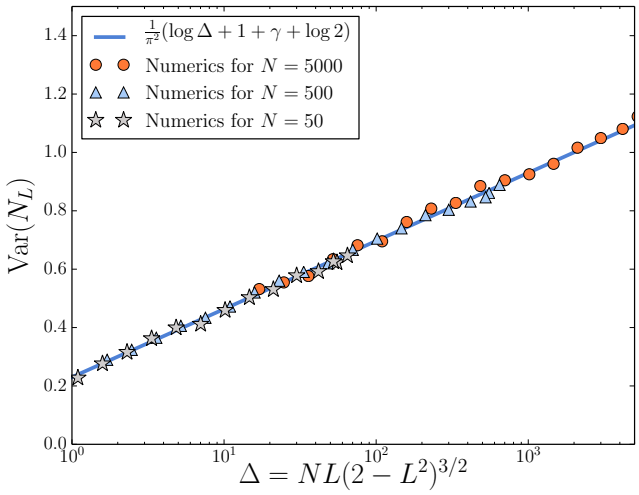


**Figure 1.9** — Simulations numériques de la variance du nombre de valeurs propres de GUE.

On fait un résume des résultats principaux de cette thèse

- L'imposition d'un mur dur dans $\zeta$ dans le spectre de la matrice aléatoire invariant peut être calculé en ajoutant un $\delta(x-\zeta)$ contribution à l'équation intégrale utilisée pour obtenir la densité moyenne. Ce résultat est largement utilisé dans les problèmes suivants

  - Le problème de l'index, en mettant un mur fort à la place zéro, voir chapitre 6.
  - Au calcul des fluctuations du nombre de valeurs propres de l'ensemble Gaussien qui tombent dans un intervalle $\mathcal{I} = [-L, L]$, voir chapitre 7.
  - Au calcul des fluctuations du nombre de valeurs propres des ensembles de Wishart et Cauchy qui tombent dans un intervalle générique $\mathcal{I} = [a, b]$, voir chapitre 8.

- La variation du nombre de valeurs propres positives dans l'ensemble de Cauchy est deux fois plus grande que la variance de valeurs propres positives de l'ensemble de Gauss. Cette différence est due à l'absence d'une densité moyenne à support compacte de valeurs propres pour l'ensemble de Cauchy, et est présenté dans le chapitre 6.

- La densité moyenne des valeurs propres pour l'ensemble de Cauchy possède comme support toute la ligne réelle, mais la densité moyenne contraint, obtenu quand nous imposons une fraction $k$ de valeurs propres à être positif et $k \neq 1/2$, est supportée dans deux intervalles disjoints, dont l'un est compact (voir figure 6.7).

- La variance du nombre $N_L$ de valeurs propres d'une matrice de Gauss à l'intérieur d'un intervalle $\mathcal{I} = [-L, L]$ dépend fortement de $L$. Résultats précédents étaient seulement en mesure de fournir des résultats pour $L \sim \frac{1}{N}$ ou $L \sim \sqrt{2}$. Nous avons fourni au chapitre 7 la fonction de densité de probabilité complète de $N_L$ pour grande $N$ et nous avons obtenu le comportement asymptotique de sa variance pour toutes les valeurs de $L$. Les nouveaux résultats que nous avons obtenus sont la variance de $N_L$ pour des valeurs de $L$ dans le "extended bulk" régime, qui sont des valeurs de $L$ l'intérieur du support, et " tail " régime, qui sont des valeurs de $L$ loin du support. Cette fonction qui lie la variance du bulk au edge régime a une importance remarquable dans le contexte d'atomes froids, et des études antérieures a essayé sans succès d'obtenir son comportement dominant pour les grands $N$ [137].

Les résultats présentés dans cette thèse ont produit 3 publications, et il y a des résultats non publiés dans cette thèse couvrant les résultats de deux articles en phase finale de préparation.

- Rodríguez-Pérez, S., Marino, R., Novaes, M., and Vivo, P. Statistics of quantum transport in weakly nonideal chaotic cavities. Phys. Rev. E **88** (2013), 052912.

- Marino, R., Majumdar, S. N., Schehr, G., and Vivo, P. Index distribution of Cauchy random matrices. J. Phys. A: Math. Theor. **47** (2014), 055001.

- Marino, R., Majumdar, S. N., Schehr, G., and Vivo, P. Phase transitions and edge scaling of number variance in gaussian random matrices. Phys. Rev. Lett. **112** (2014), 254101.

# — 2 —
# Introduction

*Every science begins as philosophy and ends as art; it arises in hypothesis and flows into achievement.*

Will Durant

## 2.1 A very brief overview of random matrix theory

In the heart of statistical physics lies the idea of abandoning specific knowledge of microscopic details of the system to gain insight into its statistical behavior. In 1947, this idea guided Wigner [150, 146] to consider ignoring the details of the strong interaction of protons and neutrons to propose a statistical approach to nuclear physics. The compound nature of the nucleus prevents any calculation of energy levels from the dynamics, so investigations on the statistics of energy levels brought Wigner to consider random matrices as a major tool to treat this scenario [147, 149]. Wigner was strongly motivated by universality, an expectation that the main features of the spectrum should not depend on microscopic details of the model, but rather on its general properties and symmetries [148].

One of the main problems studied by Wigner was the energy level spacing of the atomic nucleus. If the energy values were statistically independent, their spacing would be a random variable whose statistics is given by the Poisson distribution. Experimentally, this was not observed, energy levels exhibit level repulsion and should be described by another statistics. This repulsion, and the universality expected by Wigner, are captured by replacing the Hamiltonian with a random matrix [147], and Wigner set out to explore this domain both physically and mathematically. In a series of papers (reprinted in [118]), he laid the foundations of random matrix theory, a field whose reach would go much further than the initial ideas about nuclear spectra and energy levels.

A major development in random matrix theory (RMT) was performed by Dyson a few years later by exploring the role of symmetries in matrix ensembles [43]. Dyson introduced his general random matrix classification, the "threefold way" (see section 3.1.1), and at the same time there were breakthroughs on the mathematical side by Gaudin, Mehta,

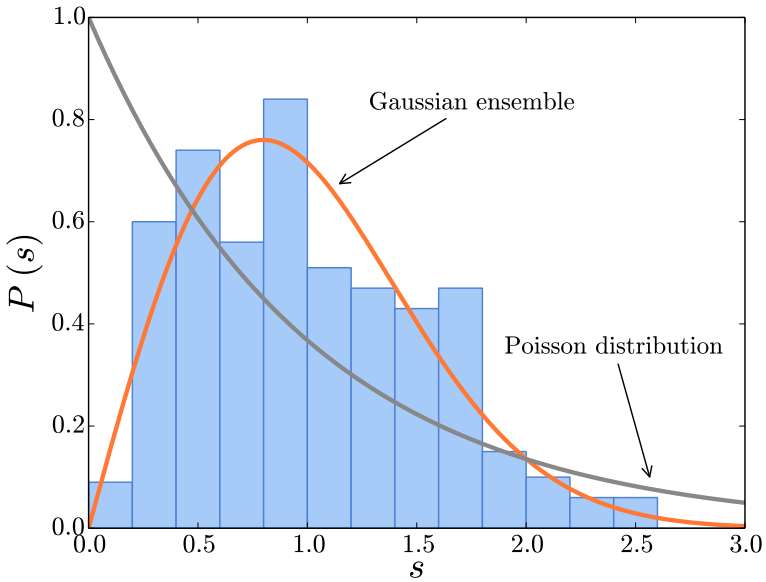


**Figure 2.1** — Data for 108 nearest neighbor spacing of energy levels in the nucleus of $^{166}$Er compared to the same quantity for a Poisson process and eigenvalues of a Gaussian Orthogonal random matrix. Graphic reproduced from [100], data is taken from [85].

Porter and Rosenzweig [119, 100]. This work is briefly reviewed in chapter 3, as it is the foundation of any work in RMT. Despite the mathematical richness, the interesting interpretation of the subject in nuclear physics and some experimental evidence, shown in figure 2.1, there was not enough data to support RMT as the fundamental tool to analyze the nuclear spectra. According to Dyson [42]

> *All of our struggles were in vain. 82 levels were too few to give a statistically significant test of the model. As a contribution to the understanding of nuclear physics, random matrix theory was a dismal failure.*

Random matrix theory remained dormant until the seventies, when H. L. Montgomery conjectured a strong connection between RMT and the zeros of the Zeta function [105, 106], arguing that the pair correlation between the zeros of the Riemann Zeta function is the same as the pair correlation function of eigenvalues of random Hermitian matrices, which is given by the sine kernel (see section 4.4.1). This conjecture remains unproven after 40 years, but has collected a significant amount of numerical data corroborating it.

The applications of RMT in nuclear physics led to the development of tools to deal with statistics of many-body physics and scattering, which proved to be fundamental to understand classical and quantum chaos in the following decade. By exploring the Sinai's billiard problem, a strongly chaotic system, Bohigas, Giannoni and Schmit [17] conjectured that level fluctuations of the quantum Sinai's billiard are consistent with the fluctuations of eigenvalues of the Gaussian orthogonal ensemble of random matrices,

shown in figure 2.2 [1]. This result is particularly interesting because it represents a powerful application of RMT for a case of high complexity, but low particle number. As the authors mentioned [17]

> *Is this a surprising result? With a few inconclusive exceptions (see a discussion on small metallic particles, for instance in Ref. 2), the basic hypotheses leading to RMT have always been put forward by invoking the complexity of as essential that one is dealing with a many-particle system (system with many degrees of freedom). Our results indicate that this is by no means a necessary condition. Indeed, the quantum chaotic system with two degrees of freedom studied here (a one-particle system in two dimensions) shows also GOE [Gaussian Orthogonal Ensemble] fluctuations. [...] In summary, the question at issue is to prove or disprove the following conjecture: Spectra of time-reversal-invariant systems whose classical analogs are K [strongly chaotic] systems show the same fluctuation properties as predicted by GOE.*

Once again, we see the unifying point of random matrix theory: the argument that in a very complicated system, symmetries should play a more fundamental role than details about the microscopic nature of the model.

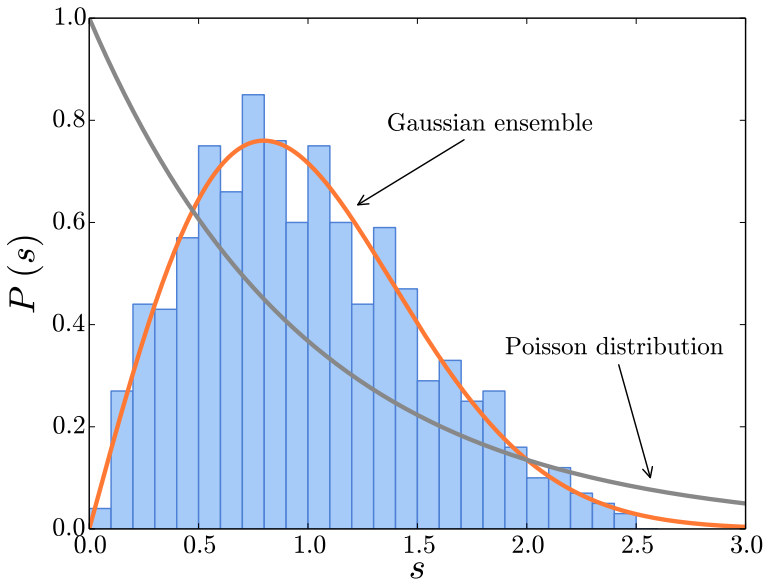


**Figure 2.2** — Data for 720 nearest neighbor spacing of energy levels for desymmetrized Sinai's billiard. Graphic reproduced from [17].

After that, a vast number of applications of random matrix theory emerged, in fields such as cosmology [131, 40], quantum transport [14], wireless communications [78], cold

[1] Oriol Bohigas was a dear member of our laboratory and the result in this figure is present in the logo of the LPTMS, in the upper-right corner of the cover of this thesis.

atoms [31, 137, 97, 28], finance [117, 82] and many others. There has been a large increase in interest in RMT in the last decade and the number of applications has become too large to mention individually. I refer to [2] for a very complete overview of the state of the field in 2011.

Random matrix theory, in an exaggerated reduction, is about answering one question: given a matrix whose entries are random variables, what can be said about its eigenvalues and eigenvectors? This question will surely be followed by many others, such as: can we obtain results for all matrix sizes? What happens when the matrix size becomes very large? Can we obtain the joint probability density function (j.p.d.f.) for the eigenvalues? Is there an equivalent of the central limit theorem for random matrices? Great mathematical and physical progress has been made towards answering these questions, and we present a brief overview of classical results in chapters 3 to 5.

Among these problems, the question about matrix size is of fundamental importance. Naturally, a random matrix problem grows in complexity as we increase the matrix size; however, once the matrix size becomes very large, we can apply techniques from statistical mechanics to gain insight into the leading behavior of the quantities we want to study. For very large $N \times N$ matrices, the leading $N$ behavior of spectral properties yields defining features of the model, and statistical physics is a fundamental tool to obtain these results. As noted by Wigner [148], after introducing the j.p.d.f. $P(\boldsymbol{\lambda})$ for the eigenvalues $\boldsymbol{\lambda} = (\lambda_1, \ldots, \lambda_N)$ of a $N \times N$ Gaussian real matrix (equation (3.17)):

$$P(\boldsymbol{\lambda}) = \frac{1}{Z_{N,\beta}} e^{-\frac{1}{2}\sum_{i=1}^{N} \lambda_i^2} \prod_{i<j} |\lambda_i - \lambda_j|. \tag{2.1}$$

> *You see again this characteristic factor which shows that the probability of two roots coinciding is 0. If you want to calculate from this formula, the probability that two successive roots have a distance $X$, then you have to integrate over all of them except two. This is very easy to do for the first integration, possible to do for the second integration, but when you get to the third, fourth and fifth, etc., integrations you have the same problem as in statistical mechanics, and presumably the solution of the problem will be accomplished by one of the methods of statistical mechanics.*

It is therefore natural to dispose of several tools emerging from statistical mechanics to solve problems that could otherwise be considered pure exercises in algebra of random variables. As an example, we can manipulate the j.p.d.f. of the eigenvalues of a Gaussian random matrix to show that their statistics is equivalent of that of charged particles in two dimensions confined to the real line and submitted to a harmonic potential. This new framework, called the Coulomb-gas method (described in section 4.1), transforms a purely mathematical problem, computing moments and observables of eigenvalues of a Gaussian matrix, into an electrostatic problem. Using this connection, the limit of large matrix size becomes the familiar thermodynamical limit, when charges are too numerous and we may replace their individual positions by a charge density. We can then import many techniques and physical intuition from electrostatics to solve problems in random matrix theory. This equivalence between different approaches that share the same statistics is

of central importance to this thesis, and it is one of the core features of random matrix theory.

## 2.2 Applications to cold fermions

I centered my thesis around a specific connection between statistical physics and RMT: the fact that the statistics of one-dimensional cold fermions submitted to a harmonic potential is equivalent to that of eigenvalues of a Gaussian Hermitian random matrix. This correspondence allows us to exchange a complicated many-body quantum problem into the calculation of observables of the Gaussian unitary ensemble, and there are many tools provided by RMT available to tackle several questions that might be complicated in the framework of many-body quantum systems.

One of the most fundamental of these questions is the problem of fluctuations of cold fermions. After the achievement of cooling trapped fermions to the point where Fermi statistics becomes dominant [95], experiments were able to explore this remarkable property of Fermi gases [116, 60, 16]. Non-interacting fermions exhibit non-trivial quantum effects, arising from Pauli exclusion principle, and even one-dimensional fermion exhibit complicated behavior emerging from the strong correlation brought by the Pauli repulsion. While confined bosons may collapse to the lowest level of the trap, low temperature fermions experience an effective repulsion of quantum nature, regardless of their original interaction. This induces a Fermi motion, a forced, which is a purely quantum phenomenon from the repulsion of the Pauli principle and is the main factor for the diluteness, suppressing the role of individual interactions among the fermions, which can be, in many cases, neglected or treated as a small perturbation. These properties are in reach of current experiments in one-dimensional cold fermions, and much progress has been done in this area in the last decade [80, 130, 114]. This turns the ideal Fermi gas into the first natural step to discuss the properties of Fermi gases.

We will explore this phenomenon by analyzing the number statistics of trapped fermions. This means counting the number $N_{\mathcal{I}}$ of fermions inside an interval and study how this number evolves as the interval grows in size. For the ideal bosonic case at zero temperature, all particles are concentrated on the ground state, centered at the minimum of the trap. They are uncorrelated and their number statistics can be easily determined. The fermionic case, due to the role of Fermi motion and quantum repulsion, leads to the natural and more complicated question of how many fermions $N_{\mathcal{I}}$ fall inside the interval $\mathcal{I}$.

Surprisingly, the observable $N_{\mathcal{I}}$ has a rich and highly non-trivial dependence on the interval size. Consider one of the simplest possible cases, the harmonically trapped one dimensional ideal gas of fermions at zero temperature, and we consider the symmetric interval $\mathcal{I} = [-L, L]$. It is known [137, 28] that the average density of harmonically trapped fermions, for a large number $N$ of particles, has a leading behavior given by Wigner's semicircle law (see figure 2.3 and section 4.2). The quantity $\mathrm{Var}(N_{\mathcal{I}})$, which represents the stiffness of the subsystem, grows logarithmically with $L$ when the interval is small, but presents a sharp drop [137, 31, 8, 46] near the semicircle edge $L \sim \sqrt{2N}$. The

reasons of the drop are clear: if $L$ is much larger than the semicircle edge, all eigenvalues will lie inside the interval and fluctuations are exponentially rare, hence the variance is effectively zero.

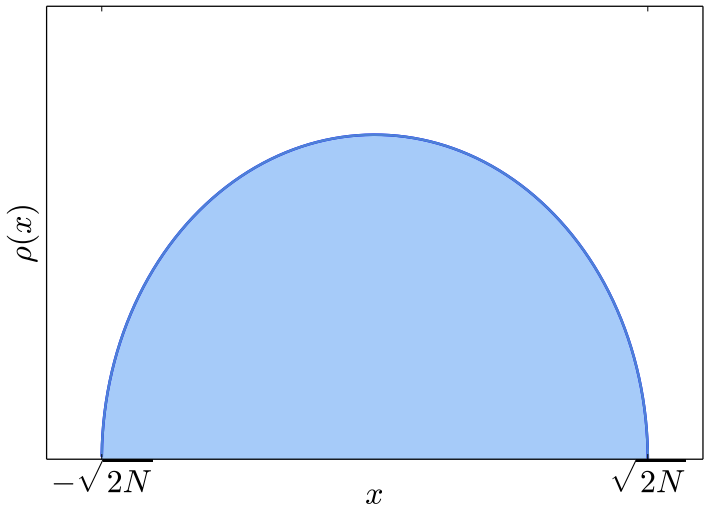


**Figure 2.3** — Wigner's semicircle law, given by equation (3.22), which is the leading behavior of the average density of harmonically trapped cold fermions.

This striking behavior of the fluctuations of cold fermions when system size increases is a purely quantum phenomenon, dictated by Pauli exclusion principle, and represents an interesting way to probe the effects of fluctuations in many-body systems. Number variance has been studied for several lattice models of fermions [48, 47] and, recently, it was shown that the entanglement entropy in the ground state of a confined Fermi gas is exactly proportional to its number variance when fluctuations are Gaussian around its mean [28].

This problem will be explored in chapter 7, where I present the correspondence between Gaussian random matrix eigenvalues and confined cold fermions. The observable $N_{\mathcal{I}}$, the number of fermions inside an interval, translates into counting Gaussian eigenvalues inside an interval, and we dispose of many tools to deal with this problem. In other words, we translate a cold atoms problem into a random matrix problem, to again write it as an electrostatic problem and solve it using classical statistical mechanics tools.

## 2.3 Thesis overview

While centered around its applications in cold fermions, this thesis treats the counting problem more generally. In a nutshell, the main question this work approaches is: given a random matrix with real eigenvalues, what is the chance of finding $k$ eigenvalues between $a$ and $b$? This counting problem is at the center of many applications of RMT, and it has motivated most of the work presented in this thesis. For confined fermions, it

represents the full counting statistics of a general interval, including intervals whose size is comparable to the system size. Most of the previous work about counting eigenvalues has approached this question in localized regimes, either confining the interval to a very narrow strip of the spectrum or considering interval ranging from one point to infinity. Results for a general interval $[a, b]$ were almost inexistent, and they represent the core of this work.

I begin by recalling a large number of classical results and techniques in random matrix theory (chapters 3 to 5). A general presentation of RMT is given in chapter 3, where I introduce Dyson's threefold way. Rotationally invariant random matrices are discussed in detail, and I present classical results, such as that their eigenvalues j.p.d.f. share a similar structure, and I introduce three classical random matrix ensembles that we will explore in detail in their work: Gaussian, Wishart and Cauchy ensembles.

Following this introducing chapter, I present in chapter 4 two techniques to analyze random matrix problems, namely orthogonal polynomials theory and the Coulomb gas method. Orthogonal polynomials are a powerful algebraic tool to deal with determinantal point processes, a class of random process that includes the eigenvalues of a large class of matrices. Although very powerful, it is not evident how to derive the behavior for large $N$ systems from orthogonal polynomials. To this end, I introduce the Coulomb gas method. These techniques will be used in conjunction to obtain results in different regions of the spectrum, which together with their scaling are discussed in section 4.4.

I also must recall some classical results in counting statistics of eigenvalues, and I do so in chapter 5. I compare the counting problem for independent variables with the case of Gaussian eigenvalues, and present the classical result of Dyson and Mehta for the number variance of small intervals, as well as the number variance for the edge of the average density. The number variance is the variance of the number of eigenvalues inside an interval. I also introduce important definitions, such as the moment generating function, the overlap matrix and the Fredholm determinant, and I exemplify the use of these objects in the classical derivation of the Tracy-Widom distribution.

During my PhD, I explored the question of the *index distribution*, the statistics of the number of positive eigenvalues in a random matrix. Previous results were available for the Gaussian and Wishart ensembles, I obtained the full probability density function of this variable for the Cauchy ensemble and was able to derive its number variance for typical fluctuations [96]. These results are reviewed in chapter 6, where I also present calculations for a simpler case, the Gaussian ensemble, whose index statistics was obtained in [89, 90]. The Cauchy ensemble presents a fundamental difference with respect to the Gaussian ensemble. While the latter presents a compact support for its average density of eigenvalues, seen above in figure 2.3, the average density for the Cauchy eigenvalues is supported on the whole real line. This difference changes the behavior of the variance of the index, and represents a fascinating comparison with previously known results for other ensembles.

These results required deeper investigation, and I was naturally led to consider the case of the symmetrical interval $[-L, L]$. Increasing the value of $L$ implies a transition from small to large intervals, exploring the mesoscopic scale, when intervals are of the

order of the system size. This regime was rarely explored in the literature, and is of great importance in the context of cold fermions. By calculating the full counting statistics of eigenvalues for intervals whose size is comparable to the whole system, I was able to determine the full p.d.f. of the number of Gaussian eigenvalues inside an interval $[-L, L]$ and, in particular, to obtain its variance for typical fluctuations around the mean [97]. This variance is connected to the calculation of the entanglement entropy of trapped cold fermions [46, 28], and the calculation of the full probability of this number statistics is described in chapter 7.

The method used to obtain the previous results, the Coulomb gas method, can be greatly generalized. This is done is chapter 8, where I apply the same calculation to Wishart and Cauchy ensembles. Each ensemble presents particularities that justify its study, and the comparison between results in three ensembles, Gaussian Wishart and Cauchy, reveals many general properties of number statistics in eigenvalues of random matrices.

Finally, I mention one more interesting application of random matrix theory in chapter 9, in the context of quantum transport of electrons. This model requires a different ensemble, the Jacobi ensemble, and statistics of the transmission and reflection eigenvalues of the scattering problem in quantum chaotic cavities are well known for the case of an ideal coupling between the cavity and its leads. The presence of a non ideal coupling, or impurities, changes the statistical behavior of these transmission eigenvalues. During my PhD I was able to show that the presence of impurities in the transmission channels can be calculated by expanding the j.p.d.f. of transmission eigenvalues into Schur polynomials. This allows us to write moments calculated in the model with impurities in terms of moments of the ideal case, which are well known. Conclusions and perspectives are left to chapter 10, where I detail this overview with results and a substantial number of questions that emerged from this work.

# — 3 —
# Invariant random matrix ensembles

*— What is jazz, Mr. Armstrong?*
*— My dear lady, as long as you have to ask this question, you will never understand it.*

## 3.1 Classification of random matrices

### 3.1.1 Invariant and independent matrices

A matrix whose entries are random variables is a random matrix. This very general definition covers a large number of mathematical objects, and we shall restrict our study to a more specific type: $N \times N$ random matrices with real spectrum. This category contains three cases:

- Real symmetric matrices $X = X^t$, which are defined by $\frac{N(N+1)}{2}$ real random variables and are diagonalizable by an orthogonal matrix $O$, which is a real matrix such that: $OO^t = O^tO = \mathbb{1}$.
- Complex Hermitian matrices $H = H^\dagger$, which are defined by $N^2$ real random variables and are diagonalizable by a unitary matrix $U$, which is a complex matrix such that: $UU^\dagger = U^\dagger U = \mathbb{1}$.
- Quaternionic self-dual matrices $Q = Q^\star$, which are defined by $2N^2 - N$ real random variables and are diagonalizable by a symplectic matrix $S$, which is a quarternionic matrix such that $SS^\star = S^\star S = \mathbb{1}$.

As mentioned in the introduction, one of the most important aspects of a random matrix ensemble is its symmetry class. When deciding for a random matrix model to a Hamiltonian with no particular symmetries, its description should be given by a complex Hermitian random matrix. If the system is invariant under time reversal, there are two possibilities: if the system has odd-spin, it is described by a quaternionic self-dual matrix; if it has even spin, it is described by a real symmetric matrix. These three options, called *Dyson's threefold way* [44], are a cornerstone in random matrix theory and represent the

classical general classification of random matrices. It is worth mentioning that generalizations of Dyson's threefold way have been an important subject of study, and other symmetry classes are obtained by replacing the Hilbert space by the structure of a Fock space [153, 64]. The threefold way is described in more detail in the next section.

Among these three cases, two classes of random matrices are usually considered: matrices with independent entries and invariant matrices.

- A random matrix whose entries are independent random variables. In the case of real matrices, their probability density can be written as

$$P(X) = \prod_{i \leq j} p_{ij}(x_{ij}). \tag{3.1}$$

  This class of matrices is known as Wigner matrices [149].

- A random matrix $X$ is said to be invariant (or rotationally invariant) when another matrix $X'$ obtained by a similarity transformation by an orthogonal, unitary or symplectic matrix has the same probability.

$$P(X) = P(X') \qquad \text{if} \quad X' = U^\dagger X U, \tag{3.2}$$

  and $U$ is an orthogonal matrix if $X$ is real symmetric, unitary if $X$ is complex Hermitian and symplectic if $X$ is quaternionic self-dual.

Random matrices with independent entries are a vast field of research whose applications are ubiquitous, but there are very few tools available to analyze spectral properties of this class of random matrices. There are few results for these ensembles of matrices, universal properties are rare and results for finite-$N$ are virtually non-existent.

We note that condition (3.2), the invariance of the probability density of a matrix, implies that the probability is rotationally invariant. In other words, given two matrices connected by a similarity transformation $H' = UHU^\dagger$, where $U$ is orthogonal, unitary or symplectic, then the probability of both matrices is the same, which means

$$P(H')\mathrm{d}H' = P(H)\mathrm{d}H. \tag{3.3}$$

Condition (3.2) only imposes that the densities should be the same, but the probabilities coincide because the flat measure $\mathrm{d}H$ is invariant under orthogonal (or unitary, or symplectic) transformations. This invariance $\mathrm{d}H = \mathrm{d}H'$ is not a trivial result. When a measure is invariant under the action of a group, it is called the Haar measure associated with this group. In this case, the flat measure is the Haar measure of $\mathbb{R}^N$ under the action of the orthogonal group.

### 3.1.2 The j.p.d.f. of eigenvalues

As mentioned before, one of the main questions in random matrix theory is: given a random matrix ensemble, what can be said about its eigenvalues? The rotational invariance

property is very valuable to explore this question, as it allows us to derive a the j.p.d.f. of the eigenvalues of the ensemble.

Using the fact that the probability is invariant under a unitary transformation (in the complex case), we can change the coordinates of the probability to obtain the statistics of its eigenvalues. The main goal of this section is to derive the j.p.d.f. of the eigenvalues of invariant random matrices with real spectrum. One way to do it is start from the probability of the matrix $P(X)\mathrm{d}X$ and change coordinates to write the probability as a function of eigenvalues and eigenvectors. This means $\{x_{ij}\} \to (U, \Lambda)$, where $U = \{U_{ij}\}$ is the orthogonal, unitary or symplectic matrix that diagonalizes $X$ and $\Lambda = \{\lambda_i\}$ are its eigenvalues.

The rotationally invariant property (3.2) restricts $P(X)$ to depend only on traces of the powers of $X$, since they are the invariants of the matrix. Indeed, all invariants of $X$ under a non-singular similarity transformation $H \to H' = AHA^{-1}$ can be written in terms of traces of the first $N$ powers of $X$ [100, 145]. Using this fact, we write

$$P(X)\mathrm{d}X = P(\{\mathrm{Tr}X^n\}_{1\leq n\leq N})\mathrm{d}X = P\left(\sum_i \lambda_i, \sum_i \lambda_i^2, \ldots, \sum_i \lambda_i^N\right) J[U,\Lambda] \prod_i \mathrm{d}\lambda_i \mathrm{d}\mu(U). \tag{3.4}$$

To obtain the j.p.d.f. of eigenvalues, we need the Jacobian $J[U, \Lambda]$ of the transformation $\{x_{ij}\} \to (U, \Lambda)$. This Jacobian turns out to be a power of the Vandermonde determinant of the eigenvalues

$$\mathrm{d}X = \prod_{i<j} |\lambda_i - \lambda_j|^\beta \prod_{i=1}^N \mathrm{d}\lambda_i \mathrm{d}\mu(U), \tag{3.5}$$

where $\mathrm{d}\mu(U)$ is the Haar measure of the orthogonal, unitary or symplectic group under its own action. This exponent $\beta$ is a defining feature of the ensemble and takes only three possible values. We denote it $\beta$, and $\beta = 1, 2, 4$ represents its symmetry class, as prescribed by Dyson's threefold way. We name the ensemble according to its invariance group, and we attribute its correspondent value of $\beta$. An ensemble of real symmetric random matrices takes $\beta = 1$ and its probability is invariant under transformations by an orthogonal matrix, it is hence called an orthogonal ensemble. For complex Hermitian random matrices, we find $\beta = 2$ and we denote them unitary ensembles. Self-dual quaternionic matrices take $\beta = 4$ and are known as symplectic ensemble.

One particularly interesting case of invariant random ensemble are matrices whose j.p.d.f. is given by

$$P(X) \propto e^{-\beta \mathrm{Tr}V(X)}, \tag{3.6}$$

where $V$ is an analytic function. These ensembles, by the cyclicity of the trace, are rotationally invariant. Using the results provided above, we can immediately write the j.p.d.f. of their eigenvalues

$$P(\lambda_1, \ldots, \lambda_N) \propto e^{-\beta \sum_{i=1}^N V(\lambda_i)} \prod_{i<j} |\lambda_i - \lambda_j|^\beta \mathrm{d}\lambda_i, \tag{3.7}$$

where we note that, given the fact that neither the probability nor the Jacobian depend on the eigenvectors, we can integrate them out and obtain the full j.p.d.f. of the eigenvalues. We consider in this thesis the ensembles whose probability that can be written like

equation (3.6), and they will differ only on the function $V(\lambda)$. This function is named the *potential* of the ensemble, and the reason for this naming convention will become clear when the Coulomb gas analogy is presented (section 4.1).

The Jacobian of the transformation $\{x_{ij}\} \to (U, \Lambda)$ is highly non-trivial, and we present a demonstration of the $\beta = 2$ case that follows closely the introduction [58]. In this case, there is an interesting geometrical derivation that can be performed to obtain the coordinate substitution and its associated Jacobian.

### 3.1.3 The invariant integration measure

The length element of the flat measure $\mathrm{d}s$, which is invariant by unitary transformations, is given by the trace $(\mathrm{d}s)^2 = \mathrm{Tr}\,(\mathrm{d}M\mathrm{d}M^\star)$. This metric yields the integration measure we need to define the probability space of our matrix ensemble. When the length element is given by $(\mathrm{d}s)^2 = \sum_{i,j}^N g_{ij}\mathrm{d}q_i\mathrm{d}q_j$, the integration measure can be calculated as

$$\mathrm{d}\mu = \sqrt{|\det(g_{ij})|}\mathrm{d}q_{11}\ldots\mathrm{d}q_{NN}. \tag{3.8}$$

As an example, let us take the space of $N \times N$ Hermitian matrices $H = \{z_{ij}\} = \{x_{ij} + iy_{ij}\}$. The imposition $x_{ij} = x_{ji}$, $y_{ij} = -y_{ji}$ yields the following expression for the length element

$$(\mathrm{d}s)^2 = \mathrm{Tr}(\mathrm{d}H\mathrm{d}H^\dagger) = \sum_i (\mathrm{d}x_{ii})^2 + 2\sum_{i<j}\left[(\mathrm{d}x_{ij})^2 + (\mathrm{d}y_{ij})^2\right], \tag{3.9}$$

from which we may extract the integration measure

$$\mathrm{d}\mu(H) = 2^{\frac{N(N-1)}{2}} \prod_i \mathrm{d}x_{ii} \prod_{i<j} \mathrm{d}x_{ij}\mathrm{d}y_{ij}. \tag{3.10}$$

While writing the integration measure as a function of the differential of the entries is straightforward, it is not very practical when exploring statistical properties of the spectrum. Let us change coordinates to best suit our needs. The spectral theorem states that the $N \times N$ Hermitian matrix $H = \{x_{ij}\}$ is diagonalizable by a unitary matrix $U$ and has $N$ real eigenvalues $\Lambda = \mathrm{diag}(\{\lambda_i\})$. We seek to change coordinates $\{x_{ij}\} \to (U, \Lambda)$ and evaluate the integration measure in these new coordinates[1]. Using the unitary property, we write $\mathrm{d}(U^\dagger U) = \mathrm{d}U^\dagger U + U^\dagger \mathrm{d}U = 0$. Noting $\delta U = U^\dagger \mathrm{d}U$, we see that the unitary condition implies the anti-Hermicity condition $\delta U^\dagger = -\delta U$. Since $H = U\Lambda U^\dagger$, we find

$$\mathrm{d}H = U\left[\mathrm{d}\Lambda + \delta U\Lambda - \Lambda\delta U\right]U^\dagger, \tag{3.11}$$

from which we can calculate the length element $(\mathrm{d}s)^2 = \mathrm{Tr}(\mathrm{d}H\mathrm{d}H^\dagger)$

$$(\mathrm{d}s)^2 = \mathrm{Tr}\left[(\mathrm{d}\Lambda)^2 + 2\mathrm{d}\Lambda(\delta U\Lambda - \Lambda\delta U) + (\delta U\Lambda)^2 + (\Lambda\delta U)^2 - 2\delta U\Lambda^2\delta U\right]. \tag{3.12}$$

[1] This correspondence is not unique, but this can be solved by considering the coset $U(N)/U(1)^N$. This detail is not important for the following, as we will see.

Because $\Lambda$ is diagonal and the diagonal elements of the commutator $\delta U\Lambda - \Lambda\delta U$ are zero, we find $2\mathrm{Tr}\left[\mathrm{d}\Lambda(\delta U\Lambda - \Lambda\delta U)\right] = 0$. We may add up the remaining terms using the cyclicity of the trace. The third, forth and fifth elements of (3.12) added up yield

$$2\mathrm{Tr}\left[\delta U\delta U\Lambda - \delta U^2\Lambda^2\right] = 2\sum_{i,j}\left[\delta U_{ij}\lambda_j\delta U_{ji}\lambda_i - \lambda_i^2\delta U_{ij}\delta U_{ji}\right] = -\sum_{i,j}(\lambda_i-\lambda_j)^2\delta U_{ji}\delta U_{ij}. \tag{3.13}$$

We write the length element using this result

$$(\mathrm{d}s)^2 = \sum_i \mathrm{d}\lambda_i^2 + \sum_{i<j}(\lambda_i-\lambda_j)^2\delta\bar{U}_{ij}\delta U_{ij}. \tag{3.14}$$

From (3.14), we calculate the integration measure using eigenvalues and eigenvectors as coordinates

$$\mathrm{d}\mu(H) = \prod_{i<j}(\lambda_i-\lambda_j)^2\prod_i \mathrm{d}\lambda_i\mathrm{d}\mu(U), \tag{3.15}$$

where $\mathrm{d}\mathcal{M}(U)$ is the part of the measure that depends exclusively on the $U$ variables. Analyzing it carefully, this measure turns out to be, up to a constant factor, the Haar measure of the unitary group under its own action. This measure is obtained by repeating the previous procedure using the length element $(\mathrm{d}s)^2 = \mathrm{Tr}(\mathrm{d}U\mathrm{d}U^\dagger)$ with $U$ a unitary matrix and extracting the integration measure associated to it.

The integration measure (3.15) depends only on the fact that $H$ is Hermitian. The Jacobian of the transformation $\{x_{ij}\} \to (U,\Lambda)$ is $\prod_{i<j}(\lambda_i-\lambda_j)^2$, which is the Vandermonde determinant of the eigenvalues. This term will strongly couple all eigenvalues and will be present in all j.p.d.f. of eigenvalues we will encounter during this work. It is the source of many interesting phenomena we will observe, and plays a role in creating a "repulsive" interaction among the eigenvalues.

## 3.2 Examples of $\beta$-ensembles

As discussed in section 3.1.3, we are interested in ensembles whose j.p.d.f. of eigenvalues can be written as (3.7). The statistical properties of the spectrum of an ensemble will be then defined by the potential $V(\lambda)$, and, in the following, we will describe three classical examples of invariant ensembles and obtain the potential for each case.

### 3.2.1 Gaussian ensemble

The Gaussian ensemble is composed of square self-adjoint matrices $X$ whose probability density function is given by $P(X) = e^{-\mathrm{Tr}Q(X)}$, and $Q(x) = ax^2 + bx + c$. Without loss of generality, we will make a wise choice of normalization and origin to write a more compact version of the probability:

$$P(X) \propto e^{-\frac{\beta}{2}\mathrm{Tr}X^2}, \tag{3.16}$$

where $\beta$ is the Dyson index of the ensemble.

To obtain the j.p.d.f. for the eigenvalues, we follow the recipe provided in section 3.1.3 to obtain

$$P(\boldsymbol{\lambda}) = \frac{1}{Z_{N,\beta}} e^{-\frac{\beta}{2}\sum_{i=1}^{N}\lambda_i^2} \prod_{i<j} |\lambda_i - \lambda_j|^\beta. \tag{3.17}$$

Naturally, we identify the potential of the Gaussian ensemble $V(x) = x^2/2$.

This ensemble has so many applications that it is hard to overstate its importance. One of the reasons of its omnipresence in physics and mathematics is inherited from the Gaussian distribution. Suppose we are trying to find a matrix "as random as it can be". In other words, we want to find the ensemble that maximizes the Shannon entropy given its constraints. Most applications require the average of the trace of the matrix to be finite, as well as the average of the trace of its square, so we restrict our study to distribution with thin tails. Given those constraints, we want to maximize the functional

$$I[P(H)] = -\int \mathrm{d}\mu(H) P(H) \left[\log P(H) - \xi_1 \mathrm{Tr} H - \xi_2 \mathrm{Tr} H^2\right]. \tag{3.18}$$

Differentiating it functionally wields

$$\frac{\delta I}{\delta P} = 1 + \log P(H) - \xi_1 \mathrm{Tr} H - \xi_2 \mathrm{Tr} H^2 = 0, \tag{3.19}$$

whose solution is

$$P(H) = \frac{1}{Z_N} e^{-\xi_1 \mathrm{Tr} H - \xi_2 \mathrm{Tr} H^2}. \tag{3.20}$$

The Gaussian ensemble is, therefore, the ideal candidate to model a random system whose averages of the trace of first and second powers are fixed. This ensemble is also relevant as a fixed point in renormalization group techniques introduced in [21]. This means that the correlation between eigenvalues of a large class of random matrices, properly scaled, is equivalent to Gaussian statistics [20].

For Wigner matrices, we mention briefly that some results equivalent to a central limit theorem for random matrices are available [88, 125, 49, 10].

Gaussian ensembles are named after their symmetry group associated.

- Real symmetric Gaussian matrices are described by a probability that is invariant under similarity transformations by orthogonal matrices, they compose the **Gaussian Orthogonal Ensemble (GOE)** and the j.p.d.f. of their eigenvalues is given by (3.17) with $\beta = 1$.

- Complex Hermitian Gaussian matrices are described by a probability that is invariant under similarity transformations by unitary matrices and are named the **Gaussian Unitary Ensemble (GUE)**, their eigenvalues are distributed according to equation (3.17) with $\beta = 2$.

- Quaternionic self-dual Gaussian matrices are described by a probability that is invariant under similarity transformations by symplectic matrices and are named the **Gaussian Symplectic Ensemble (GSE)**, their eigenvalues are distributed according to equation (3.17) with $\beta = 4$.

Gaussian random ensembles occupy a unique position among random matrix ensembles. When we described two classes of random matrix, those with independent entries and those whose probability is rotationally invariant, we did not explore the possibility of imposing these two conditions simultaneously. It turns out that these conditions are extremely restrictive, and only one ensemble, the Gaussian ensemble, is able to fulfill them both. This result is a theorem due to Porter and Rosenzweig [119], and is represented in figure 3.1.

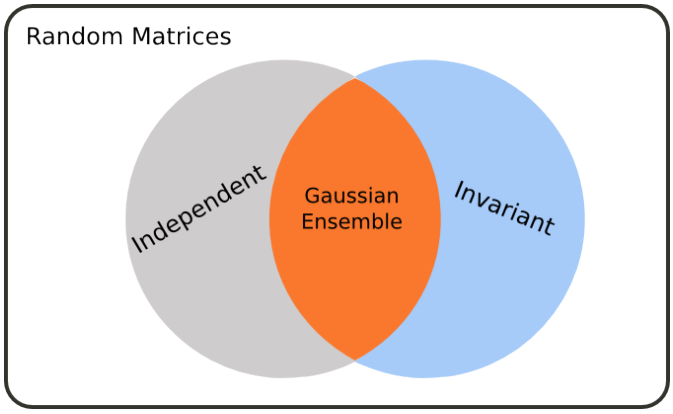


**Figure 3.1** — Diagram representing Porter-Rosenzweig theorem.

One fundamental quantity of a random matrix ensemble is the average distribution of eigenvalues $\rho(\lambda)$. To obtain it, we integrate the j.p.d.f. of the eigenvalues in all variables but one.

$$\rho_N(\lambda) = \int \cdots \int \mathrm{d}\lambda_2 \ldots \mathrm{d}\lambda_N P(\lambda, \lambda_2, \ldots, \lambda_N). \tag{3.21}$$

Although the eigenvalues are strongly all-in-all correlated, the average density of eigenvalues for the Gaussian ensemble has a surprisingly simple limit when $N$ is large. This result was first obtained by Wigner for a specific class of matrices, arising from quantum mechanical investigations [147], and then generalized to a much larger class [149], which includes the Gaussian Orthogonal ensemble.

The average density of eigenvalues for the Gaussian ensemble when $N$ is large is given by

$$\rho_N(\lambda) \xrightarrow{\text{large } N} \frac{1}{\sqrt{N}} \rho_{sc}\left(\frac{\lambda}{\sqrt{N}}\right), \qquad \rho_{sc}(x) = \frac{1}{\pi}\sqrt{2 - x^2}, \tag{3.22}$$

where $\rho_{sc}(x)$ is named Wigner's semicircle law and is represented in figure 3.2a. Wigner was able to determine the average distribution of eigenvalues of the Gaussian ensemble using results due to Wishart found, according to Wigner, by accident in a statistics book by S. S. Wilks [151].

Equation (3.22) clearly reveals the scaling of the eigenvalues of a Gaussian random matrix with $\sqrt{N}$. It is convenient to rescale the eigenvalues by $\sqrt{N}$ to make the average density independent of the size of the matrix.

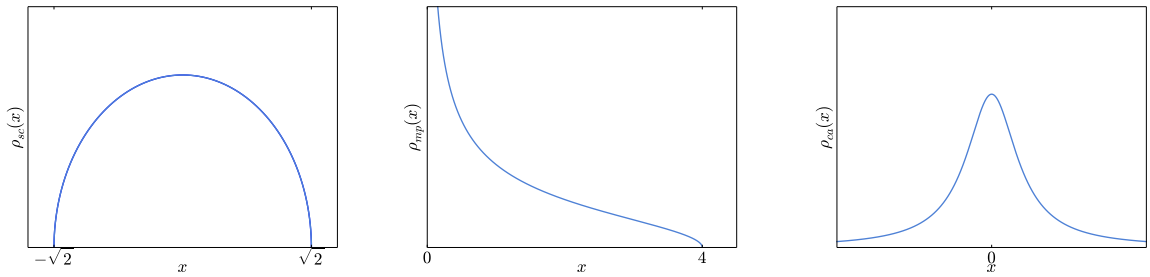


**(a)** **(b)** **(c)**

**Figure 3.2** — (a) Semicircle law, (b) Marčenko Pastur law, (c) Cauchy distribution.

### 3.2.2 Wishart ensemble

Let $X$ be a $M \times N$ matrix whose entries are Gaussian i.i.d. random variables (real, complex or quaternions). We define a Wishart matrix $W$ as the $N \times N$ covariance matrix $W = X^\dagger X$ of the Gaussian data matrix $X$. This ensemble is also know as the Laguerre ensemble, due to the class of orthogonal polynomials associated to it. Wishart matrices are positive semi-definite and symmetric. This ensemble has been introduced by Wishart in 1928 [152] and extensively studied by statisticians [66, 53] long before the official birth of RMT in physics.

The importance of this ensemble is clear. Covariance matrices are ubiquitous is statistical analysis, and the Wishart ensemble represents the set of covariance matrices emerging from random normally-distributed data.

The j.p.d.f. of its eigenvalues is given by [72]

$$P(\boldsymbol{\lambda}) = \frac{1}{Z_N} e^{-\frac{\beta}{2}\sum_{i=1}^{N} x} \prod_{i=1}^{N} \lambda_i^{\beta\alpha} \prod_{j<k} |\lambda_k - \lambda_j|^\beta, \tag{3.23}$$

where the constant $\alpha$ is given by $\alpha = \beta(1 + M - N)/2 - 1/\beta$. We identify the potential $V(x) = \frac{x}{2} - \alpha \ln x$. When $N$ is large and $N/M$ is kept fixed, the logarithm term of the potential becomes sub-dominant with respect to the linear term and may be neglected.

The average spectral density in the large-$N, M$ limit (with $N/M = c \leq 1$ fixed) for Wishart matrices was obtained by Marčenko and Pastur [98] (see Fig. 3.2b for the $N = M$ case) and given by

$$\rho_N(\lambda) \to \frac{1}{N}\rho_{mp}\left(\frac{\lambda}{N}\right) \qquad \rho_{mp}(x) = \frac{1}{2\pi x}\sqrt{(x - x_-)(x_+ - x)}, \tag{3.24}$$

where $x_\pm = (1 \pm 1/\sqrt{c})^2$. In this thesis, for simplicity, we will only deal with the symmetrical case of Wishart ($c = 1$), although a general treatment is certainly possible.

We note that Wishart eigenvalues scale as $N$, and its maximum eigenvalue has an average position $N(1+1/\sqrt{c})^2$. The eigenvalues of the correlation matrix are fundamental to a technique named *Principal Component Analysis* (PCA). This technique consists in

reducing the dimension of a sample size while keeping intact the information it contains. Let $\boldsymbol{X} = \{X_i\}_{1\leq i\leq N}$ be a random variable of dimension $N$ that we sample $M$ times. We obtain the empirical data matrix whose row $j$ is the $j$-th realization of variable $\boldsymbol{X}$

$$A = \begin{pmatrix} X_{11} & \cdots & X_{1N} \\ \vdots & \ddots & \vdots \\ X_{M1} & \cdots & X_{MN} \end{pmatrix}. \tag{3.25}$$

We define $W = A^T A$ the covariance matrix. It is a fact that the direction of the eigenvector associated with the largest eigenvalue yields the direction of largest fluctuation of the sample $A$, we call this a *principal direction*. If the smallest eigenvalue is negligible with respect to the largest, this means that fluctuations of data on the direction of the eigenvector associated to the smallest eigenvalue are negligible with respect to fluctuations on the direction of the eigenvector associated to the largest eigenvalue. Without entering in the details of the technique [107], we may say that projecting the data in the $P$ principal directions is the optimal way to reduce the dimension from $N$ to $P$ while preserving most of the information, which in this case is given by the correlations. Wishart matrices are a very natural "null" model for covariance matrices, as they represent the covariance of uncorrelated, Gaussian distributed data, which is noise. This comparison is fundamental to create a good criterion of selection of directions to neglect and directions to keep in the PCA technique.

### 3.2.3 Cauchy ensemble

We consider $N \times N$ matrices which might be symmetric ($\beta = 1$), Hermitian ($\beta = 2$) or self-dual ($\beta = 4$) drawn from the distribution

$$P(\mathbf{H}) \propto \left[\det\left(\mathbb{1}_N + \mathbf{H}^2\right)\right]^{-\beta(N-1)/2-1}, \tag{3.26}$$

where $\mathbb{1}_N$ is the identity matrix $N \times N$.

Originally devised as a suitable replacement for the Gaussian ensemble in the context of quantum transport [22], the Cauchy ensemble has also found use in the context of free probability [23, 24, 59]. This probability can also be written in the form (3.6), and we can find its eigenvalues j.p.d.f. using the procedure described above:

$$P(\lambda_1, \cdots, \lambda_N) = \frac{1}{Z_N} \prod_{j=1}^{N} \frac{1}{(1+\lambda_j^2)^{\beta(N-1)/2+1}} \prod_{i<k} |\lambda_i - \lambda_k|^\beta . \tag{3.27}$$

The Cauchy ensemble is also one of the few exactly solvable ensembles whose average spectral density has fat tails extending over the full real axis, and given by (see Fig. 3.2c)

$$\rho_N(\lambda) = \frac{1}{\pi} \frac{1}{1+\lambda^2}. \tag{3.28}$$

Remarkably, the average density does *not* depend on $N$ (it is the same for any $N$).

The main feature that lead us to consider this ensemble is the fat tail in the average density. Many features of the number statistics change drastically once an "edge" is reached, once the considered interval for counting eigenvalues crosses the edge of the average density if this density has a compact support. In the absence of a compact support, we expect to obtain a different behavior, and we were able to compare it with results in the other ensembles. Wigner matrices whose probability have fat tails were studied by [15] and the Cauchy ensemble represents an interesting equivalent in the invariant domain.

# — 4 —
# Two complementary methods

*Two roads diverged in a yellow wood,*
*And sorry I could not travel both*
*And be one traveler, long I stood*
*And looked down one as far as I could*
*To where it bent in the undergrowth;*

Robert Frost

## 4.1 The Coulomb gas method

In the following, we will describe the main method applied to solve the problems treated in this thesis. This procedure is called the Coulomb-gas method. It was introduced by Dyson and Mehta on the founding papers of the subject [43, 45], and has since found numerous applications, such as the study principal component analysis in random sets of data [94], the evaluation of resistance, conductance and shot noise power in chaotic mesoscopic cavities [61, 140, 142], the study of mutual information and data transmission in multiple input multiple output (MIMO) channels [78], bipartite entanglement of quantum systems [28, 51, 108, 109], on the top eigenvalue of Gaussian and Wishart matrices [91, 37] and many others.

We will explore this method in a very general framework. All the ensembles presented above share the same form (equation (3.7)) for the j.p.d.f. of their eigenvalues, so the method applies for any sufficiently confining potential $V(x)$. .

### 4.1.1 Physical interpretation, density and scaling

#### Probability as a Boltzmann weight

We take a random matrix ensemble whose eigenvalue j.p.d.f. is given by

$$P(\boldsymbol{x}) = \frac{1}{Z_{N,\beta}} e^{-\beta N \sum_{i=1}^{N} V(x_i)} \prod_{j<k} |x_k - x_j|^{\beta}. \tag{4.1}$$

We can rewrite this probability by inserting the Vandermonde determinant into the exponential

$$P(\boldsymbol{x}) = \frac{1}{Z_{N,\beta}} e^{-\beta N \sum_{i=1}^{N} V(x_i) + \beta \sum_{k<j} \log|x_k - x_j|}. \tag{4.2}$$

Note that we rescaled the potential $V(x)$ by a factor $N$. This is a more convenient scaling, because the potential term and the logarithmic term will be comparable, both will be of order $N^2$. This yields eigenvalues $\{x_i\}$ of the order of unity, which are more convenient to work with. In the case of the Gaussian ensemble, this is equivalent to scaling the eigenvalues by a factor: $x_i = \lambda_i/\sqrt{N}$, where $\lambda_i$ are the eigenvalues of a matrix whose probability is given by $P(X) \propto e^{-\frac{\beta}{2}\mathrm{Tr}X^2}$. We can find many different choices of scaling in the random matrix literature, and we choose the one described by equation (4.1). It yields eigenvalues of the order of unity and average distribution of eigenvalues that are independent of both $N$ and $\beta$.

Probability (4.2) can be interpreted as the Boltzmann weight of an associated electrostatic system. Take $N$ charges in a 2-dimensional gas confined to a line and submitted to a potential $N.V(x)$. The 2-d electrostatic repulsion is logarithmic, and the probability of finding the charges at positions $\boldsymbol{x} = (x_1, \ldots, x_N)$ will be given by

$$P(\boldsymbol{x}) = \frac{1}{Z_{N,\beta}} e^{-\beta E[\boldsymbol{x}]} \qquad E[\boldsymbol{x}] = N \sum_{i=1}^{N} V(x_i) - \sum_{j<k} \log|x_j - x_k|. \tag{4.3}$$

Written like this, the statistics of eigenvalues in random matrix ensembles whose j.p.d.f. is written as (4.1) is equivalent to the Boltzmann weight of a physical system of charges placed in positions $\boldsymbol{x}$ whose energy is $E[\boldsymbol{x}]$ and $Z_{N,\beta}$ is the partition function of the system. This fundamental correspondence between charged particles and random eigenvalues allows us to import many techniques from statistical mechanics to treat this problem. A system described by the energy $E[\boldsymbol{x}]$ is called a Coulomb gas, or log-gas.

### Density of eigenvalues

We are interested in matrices of large size. In the language of statistical mechanics for the associated physical system, we study charges in the thermodynamical limit. A large number of eigenvalues will translate into a large number of charges, and, as it is customary in electrostatics, we may treat a large number of charges by defining a density of charges.

Let $\boldsymbol{x} = \{x_i\}_{1 \le i \le N}$ be the eigenvalues of a random matrix. We denote the *empirical density of eigenvalues* $\hat{\rho}(x)$ and the *average density of eigenvalues* $\rho(x)$ as

$$\hat{\rho}(x) = \frac{1}{N} \sum_{i=1}^{N} \delta(x_i - x) \qquad \rho(x) = \langle \hat{\rho}(x) \rangle = \frac{1}{N} \sum_{i=1}^{N} \langle \delta(x_i - x) \rangle . \tag{4.4}$$

$\hat{\rho}(x)$ is a distribution defined by random variables, effectively a "counting function" for the eigenvalues. $\rho(x)$ is a real function, the same function defined in (3.21). We also denote the two-point density

$$\hat{\rho}_2(x, x') = \frac{1}{N(N-1)} \sum_{i \neq j} \delta(x_i - x)\delta(x_j - x'). \tag{4.5}$$

One very important property of the empirical density is that it is a *self-averaging* function in the sense of distribution. This means that, for all test function $\phi(x)$ and a fixed domain $A$, we have

$$\lim_{N\to\infty} \int_A \phi(x)\hat{\rho}(x)\mathrm{d}x = \int_A \phi(x)\left\langle\hat{\rho}(x)\right\rangle \mathrm{d}x = \int_A \phi(x)\rho(x)\mathrm{d}x. \tag{4.6}$$

This limit is what we mean when writing that, in the large $N$ limit, we find $\hat{\rho} \sim \rho$. It is tempting to write $\lim_{N\to\infty} |\hat{\rho}(x) - \rho(x)| = 0, \forall x$, but not only this is mathematically inaccurate, it is also not true for all values of $x$. If the integration domain $A$ on equation (4.6) scales with $N$, the convergence is compromised. In particular, if $\rho(x)$ is a function whose support is compact and presents an edge, the convergence from $\hat{\rho}(x)$ to $\rho(x)$ is not uniform around the edge and the Coulomb gas method cannot be applied to evaluate quantities around the edge of the distribution. This fact will force us to resort to other techniques to evaluate this "edge regime", which is responsible for a rich transitional behavior for many quantities studies in this thesis. This self-averaging property is also true for the 2-point density function.

This convergence represents a macroscopic behavior for the charges and cannot incorporate fluctuations of the order of the microscopic level of the ensemble. This is one of the main limitations of the Coulomb gas method. Further in this chapter, we will introduce another method able to probe into the microscopic details of the ensemble.

### 4.1.2 From discrete to continuum

Our aim is to show how to relate the integral on the eigenvalues $\int \mathrm{d}x_1 \dots \mathrm{d}x_N$ to a functional integral on the average density. For this purpose, we use the self-averaging property of the density and the large $N$ limit to exchange the sums of random variables $x_i$ in $E[\boldsymbol{x}]$ in equation (4.3) into integrals of an average density $\rho(x)$. This passage is intuitive from the electrostatic point of view, we exchange a treatment dealing with a large number of point charges to a treatment of the charge density. I reproduce in the following the necessary steps of this exchange, following closely the accounts in [107, 38, 43]. Our steps are the following:

1. We first write the potential and the repulsive elements of the energy as integrals on the empirical densities.

2. We explore the large $N$ limit to exchange the empirical densities with average densities.

3. We write the integration measure as a functional integral with respect to $\rho$.

4. We complete by enforcing the normalization of $\rho$.

These steps are in the core of all the results of this thesis, and in this section I intend to present them with a sufficient level of detail. For a more mathematical treatment, we refer to [50].

### Empirical densities to average densities

Using the empirical density $\hat{\rho}(x)$, we can write a functional $\sum_i V(x_i)$ as an integral on the empirical density and apply the large $N$ limit to obtain it as an integral on the average density.

$$N\sum_{i=1}^{N} V(x_i) = N^2 \int \hat{\rho}(x)V(x)\mathrm{d}x \xrightarrow{\text{large } N} N^2 \int \rho(x)V(x)\mathrm{d}x. \tag{4.7}$$

The repulsion term should be expressed using the 2-point density

$$\sum_{i<j} \log|x_i - x_j| = \frac{1}{2}\sum_{i\neq j} \log|x_i - x_j| = \frac{N(N-1)}{2}\int \mathrm{d}x \int \mathrm{d}x' \hat{\rho}_2(x,x') \log|x - x'|. \tag{4.8}$$

We note that

$$\hat{\rho}_2(x,x') = \frac{N}{N-1}\hat{\rho}(x)\hat{\rho}(x') - \frac{1}{N-1}\hat{\rho}(x)\delta(x-x'), \tag{4.9}$$

where the last term is the self interaction. In the large $N$ limit, the product of empirical densities converges in the sense of distribution to the product of average densities. The self-interacting term can be dealt with considering the following argument by Dyson [43, 38]. In the large $N$ limit we may write

$$\int \mathrm{d}x \int \mathrm{d}x' \hat{\rho}(x)\delta(x-x') \log|x-x'| \sim \int \mathrm{d}x \rho(x) \log|l(x)|, \tag{4.10}$$

where $l(x)$ represents a position-dependent cutoff. Dyson's argument consists in taking the cutoff as the average distance between eigenvalues at the point $x$, which is simply the inverse of the average density $\rho(x)$. In the large $N$ limit, we may write the interaction term as

$$\sum_{i<j} \log|x_i - x_j| \xrightarrow{\text{large } N} \frac{N^2}{2}\iint \mathrm{d}x\mathrm{d}x' \rho(x)\rho(x') \log|x-x'| + \frac{N}{2}\int \rho(x)\log\rho(x)\mathrm{d}x. \tag{4.11}$$

And the energy can then be written as

$$\begin{aligned} E[\boldsymbol{x}] \xrightarrow{\text{large } N} & N^2 \int \rho(x)V(x)\mathrm{d}x \\ & - \frac{N^2}{2}\iint \mathrm{d}x\mathrm{d}x' \rho(x)\rho(x') \log|x-x'| \\ & - \frac{N}{2}\int \rho(x)\log\rho(x)\mathrm{d}x. \end{aligned} \tag{4.12}$$

### Calculating the integration measure

The final step to complete the transition from discrete to continuum is to determine the Jacobian of the transformation $\{x_i\} \to \rho(x)$. Physically, we expect this Jacobian to take into account the entropy associated with the transformation, since the points $\{x_i\}$ are ordered and distinguishable while the average density is a single variable real function.

We calculate the Jacobian

$$J[\rho] = C_N \int \prod_{i=1}^{N} \mathrm{d}x_i \delta \left[ N\rho(x) - \sum_{i=1}^{N} \delta(x - x_i) \right], \tag{4.13}$$

where $C_N$ is a constant. We write the delta function as a functional Fourier transform with parameter $g(x)$

$$J[\rho] = C'_N \int \prod_{i=1}^{N} \mathrm{d}x_i \mathcal{D}g \, e^{\int \mathrm{d}x g(x) \left[ N\rho(x) - \sum_{i=1}^{N} \delta(x - x_i) \right]}. \tag{4.14}$$

The integral on $x_i$ can be performed

$$J[\rho] = C'_N \int \mathcal{D}g \, e^{N \int \mathrm{d}x g(x)\rho(x) + N \log\left[ \int \mathrm{d}x \exp[-g(x)] \right]} = \int \mathcal{D}g \, e^{-NZ[g,\rho]}, \tag{4.15}$$

where

$$Z[g, \rho] = -\int \mathrm{d}x g(x)\rho(x) - \log \left[ \int \mathrm{d}x e^{-g(x)} \right]. \tag{4.16}$$

This integral can be evaluated for large $N$ by the saddle point method. We differentiate it functionally with respect to $g$ to obtain

$$\left. \frac{\delta Z}{\delta g} \right|_{g^\star} = 0 = -\rho(x) + \frac{e^{-g^\star(x)}}{\int \mathrm{d}x e^{-g^\star(x)}}. \tag{4.17}$$

whose solution $g^\star(x)$ can be given implicitly by

$$\rho(x) = \frac{e^{-g^\star(x)}}{\int \mathrm{d}x' e^{-g^\star(x')}}. \tag{4.18}$$

Replacing this result in the functional $Z[g, \rho]$ yields

$$Z[g^\star, \rho] = \int \mathrm{d}x \rho(x) \log \rho(x) + \underbrace{\int \mathrm{d}x \rho(x)}_{=1} \log \left[ \int \mathrm{d}x' e^{-g^\star(x')} \right] - \log \left[ \int \mathrm{d}x' e^{-g^\star(x')} \right] \tag{4.19}$$

$$= \int \mathrm{d}x \rho(x) \log \rho(x). \tag{4.20}$$

And we obtain the Jacobian

$$J[\rho] = C'_N e^{-N \int \mathrm{d}x \rho(x) \log \rho(x)}. \tag{4.21}$$

Indeed, this term matches the entropy of the average density $\rho$, as expected. The energy written as a functional of the average density becomes

$$E[\boldsymbol{x}] \xrightarrow{\text{large } N} N^2 \left[ \Sigma[\rho] - \frac{1}{N} \left( \frac{1}{2} - \frac{1}{\beta} \right) \int \rho(x) \log \rho(x) \mathrm{d}x \right], \tag{4.22}$$

where

$$\Sigma[\rho] = \int \rho(x)V(x)\mathrm{d}x - \frac{1}{2}\iint \mathrm{d}x\mathrm{d}x'\rho(x)\rho(x')\log|x-x'|. \tag{4.23}$$

The functional form of the energy contains a sub-dominant term, which is composed by the entropic term and the self-interacting part of the repulsion. Interestingly, this term cancels out in the case of $\beta = 2$, when the ensemble is considered for complex matrices. For other values of $\beta$, this term can be neglected when $N$ is large. From this point on, we consider this term to be negligible.

We note a special case in which $\beta$ can scale with $N$ ($\beta \sim 1/N$). It is possible to construct such ensembles, deriving them from Brownian motion investigations [4]. This scaling will turn the entropic term into a relevant contribution for the energy and the behavior of the $\beta$-ensemble will change drastically (see [5]).

**Enforcing normalization**

We recall the j.p.d.f. of the eigenvalues

$$P(\boldsymbol{x})\prod_{i=1}^{N}\mathrm{d}x_i \propto \prod_{i=1}^{N}\mathrm{d}x_i e^{-\beta E[\boldsymbol{x}]} \xrightarrow{\text{large } N} \mathcal{D}\rho\, e^{-\beta N^2\Sigma[\rho]}\delta\left(\int\rho(x)\mathrm{d}x - 1\right), \tag{4.24}$$

where we introduced a supplementary $\delta$ to enforce normalization, since all integrals of this probability must be performed in the space of normalized densities. This condition can be incorporated into the exponent by writing it in its exponential representation.

$$P(\boldsymbol{x})\prod_{i=1}^{N}\mathrm{d}x_i \xrightarrow{\text{large } N} \frac{1}{Z_{N,\beta}}\mathcal{D}\rho\int\mathrm{d}\eta e^{-\beta N^2 S[\rho]}, \tag{4.25}$$

where

$$S[\rho] = \int\rho(x)V(x)\mathrm{d}x - \frac{1}{2}\iint\mathrm{d}x\mathrm{d}x'\rho(x)\rho(x')\log|x-x'| + \eta\left(\int\rho(x)\mathrm{d}x - 1\right) \tag{4.26}$$

is called the *action*. This functional replaces the role of the energy and allows us to calculate many observables using a saddle-point approximation. We now illustrate this method on the computation of the Wigner semi-circle law.

## 4.2 An example: calculating the semi-circle law

We want to calculate the average density of eigenvalues of the Gaussian ensemble. By the self-averaging property in the large $N$ limit, we know that the average density of eigenvalues will also be the density whose probability is the highest. We recall the j.p.d.f. of the eigenvalues of the Gaussian ensemble.

$$P(\boldsymbol{x}) = \frac{1}{Z_{N,\beta}}e^{-\frac{\beta N}{2}\sum_{i=1}^{N}x_i^2}\prod_{i<j}|x_i - x_j|^\beta. \tag{4.27}$$

We apply the formalism described above, using the potential $V(x) = x^2/2$. This probability becomes

$$P(\boldsymbol{x}) \xrightarrow{\text{large } N} \frac{1}{Z_{N,\beta}} e^{-\beta N^2 S[\rho,\eta]}, \tag{4.28}$$

where

$$S[\rho,\eta] = \int \rho(x)\frac{x^2}{2}\mathrm{d}x - \frac{1}{2}\iint \mathrm{d}x\mathrm{d}x'\rho(x)\rho(x')\log|x-x'| + \eta\left(\int \rho(x)\mathrm{d}x - 1\right). \tag{4.29}$$

We want to obtain the density $\rho^\star$ that contributes the most to the probability, and this is obtained by minimizing the functional $S$. We find

$$\left.\frac{\delta S}{\delta \rho}\right|_{\rho^\star} = 0 = \frac{x^2}{2} - \int \mathrm{d}x'\rho^\star(x')\log|x-x'| + \eta, \quad x \in \text{supp } \rho^\star \tag{4.30}$$

Equation (4.30) has a clear physical interpretation. In the electrostatic context, it means that for each point in the average density, potential and repulsion are balanced. This is of course expected as the system is in equilibrium. We differentiate this relation with respect to $x$ to obtain

$$x = \fint \frac{\rho^\star(x')}{x-x'}\mathrm{d}x', \quad x \in \text{supp } \rho^\star, \tag{4.31}$$

where $\fint$ represent the Cauchy principal value of the integral. Solving equation (4.31) and inserting the result into the action $S[\rho]$ is the main technical challenge of the Coulomb gas method. For this simpler case, we shall provide a detailed solution. We propose two methods: the Tricomi formula and the resolvent method.

### 4.2.1 Tricomi formula

Assuming that the support of $\rho^\star(x)$ is $A = [a,b]$, a compact simply connected support where $a$ and $b$ will be found afterwards, we can solve equation (4.31) directly using a formula due to Tricomi [136]. Given a sufficiently smooth real function $g(x)$ that satisfies

$$g(x) = \fint \frac{\rho(x')}{x-x'}\mathrm{d}x', \quad x \in [a,b], \tag{4.32}$$

when $\rho(x)$ is a function whose support is a single interval $[a,b]$, then this relation can be inverted and yields

$$\rho(x) = \frac{1}{\pi\sqrt{x-a}\sqrt{b-x}}\left[C - \fint_a^b \frac{\mathrm{d}x'}{\pi}\frac{\sqrt{x'-a}\sqrt{b-x'}}{x-x'}g(x')\right], \tag{4.33}$$

where

$$C = \int_a^b \rho(x)\mathrm{d}x. \tag{4.34}$$

To apply this theorem directly in order to find the solution of (4.31), we need some information about the support of the average density. Let us suppose that the average density of eigenvalues for the Gaussian ensemble has indeed a compact support $[-a, a]$, where the symmetry arises from the symmetry of the j.p.d.f. with respect to $x_i \to -x_i$ transformations. The constant $C$, by definition, is equal to 1. We solve the following integral

$$I_A(x) = \fint_{-a}^{a} \frac{\mathrm{d}x'}{\pi} \frac{\sqrt{x'+a}\sqrt{a-x'}}{x-x'} x' = x^2 - \frac{a^2}{2}. \tag{4.35}$$

And we obtain the density

$$\rho^\star(x) = \frac{1}{\pi\sqrt{a^2-x^2}} \left[1 - I_A(x)\right] = \frac{1 + a^2/2 - x^2}{\pi\sqrt{a^2-x^2}}. \tag{4.36}$$

The support of the distribution is $[-a, a]$, which means that $\rho(a) = 0$. This imposes $a = \sqrt{2}$, and we find the final formula for $\rho(x)$

$$\rho^\star(x) = \frac{\sqrt{2-x^2}}{\pi}, \tag{4.37}$$

which is, as expected, Wigner's semi circle law.

In general, we can guess by physical intuition or numerical analysis when the support is a single compact interval. When this is not the case, Tricomi's formula cannot be applied directly. When dealing with a two-interval support, $A = [a, b] \cup [c, d]$, we may use Tricomi's formula twice, one on each support, splitting the integral and bootstrapping the result from one equation to the other. This increases the complexity of the integrals performed, but it is possible and it is done in [107, 90, 89]. For more complex supports, we should resort to other tools to solve integral equation (4.31).

### 4.2.2 Resolvent method

Let $G(z)$ be a holomorphic function, called the *resolvent* (or Green's function), defined as

$$G(z) = \int \frac{\rho^\star(y)}{z-y} \mathrm{d}y, \quad z \in \mathbb{C} \setminus \operatorname{supp} \rho^\star. \tag{4.38}$$

Normalization of $\rho^\star$ to 1 implies that $G(z)$ behaves as $1/z$ when $|z|$ is large. We recall a standard identity involving the Dirac delta

$$\lim_{\varepsilon \to 0^+} G(x + i\varepsilon) = \lim_{\varepsilon \to 0^+} \int_a^b \frac{\rho^\star(y)}{x + i\varepsilon - y} \mathrm{d}y = -i\pi\rho^\star(x) + \fint_a^b \frac{\rho^\star(y)}{x-y} \mathrm{d}y. \tag{4.39}$$

We notice that, having $G(z)$, we obtain $\rho^\star(x)$ by performing

$$\rho^\star(x) = -\frac{1}{\pi} \lim_{\varepsilon \to 0^+} \left[\operatorname{Im} G(x + i\varepsilon)\right]. \tag{4.40}$$

We illustrate this method on the determination of the semicircle law. To find an equation for $G(z)$ in this case, we multiply equation (4.31) by $\frac{\rho^\star(x)}{z-x}$ and integrate it over $x$. This yields

$$\int x\frac{\rho^\star(x)}{z-x}\mathrm{d}x = \iint \frac{\rho^\star(x)}{z-x}\frac{\rho^\star(y)}{x-y}\mathrm{d}y\mathrm{d}x. \tag{4.41}$$

The RHS of equation (4.41) can be expressed in terms of $G(z)$ with the following manipulation. We use the identity

$$\frac{1}{(z-x)(x-y)} = \left(\frac{1}{z-x}+\frac{1}{x-y}\right)\frac{1}{z-y}, \tag{4.42}$$

to write the RHS as

$$\iint \frac{\rho^\star(x)}{z-x}\frac{\rho^\star(y)}{x-y}\mathrm{d}x\mathrm{d}y = \iint \frac{\rho^\star(x)\rho^\star(y)}{(z-x)(z-y)}\mathrm{d}x\mathrm{d}y - \iint \frac{\rho^\star(x)}{z-x}\frac{\rho^\star(y)}{x-y}\mathrm{d}x\mathrm{d}y. \tag{4.43}$$

Since the first term of the RHS of equation (4.41) is $G^2(z)$ and the second is the RHS of equation (4.41) with the sign changed, this implies that the RHS of equation (4.41) is $G^2(z)/2$.

The manipulations required to express the LHS in terms of $G(z)$ are straightforward in the Gaussian case. The LHS of equation (4.41) reads

$$\int x\frac{\rho^\star(x)}{z-x}\mathrm{d}x = \int (x-z+z)\frac{\rho^\star(x)}{z-x}\mathrm{d}x = -1+zG(z). \tag{4.44}$$

The final equation for the resolvent thus reads

$$-1+zG(z)+ = \frac{1}{2}G^2(z). \tag{4.45}$$

And its solution is evident

$$G(z) = z \pm \sqrt{z^2-2}. \tag{4.46}$$

The sign of the resolvent is chosen according to the normalization condition $G(z) \to 1/z$ when $|z| \to \infty$. We note that the resolvent is well defined on the real line outside of the support of $\rho^\star(x)$, and the sign choice for points in the real line is given by

$$G(x) = \begin{cases} G_-(x) \text{ for } x > \sqrt{2} \\ G_+(x) \text{ for } x < \sqrt{2} \end{cases} \tag{4.47}$$

We apply the identity (4.39) to obtain

$$-\frac{1}{\pi}\lim_{\varepsilon\to 0^+}\operatorname{Im} G(x+i\varepsilon) = \frac{\sqrt{2-x^2}}{\pi}. \tag{4.48}$$

As expected, we obtain Wigner semicircular law for the average density of eigenvalues of Gaussian random matrices. For other ensembles, equation (4.31) takes a different form, and resolution of this equation by the resolvent method is not always as simple.

## 4.3 Orthogonal polynomials

A second technique we introduce to tackle calculations of quantities involving eigenvalues of an invariant random matrix is due to Mehta and Gaudin [100], named the orthogonal polynomial technique. It is a very powerful tool arising from a brilliant insight in manipulating the j.p.d.f. (3.7). While elements of this technique can be developed for $\beta = 1$ and $\beta = 4$ with the use of pfaffians, we present only the simpler $\beta = 2$ version. In this entire section, we consider only the complex-valued matrix case with Dyson index $\beta = 2$.

The Coulomb gas method is very powerful, but has its limitations. As discussed in section 4.1.2, the empirical densities converges to the average, but not uniformly. There are scales in which the convergence of the average density of eigenvalues is problematic, and the Coulomb gas is not suitable to deal with these regimes. The orthogonal polynomials technique works in all regimes and scales, but large-$N$ results are very hard to obtain if we do not restrict our interest to specific regimes in which the asymptotic behavior of fundamental quantities of the ensemble are known. Loosely speaking, the orthogonal polynomial technique is well suited to study local fluctuations. Major results such as the sine kernel or the Airy kernel cannot be obtained via Coulomb gas. To deal with local regimes, we must resort to the orthogonal polynomials.

### 4.3.1 Correlation functions

In the section above, we defined the average and 2-point density functions of a random matrix ensemble. This definition is of course not restricted to 2, and we have great interest in generalizing it. Let $H$ be a Hermitian random matrix whose eigenvalues are given by $\{x_i\}$. We define the *empirical n-point density* $\hat{\rho}_n : \mathbb{R}^n \to \mathbb{R}$

$$\hat{\rho}_n(y_1, \dots, y_n) = \frac{(N-n)!}{N!} \sum_{i_1 \neq \dots \neq i_n} \delta(y_1 - x_{i_1}) \dots \delta(y_n - x_{i_n}). \tag{4.49}$$

The average of this random distribution is naturally given by the *average n-point density*

$$\begin{aligned} \rho_n(y_1, \dots, y_n) &= \langle \hat{\rho}_n(y_1, \dots, y_n) \rangle & (4.50) \\ &= \int \mathrm{d}y_{n+1} \dots \int \mathrm{d}y_N P(y_1, \dots, y_N), & (4.51) \end{aligned}$$

where $P$ is the j.p.d.f. of the eigenvalues.

We note that densities are always normalized to 1 when integrated over all their variables. A similar definition, but more convenient to our purposes, is the *n-point correlation function* $R_n$

$$\begin{aligned} R_n(y_1, \dots, y_n) &= \frac{N!}{(N-n)!} \rho_n(y_1, \dots, y_n) & (4.52) \\ &= \sum_{i_1 \neq \dots \neq i_n} \langle \delta(y_1 - x_{i_1}) \dots \delta(y_n - x_{i_n}) \rangle & (4.53) \end{aligned}$$

$$= \frac{N!}{(N-n)!} \int \mathrm{d}y_{n+1} \dots \int \mathrm{d}y_N P(y_1, \dots, y_N). \tag{4.54}$$

In particular, $R_1(x) = N\rho(x)$ and $R_2(x, x') = N(N-1)\rho_2(x, x')$.

Correlation functions are fundamental quantities for point processes, and in particular to the analysis of the spectrum of the random matrix ensembles we described. They represent the probability density of finding an eigenvalue around each of the points $y_1 \dots, y_n$, the position of the remaining levels being unobserved. They allow us to express averages of symmetric sums as a convenient integral, a procedure already used in the Coulomb gas method with the first and second $n$-point densities in section 4.1.2. Let $f : \mathbb{R}^k \to \mathbb{R}$ be a test function, we may write

$$\left\langle \sum_{\substack{i_1,\dots,i_k \\ i\text{'s distinct}}} f(x_{i_1}, \dots, x_{i_k}) \right\rangle = \int_{\mathbb{R}^k} f(y_1, \dots, y_k) R_k(y_1, \dots, y_k) \mathrm{d}y_1 \dots \mathrm{d}y_k. \tag{4.55}$$

The LHS is summed over all $k$-tuples of eigenvalues. We write the first two cases of this sum

$$\left\langle \sum_{i=1}^{N} f(x_i) \right\rangle = \int f(y) R_1(y) \mathrm{d}y \tag{4.56}$$

$$\left\langle \sum_{i \neq j} f(x_i, x_j) \right\rangle = \int f(y, y') R_2(y, y') \mathrm{d}y \mathrm{d}y'. \tag{4.57}$$

### 4.3.2 Orthogonal polynomials

We will introduce the building blocks of the powerful theory of orthogonal polynomials. We emphasize that we consider only the case for complex matrices, which implies a Dyson index $\beta = 2$. It is possible to generalize many of these results to other values of $\beta$ [100], but these generalizations are not straightforward and lie outside the interest of this work.

We are interested in ensembles whose eigenvalues are described by a j.p.d.f. of the form (4.1) with $\beta = 2$, which we recall here

$$P(x_1, \dots, x_N) = \frac{1}{Z_N} e^{-2N \sum_{i=1}^{N} V(x_i)} \det \left[ x_i^{j-1} \right]^2, \tag{4.58}$$

where we wrote the Vandermonde determinant in its determinantal form for future convenience.

One special type of point process that has correlation functions is the *determinantal point process*. Let $K_N : \mathbb{R}^2 \to \mathbb{R}$. We define a determinantal point process as a $N$ point process whose $n$-point correlation functions exist and are written as

$$R_n(x_1, \dots, x_n) = \det \left[ K_N(x_i, x_j) \right]_{1 \leq i,j \leq n}, \tag{4.59}$$

In particular, $R_1(x) = K_N(x, x)$ and $R_2(x, y) = K_N(x, x)K_N(y, y) - K_N(x, y)K_N(y, x)$.

We are going to show that a process defined by the probability law (4.58) is actually a determinantal point process, and we can write its kernel explicitly.

We want to calculate $n$-point correlation functions of this process, which are integrals of the probability (4.58) for $N-n$ variables. These integrals of determinants can be performed immediately using a powerful "integrating-out" lemma due to Dyson, Mehta and Gaudin [100]. This lemma states

- Let $J_n = (J_{ij})_{1\leq i,j\leq n}$ be an $n\times n$ matrix whose entries are defined by a real vector $\boldsymbol{x} = (x_1,\dots,x_n)$ and given by a function of the form $K_N(x_i,x_j)$. Suppose this function $K_N(x,y)$ satisfies a *reproducing kernel property*, which is

$$\int K_N(x,y)K_N(y,z)\mathrm{d}y = K_N(x,z), \tag{4.60}$$

  then

$$\int \det J_n(\boldsymbol{x})\mathrm{d}\mu(x_n) = [q-(n-1)]\det J_{n-1}, \tag{4.61}$$

  where $q = \int K_N(x,x)\mathrm{d}\mu(x)$.

To apply this lemma, we need only to write the j.p.d.f. of eigenvalues (4.58) as the determinant of a kernel $K_N(x,y)$ that satisfies the reproducing property. This probability can be manipulated to be written as a determinant of a reproducing kernel using the fact that adding or subtracting rows from a determinant only changes its prefactor. The idea is to add and subtract rows from the Vandermonde matrix to build a matrix whose entries are polynomials orthogonal to the weight $e^{-2NV(x)}$. In other words, let $\pi_i(x)$ be a polynomial of degree $i$ such that

$$\int \pi_i(x)\pi_j(x)e^{-2NV(x)}\mathrm{d}x = c_i\delta_{ij}, \tag{4.62}$$

where $c_i$ is a constant. This defines the family of polynomials orthogonal to the weight $e^{-2NV(x)}$. We add and subtract rows from the Vandermonde matrix to obtain a proportional determinant of a matrix composed of orthogonal polynomials.

$$\det\left[x_i^{j-1}\right] = \begin{vmatrix} 1 & \cdots & 1 \\ x_1 & \cdots & x_N \\ \vdots & \ddots & \vdots \\ x_1^{N-1} & \cdots & x_N^{N-1} \end{vmatrix} \propto \begin{vmatrix} \pi_0(x_1) & \cdots & \pi_0(x_N) \\ \pi_1(x_1) & \cdots & \pi_1(x_N) \\ \vdots & \ddots & \vdots \\ \pi_{N-1}(x_1) & \cdots & \pi_{N-1}(x_N) \end{vmatrix} = \det\left[\pi_{j-1}(x_i)\right]. \tag{4.63}$$

This allows us to write the j.p.d.f. of eigenvalues as

$$P(x_1,\dots,x_N) \propto \det\left[K_N(x_i,x_j)\right], \tag{4.64}$$

where

$$K_N(x,y) = e^{-N(V(x)+V(y))}\sum_{k=0}^{N-1}\pi_k(x)\pi_k(y) = \sum_{k=0}^{N-1}\phi_k(x)\phi_k(y). \tag{4.65}$$

is called the *kernel*, where we defined the function $\phi_k(x)$, given by $e^{-NV(x)}\pi_k(x)$. This kernel satisfies the reproducing property, and we may apply the integrating-out lemma to

obtain the $n$-point correlation functions as the determinant of this same kernel. Indeed, we obtain

$$\int \cdots \int \det\left[K_N(x_i,x_j)\right]_{1\leq i,j\leq N} \mathrm{d}x_{k+1}\ldots\mathrm{d}x_N = (N-k)!\det\left[K_N(x_i,x_j)\right]_{1\leq i,j\leq k}. \quad (4.66)$$

Recalling equation (4.54), we can write a direct relation between the correlation function and the kernel

$$R_n(x_1,\ldots,x_n) = \det\left[K_N(x_i,x_j)\right]_{1\leq i,j\leq n}, \quad (4.67)$$

which proves that the eigenvalues of a complex rotationally invariant random matrix whose eigenvalues j.p.d.f. is given by (4.1) form a determinantal point process whose statistics is completely described by a kernel $K_N(x,y)$.

### 4.3.3 Gaussian Unitary Ensemble

The ideas presented in the previous section are very general, and we detail the special case of the Gaussian Unitary Ensemble. The potential of GUE is given by $V(x) = x^2/2$, and the family of polynomials orthogonal with respect to this weight is the family of *Hermite polynomials* $H_n\left(x\sqrt{N}\right)$, defined as

$$H_n(x) = e^{x^2}\left(-\frac{\mathrm{d}}{\mathrm{d}x}\right)^n e^{-x^2} = n!\sum_{i=0}^{[n/2]}(-1)^i\frac{(2x)^{n-2i}}{i!(n-2i)!}. \quad (4.68)$$

These polynomials are orthogonal with respect to the measure $e^{-Nx^2}$, yielding

$$\int_{-\infty}^{\infty} H_n\left(x\sqrt{N}\right)H_m\left(x\sqrt{N}\right)e^{-Nx^2}\mathrm{d}x = 2^n\frac{n!}{\sqrt{N}}\sqrt{\pi}\delta_{mn}. \quad (4.69)$$

This calls for the definition of the function $\phi_n(x)$

$$\phi_n(x) = \left(2^n\frac{n!}{\sqrt{N}}\sqrt{\pi}\right)^{-\frac{1}{2}} e^{-N\frac{x^2}{2}}H_n\left(x\sqrt{N}\right). \quad (4.70)$$

Due to the similarity with the wave function of the quantum harmonic oscillator, these function are named *oscillator wave functions*. This similarity will play a crucial role in chapter 7. From its definition, it is clear that the oscillator wave functions are orthonormal and the kernel reads

$$K_N(x,y) = \sum_{k=0}^{N-1} e^{-N\frac{(x^2+y^2)}{2}}\frac{H_k\left(x\sqrt{N}\right)H_k\left(y\sqrt{N}\right)}{2^k k!\sqrt{\pi/N}} = \sum_{k=0}^{N-1}\phi_k(x)\phi_k(y). \quad (4.71)$$

In particular the average density of eigenvalues is given by

$$N\rho(x) = R_1(x) = K_N(x,x) = \sum_{k=0}^{N-1}\phi_k(x)^2. \quad (4.72)$$

If we want to explore the large $N$ limit of the random matrix ensemble, we need to study the asymptotics of its orthogonal polynomials. This is simplified by the fact that orthogonal polynomials satisfy a three-term recurrence relation, which implies a formula involving the sums of products of orthogonal polynomials, named the *Christoffel-Darboux formula*.

- Let $P_n(x)$ be a family of orthogonal polynomials whose leading coefficient is $k_n$. We denote $\|P_k\|_{L_2} = h_k$ the square integral norm. Then

$$\sum_{k=0}^{N-1} \frac{P_k(x)P_k(y)}{h_k} = \frac{k_{N-1}}{k_N h_{N-1}} \frac{P_N(x)P_{N-1}(y) - P_N(y)P_{N-1}(x)}{x-y}. \tag{4.73}$$

The LHS of the formula is precisely the sum required to obtain the kernel. This theorem exchanges the asymptotic of the sum of $N$ terms with a single asymptotic evaluation on Hermite polynomials to obtain the behavior of the kernel at large $N$.

The orthogonal polynomials method and the Coulomb gas method have advantages and limitations. Coulomb gas can easily provide results in leading order in $N$ for many observables, but it is unable to explore local fluctuations. The orthogonal polynomials method is valid for $\beta = 2$ only and calculations for large $N$ are usually difficult, but it is able to probe into local fluctuations. For these reasons, we decided to split the spectrum of eigenvalues of a random matrix into different interval, or regimes, and treat each part with a different method. These techniques complement each other and the matching of the calculated quantities in the cross-over between the regimes is a good test of consistency of our results.

## 4.4 Scaling regimes in invariant random matrices

Using the orthogonal polynomials method, we can write all observables of a complex invariant random matrix ensemble in terms of the kernel $K_N(x, y)$. This is a very powerful result, as it simplifies many calculations into the computation of the behavior of a single two-variable function. This function, however, is not simple. We recall its general form

$$K_N(x, y) = e^{-N(V(x)+V(y))} \sum_{k=0}^{N-1} \pi_k(x)\pi_k(y), \tag{4.74}$$

where $\pi_k(x)$ are a family of polynomials orthogonal to the weight $e^{-2NV(x)}$. This sum becomes very difficult for large values of $N$, even using Christoffel-Darboux's formula, but there are two particular scaling regimes for the variables $x$ and $y$ in which the kernel has a simple limit. We present both regimes for the GUE case, but the generalization is straightforward.

- **Bulk Regime**: $|x-y| \sim 1/N$. This is the situation in which $x$ and $y$ are very close, their distance is of the order of the average distance between the eigenvalues. Since

the eigenvalues in this regime are so close, the potential does not play an important role in its statistics and we are "zooming in" on the spectrum to obtain only the contribution of the logarithmic repulsion.

- **Edge Regime**: $|x - \sqrt{2}| \lesssim N^{-2/3}$, and the symmetric correspondent. This regime is obtained by "zooming in" at the edge of the average distribution of eigenvalues. The width of the edge regime was introduced by Tracy and Widom in their seminal paper [134] calculating for the first time statistics for the largest eigenvalue of a Gaussian random matrix, the so-called Tracy-Widom distribution.

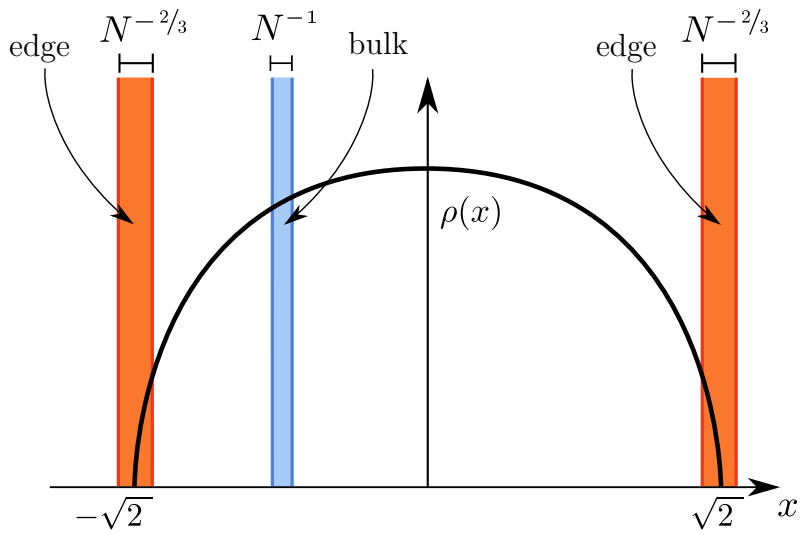


**Figure 4.1** — Representation of bulk and edge regimes for the Gaussian ensemble. The representation of the bulk is placed at an arbitrary location, since it is translational invariant inside the support.

These regimes are summarized in picture 4.1. Both regimes are local and their width decreases as $N$ becomes large. Their scaling is crucial to ignore the form of the potential and reveal properties arising only from the logarithmic repulsion of the eigenvalues.

Loosely speaking, the bulk and edge regime are "zoomed in" regions of different parts of the spectrum. Inside the support of the average density and away from the edges, we find the bulk regime when we change our scale to the interparticle distance. In this "zoomed in" situation, distances are so small that the potential, a smooth function on the real line, can be treated as a constant, and analysis on this regime cannot see the specific form of the potential. In the edge regime, the average density presents a singularity, which changes completely the asymptotic behavior of the kernel. In the appropriate scale around the edge, the potential can be linearized and once again we find local universality for the kernel.

We describe the classical results for the asymptotics of the kernel in the bulk and edge regime.

### 4.4.1 Bulk regime and the sine kernel

Our goal is to obtain a more useful expression for the kernel on the bulk of GUE than the sum of products of orthogonal polynomials (4.71). The standard procedure to do so is to write the Christoffel-Darboux formula (4.73) applied to the oscillator wave functions $\phi_k(x)$ (4.70) and use asymptotics of Hermite polynomials (those can be found in [12]) in the bulk regime to obtain the asymptotic behavior of the kernel. The calculations required to do so, however, are complicated and not particularly interesting to reveal the universal character of the sine kernel. So instead of going through the usual route, we will use some results of functional analysis to explore the limiting behavior of $K_N(x, y)$ when $N$ is large and when the variables are scaled according to the bulk limit. This approach follows [132].

We recall the formula of the kernel as a sum of products of its oscillator wave functions

$$K_N(x, y) = \sum_{k=0}^{N-1} \phi_k(x)\phi_k(y). \tag{4.75}$$

As their name suggests, these functions are eigenfunctions of the harmonic oscillator operator

$$\mathscr{L} = -\frac{1}{2N}\frac{\mathrm{d}^2}{\mathrm{d}x^2} + \frac{Nx^2}{2}, \tag{4.76}$$

whose eigenvalues are

$$\mathscr{L}\phi_k = \left(k + \frac{1}{2}\right)\phi_k. \tag{4.77}$$

The role played by the kernel $K_N$ is, hence, the integral kernel of the spectral projection $\mathscr{P}$ into the eigenfunctions of the operator $\mathscr{L}$. To make this clear, we notice how its action on a test function $\phi$ is given by

$$\mathscr{P}\phi(x) = \int K_N(x, y)\phi(y)\mathrm{d}y = \int \sum_{k=0}^{N-1} \phi_k(x)\phi_k(y)\phi(y)\mathrm{d}y = \sum_{k=0}^{N-1} \langle \phi, \phi_k \rangle \, \phi_k(x). \tag{4.78}$$

So $K_N$ is an integral kernel responsible for projecting the test function in the space of eigenfunctions of the operator $\mathscr{L}$, with a caveat: it only projects it in the eigenfunctions associated with the first $N$ eigenvalues. We note this region by $\mathscr{L} \leq N - 1/2$, which means that the projection only takes into account eigenfunctions $\phi_k$ such that $\mathscr{L}\phi_k \leq (N - 1/2)\phi_k$.

We now place ourselves in the bulk limit. We chose a fixed point inside the bulk, $x_0$, where $x_0 \in ]-\sqrt{2}, \sqrt{2}[$. We pick small fluctuations around this value, of the order of the interparticle distance, which is given by $1/(N\rho_N(x_0))$, where $\rho(x) = \sqrt{2 - x^2}/\pi$.

$$x = x_0 + \frac{u}{\sqrt{2}N\rho(x_0)}. \tag{4.79}$$

This transformation is also named the unfolding of the spectrum. In these coordinates, the operator $\mathcal{L}$ becomes

$$\mathscr{L} = -\frac{N\rho(x_0)^2}{2}\frac{\mathrm{d}^2}{\mathrm{d}u^2} + \frac{N}{2}\left(x_0 + \frac{u}{\sqrt{2}N\rho(x_0)}\right)^2. \tag{4.80}$$

Since the kernel is responsible for projecting functions in the spectral region of eigenvalues smaller than $N - 1/2$, which we denote by $\mathscr{L} \leq N - 1/2$, we then write

$$-\frac{N\rho(x_0)^2}{2}\frac{\mathrm{d}^2}{\mathrm{d}u^2} + \frac{N}{2}\left(x_0 + \frac{u}{\sqrt{2}N\rho(x_0)}\right)^2 \leq N - \frac{1}{2}. \tag{4.81}$$

This inequality only denotes the region of the spectrum where the kernel projects the functions to, and we may apply the large $N$ limit on both sides to determine what is the limit of this projection region. Taking the large $N$ limit yields

$$-\frac{\mathrm{d}^2}{\mathrm{d}u^2} \leq \pi^2 \tag{4.82}$$

It is clear that we just need to find the integral kernel of the projection into the spectral functions of the operator $-\frac{\mathrm{d}^2}{\mathrm{d}u^2}$ in its spectral region of eigenvalues smaller that $\pi^2$. To do so, we send our problem to Fourier space. Confining the projection to eigenvalues smaller than $\pi^2$ is equivalent to confining the frequency variable in Fourier space to a certain interval. Indeed, we may use a semiclassical argument to write the region described above as: $\mathcal{F}[-\frac{\mathrm{d}^2}{\mathrm{d}u^2}] = |\xi|^2 4\pi^2 \leq \pi^2$, which yields the following region for the frequency variable

$$|\xi|^2 \leq \frac{1}{4}. \tag{4.83}$$

Going back to physical space we obtain

$$\mathscr{P}\phi(u) = \int_{-\frac{1}{2}}^{\frac{1}{2}} e^{2\pi i\xi u}\hat{\phi}(\xi)\mathrm{d}\xi = \int_{-\infty}^{\infty}\int_{-\frac{1}{2}}^{\frac{1}{2}} e^{2\pi i\xi u}e^{-2\pi i\xi v}\phi(v)\mathrm{d}\xi\mathrm{d}v \tag{4.84}$$

$$= \int_{-\infty}^{\infty} \frac{\sin(\pi(u-v))}{\pi(u-v)}\phi(v)\mathrm{d}v. \tag{4.85}$$

Where we recognize the sine kernel as playing the role of the integral kernel of the spectral projection of this operator. We have, therefore, that the GUE kernel converges, in the bulk limit for large values of $N$, to the sine kernel. In summary, we have that, given the scaling

$$x = x_0 + \frac{u}{\sqrt{2}N\rho(x_0)} \qquad \text{and} \qquad y = x_0 + \frac{v}{\sqrt{2}N\rho(x_0)}, \tag{4.86}$$

with $x_0, y_0 \in ]-\sqrt{2}, \sqrt{2}[$, the kernel has the limit

$$\lim_{N\to\infty} \frac{1}{\sqrt{2}N\rho(x_0)} K_N(x, y) = \frac{\sin(\pi(u-v))}{\pi(u-v)} = K_{sk}(u-v), \tag{4.87}$$

where $K_{sk}$ known as the *sine kernel*.

This method of obtaining the asymptotic behavior for the sine kernel reveals part of the universality of this asymptotic behavior. All orthogonal polynomials are associated with a second order differential operator and this scaling is responsible for neglecting the role of

the potential into calculations. This means that this procedure can be reproduced for all ensembles presented above, as the potential associated with the ensemble does not play a role once the correct scaling is applied. Hence, the sine kernel described the asymptotic of the kernel in the bulk of Gaussian, Wishart, Cauchy and many other ensembles for $\beta = 2$.

Physically, we use the charged particle analogy to note that in the interparticle distance scale, the potential, as a smooth function, can be treated as constant. The universality arises from the fact that the potential is negligible in this scale and log repulsion is responsible for correlations. Hence, this scaling limit of the kernel is universal for all ensembles whose j.p.d.f. of eigenvalues is described by (4.1) for $\beta = 2$.

### 4.4.2 Edge regime and the Airy kernel

Hermite polynomials may also be scaled in the edge of the average density. Our goal is to expand the Hermite polynomials around the average value of the largest eigenvalue of GUE, $\sqrt{2}$, and scale this variable by the typical fluctuation of the largest eigenvalue. Heuristically, we can argue that this scale of fluctuations of the largest eigenvalue $x_{\max}$ is given by saying that between the point $x_{\max}$ and $\sqrt{2}$ there is only one eigenvalue. In other words,

$$\int_{x_{\max}}^{\sqrt{2}} \sqrt{\sqrt{2} - x}\mathrm{d}x \sim \frac{1}{N}, \tag{4.88}$$

from which we deduce $\sqrt{2} - x_{\max} \sim O(N^{-\frac{2}{3}})$. While the bulk scaling was expected, it corresponds to the interparticle distance, the scaling for the edge regime is not intuitive. This edge width is related to the typical fluctuations of the largest eigenvalue, the so-called Tracy-Widom distribution. The p.d.f. for the maximum eigenvalue was first obtained by Tracy and Widom for GUE [134], generalized to GOE and GSE [135] and proven extremely resilient to changes in the ensemble, representing a true universal property emerging from the presence of an edge in strongly correlated systems [91].

We set

$$x = \sqrt{2} + \frac{\xi_1}{\sqrt{2}N^{\frac{2}{3}}} \quad \text{and} \quad y = \sqrt{2} + \frac{\xi_2}{\sqrt{2}N^{\frac{2}{3}}}, \tag{4.89}$$

Using this normalization, we find the following asymptotic behavior for the Hermite polynomials [56]

$$e^{-N\frac{x^2}{2}} H_N\left(x\sqrt{N}\right) = \pi^{\frac{1}{4}} 2^{\frac{N}{2}+\frac{1}{4}} \frac{\sqrt{N!}}{N^{\frac{1}{12}}} \left[\mathrm{Ai}(\xi_1) + O(N^{-2/3})\right] \tag{4.90}$$

Using the fact that $N$ is large, we can Taylor expand the Airy function and apply the result to Christoffel-Darboux formula [115]. We obtain

$$K_N(x, y)\mathrm{d}y \xrightarrow{\text{large } N} \frac{\mathrm{Ai}(\xi_1)\mathrm{Ai}'(\xi_2) - \mathrm{Ai}(\xi_2)\mathrm{Ai}'(\xi_1)}{\xi_1 - \xi_2}\mathrm{d}\xi_2 = K_{\mathrm{Ai}}(\xi_1, \xi_2)\mathrm{d}\xi_2, \tag{4.91}$$

where $K_{\mathrm{Ai}}$ is known as the *Airy kernel* and $\mathrm{Ai}(x)$ is the Airy function, the solution of the differential equation

$$\mathrm{Ai}''(x) = x\mathrm{Ai}(x), \quad \mathrm{Ai}(x) \xrightarrow{x\to\infty} 0. \tag{4.92}$$

# — 5 —
# Counting statistics

*Man is fond of counting his troubles,*
*but he does not count his joys.*

Fyodor Dostoyevsky

The problem of counting eigenvalues is an old, rich and fundamental subject in random matrix theory. Many problems can be transformed into a counting problem of the number of eigenvalues of a random matrix ensemble inside an interval. Several previous results have explored this observable in many different ways, and we discuss some of them in this chapter.

We are interested in the observable $N_{\mathcal{I}}$, the number of eigenvalues $\{x_i\}$ inside an interval $\mathcal{I} = [a, b]$. By definition

$$N_{\mathcal{I}} = \sum_{i=1}^{N} \mathbb{1}_{\mathcal{I}}(x_i), \tag{5.1}$$

where $\mathbb{1}_{\mathcal{I}}(x)$ is the characteristic function whose value is 1 if $x \in \mathcal{I}$ and zero otherwise. We recall that we consider only eigenvalues $x_i$ distributed according to the j.p.d.f. (4.1)

$$P(\boldsymbol{x}) = \frac{1}{Z_{N,\beta}} e^{-\beta N \sum_{i=1}^{N} V(x_i)} \prod_{j<k} |x_k - x_i|^{\beta}. \tag{5.2}$$

$N_{\mathcal{I}}$ is a random variable. One of the main questions during my PhD was the following: what is the statistics of $N_{\mathcal{I}}$ for invariant self-adjoint random matrices? In other words, how many eigenvalues from an invariant ensemble lie between $a$ and $b$? This study is named number statistics, or full counting statistics. In this chapter, we present the classical results for the statistics of the variable $N_{\mathcal{I}}$. These results are both powerful and necessary, as they will be the reference to compare with new results we obtained in chapters 6, 7 and 8.

## 5.1 Counting uncorrelated variables

The j.p.d.f. of eigenvalues of an invariant random matrix contains a Vandermonde determinant coupling all eigenvalues. The presence of the Vandermonde will greatly impact the behavior of the number statistics, and this impact becomes clear when we compare to the case of uncorrelated variables.

We begin by exploring this case, when points are distributed on a line according to independent probabilities. We consider the i.i.d. variables $\{x_1, \dots, x_n\}$. We set

$$P(x_1, \dots, x_n) = p(x_1) \dots p(x_n) \tag{5.3}$$

We recall the definition of empiric density and average density of points

$$\hat{\rho}(x) = \frac{1}{N} \sum_{i=1}^{N} \delta(x - x_i) \qquad \rho(x) = \frac{1}{N} \left\langle \sum_{i=1}^{N} \delta(x - x_i) \right\rangle . \tag{5.4}$$

We introduce the moment generating function

$$\chi_{\mathcal{I}}(z) = \sum_{N_{\mathcal{I}}} (1-z)^{N_{\mathcal{I}}} P(N_{\mathcal{I}}) = \left\langle (1-z)^{N_{\mathcal{I}}} \right\rangle . \tag{5.5}$$

Using the statistical independence of the points with definition (5.1), we may write $\chi_{\mathcal{I}}(z)$ as

$$\chi_{\mathcal{I}}(z) = \left\langle \prod_i (1-z)^{\mathbb{1}_{\mathcal{I}}(x_i)} \right\rangle = \prod_i \langle 1 - z\mathbb{1}_{\mathcal{I}}(x_i) \rangle = \left[ 1 - z \int_{\mathcal{I}} \rho(x) \mathrm{d}x \right]^N . \tag{5.6}$$

We write $q_{\mathcal{I}} = \int_{\mathcal{I}} \rho(x) \mathrm{d}x$ the average number of points inside $\mathcal{I}$. We set $1 - z = s$, and this last term becomes $(1 - q_{\mathcal{I}} + s q_{\mathcal{I}})^N$. Comparing the second term in (5.5) and this last term yields

$$\sum_{k=0}^{N} s^k P(N_{\mathcal{I}} = k) = (1 - q_{\mathcal{I}} + s q_{\mathcal{I}})^N = \sum_{k=0}^{N} \binom{N}{k} q_{\mathcal{I}}^k (1 - q_{\mathcal{I}})^{N-k} s^k . \tag{5.7}$$

By simple comparison we find

$$P(N_{\mathcal{I}} = k) = \binom{N}{k} q_{\mathcal{I}}^k (1 - q_{\mathcal{I}})^{N-k} . \tag{5.8}$$

The probability law for $N_{\mathcal{I}}$ in uncorrelated variables is given by the binomial distribution. The average number of points inside the interval $\mathcal{I}$ will be given by $\langle N_{\mathcal{I}} \rangle = N q_{\mathcal{I}}$ and the variance of $N_{\mathcal{I}}$ will be given by $\langle N_{\mathcal{I}}^2 \rangle - \langle N_{\mathcal{I}} \rangle^2 = N q_{\mathcal{I}} (1 - q_{\mathcal{I}})$.

If we consider the interval $\mathcal{I}$ to be very small (and hence $q_{\mathcal{I}}$ small), $N$ to be very large and $N q_{\mathcal{I}} = \lambda$ to be fixed, we obtain the standard Poisson limit to the binomial distribution.

$$\lim_{\substack{N \to \infty \\ \lambda \, fixed}} P(N_{\mathcal{I}} = k) = \frac{\lambda^k}{k!} e^{-\lambda} , \tag{5.9}$$

whose average and variance are given by $\langle N_{\mathcal{I}} \rangle = \lambda$ and $\mathrm{Var}(N_{\mathcal{I}}) = \lambda$.

This result shows that the variance of an i.i.d. particles process grows linearly with $\lambda$, which is given by $N \int_{\mathcal{I}} \rho(\lambda) \mathrm{d}\lambda$. We consider a very small interval $\mathcal{I} = [a, b]$. We can then write $\lambda \simeq N\rho(a)(b-a)$, and we note that, in this scale, the variance grows linearly with the system size. This scale is ideal to compare to the equivalent bulk limit case for strongly correlated variables such as the eigenvalues of a Gaussian random matrix.

## 5.2 Kernel formulas for counting statistics

Since $N_{\mathcal{I}}$ and all its powers are symmetric sums of functions of the eigenvalues, we may write all moments of $N_{\mathcal{I}}$ in terms of the correlation functions of the ensemble, according to equation (4.55). The correlation functions, as seen in the last chapter, can be expressed as a combination of the kernel of the ensemble. The average is the simplest moment, and it is given by

$$\langle N_{\mathcal{I}} \rangle = \int \left( \sum_{i=1}^{N} \mathbb{1}_{\mathcal{I}}(x_i) \right) P(\boldsymbol{x}) \mathrm{d}\boldsymbol{x} = N \int_{\mathcal{I}} \rho(x) \mathrm{d}x = \int_{I} K_N(x, x) \mathrm{d}x. \tag{5.10}$$

The variance of $N_{\mathcal{I}}$ is a more complicated object. To obtain it, we recall the 1 and 2-point correlation functions

$$R_1(x) = N \int \cdots \int \mathrm{d}x_2 \ldots \mathrm{d}x_N P(x, x_2, \ldots, x_N) \tag{5.11}$$

$$R_2(x, x') = N(N-1) \int \cdots \int \mathrm{d}x_3 \ldots \mathrm{d}x_N P(x, x', x_2, \ldots, x_N). \tag{5.12}$$

Our goal is to express the variance in terms of correlation functions, and finally to express them as combinations of the kernel $K_N(x, y)$. We rewrite the second moment as

$$\left\langle N_{\mathcal{I}}^2 \right\rangle = \int \left( \sum_{i=1}^{N} \mathbb{1}_{\mathcal{I}}(x_i) \right)^2 P(\boldsymbol{x}) \prod_{i=1}^{N} \mathrm{d}x_i = \int \sum_{i,j}^{N} \mathbb{1}_{\mathcal{I}}(x_i) \mathbb{1}_{\mathcal{I}}(x_j) P(\boldsymbol{x}) \prod_{i=1}^{N} \mathrm{d}x_i. \tag{5.13}$$

We recall equation (4.55) and we specify the cases for $R_1$ and $R_2$.

$$\left\langle \sum_{i=1}^{N} f(x_i) \right\rangle = \int f(x) R_1(x) \mathrm{d}x \tag{5.14}$$

$$\left\langle \sum_{i \neq j} f(x_i, x_j) \right\rangle = \int f(x, y) R_2(x, y) \mathrm{d}x \mathrm{d}y. \tag{5.15}$$

By expanding the sums of equation (5.13) and separating the $i = j$ and $i \neq j$, we obtain

$$\begin{aligned} \langle N_{\mathcal{I}}^2 \rangle &= \int \mathrm{d}x R_1(x) \mathbb{1}_{\mathcal{I}}(x) + \iint \mathrm{d}x \mathrm{d}y \mathbb{1}_{\mathcal{I}}(x) \mathbb{1}_{\mathcal{I}}(y) R_2(x, y). \\ &= \int_{\mathcal{I}} R_1(x) \mathrm{d}x + \int_{\mathcal{I}} \int_{\mathcal{I}} R_2(x, y) \mathrm{d}x \mathrm{d}y \end{aligned} \tag{5.16}$$

We note how the variancecan be written in terms of integrals of the correlation functions.

$$\begin{aligned}\mathrm{Var}(N_I) &= \left\langle N_{\mathcal{I}}^2 \right\rangle - \langle N_{\mathcal{I}} \rangle^2 \\ &= \int_{\mathcal{I}} R_1(x)\mathrm{d}x + \int_{\mathcal{I}}\int_{\mathcal{I}} R_2(x,y)\mathrm{d}x\mathrm{d}y - \left(\int_{\mathcal{I}} R_1(x)\mathrm{d}x\right)^2 \end{aligned} \tag{5.17}$$

As discussed in the previous chapter, for $\beta = 2$ we can define a kernel $K_N(x,y)$ that contains all the information about the statistics of the eigenvalues. The correlation functions can be written as a determinant of $K_N$, and the variance has a direct expression as a function of it. We need only to replace $R_1$ and $R_2$ in (5.17) by their expressions in terms of the kernel to obtain

$$\mathrm{Var}(N_I) = \int_{\mathcal{I}} K_N(x,x)\mathrm{d}x - \int_{\mathcal{I}}\int_{\mathcal{I}} K_N(x,y)^2\mathrm{d}x\mathrm{d}y \tag{5.18}$$

## 5.3 Number variance in edge and bulk regimes

If we know the kernel, we can find the fluctuations of eigenvalues inside the interval $\mathcal{I}$. We consider the case of GUE, where the kernel is given by equation (4.71). Our goal is to use the known asymptotic behavior of the GUE kernel in both the bulk and edge regime, presented in section 4.4, to obtain the variance of the number of eigenvalues inside an interval $\mathcal{I}$ in these regimes. We begin by the simpler case, the number variance in the bulk regime.

### 5.3.1 Number variance in the bulk limit

While the average of $N_{\mathcal{I}}$ is simply the integral of the average density in the interval $\mathcal{I}$, the full probability density function for the counting statistics is a much more complex object. This problem was originally studied by Dyson [43] in 1963 for the Gaussian ensemble. Dyson considered a small interval around the origin whose size is of the order of the mean spacing between the eigenvalues, the so-called bulk regime (see figure 4.1).

As described in 4.4.1, the GUE kernel can be evaluated in the asymptotic limit of the bulk, when distances are comparable to the interparticle distance (which is $\sim N^{-1}$). This limit, equation (4.86), allows us to evaluate the variance of the random variable $N_{\mathcal{I}}$ when we apply it to the formula (5.18).

We recall the asymptotic limit of the GUE kernel when evaluated in the bulk. We consider values around the origin scaled according to the interparticle distance at the origin: $1/(N\rho(0)) = \pi/\sqrt{2}N$. We denote this scaled variable as $x = u\pi/\sqrt{2}N$. We find

$$\lim_{N\to\infty} \frac{\pi}{\sqrt{2}N} K\left(\frac{u\pi}{\sqrt{2}N}, \frac{u'\pi}{\sqrt{2}N}\right) = \frac{\sin(\pi v)}{\pi v}, \tag{5.19}$$

where $v = u - u'$.

We evaluate expression (5.18) in the bulk limit, taking the interval $\mathcal{I}$ as $[-L, L]$ and considering values of $L$ of the order of $1/N$. We define the scaled interval size $s =$

$L\sqrt{2}N/\pi$, so $s$ is the interval size measured in units of the interparticle distance. Noting that $K_N(x,x) = N\rho(x) = N\sqrt{2-x^2}/\pi$, we write

$$\begin{aligned}
\mathrm{Var}(N_{[-L,L]}) &= \left\langle N_{[-L,L]}^2 \right\rangle - \left\langle N_{[-L,L]} \right\rangle^2 \\
&= \int_{-L}^{L} K_N(x,x)\mathrm{d}x - \int_{-L}^{L}\int_{-L}^{L} K_N(x,y)^2 \mathrm{d}x\mathrm{d}y && (5.20)\\
&= \int_{-s}^{s} \sqrt{1-\left(\frac{u\pi}{\sqrt{2}N}\right)^2}\mathrm{d}u - \int_{-s}^{s}\int_{-s}^{s} \frac{\pi^2}{2N^2} K\left(\frac{u\pi}{\sqrt{2}N}, \frac{u'\pi}{\sqrt{2}N}\right)^2 \mathrm{d}u\mathrm{d}u' && (5.21)\\
&\xrightarrow{N\to\infty} 2s - \int_{-s}^{s}\int_{-s}^{s} \left(\frac{\sin(\pi(u-u'))}{\pi(u-u')}\right)^2 \mathrm{d}u\mathrm{d}u' && (5.22)\\
&= 2s - 2\int_0^{2s} (2s-v)\left(\frac{\sin(\pi v)}{\pi v}\right)^2 \mathrm{d}v && (5.23)
\end{aligned}$$

This integral can be analyzed in two different limits. When $s \to 0$, we obtain the limit when the interval is small even compared to the average interparticle distance. When $s \to \infty$, we are observing the behavior for an interval small with respect to the whole spectrum and large with respect to the interparticle distance. This latter limit was studied by Dyson and Mehta, and both limits yield

$$2s - 2\int_0^{2s} (2s-v)\left(\frac{\sin(\pi v)}{\pi v}\right)^2 \mathrm{d}v = \begin{cases} \frac{1}{\pi^2}\left(\log s + 1 + \gamma + \log(4\pi)\right), & \text{for } s \to \infty \\ 2s(1-s) & \text{for } s \to 0 \end{cases} \quad (5.24)$$

Replacing the value of $s$ for GUE we obtain for $s$ large, *i.e.* $L \gg 1/N$

$$\mathrm{Var}(N_{[-L,L]}) = \frac{1}{\pi^2}\log(NL) + \underbrace{\frac{1}{\pi^2}\left(\frac{5}{2}\log 2 + 1 + \gamma\right)}_{=B_2}. \quad (5.25)$$

Dyson and Mehta calculated this variance for values of $\beta = 1$, 2 and 4, and found that, in the bulk limit, we have

$$\left\langle (N_{\mathcal{I}} - \langle N_{\mathcal{I}}\rangle)^2 \right\rangle \sim \frac{2}{\beta\pi^2}\log(NL) + B_\beta, \quad (5.26)$$

where $B_\beta$ is a constant determined depending on $\beta$ (see Appendix A.38 of [100]).

The comparison of equation (5.26) with the variance with independent variables, whose variance behaves linearly with the size of the interval in the bulk limit, reveals that the all-in-all correlations brought by the Vandermonde determinant reduce the fluctuations of eigenvalues inside the interval. This result depends only on the behavior of the eigenvalues around the origin, the so-called sine kernel in the bulk limit (equation (4.87)). Since Gaussian, Wishart and Cauchy all share the sine kernel in this limit, this result holds for all three ensembles when considering the interval $\mathcal{I}$ to have dimensions of the order of the interparticle distance.

After Dyson and Mehta, interest in the variable $N_{\mathcal{I}}$ re-emerged as this quantity was studied in different contexts, such as quantum chaos [9] and statistics of unitary matrices [39]. These references contain conjectures and results that foreshadow a greater theorem, proven by Costin and Lebowitz [33], which states

**Theorem 1** *Let $N(L)$ be the number of eigenvalues, in an interval of length $L$, of a $N \times N$ matrix chosen at random from the Gaussian ensemble. We consider the case $N \to \infty$ and $L \to \infty$ in the bulk-limit. Then all cumulants of the variable $\zeta = [N(L) - \langle N(L) \rangle]/\sqrt{\log L}$ approach those of a Gaussian distribution.*

While this is the original statement of the theorem, further work has shown that this result is much more general. Generalizations of this theorem can be found in [73, 74, 127]. Historically, Wigner calculated the first moment of $N_{\mathcal{I}}$, Dyson and Mehta calculated the second moment for $N_{\mathcal{I}}$ when $|\mathcal{I}|$ is small and Costin and Lebowitz proved that the following moments of $N_{\mathcal{I}}$ in this limit tend to zero.

Parallel to Costin and Lebowitz's result, and closely related to the work presented in this thesis, Fogler and Shklovskii [54] showed that the probability density of the quantity $N_{\mathcal{I}}$ for any invariant random matrix, in Dyson's bulk limit, is given asymptotically and for typical fluctuations (small values of $\delta N$) around the average by

$$P(N_{\mathcal{I}}) \approx \exp\left(-\frac{\pi^2\beta}{4}\frac{\delta N^2}{\log(\langle N_{\mathcal{I}}\rangle/\delta N) + B}\right), \tag{5.27}$$

where $\delta N = N_{\mathcal{I}} - \langle N_{\mathcal{I}}\rangle$ and $B$ depends weakly on $\delta N$. This result was obtained by taking the Coulomb-gas analogy further and transforming the spectral statistics problem into the calculation of the average charge density for a two-dimensional semi infinite split-gate device.

### 5.3.2 Number variance in the edge limit

We proceed to calculate the number variance for the interval $\mathcal{I} = [-L, L]$ when $L$ is very close to the soft edge of the distribution and $\beta = 2$. We take the case of GUE, where the edge is $\sqrt{2}$. This calculation is valid for every ensemble with a soft edge, in particular the Wishart ensemble can be calculated using the same procedure. This is possible due to the universality of the Airy kernel in the edge regime.

For Gaussian unitary matrices, with $\beta = 2$, we recall equation (5.18):

$$\mathrm{Var}(N_{\mathcal{I}}) = \int_{\mathcal{I}} K_N(x,x)\mathrm{d}x - \int_{\mathcal{I}}\int_{\mathcal{I}} K_N(x,y)^2 \mathrm{d}x\mathrm{d}y, \tag{5.28}$$

where $K_N(x,y)$ is the Christoffel-Darboux kernel

$$K_N(x,y) = \sqrt{\frac{N}{\pi}}\frac{1}{2^N(N-1)!}\mathrm{e}^{-N\frac{x^2+y^2}{2}}\frac{H_N(x\sqrt{N})H_{N-1}(y\sqrt{N}) - H_N(y\sqrt{N})H_{N-1}(x\sqrt{N})}{\sqrt{N}(x-y)}, \tag{5.29}$$

and $H_N(x)$ are Hermite polynomials. The kernel satisfies the property

$$\int_{-\infty}^{\infty} \mathrm{d}z K_N(x,z)K_N(z,y) = K_N(x,y) \tag{5.30}$$

as well as the symmetry relation

$$K_N(-x,-y) = K_N(x,y), \tag{5.31}$$

and the average density may be written as $K_N(x,x) = N\rho_{sc}(x)$, where $\rho_{sc}(x) = \sqrt{2-x^2}/\pi$ is the semicircle.

In the $L$-box case, we have $\mathcal{I} = [-L, L]$. We split the integral (5.28) in three contributions

$$\begin{aligned}\int_{-L}^{L}\mathrm{d}x\left(\int_{-\infty}^{-L}\mathrm{d}y + \int_{L}^{\infty}\mathrm{d}y\right) K_N(x,y)^2 = \int_{-L}^{\infty}\mathrm{d}x\int_{-\infty}^{-L}\mathrm{d}y K_N(x,y)^2 + \int_{L}^{\infty}\mathrm{d}x\int_{-\infty}^{L}\mathrm{d}y K_N(x,y)^2 \\ - 2\int_{L}^{\infty}\mathrm{d}x\int_{-\infty}^{-L}\mathrm{d}y K_N(x,y)^2.\end{aligned} \tag{5.32}$$

We notice that the first two terms of the RHS of equation (5.32) are $\mathrm{Var}(N_{(-\infty,L]})$ and $\mathrm{Var}(N_{[L,\infty]})$, respectively. It remains to show that, when $L$ is near $\sqrt{2}$, the last term of the RHS vanish when $N$ is large. We place ourselves in the *edge* regime, where the value of $L$ is close to $\sqrt{2}$ and we define the scaled variable $s = (L-\sqrt{2})\sqrt{2}N^{2/3}$. When $s$ is of order 1, this is the region in which the kernel behaves asymptotically as the Airy kernel [134, 135]

$$K_N\left(\sqrt{2}+\frac{u}{\sqrt{2}N^{2/3}}, \sqrt{2}+\frac{v}{\sqrt{2}N^{2/3}}\right) \overset{\text{large } N}{\sim} \sqrt{2}N^{2/3}K_{\mathrm{Ai}}(u,v)\ , \tag{5.33}$$

$$K_{\mathrm{Ai}}(u,v) = \frac{\mathrm{Ai}(u)\mathrm{Ai}'(v) - \mathrm{Ai}(v)\mathrm{Ai}'(u)}{u-v}\ , \tag{5.34}$$

where $\mathrm{Ai}(x)$ is the Airy function. We study the last term of the RHS of (5.32) in this regime. By changing variables $x = \sqrt{2}+\frac{u}{\sqrt{2}N^{2/3}}$, $y = \sqrt{2}+\frac{v}{\sqrt{2}N^{2/3}}$ and applying the large $N$ limit we find

$$2\int_{L}^{\infty}\mathrm{d}x\int_{-\infty}^{-L}\mathrm{d}y K_N(x,y)^2 \overset{\text{large } N}{\longrightarrow} 2\int_{s}^{\infty}\mathrm{d}u\int_{-\infty}^{-4N^{2/3}-s}\mathrm{d}v K_{\mathrm{Ai}}(u,v)^2 \to 0. \tag{5.35}$$

Since the integrand is finite and the domain on integration shrinks to zero as $N$ increases, this term is negligible for any $s$ in this scaling and, using the box symmetry, we may write

$$\mathrm{Var}\left(N_{[-L,L]}\right) \overset{\text{large } N}{\sim} \mathrm{Var}\left(N_{(-\infty,-L]}\right) + \mathrm{Var}\left(N_{[L,\infty)}\right) = 2\,\mathrm{Var}\left(N_{[L,\infty)}\right), \text{ for } L\sim\sqrt{2}, \tag{5.36}$$

which is expected, since, for large $N$ and when $L$ is around the edge, the intervals $(-\infty,-L]$ and $[L,\infty)$ are sufficiently far apart and the variables $N_{(-\infty,-L]}$ and $N_{[L,\infty)}$ can be treated as independent variables when fluctuating around their average values.

Writing $\mathrm{Var}(N_{[-L,L]})$ as the sum (5.36) is convenient because asymptotics of $\mathrm{Var}(N_{[L,\infty)})$ are known, they were obtained in [62] using asymptotics of the Airy kernel. Using the scaling $s = (L - \sqrt{2})\sqrt{2}N^{2/3}$ we find

$$2\,\mathrm{Var}\left(N_{[L,\infty)}\right) = \tilde{V}_2(s) = 2\int_s^\infty \mathrm{d}u \int_{-\infty}^s \mathrm{d}v K_{\mathrm{Ai}}^2(u,v). \tag{5.37}$$

The variance of the number of eigenvalues inside the $L$-box is, in the edge regime for $\beta = 2$, given by

$$\mathrm{Var}(N_{[-L,L]}) = \tilde{V}_2(s), \quad \text{for } L = \sqrt{2} + \frac{s}{\sqrt{2}N^{2/3}}. \tag{5.38}$$

Asymptotics of $\tilde{V}_2(s)$ on the scaling variable $s$, studied by [62], are given by

$$\tilde{V}_2(s) \sim \begin{cases} \frac{3}{2\pi^2}\ln|s|, & \text{for } s \to -\infty \\ \frac{1}{8\pi s^{3/2}}\exp\left(-\frac{4}{3}s^{3/2}\right), & \text{for } s \to \infty \end{cases}. \tag{5.39}$$

The asymptotic behavior of the number variance at the edge is not a trivial result, and involves a series of long calculations and we refer to [62] for the complete derivation of this result.

## 5.4 The moment generating function

The average and variance of $N_{\mathcal{I}}$ are not the only moments that can be expressed as integrals of the kernel, all moments of $N_{\mathcal{I}}$ can be written as a sum of integrals of $K_N(x,y)$. One very important result of determinantal point processes is the relation between moment generating function, kernel and probability, which we will explore in this section. We present a systematic procedure to obtain all moments of $N_{\mathcal{I}}$ in terms of the kernel and introduce elements, such as the overlap matrix and the Fredholm determinant, that are fundamental for the analysis of the counting problem. A more complete presentation of these techniques can be found in [56, 100].

### 5.4.1 Definition

We recall the definition of the moment generating function.

$$\chi_B(z) = \left\langle (1-z)^{N_B} \right\rangle = \sum_{N_B} (1-z)^{N_B} P(N_B), \tag{5.40}$$

where $P(N_B)$ is the p.d.f. of the variable $N_B$. The expansion of $\chi_B(z)$ around $z = 0$ provides all moments of the distribution of $N_B$, and this object yields information about many properties of the counting statistics of a process, as we will see. Using the fact that that $\mathbb{1}_B(x)$ can only take values zero and one, we may write

$$\chi_B(z) = \left\langle (1-z)^{N_B} \right\rangle = \left\langle (1-z)^{\sum_{i=1}^N \mathbb{1}_B(x_i)} \right\rangle = \left\langle \prod_{i=1}^N (1-z)^{\mathbb{1}_B(x_i)} \right\rangle \tag{5.41}$$

$$= \left\langle \prod_{i=1}^{N} [1 - z\mathbb{1}_B(x_i)] \right\rangle = \int \prod_{i=1}^{N} [1 - z\mathbb{1}_B(x_i)]\, P(\boldsymbol{x}) \mathrm{d}x_1 \dots \mathrm{d}x_N. \tag{5.42}$$

The expected value of the polynomial $\prod_{i=1}^{N} [1 - z\mathbb{1}_B(x_i)]$ is our main object of interest. We may expand its first few terms to observe its general form. For $N = 2$ we obtain

$$[1 - z\mathbb{1}_B(x_1)]\,[1 - z\mathbb{1}_B(x_2)] = 1 - z\,[\mathbb{1}_B(x_1) + \mathbb{1}_B(x_2)] + z^2 \mathbb{1}_B(x_1)\mathbb{1}_B(x_2). \tag{5.43}$$

For $N = 3$ we obtain

$$\begin{aligned} \prod_{i=1}^{3} [1 - z\mathbb{1}_B(x_i)] =& 1 - z\,[\mathbb{1}_B(x_1) + \mathbb{1}_B(x_2) + \mathbb{1}_B(x_3)] \\ &+ z^2\,[\mathbb{1}_B(x_1)\mathbb{1}_B(x_2) + \mathbb{1}_B(x_2)\mathbb{1}_B(x_3) + \mathbb{1}_B(x_3)\mathbb{1}_B(x_1)] \\ &- z^3 \mathbb{1}_B(x_1)\mathbb{1}_B(x_2)\mathbb{1}_B(x_3). \end{aligned} \tag{5.44}$$

We deduce that the general form of the $k$-th coefficient $c_k$ of this polynomial is

$$\prod_{i=1}^{N} [1 - z\mathbb{1}_B(x_i)] = \sum_{k=0}^{N} c_k z^k, \qquad c_k = (-1)^k \sum_{\sigma} \left[\mathbb{1}_B(x_{\sigma(1)}) \dots \mathbb{1}_B(x_{\sigma(k)})\right], \tag{5.45}$$

where $\sigma$ represents the $\binom{N}{k}$ permutations of $N$ index in groups of $k$.

The expected value of each product of $\mathbb{1}_B(x_1) \dots \mathbb{1}_B(x_k)$ can be written in terms of correlation functions. We recall the correlation function $R_k$.

$$R_k(x_1, \dots, x_k) = \frac{N!}{(N-k)!} \int P(\boldsymbol{x}) \mathrm{d}x_{k+1} \dots \mathrm{d}x_N \tag{5.46}$$

It follows from this definition that

$$\int \mathbb{1}_B(x_1) \dots \mathbb{1}_B(x_k) P(\boldsymbol{x}) \mathrm{d}x_1 \dots \mathrm{d}x_N = \int_B \mathrm{d}x_1 \dots \mathrm{d}x_k \int P(\boldsymbol{x}) \mathrm{d}x_{k+1} \dots \mathrm{d}x_N \tag{5.47}$$

$$= \frac{(N-k)!}{N!} \int_B R_k(x_1, \dots, x_k) \mathrm{d}x_1 \dots \mathrm{d}x_k. \tag{5.48}$$

We recall that all correlation functions of a determinantal point process can be written as a determinant of its kernel $K_N(x, y)$ (equation (4.59)).

$$R_n(x_1, \dots, x_n) = \det\left[K_N(x_i, x_j)\right]_{1 \le i,j \le n}, \tag{5.49}$$

and the moment generating function can then be written as

$$\chi_B(z) = \sum_{k=0}^{N} \frac{(-1)^k z^k}{k!} \int_B R_k(z_1, \dots, x_k) \mathrm{d}x_1 \dots \mathrm{d}x_k \tag{5.50}$$

$$= \sum_{k=0}^{N} \frac{(-z)^k}{k!} \int_B \det\left[K_N(x_i, x_j)\right]_{1 \le i,j \le k} \mathrm{d}x_1 \dots \mathrm{d}x_k = \sum_{N_B=0}^{N} (1-z)^{N_B} P(N_B). \tag{5.51}$$

This means that if we know the kernel, in principle, we can determine $\chi_B(z)$ and, therefore, $P(N_B)$. One particular limit of the moment generating function is its value when $z \to 1$. Since the polynomial $(1-z)^{N_B}$ is null for all powers of $N_B$ except $N_B = 0$, the moment generating function in this limit corresponds to the *hole probability*, the probability of finding zero eigenvalues inside the interval $B$.

$$\lim_{z\to 1} \chi_B(z) = P(N_B = 0). \tag{5.52}$$

As discussed above, the kernel of a determinantal point process can be expressed as a sum of products of orthogonal functions. We take $\beta = 2$. We write

$$P(\boldsymbol{x}) = \frac{1}{N!} \det[\phi_i(x_j)] \det[\phi_i(x_j)]. \tag{5.53}$$

And the moment generating function will be written as

$$\chi_B(z) = \left\langle \prod_{i=1}^{N} (1 - z\mathbb{1}_B(x_i)) \right\rangle = \frac{1}{N!} \int \prod_{i=1}^{N} (1 - z\mathbb{1}_B(x_i)) \det[\phi_i(x_j)] \det[\phi_i(x_j)] \prod_i \mathrm{d}x_i. \tag{5.54}$$

This integral of determinants can be refolded into the determinant of a single integral, using a powerful identity proven by Andréief [7].

**Theorem 2 (Andréief's (or Cauchy-Binet) identity)** *Let $f$ and $g$ be integrable real functions. Then*

$$\int \cdots \int_{\mathbb{R}^n} \det\left[f_i(x_j)\right] \det\left[g_i(x_j)\right] \prod_{i=1}^{n} \mathrm{d}\mu(x_i) = n! \det\left[\int_{\mathbb{R}} f_i(x) g_j(x) \mathrm{d}\mu(x)\right]. \tag{5.55}$$

This powerful algebraic identity allows us to exchange the multiple integral of determinants by the determinant of a single integral. This result can be easily proven by expanding the determinants as a sum of permutations and folding the result back into a single determinant (see appendix B of [120]). We may incorporate the polynomial $\prod_{i=1}^{N}(1 - z\mathbb{1}_B(x_i))$ into the measure $\mathrm{d}x$:

$$(1 - z\mathbb{1}_B(x_i))\mathrm{d}x_i = \mathrm{d}\mu(x_i). \tag{5.56}$$

And $\chi_B(z)$ can be refolded using Andréief's identity (5.55)

$$\begin{aligned}
\chi_B(z) &= \det\left[\int (1 - z\mathbb{1}_B(x))\phi_i(x)\phi_j(x)\mathrm{d}x\right] \\
&= \det\left[\int \phi_i(x)\phi_j(x)\mathrm{d}x - z\int \mathbb{1}_B(x)\phi_i(x)\phi_j(x)\mathrm{d}x\right] \qquad (5.57) \\
&= \det\left[\delta_{ij} - z\int_B \phi_i(x)\phi_j(x)\mathrm{d}x\right]. \qquad (5.58)
\end{aligned}$$

The moment generating function can thus be fully determined by $\int_B \phi_i(x)\phi_j(x)\mathrm{d}x$. This is a very special object, named the *overlap matrix*, and it is the key to connect the moment generating function, kernel and number statistics. We explore this connection in the next section.

### 5.4.2 The overlap matrix

We take a determinantal point process whose orthogonal functions are given by the family $\{\phi_i(x)\}$. We define the overlap matrix $A = \{A_{ij}\}$ for the counting statistics of the interval $B$ such that

$$A_{ij} = \int_B \phi_i(x)\phi_j(x)\mathrm{d}x. \tag{5.59}$$

Naturally, if $B = \mathbb{R}$, the overlap matrix is the identity, by orthogonality of the family of functions $\{\phi_i(x)\}$. We denote the eigenvalues of the overlap matrix by $\{a_i\}$. According to equation (5.58), we have

$$\chi_B(z) = \left\langle (1-z)^{N_B} \right\rangle = \sum_{N_B} (1-z)^{N_B} P(N_B) = \det[\mathbb{1} - zA] = \prod_{i=1}^{N} (1 - za_i). \tag{5.60}$$

This shows that the knowledge of the eigenvalues of the overlap matrix is enough to obtain the moment generating function. The hole probability can also be cast in terms of eigenvalues of the overlap matrix.

$$\chi_B(z=1) = \lim_{z\to 1} \sum_{N_B} (1-z)^{N_B} P(N_B) = P[N_B = 0] = \det[\mathbb{1} - A] = \prod_{i=1}^{N} (1 - a_i). \tag{5.61}$$

So far, we have not used the kernel. The connection between the overlap matrix and the kernel can be obtained by exploring the eigenvectors of $A$. Let

$$\sum_j A_{ij} C_j^{(a)} = a C_i^{(a)}, \tag{5.62}$$

where $C_j^{(a)}$ are the eigenvectors of the overlap matrix associated with the eigenvalue $a$. We recall the definition of the kernel in terms of the orthogonal functions $\{\phi_i\}$

$$K_N(x,y) = \sum_{k=1}^{N} \phi_k(x)\phi_k(y). \tag{5.63}$$

We define the function

$$\psi^{(a)}(x) = \sum_{j=1}^{N} C_j^{(a)} \phi_j(x). \tag{5.64}$$

We will show that the function $\psi^{(a)}(x)$ is in fact an eigenfunction of the Fredholm operator of kernel $K_N(x,y)$ associated with the eigenvalue $a$. We consider the following integral

$$\int_B K_N(x,y)\psi^{(a)}(y)\mathrm{d}y = \int_B \left[\sum_{k=1}^{N} \phi_k(x)\phi_k(y)\right] \left[\sum_{j=1}^{N} C_j^{(a)} \phi_j(y)\right] \mathrm{d}y \tag{5.65}$$

$$= \sum_{k,j} \phi_k(x) C_j^{(a)} \underbrace{\int_B \phi_k(y)\phi_j(y)\mathrm{d}y}_{A_{kj}} \tag{5.66}$$

$$= \sum_{k,j} \phi_k(x) A_{kj} C_j^{(a)} \tag{5.67}$$

$$= \sum_{k,j} \phi_k(x)\, a\, C_j^{(a)} = a\psi^{(a)}(x). \tag{5.68}$$

So we can find the eigenvalues of the overlap matrix, and hence the moment generating function, by solving the Fredholm integral equation

$$\int_B K_N(x,y)\psi^{(a)}(y)\mathrm{d}y = a\psi^{(a)}(x). \tag{5.69}$$

We note that $K_N(x,y)$ is a trace-class operator in which the integral

$$\mathrm{Tr}_B K = \int_B K_N(x,x)\mathrm{d}x, \tag{5.70}$$

is well defined. This implies that the determinant $\det(\mathbb{1} - K)$ is also well defined and yields

$$\det(\mathbb{1} - K) = e^{-\sum_{n=1}^{\infty} \frac{\mathrm{Tr}K^n}{n}}, \tag{5.71}$$

where

$$\mathrm{Tr}K^n = \int \mathrm{d}x_1 \ldots \mathrm{d}x_n K_N(x_1,x_2)K_N(x_2,x_3)\ldots K_N(x_n,x_1). \tag{5.72}$$

Using this fact, we may write the moment generating function as

$$\chi_B(z) = \det(\mathbb{1} - zA) = \prod_{i=1}^{N}(1 - za_i) = \det[\mathbb{1} - zP_B K P_B] = e^{-\sum_{n=1}^{\infty} \frac{z^n}{n}\mathrm{Tr}_B(K_N^n)}, \tag{5.73}$$

where $P_B$ restricts the integration to the interval $B$, transforming the trace into a partial trace on $B$. Equation (5.73) is a Fredholm determinant of the kernel $K$. From this equation, we may also write the hole probability as a function of the kernel.

$$P(N_B = 0) = \lim_{z\to 1} \chi_B(z) = \det\left[\mathbb{1} - P_B K P_B\right] = e^{-\sum_{n=1}^{\infty} \frac{1}{n}\mathrm{Tr}_B K^n}. \tag{5.74}$$

And we also remark that the overlap matrix $A$ and the restricted kernel $P_B K P_B$ have the same eigenvalues, and, as a consequences, $\mathrm{Tr}_B K^n = \mathrm{Tr}A^n, \forall n$.

Finally, we want to write the third moment of $N_B$ as integrals of the kernel. We first expand the LHS of equation (5.73) to obtain the coefficient of $z^3$ term

$$\chi_B(z) = \left\langle (1-z)^{N_B} \right\rangle = 1 - \langle N_B \rangle z + \frac{\langle N_B(N_B-1)\rangle}{2!}z^2 - \frac{\langle N_B(N_B-1)(N_B-2)\rangle}{3!}z^3 + O(z^4) \tag{5.75}$$

And we expand the RHS to retrieve the matching coefficient of $z^3$

$$e^{-\sum_{n=1}^{\infty} \frac{z^n}{n}\mathrm{Tr}_B(K_N^n)} = \exp\left[-z\mathrm{Tr}_B(K_N) - \frac{z^2}{2}\mathrm{Tr}_B(K_N^2) - \frac{z^3}{3}\mathrm{Tr}_B(K_N^3) + O(z^4)\right] \tag{5.76}$$

$$= 1 - z\mathrm{Tr}_B(K_N) + \frac{\mathrm{Tr}_B(K_N)^2 - \mathrm{Tr}_B(K_N^2)}{2}z^2$$

$$- \left[\mathrm{Tr}_B(K_N)^3 - 3\mathrm{Tr}_B(K_N)\mathrm{Tr}_B(K_N^2) + 2\mathrm{Tr}_B(K_N^3)\right] \frac{z^3}{6} + O(z^4). \tag{5.77}$$

We compare the $z^3$ coefficients to obtain

$$\langle N_B(N_B-1)(N_B-2)\rangle = \mathrm{Tr}_B(K_N)^3 - 3\mathrm{Tr}_B(K_N)\mathrm{Tr}_B(K_N^2) + 2\mathrm{Tr}_B(K_N^3). \tag{5.78}$$

Since we know the expression of $\langle N_B^2\rangle$ and $\langle N_B\rangle$ in terms of integrals of the kernel, we can show that

$$\mu_3 = \left\langle (N_B - \langle N_B\rangle)^3 \right\rangle = \mathrm{Tr}_B(K_N) - 3\mathrm{Tr}_B(K_N^2) + 2\mathrm{Tr}_B(K_N^3) \tag{5.79}$$

$$= \int_B K_N(x,x)\mathrm{d}x - 3\int_B\int_B K_N(x,y)^2\mathrm{d}x\mathrm{d}y + 2\int_B\int_B\int_B K_N(x,y)K_N(y,z)K_N(z,x)\mathrm{d}x\mathrm{d}y\mathrm{d}z. \tag{5.80}$$

The third moment is very different from the variance, and we see coefficients for the integrals of the kernel that are not evident. This shows the interest of obtaining a systematic approach to calculation of higher moments of counting statistics.

## 5.5 An example: statistics of the maximum eigenvalue

We will apply the techniques presented above to a specific example: the probability distribution of the largest eigenvalue of a Gaussian random matrix. We define $B = [M, \infty)$, and we note that the hole probability of $B$ is equivalent to the cumulative distribution of the largest eigenvalue

$$P(N_B = 0) = P\left(\text{interval } [M,\infty) \text{ is empty}\right) = P\left(\text{all eigenvalues} \leq M\right) = P\left(x_{\max} \leq M\right). \tag{5.81}$$

We place ourselves in the edge regime

$$x = \sqrt{2} + \frac{u}{\sqrt{2}N^{\frac{2}{3}}} \quad \text{and} \quad y = \sqrt{2} + \frac{v}{\sqrt{2}N^{\frac{2}{3}}}. \tag{5.82}$$

Let $P\left(x_{\max} \leq M\right) = Q(M)$ be the cumulative distribution of the largest eigenvalue of GUE. Then

$$Q(M) = e^{-\sum_{n=1}^{\infty}\frac{1}{n}\mathrm{Tr}_B K^n}. \tag{5.83}$$

As we discussed before, the GUE kernel converges to the Airy kernel in this regime, as in equation (4.91). The traces of the powers of the kernel become

$$\mathrm{Tr}_B K = \int_M^{\infty} K_N(x,x)\mathrm{d}x = \int_{\frac{M-\sqrt{2}}{\sqrt{2}N^{2/3}}}^{\infty} K_{Ai}(u,u)\mathrm{d}u \tag{5.84}$$

$$\mathrm{Tr}_B K^2 = \int_M^\infty K_N(x,y)^2 \mathrm{d}x\mathrm{d}y = \int_{\frac{M-\sqrt{2}}{\sqrt{2}N^{2/3}}}^\infty \int_{\frac{M-\sqrt{2}}{\sqrt{2}N^{2/3}}}^\infty K_{Ai}(u,v)^2 \mathrm{d}u\mathrm{d}v, \tag{5.85}$$

where

$$K_{Ai}(x,y) = \frac{\mathrm{Ai}(x)\mathrm{Ai}'(y) - \mathrm{Ai}(y)\mathrm{Ai}'(x)}{x-y}. \tag{5.86}$$

Hence, in the edge regime we find

$$Q(M) \xrightarrow{M\to\sqrt{2}} \mathcal{F}_2\left[\frac{M-\sqrt{2}}{\sqrt{2}N^{2/3}}\right] = e^{-\sum_{n=1}^\infty \frac{1}{n}\mathrm{Tr}_B K_{Ai}^n}. \tag{5.87}$$

It is remarkable that we can deduce that the probability of the largest eigenvalue of GUE, for typical deviations, will depend on this scaling variable $(M-\sqrt{2})/\sqrt{2}N^{2/3}$ and can be calculated by the exponential of traces of powers of the Airy kernel. This exponential, however, is not simple. In 1994, Tracy and Widom [134] were able to show that this scaling function $\mathcal{F}_2(z)$ can be expressed in a more direct form, as

$$\mathcal{F}_2(z) = e^{-\int_z^\infty (u-z)q^2(u)\mathrm{d}u}, \tag{5.88}$$

where $q(u)$ is the solution of a Painlevé II equation

$$q''(u) = 2q^3(u) + uq(u), \quad q(u) \xrightarrow{u\to\infty} \mathrm{Ai}(u). \tag{5.89}$$

The elements we introduced in this chapter, the moment generating function, overlap matrix and Fredholm determinant, form the pillars of the standard approach to number statistics and the Tracy-Widom distribution is only one of the major breakthroughs obtained by this method. Due to the use of the kernel, this approach is most useful in regions where the behavior of the kernel is known, namely the bulk and edge regime. To deal with larger scales, the mesoscopic bulk or the whole positive semi-line, the Coulomb gas method is a powerful tool; and the results presented here for bulk and edge should match larger scales when the correct limit is taken.

# — 6 —
# Index distribution of random matrices

*Positive anything is better than negative nothing.*

Elbert Hubbard

## 6.1 The index function

It is important to note that most results presented in the previous chapter take place in a very small interval with respect to the size of the support of the density distribution, and only typical fluctuations are considered for the asymptotic analysis. First efforts to overcome this limitation focused on the behavior around the *edge* of the average density distribution [128, 47]. Interest in the edge behavior coincided with the study of $N_{\mathcal{I}}$ for a much larger interval, the positive semi-axis $\mathcal{I} = [0, +\infty)$. The number of eigenvalues larger than a certain threshold $\zeta$ is called the $\zeta$-*index*, and is simply noted *index* when $\zeta = 0$. The index effectively counts the number of positive eigenvalues and we note it $N_{\mathcal{I}} = N_+$.

The importance of the index was first noted by May [99], in the field of theoretical ecology. In his work, May studied a complex system of the form $\frac{\mathrm{d}\boldsymbol{x}}{\mathrm{d}t} = A\boldsymbol{x}$ where the elements $a_{ij}$ of $N \times N$ matrix $A$ were taken from a random distribution of variance $\alpha$ and average zero. He determined that the system was almost surely stable if $\alpha < N^{-1/2}$ and almost surely unstable if $\alpha > N^{-1/2}$, the transition between both regime being sharp, its width scaling as $N^{-2/3}$. When the variance is kept fixed, the system will be almost surely be unstable, the probability of having all eigenvalues negative decreases very fast when the size of the system increases. Although this regime transition obtained by May foreshadowed a much deeper development in random matrix theory, the question of how exactly this probability decreases with $N$ remained unanswered until 2006 [37].

First calculations of this probability for Gaussian matrices were performed by Cavagna *et al.* [32] in the context of multidimensional potential landscapes, the so-called random Hessian model. The set $\{x_i\}$ represents a configuration of the system and $V(\{x_i\})$ is the potential landscape, the system is described by an equation $\frac{\mathrm{d}x_i}{\mathrm{d}t} = \nabla_{x_i} V$. The Hessian matrix $H_{ij} = \mathrm{d}^2 V / \mathrm{d}x_i \mathrm{d}x_j$ defines the nature of the stationary point, and the number of

positive eigenvalues (hence the index) provides information about the typical stability pattern of the system [144].

In absence of more information about the system, a sensible choice for a random Hessian in GOE. This random Gaussian Hessian model was studied in many different contexts and has found use in string theory [131] and cosmology [1].

In [32], the authors were able to show that $N_+$ has typical fluctuations of $\mathcal{O}(\log N)$ for large $N$ around its mean value, and that the distribution of these typical fluctuations is given by a Gaussian distribution whose variance is modulated by $\log N$, i.e., $\operatorname{Var} N_+ \sim \log N/\pi^2$ for $\beta = 1$.

The Gaussian behavior for typical fluctuations of $N_+$ is contrasted with the atypical case where all eigenvalues are positive, $N_+ = N$. This extreme case was considered for the evaluation of the number of stationary points in a Gaussian energy landscape [40]. The asymptotic behavior for large $N$ of the probability density in this case was computed by Dean and Majumdar [37]

$$P(N_+ = N) \approx \mathrm{e}^{-\beta \frac{\log 3}{4} N^2}. \tag{6.1}$$

This stark difference in behavior between the Gaussian typical fluctuations and (6.1) was addressed in [89, 90], where the authors obtained by the Coulomb-gas method the full probability density of the index for the Gaussian ensemble.

During my PhD, I was able to obtain the statistics of the index for the Cauchy ensemble. This case differs from the Gaussian due to the absence of compact support for the average density of eigenvalues. This changes drastically the asymptotic behavior of $\operatorname{Var}(N_+)$, as we will see.

Before describing our results for the Cauchy ensemble, it is instructive to re-derive the result for the Gaussian ensemble using the Coulomb gas technique. This was done in [89, 90] using a slightly different technique that the one presented here. The authors applied Tricomi theorem to solve the main integral equation and also used the resolvent method by guessing the resolvent function, while we present a clear derivation of the resolvent.

## 6.2 Positive eigenvalues of a Gaussian random matrix

### 6.2.1 The Coulomb gas

We want to calculate the full probability density function of the index of a $N \times N$ Gaussian random matrix. We recall the j.p.d.f. of the eigenvalues is given by

$$P(\mathbf{x}) = \frac{1}{Z_{N,\beta}} \mathrm{e}^{-\frac{\beta N}{2} \sum_{i=1}^{N} x_i^2} \prod_{j<k} |x_k - x_j|^\beta. \tag{6.2}$$

The variable $N_+$ has a p.d.f. that reads, by definition

$$P(N_+ = kN) = \frac{1}{Z_{N,\beta}} \int \prod_i \mathrm{d}x_i P(\mathbf{x}) \delta \left( \sum_i \mathbb{1}_{[0,\infty)}(x_i) - kN \right). \tag{6.3}$$

As presented in section 4.1, we apply the Coulomb gas method to obtain the large deviation function for the variable $N_+$. The key is to write the p.d.f. (6.3) as the Gibbs-Boltzmann weight of an associated physical system, use the large-$N$ hypothesis to apply a saddle-point method and derive the large deviation function for $N_+$. We begin by using the exponential representation of the delta to write

$$P(N_+ = kN) = \frac{1}{Z_{N,\beta}} \int \prod_i \mathrm{d}x_i \int \mathrm{d}\mu \mathrm{e}^{-\frac{\beta N}{2}\sum_i x_i^2 + \beta \sum_{k>j} \log|x_k - x_j| + \beta\mu\left(\sum_i \mathbb{1}_{[0,\infty)}(x_i) - kN\right)} \tag{6.4}$$

$$= \frac{1}{Z_{N,\beta}} \int \prod_i \mathrm{d}x_i \int \mathrm{d}\mu \mathrm{e}^{-\beta E(\mathbf{x},\mu)}, \tag{6.5}$$

where

$$E(\mathbf{x},\mu) = N\sum_{i=1}^{N} \frac{x_i^2}{2} - \frac{1}{2}\sum_{i\neq j} \log|x_i - x_j| + \mu\left(\sum_{i=1}^{N} \mathbb{1}_{[0,\infty)}(x_i) - kN\right) \tag{6.6}$$

is said the *e*nergy of the configuration $\{x_i\}$. In section 4.1.1 we mentioned the analogy between the p.d.f. of the eigenvalues of the Gaussian ensemble and an associated system of 2-dimensional charges confined to a line submitted to a harmonic potential. This result still applies to the index case, the p.d.f. (6.5) is also the Gibbs-Boltzmann weight of the same electrostatic system, with a small shift in the potential, a jump of height $\mu$. (see figure 6.1).

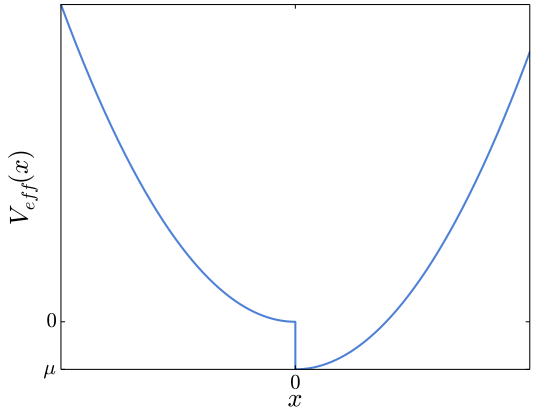


**Figure 6.1** — Sketch of the harmonic potential to which the associated system of equation (6.5) is submitted, for the case $\mu < 0$.

The Lagrange multiplier $\mu$ has the role of ensuring the condition $N_+ = kN$. In the electrostatic analogy, this shift in the potential will ensure that the fraction of positive eigenvalues is indeed $k$. This quantity will be compared to the average fraction of positive eigenvalues, $k^\star = 1/2$, and we expect an abrupt change in the behavior of the system when $k$ goes from $< 1/2$ to $> 1/2$.

To analyze the probability function (6.5), we will transform the discrete approach on the position of the eigenvalues to a continuum functional integral over the density $\rho$, as

described before in section 4.1.2. Re-scaling $\mu \to N^2\mu$ we find

$$E[\mathbf{x}, \mu] \xrightarrow{N \text{ large}} N^2 S[\rho], \tag{6.7}$$

where

$$\begin{aligned} S[\rho] = &\int \frac{x^2}{2}\rho(x)\mathrm{d}x - \frac{1}{2}\iint \rho(x)\rho(x')\log|x-x'|\mathrm{d}x\mathrm{d}x' \\ &+ \mu\left(\int_0^\infty \rho(x)\mathrm{d}x - k\right) + \eta\left(\int_{-\infty}^\infty \rho(x)\mathrm{d}x - 1\right) \end{aligned} \tag{6.8}$$

is the action.

As in the example in section 4.1.2, we added a supplemental Lagrange multiplier $\eta$ to enforce the normalization of the density $\rho$. Using the large-$N$ hypothesis, we apply a saddle-point approximation to the probability function (6.5).

$$\frac{1}{Z_{N,\beta}}\int \prod_i \mathrm{d}x_i \int \mathrm{d}\mu \mathrm{e}^{-\beta N^2 S[\rho]} = \frac{1}{Z_{N,\beta}}\mathrm{e}^{-\beta N^2 S[\rho^\star]}, \tag{6.9}$$

where $\rho^\star$ minimizes the functional $S[\rho]$.

To obtain it, we differentiate (6.8) functionally with respect to $\rho$.

$$\left.\frac{\delta S}{\delta \rho}\right|_{\rho^\star} = 0 = \frac{x^2}{2} - \int \rho^\star(x')\log|x-x'|\mathrm{d}x' + \mu \mathbb{1}_{[0,\infty)} + \eta, \quad x \in \mathrm{supp}(\rho^\star). \tag{6.10}$$

And we differentiate it with respect to $x$ to obtain

$$x + \mu\delta(x) = \fint \frac{\rho^\star(x')}{x-x'}\mathrm{d}x', \quad x \in \mathrm{supp}(\rho^\star), \tag{6.11}$$

where $\fint$ represents the principal part of the integral.

The integral equation (6.11) is very similar to the equation (4.41) solved in section 4.2.2, the only difference being the extra delta factor. We mentioned that equation (6.10) is a balance of energy for the Coulomb gas problem, ensuring that repulsion and potential are balanced in every point of the support of the average density. The calculation of the index adds the Lagrange multiplier $\mu$, which can be interpreted as a *chemical potential* added to the interval $[0, \infty)$. In other words, we are either adding or reducing the energy cost to place a charge on the positive side to force the system to obey the condition $N_+ = kN$.

This interpretation is important to estimate the shape of the average density distribution that will emerge from equation (6.11). In the case $k > \frac{1}{2}$, we are forcing more eigenvalues to be positive than the average value. This is equivalent to add a negative chemical potential. The discontinuity of this potential will create a divergence of charge in zero. Charges on the positive side will stack up at the origin, while charges on the negative side will be repelled by this stacking. This is indeed the image we observe when solving equation (6.11), as we will see.

By this description, it is clear that we expect the support to have multiple disjoint compact parts. This turns the Tricomi theorem into an unfavorable option. Although this was the method used to first calculate this quantity in [89], we prefer using the resolvent option both for convenience and for uniformity with the rest of calculations in this thesis. Some results in this thesis involve a three-cut support, Tricomi's theorem would require extensive calculation that can be more easily performed with the resolvent method.

### 6.2.2 The resolvent method

We recall the resolvent function

$$G(z) = \int \frac{\rho^\star(x)}{z-x}\mathrm{d}x. \tag{6.12}$$

Following the recipe provided in 4.2.2, we multiply both sides of the equation by $\frac{\rho^\star(x)}{z-x}$ and we integrate it over $x$. Our goal is to write equation (6.11) as an algebraic equation on the resolvent, obtain the resolvent and use relation (4.40) to obtain the constrained average density $\rho^\star(x)$, which is the average density submitted to the constraint of having a fraction $k$ of eigenvalues on its positive side.

$$\int x\frac{\rho^\star(x)}{z-x}\mathrm{d}x + \mu\int \delta(x)\frac{\rho^\star(x)}{z-x}\mathrm{d}x = \iint \frac{\rho^\star(x')}{x-x'}\frac{\rho^\star(x)}{z-x}\mathrm{d}x'\mathrm{d}x, \quad x\in\mathrm{supp}(\rho^\star), \tag{6.13}$$

Some regularization is required to perform the integral on the delta, as simply setting $x=0$ in the integrand is not possible because the density $\rho(x)$ diverges at zero. We may regularize this integral by setting $x\to 0+\varepsilon$ and taking $\varepsilon\to 0$. This procedure converges, and the integral is finite and independent of the regularization used. This shows that the contribution of the hard wall to the algebraic equation of the resolvent is simply the pole $A/z$. This is one of the main results of this work, as it is independent of ensemble and position of the wall. As we will see, we can apply this procedure to more general intervals, other ensembles and in all cases the algebraic equation of the resolvent can be adapted by adding an extra term of the order of $z^{-1}$.

Integrating equation (6.11), repeating the same steps described in section 4.2.2, yields

$$-1+G(z)+\frac{A}{z} = \frac{1}{2}G(z)^2, \tag{6.14}$$

whose solution is straightforward

$$G(z) = z\pm\sqrt{\frac{2A-2z+z^3}{z}} = z\pm\sqrt{\frac{(z-b_1)(z-b_2)(z-a)}{z}}. \tag{6.15}$$

The extra term in the algebraic equation $A/z$ brought by the imposition of a hard wall in zero yields, in the resolvent, a square-root convergence in $a$ and a square-root divergence in zero. These pairs of convergence-divergence will appear in all cases of imposition of

hard walls in the spectra, and can be understood in the context of Coulomb gas. The density of charged particles, when confined in excess in a region by a hard wall, will diverge at the wall at will repel the charges on the other side of this wall, creating the square-root convergence. This can be clearly seen in figure 6.2.

While $G$ has only one parameter to be calculated using the fraction $k$, it is convenient to write the resolvent in terms of the roots of the polynomial on the numerator of the square root, as presented in equation (6.15). These roots can be obtained by equating the coefficient of both polynomials.

$$a + b_1 + b_2 = 0 \tag{6.16}$$
$$ab_1 + ab_2 + b_1 b_2 = -2 \tag{6.17}$$

And to the final variable we determine it directly using the condition $\int_0^\infty \rho^\star(x)\mathrm{d}x = k$. Using the identity (4.39), we calculate the average density constrained to the condition of having a fraction $k$ of positive eigenvalues.

$$-\frac{1}{\pi}\mathrm{Im}\left[\lim_{\varepsilon\to 0^+} G(x+i\varepsilon)\right] = \frac{1}{\pi}\sqrt{\frac{(b_1-x)(x-b_2)(x-a)}{x}} = \rho^\star(x). \tag{6.18}$$

We notice how the roots of the polynomial become the edges of the constrained average density, whose support is $[b_1, 0[\cup[a, b_2]$ for the $k < \frac{1}{2}$ case and $[b_1, a]\cup]0, b_2]$ for the $k > \frac{1}{2}$ case. We plot two cases of this density, when $a > 0$ and when $a < 0$. There is a drastic change in behavior on the point $a = 0$, which corresponds to the $k = \frac{1}{2}$ situation, its average value. Naturally, when the fraction of positive eigenvalues is its average value we obtain the non-constrained average density, Wigner's semicircle law. This can be seen clearly in figure 6.2.

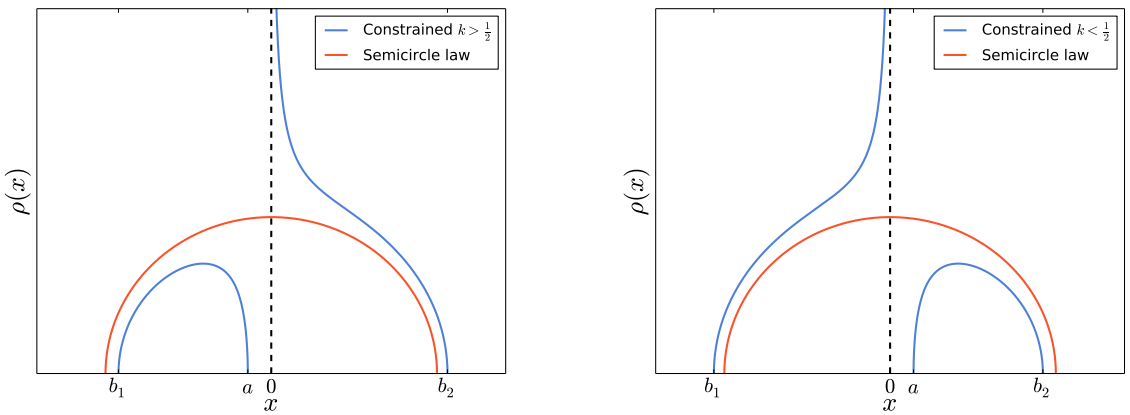


**(a)** **(b)**

**Figure 6.2** — Constrained average density (blue, two support line) and comparison with Wigner's semicircle (orange, single support line) for the index of the Gaussian ensemble in the cases (a) $k > \frac{1}{2}$ and (b) $k < \frac{1}{2}$ (equation (6.18)).

Indeed, we observe the expected divergence at the origin caused by the non-optimal constraint $k \neq k^\star = 1/2$. The eigenvalues diverge at the most populated side of the wall and converge on the opposite side, repelled by the excess of eigenvalues, and the compact single support breaks into two disjoint supports.

### 6.2.3 Obtaining the rate function

Armed with the constrained average density $\rho^\star(x)$, we calculate the full rate function. The p.d.f. of $N_+$ is given by equation (6.9). The partition function $Z_{N,\beta}$ can be easily calculated using the saddle-point method

$$Z_{N,\beta} = \int P(\boldsymbol{x})\mathrm{d}\boldsymbol{x} = \int \mathcal{D}\rho e^{-\beta N^2 S[\rho]} \approx e^{-\beta N^2 S[\rho_{sc}]} \tag{6.19}$$

Since $\rho_{sc}$ is the density that minimizes the functional $S$ without any constraints, it is clear that it is Wigner's semicircle, as calculated in section 4.2. The p.d.f. for $N_+$ becomes

$$P(N_+ = kN) = \frac{1}{Z_{N,\beta}} e^{-\beta N^2 S[\rho^\star]} = e^{-\beta N^2 \psi(k)}, \tag{6.20}$$

where $\psi(k) = S[\rho^\star] - S[\rho_{sc}]$ is called the *rate function*. By its definition, it is clear that $\psi(k)$ reaches its minimum when $k = \frac{1}{2}$.

We recall that the action $S$ calculated in $\rho^\star$ is given by equation (6.8)

$$S[\rho^\star] = \int \frac{x^2}{2}\rho^\star(x)\mathrm{d}x - \frac{1}{2}\iint \rho^\star(x)\rho^\star(x')\log|x-x'|\mathrm{d}x\mathrm{d}x' \tag{6.21}$$

$$+ \mu \underbrace{\left(\int_0^\infty \rho^\star(x)\mathrm{d}x - k\right)}_{=0} + \eta \underbrace{\left(\int_{-\infty}^\infty \rho^\star(x)\mathrm{d}x - 1\right)}_{=0}, \tag{6.22}$$

where we note the null terms, since $\rho^\star$ satisfies both conditions by definition. The remaining terms are one single integral on the quadratic potential and one double integral with a logarithm term. This double integral is problematic, and we can replace it with other terms easier to calculate. We make use of the energy balance equation (6.10) applied to $\rho^\star$ by multiplying it by $\rho^\star(x)$ and integrating it over $x$. This yields

$$\int \rho^\star(x)\frac{x^2}{2}\mathrm{d}x - \iint \rho^\star(x)\rho^\star(x')\log|x-x'|\mathrm{d}x\mathrm{d}x' + \eta \underbrace{\int \rho^\star(x)\mathrm{d}x}_{=1} + \mu \underbrace{\int_0^\infty \rho^\star(x)\mathrm{d}x}_{=k} = 0, \tag{6.23}$$

which can be rewritten as

$$\iint \rho^\star(x)\rho^\star(x')\log|x-x'|\mathrm{d}x\mathrm{d}x' = \int \rho^\star(x)\frac{x^2}{2}\mathrm{d}x - \eta - \mu k. \tag{6.24}$$

This shows that, for the case of $\rho^\star$, the energy balance equation allows us to exchange the double integral by a simple integral summed to the Lagrange multipliers. The final form of the action $S$ calculated for $\rho^\star$ becomes

$$S[\rho^\star] = \frac{1}{4}\int \rho^\star(x)x^2\mathrm{d}x - \frac{\mu k}{2} - \frac{\eta}{2}. \tag{6.25}$$

The calculation of the Lagrange multipliers $\mu$ and $\eta$ is still necessary. To perform it, we explore once again the energy balance equation (6.10). This equation is valid in any point of the support, so we calculate it on the points $a$ and 0. These are edges of the support, and we take the limit in the correct direction to obtain these equation while staying inside the support of $\rho^\star$. For simplicity, we take the case where $k < \frac{1}{2}$, which implies $a > 0$. This yields

$$\frac{a^2}{2} - H(a) + \mu + \eta = 0 \tag{6.26}$$

$$-H(0) + \eta = 0, \tag{6.27}$$

where we defined the function $H(x) = \int \rho(x') \log|x - x'| \mathrm{d}x'$.

From (6.27), we obtain $\eta = H(0)$. While the integral $H(0)$ can be treated directly, we want to avoid dealing with the integral of $\rho(x') \log|x - x'|$. Instead, we replace it in the first equation as it is, and we obtain the value of $\mu$.

$$\mu = H(a) - H(0) - \frac{a^2}{2}. \tag{6.28}$$

Remarkably, since $H$ is the primitive of $G$, the difference $H(a) - H(0)$ can be written as $\int_0^a G(x)\mathrm{d}x$. The final formula for the first Lagrange multiplier is

$$\mu = \int_0^a G(x)\mathrm{d}x - \frac{a^2}{2}. \tag{6.29}$$

Integrals of the resolvent are much easier to calculate than the value of $H$ in any point, so we perform a small manipulation to also obtain $\eta$ as an integral of the resolvent. We note that $b_1$ is the lower edge of the average density. We expand $\log|b_1 - x|$ on $x$. We obtain

$$\int \rho^\star(x) \log|b_1 - x| \mathrm{d}x = \log|b_1| - \int \sum_{n=1}^{\infty} \frac{x^n}{b_1^n} \rho^\star(x) \mathrm{d}x = \log|b_1| - \int_{b_1}^{-\infty} \left( G(x) - \frac{1}{x} \right) \mathrm{d}x. \tag{6.30}$$

Using this relation and applying equation (6.10) to $b_1$ yields

$$\eta = \log|b_1| - \frac{b_1^2}{2} - \int_{b_1}^{-\infty} \left( G(x) - \frac{1}{x} \right) \mathrm{d}x. \tag{6.31}$$

The final formula for the action becomes

$$\begin{aligned} S[\rho^\star] =& \frac{1}{4} \int \rho^\star(x) x^2 \mathrm{d}x - \frac{1}{2} \left( \int_0^a G(x)\mathrm{d}x - \frac{a^2}{2} \right) k \\ & - \frac{1}{2} \left( \log|b_1| - \frac{b_1^2}{2} - \int_{b_1}^{-\infty} \left( G(x) - \frac{1}{x} \right) \mathrm{d}x \right). \end{aligned} \tag{6.32}$$

The value of the action calculated in the semi-circle can be easily performed. The edges of the support collapse into $b_1 = -\sqrt{2}$, $b_2 = \sqrt{2}$ and $a = 0$ for the semicircle, so

the resolvent assumes the form $G(z) = z \pm \sqrt{z^2-2}$. We obtain $\mu = 0$ and the remaining integrals are straightforward. They yield

$$S[\rho_{sc}] = \frac{1}{4\pi}\int x^2\sqrt{2-x^2}\mathrm{d}x - \frac{\log 2}{4} + \frac{1}{2} + \frac{1}{2}\int_{-\sqrt{2}}^{-\infty}\left(x + \sqrt{x^2-2} - \frac{1}{x}\right)\mathrm{d}x = \frac{3}{8} + \frac{\log 2}{4}. \tag{6.33}$$

One last simplification worth mentioning is the integral $\int x^2\rho^\star(x)\mathrm{d}x$. This is the computation of the second moment of the average density, which can also be given by the expansion of the resolvent in orders of $z$

$$G(z) = \int \frac{\rho^\star(x)}{z-x}\mathrm{d}x = \frac{1}{z} + \frac{1}{z^2}\int x\rho^\star(x)\mathrm{d}x + \frac{1}{z^3}\int x^2\rho^\star(x)\mathrm{d}x + \mathcal{O}(z^{-4}). \tag{6.34}$$

Expanding the resolvent (6.15) and applying the normalization conditions (6.16) and (6.17) yields

$$G(z) = \frac{1}{z} + \frac{a(a^2-2)}{2z^2} + \frac{1}{2z^3} + \mathcal{O}(z^{-4}). \tag{6.35}$$

Which implies a result that is surprisingly edge independent

$$\frac{1}{4}\int x^2\rho^\star(x)\mathrm{d}x = \frac{1}{8}. \tag{6.36}$$

The final formula of the rate function is, then

$$\psi(k) = -\frac{1}{2}\left(\int_0^a G(x)\mathrm{d}x - \frac{a^2}{2}\right)k - \frac{1}{2}\left(\log|b_1| - \frac{b_1^2}{2} - \int_{b_1}^{-\infty}\left(G(x) - \frac{1}{x}\right)\mathrm{d}x\right) - \frac{1}{4} - \frac{\log 2}{4}. \tag{6.37}$$

The final formula for the action involves integrals that are analytically complicated, but represent no challenge numerically. We plot the numerical results of this formula in figure 6.3. Indeed, we observe the minimum at $k^\star = 1/2$ and the symmetry, consequence of the reflection invariance of the problem.

### 6.2.4 Variance of the index

The rate function, when plotted with respect to $k$, shows a clear symmetric minimum around $k = 1/2$. This invites us to study typical fluctuations of $k$ around its average, and to explore the variance of the variable $N_+$. Our goal is to expand $\psi(k)$ around $k = \frac{1}{2} + \delta$ for leading terms in small $\delta$, up to $\delta^2$. This expansion is not straightforward, and we proceed in the following way.

We know that when $k = k^\star = 1/2$, the edges $a$, $b_1$ and $b_2$ collapse to 0, $-\sqrt{2}$ and $\sqrt{2}$ respectively. We perturb the edges by a small parameter. We set

$$a = \epsilon, \qquad b_1 = -\sqrt{2} - \epsilon_2, \qquad b_2 = \sqrt{2} - \epsilon_3. \tag{6.38}$$

The normalization condition implies equations (6.16) and (6.17), this yields a relation between the perturbations

$$\epsilon - \epsilon_2 - \epsilon_3 = 0 \tag{6.39}$$

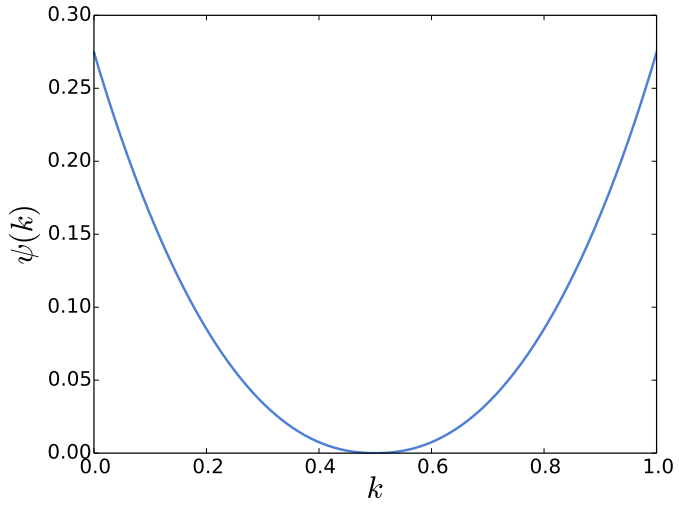


**Figure 6.3** — Rate function $\psi(k)$ for the index of the Gaussian ensemble (equation (6.37)).

$$\epsilon_2 - \epsilon_3 = 0 \tag{6.40}$$

Which implies $\epsilon = 2\epsilon_2 = 2\epsilon_3$. The relation between $\epsilon$ and $\delta$ will be given by the final condition $\int_0^\infty \rho^\star(x)\mathrm{d}x = k = \frac{1}{2} + \delta$. We replace the edges by the perturbed values and we expand the resolvent in powers of $\epsilon$, to perform the integrations required.

Since the cases $k > \frac{1}{2}$ and $k < \frac{1}{2}$ are symmetrical, we focus our attention to the latter, which implies $\epsilon > 0$. This will only play a minor roll when expressing the value of $k$ in terms of $\epsilon$, and both cases provide equivalent results.

### Calculation of $\mu$

We recall the formula for $\mu$ and we replace the edges

$$\mu = \int_0^a G(x)\mathrm{d}x - \frac{a^2}{2} = \int_0^\epsilon \sqrt{\frac{(x-\sqrt{2}+2\epsilon)(x+\sqrt{2}+2\epsilon)(x-\epsilon)}{x}}\mathrm{d}x. \tag{6.41}$$

We will repeat this kind of integration many times in this thesis, and the technique is the same. Since the integrating interval is very small, we split the slow variating and the fast variating parts of the integral and we treat them separately. The slow variating parts can just be evaluated taking $x = 0$ and the perturbation associated to it to be zero, while the fast variating are integrated. The procedure goes as follows

$$\mu = \int_0^\epsilon \sqrt{\frac{(x-\sqrt{2}+\epsilon/2)(x+\sqrt{2}+\epsilon/2)(x-\epsilon)}{x}}\mathrm{d}x = \sqrt{2}\int_0^\epsilon \sqrt{\frac{\epsilon - x}{x}}\mathrm{d}x + o(\epsilon) = \frac{\pi}{\sqrt{2}}\epsilon + o(\epsilon). \tag{6.42}$$

### Calculation of $\eta$

First, we calculate the integral $I = \int_{b_1}^{-\infty} \left(G(x) - \frac{1}{x}\right) \mathrm{d}x$ by splitting the domain of integration into two parts:

$$I = \underbrace{\int_{b_1}^{-\sqrt{2}} \left(G(x) - \frac{1}{x}\right) \mathrm{d}x}_{I_1} + \underbrace{\int_{-\sqrt{2}}^{-\infty} \left(G(x) - \frac{1}{x}\right) \mathrm{d}x}_{I_2}. \tag{6.43}$$

For $I_1$, we proceed as equation (6.42).

$$I_1 = \int_{b_1}^{-\sqrt{2}} \left(x - \frac{1}{x}\right) \mathrm{d}x + \int_{b_1}^{-\sqrt{2}} \sqrt{\frac{(x - \sqrt{2} + \epsilon/2)(x + \sqrt{2} + \epsilon/2)(x - \epsilon)}{x}} \mathrm{d}x \tag{6.44}$$

$$= -\frac{\epsilon}{2\sqrt{2}} + 2^{\frac{3}{4}} \int_{b_1}^{-\sqrt{2}} \sqrt{x + \sqrt{2} + \frac{\epsilon}{2}} \mathrm{d}x + o(\epsilon) \tag{6.45}$$

$$= -\frac{\epsilon}{2\sqrt{2}} + o(\epsilon). \tag{6.46}$$

For $I_2$, we expand the integrand in powers of $\epsilon$ and we integrate it term by term from $-\sqrt{2}$ to $-\infty$. The splitting of the domain was important to ensure the convergence of this procedure

$$I_2 = \int_{-\sqrt{2}}^{-\infty} \left(x + \sqrt{x^2 - 2} - \frac{1}{x}\right) \mathrm{d}x + \int_{-\sqrt{2}}^{-\infty} \frac{\epsilon}{x\sqrt{x^2 - 2}} \mathrm{d}x + o(\epsilon) \tag{6.47}$$

$$= -\frac{1}{2} + \log 2 + \frac{\pi\epsilon}{2\sqrt{2}}. \tag{6.48}$$

We add the expansion of $\log |b_1| - b_1^2/2$ to obtain the final result

$$\eta = -\frac{1}{2} - \frac{\log 2}{2} - \frac{\pi\epsilon}{2\sqrt{2}}. \tag{6.49}$$

### Calculation of $k$

We expand the average density in powers of $\epsilon$

$$\rho^\star(x) = \frac{1}{\pi}\sqrt{\frac{(x - \sqrt{2} + \epsilon/2)(x + \sqrt{2} + \epsilon/2)(x - \epsilon)}{x}} = \frac{1}{\pi}\sqrt{2 - x^2} - \frac{\epsilon}{\pi x\sqrt{2 - x^2}} + o(\epsilon). \tag{6.50}$$

The value of $k$ can be easily calculated. We focus our attention to the case $k < \frac{1}{2}$ and $\epsilon > 0$. As they are symmetrical, we will just calculate this case. The value of $k$ is the integral between $a$ and $b_2$, and we calculate each term of the RHS of equation (6.50).

$$\int_a^{b_2} \frac{\sqrt{2 - x^2}}{\pi} \mathrm{d}x = \frac{1}{2} - \frac{\sqrt{2}}{\pi}\epsilon + o(\epsilon), \tag{6.51}$$

$$\int_a^{b_2} \frac{\epsilon}{\pi x\sqrt{2-x^2}}\mathrm{d}x = \frac{3\log 2}{2\sqrt{2}\pi}\epsilon - \frac{1}{\pi\sqrt{2}}\epsilon\log\epsilon + o(\epsilon). \tag{6.52}$$

We keep only the first two dominant orders, so we may write

$$k = \frac{1}{2} + \frac{1}{\pi\sqrt{2}}\epsilon\log\epsilon + o(\epsilon\log\epsilon). \tag{6.53}$$

Where we easily recognize the relation between $\epsilon$, the perturbation of the edges, and $\delta$ the perturbation on the fraction of positive eigenvalues $k$

$$\delta = \frac{1}{\pi\sqrt{2}}\epsilon\log\epsilon. \tag{6.54}$$

**Final expression for $\psi\left(\frac{1}{2}+\delta\right)$**

We sum the terms calculated above and, after an impressive sequence of simplifications, we obtain

$$\psi\left(\frac{1}{2}+\delta\right) = -\frac{\mu k}{2} - \frac{\eta}{2} - \frac{1}{4} - \frac{\log 2}{4} = -\frac{\pi}{2\sqrt{2}}\epsilon\delta + o(\epsilon\delta). \tag{6.55}$$

As expected, the constant term was compensated by the normalization constant $S[\rho_{sc}]$ and the linear term vanished when expanding around the minimum. The remaining term is of quadratic order, but it remains to express $\epsilon$ in terms of $\delta$ to be able to read the variance from it. We use equation (6.54). The inverse cannot be expressed by simple functions, but we may use the fact that both $\epsilon$ and $\delta$ are small to provide the following *ansatz*, correct to leading order in $\epsilon$ and $\delta$

$$\epsilon = \pi\sqrt{2}\frac{\delta}{\log\delta}. \tag{6.56}$$

This relation can be verified by inserting it in (6.54) and checking that it holds for leading order in $\delta$. The rate function becomes

$$\psi\left(\frac{1}{2}+\delta\right) = -\frac{\pi^2}{2}\frac{\delta^2}{\log\delta} + o\left(\frac{\delta^2}{\log\delta}\right). \tag{6.57}$$

As we are interested in typical fluctuations of $N_+$ around its mean $N/2$, we assume $N_+ - N/2 \ll N$. This result allows us to write

$$\log\delta = \log\left(\frac{N_+ - \frac{N}{2}}{N}\right) \approx -\log N. \tag{6.58}$$

The rate function for typical fluctuations the variable $N_+$ becomes

$$\psi(N_+) \approx \frac{\pi^2}{2N^2}\frac{(N_+ - \frac{N}{2})^2}{\log N}. \tag{6.59}$$

The p.d.f. for typical fluctuations of $N_+$ is, therefore

$$P(N_+) = e^{-\beta N^2 \psi(N_+)} \approx e^{-\beta \frac{\pi^2}{2} \frac{(N_+ - \frac{N}{2})^2}{\log N}}, \tag{6.60}$$

which yields the leading behavior of the variance for typical fluctuations

$$\operatorname{Var} N_+ = \frac{1}{\beta \pi^2} \log N + \text{cte} + o(1). \tag{6.61}$$

Agreeing with results found in [32] for $\beta = 1$ and with the full result found in [89, 90]. The constant term is very difficult to be determined using the Coulomb gas method, but it was found in [90] for $\beta = 2$ and is given by $\text{cte} = \frac{\gamma + 1 + 3\log 2}{2\pi^2} \approx 0.1852...$.

### 6.2.5 Comparison with numerics

We compare the slope of formula (6.61) and numerical simulations from eigenvalues of GOE ($\beta = 1$) in figure 6.4.

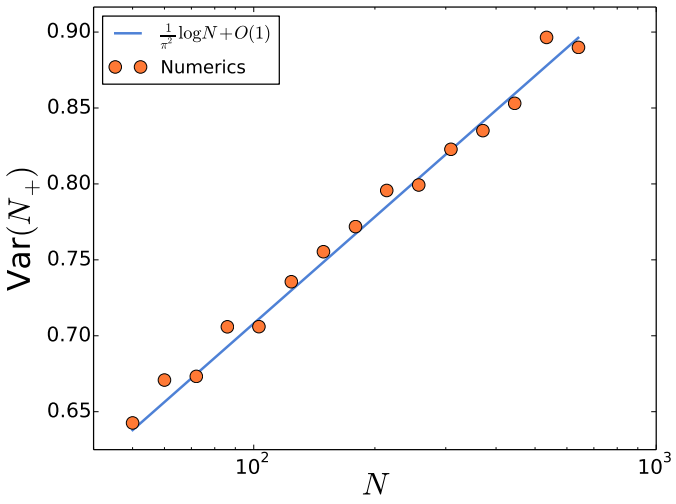


**Figure 6.4** — Comparison between the leading behavior of the variance and numerical simulations for GOE ($\beta = 1$).

## 6.3 Positive eigenvalues of a Cauchy random matrix

During my PhD, I was able to calculate the index distribution for the Cauchy ensemble [96]. This ensemble presents the remarkable property of having an average density of eigenvalues supported on the whole real line, without soft edges like the Gaussian and Wishart cases. A natural question would be: how the fact that eigenvalues can get arbitrarily large affects the fluctuations of the positive eigenvalues? To determine the

behavior of the variance of the index for this ensemble, we proceed with very similar calculations to those performed above for the Gaussian case. The procedure will be similar, but the result presents a fundamental difference emerging from the non-compact support of the average density of eigenvalues in the Cauchy ensemble, as we will see. The technical parts of this session are taken almost verbatim from our calculations in [96].

### 6.3.1 The Coulomb gas

Let $N_+$ be the number of eigenvalues of a Cauchy random matrix larger than zero. The probability density of $N_+$ is by definition

$$P(N_+) = \int \prod_i \mathrm{d}x_i P(\boldsymbol{x}) \delta \left( N_+ - \sum_{j=1}^{N} \theta(x_j) \right), \tag{6.62}$$

where $\theta$ is the Heaviside step function and $P(\boldsymbol{x})$ is defined in (3.27).

We start by writing the j.p.d.f. $P(\boldsymbol{x})$ in exponential form,

$$P(\boldsymbol{x}) \propto e^{-\beta E[\boldsymbol{x}]}, \tag{6.63}$$

where:

$$E[\boldsymbol{x}] = \left( \frac{N-1}{2} + \frac{1}{\beta} \right) \sum_{j=1}^{N} (1 + x_j^2) - \sum_{i>j} \log |x_i - x_j|. \tag{6.64}$$

In the continuum limit, according to the recipe provided in 4.2.2, the multiple integral (6.62) becomes

$$P(N_+, N) = \frac{1}{Z_{N,\beta}} \int \mathcal{D}[\rho] \int d\eta \int d\mu e^{-\beta N^2 S[\rho]}, \tag{6.65}$$

where the action $S$ is given by

$$S[\rho] = \frac{1}{2} \int_{-\infty}^{+\infty} \mathrm{d}x \rho(x) \log(1+x^2) - \frac{1}{2} \int \int_{-\infty}^{+\infty} \mathrm{d}x \mathrm{d}x' \rho(x) \rho(x') \log |x - x'| \tag{6.66}$$

$$+ \eta \left( \int_{-\infty}^{+\infty} \mathrm{d}x \rho(x) - 1 \right) + \mu \left( \int_{0}^{+\infty} \mathrm{d}x \rho(x) - k \right). \tag{6.67}$$

and $\eta, \mu$ are Lagrange multipliers, introduced to enforce the overall normalization of the density, and a fraction $k$ of positive eigenvalues.

### 6.3.2 The resolvent method

As mentioned earlier, the integral (6.65), where we neglected terms of $\mathcal{O}(N)$, can be calculated using a saddle point method for large $N$. The constrained density of eigenvalues $\rho^\star(x)$ is determined by the variational condition

$$\frac{\delta S}{\delta \rho} = \frac{\log(1+x^2)}{2} - \int_{-\infty}^{+\infty} \mathrm{d}x' \rho^\star(x') \log |x - x'| + \eta + \mu \theta(x) = 0, \tag{6.68}$$

Equation (6.68), valid for $x$ inside the support of $\rho^\star(x)$, can be differentiated once with respect to $x$ to give the following singular integral equation

$$\frac{x}{1+x^2} + \mu\delta(x) = \fint_{-\infty}^{\infty} \frac{\rho^\star(y)}{x-y}\mathrm{d}y. \tag{6.69}$$

where $\fint$ stands for Cauchy principal part. Solving (6.69) with the constraint $\int_0^\infty dx\rho^\star(x) = k$ is again the main technical challenge. The physical intuition is not enough to predict the form of the constrained average density. As before, we expect a divergence-convergence pair around the origin, but the behavior at infinity is not evident. The unconstrained average density, Cauchy's distribution, goes on both sides to infinity, but we cannot tell if this behavior is preserved when the constraint is applied. We expect the side with extra eigenvalues to continue its asymptotic behavior to infinity, but the side with less eigenvalues might collapse to a compact support. Indeed, this is the real behavior of the constrained average density, as we will prove it by solving the integral equation (6.69).

Again, we introduce the resolvent

$$G(z) = \int \frac{\rho^\star(x)}{z-x}\mathrm{d}x \ , \tag{6.70}$$

for the Cauchy case. It is an analytic function in the complex plane outside the support of the density. From the resolvent, the density can be computed in the standard way as

$$-\frac{1}{\pi}\lim_{\varepsilon\to 0^+} \mathrm{Im}\ G(x+\mathrm{i}\varepsilon) = \rho^\star(x) \ , \tag{6.71}$$

where Im stands for the imaginary part.

Writing equation (6.69) as a function of the resolvent is a more complicated problem then the Gaussian case, as the derivative of the potential is not a polynomial, but a rational function. As a warm-up exercise, we first derive the resolvent equation for the *unconstrained* case (corresponding to (6.69) when $\mu = 0$), where we expect to recover the density in equation (3.28). As before, we multiply both sides in (6.69) (dropping the principal value) by $\rho^\star(x)/(z-x)$ and we integrate it over $x$, obtaining

$$\int \frac{x}{1+x^2}\frac{\rho^\star(x)}{z-x}\mathrm{d}x = \iint \frac{\rho^\star(x)\rho^\star(y)}{(x-y)(z-x)}\mathrm{d}x\mathrm{d}y \ . \tag{6.72}$$

Our goal is to express both sides in terms of $G(z)$ and, by doing so, obtain an algebraic equation for $G(z)$. The RHS is the same as in the Gaussian case, and we refer to equation (4.43) for the details that show that it is simply $G(z)^2/2$.

The LHS of (6.72) requires a little more algebraic manipulation to be expressed in terms of $G(z)$. We manipulate this expression in two different ways and exploit the equality between the results to get rid of one integral. Using the identity

$$\frac{x}{1+x^2} = \frac{1}{x} - \frac{1}{x(1+x^2)} \tag{6.73}$$

one has

$$\int \frac{x}{1+x^2}\frac{\rho^\star(x)}{z-x}\mathrm{d}x = \int \frac{1}{x}\frac{\rho^\star(x)}{z-x}\mathrm{d}x - \int \frac{1}{x(1+x^2)}\frac{\rho^\star(x)}{z-x}\mathrm{d}x\,. \tag{6.74}$$

Using the relation (4.42), we may express the first term of the sum in (6.74) as

$$\int \frac{1}{x}\frac{\rho^\star(x)}{z-x}\mathrm{d}x = \int \left(\frac{1}{x}+\frac{1}{z-x}\right)\frac{\rho^\star(x)}{z}\mathrm{d}x = \frac{1}{z}\underbrace{\int \frac{\rho^\star(x)}{x}\mathrm{d}x}_{a_0} + \frac{1}{z}\underbrace{\int \frac{\rho^\star(x)}{z-x}\mathrm{d}x}_{G(z)} = \frac{a_0}{z}+\frac{G(z)}{z}. \tag{6.75}$$

The second term of the sum in (6.74) will not be calculated for now, and will be called $-\alpha(z)$. Using this manipulation (6.75), we have:

$$\int \frac{x}{1+x^2}\frac{\rho^\star(x)}{z-x}\mathrm{d}x = \frac{a_0}{z}+\frac{G(z)}{z}-\alpha(z). \tag{6.76}$$

Now, we use a different strategy, using the identity $x/(1+x^2) = (x-z)/(1+x^2) + z/(1+x^2)$, to obtain

$$\begin{aligned}\int \frac{x}{1+x^2}\frac{\rho^\star(x)}{z-x}\mathrm{d}x &= \int \frac{x+z-z}{1+x^2}\frac{\rho^\star(x)}{z-x}\mathrm{d}x \\ &= -\underbrace{\int \frac{\rho^\star(x)}{1+x^2}dx}_{a_1} + z\int \frac{1}{1+x^2}\frac{\rho^\star(x)}{z-x}\mathrm{d}x.\end{aligned} \tag{6.77}$$

The first term in the sum (6.77) is a constant, which we call $a_1$. Now we proceed to manipulate the second term in (6.77) to obtain

$$z\int \frac{1}{1+x^2}\frac{\rho^\star(x)}{z-x}\mathrm{d}x = z\int \frac{x-z+z}{x(1+x^2)}\frac{\rho^\star(x)}{z-x}\mathrm{d}x \tag{6.78}$$

$$= -z\underbrace{\int \frac{\rho^\star(x)}{x(1+x^2)}\mathrm{d}x}_{a_2} + z^2\underbrace{\int \frac{1}{x(1+x^2)}\frac{\rho^\star(x)}{z-x}\mathrm{d}x}_{\alpha(z)}\,. \tag{6.79}$$

Therefore, the LHS of (6.72) can also be written as $-a_1 - za_2 + z^2\alpha(z)$. We have then two distinct ways of writing the LHS, and we can use them both to cancel $\alpha(z)$.

$$\begin{gathered}\frac{a_0}{z}+\frac{G(z)}{z}-\alpha(z) = (\mathrm{RHS}) \\ -a_1 - za_2 + z^2\alpha(z) = (\mathrm{RHS}) \\ \hline -1 - a_1 + z(a_0-a_2) + zG(z) = (\mathrm{RHS})(1+z^2).\end{gathered} \tag{6.80}$$

where we have multiplied the first equation by $z^2$ and then summed the two. Since the RHS is equal to $(1/2)G(z)^2$, we find the algebraic equation for $G(z)$

$$-a_1 + z(a_0-a_2) + zG(z) = \frac{(1+z^2)}{2}G(z)^2. \tag{6.81}$$

We proceed to determine constants $a_0$, $a_1$ and $a_2$ using the normalization condition of the density $\rho^\star(x)$. From (6.70) (setting $|z| \to \infty$), it implies that $G(z)$ should asymptotically go as $G(z) \sim 1/z$. Taking the limit $|z| \to \infty$ in equation (6.81), we find equations for the coefficients

$$-a_1 + +z(a_0 - a_2) + z\left(\frac{1}{z} + O(z^{-2})\right) = \frac{z^2}{2}\left(\frac{1}{z} + O(z^{-2})\right)^2. \tag{6.82}$$

which implies $a_0 = a_2$ and $a_1 = \frac{1}{2}$. Our algebraic equation, finally, becomes:

$$(1+z^2)G(z)^2 - 2zG(z) + 1 = 0. \tag{6.83}$$

The two solutions read

$$G(z) = \frac{2z \pm \sqrt{4z^2 - 4(1+z^2)}}{2(1+z^2)} = \frac{z \pm \mathrm{i}}{1+z^2}. \tag{6.84}$$

Using (6.71), the density comes out as expected

$$-\frac{1}{\pi}\lim_{\varepsilon\to 0^+} \mathrm{Im}\; G(x+\mathrm{i}\varepsilon) = \frac{1}{\pi}\frac{1}{1+x^2} = \rho^\star(x), \tag{6.85}$$

Now, we consider the full index problem, i.e. with an extra term in the potential as in (6.69),

$$\frac{x}{1+x^2} + \mu\delta(x) = \fint_{-\infty}^{\infty} \frac{\rho^\star(y)}{x-y}\mathrm{d}y, \tag{6.86}$$

where the constant $\mu$ will be determined by the normalization condition of the rightmost blob $\int_0^\infty \rho^\star(x)\mathrm{d}x = k$. We repeat the same steps as for the unconstrained integral equation, multiplying (6.69) (without the principal value) by $\frac{\rho^\star(x)}{z-x}$ and integrating in $x$. We get an extra term from it in (6.72), arising from the Lagrange multiplier

$$\int \frac{x}{1+x^2}\frac{\rho^\star(x)}{z-x}\mathrm{d}x = \iint \frac{\rho^\star(x)\rho^\star(y)}{(x-y)(z-y)}\mathrm{d}x\mathrm{d}y - \frac{\mu}{z}. \tag{6.87}$$

We absorb this new term into the RHS and proceed to express, as before, all integrals in terms of $G(z)$. Our new algebraic equation will then be:

$$-a_1 + z(a_0 - a_2) + zG(z) = (1+z^2)\left(\frac{G(z)^2}{2} - \frac{A}{z}\right). \tag{6.88}$$

Imposing the condition that $G(z) \sim 1/z$ for $|z| \to \infty$, we get the two conditions $a_1 = 1/2$ and $a_0 - a_2 + A = 0$. Calling $A = B/2$ we find the equation

$$\frac{B}{2}z + G(z)z - \frac{1}{2} = \left(z^2+1\right)\left(\frac{B/2}{z} + \frac{G(z)^2}{2}\right), \tag{6.89}$$

whose solutions are

$$G(z) = \frac{z^2 \pm \sqrt{-Bz^3 - Bz - z^2}}{z^3 + z} \tag{6.90}$$

Using (6.71), it is then easy to derive that the constrained density is:

$$\rho^\star(x) = \frac{1}{\pi}\frac{\sqrt{B(x^3+x)+x^2}}{|x^3+x|}, \tag{6.91}$$

which is of the form

$$\rho^\star(x) = \frac{\sqrt{1}}{\pi(1+x^2)}\sqrt{\frac{B(x-a)(x-b)}{x}}\ , \tag{6.92}$$

where the edge points of the leftmost blob (for $k > 1/2$) $a, b$ are determined as a function of $B$

$$a = -\frac{1}{2B}(1-\sqrt{1-4B^2})\ , \tag{6.93}$$

$$b = -\frac{1}{2B}(1+\sqrt{1-4B^2})\ , \tag{6.94}$$

In particular, we note $ab = 1$ and $a + b = -1/B$. $B$ can be found as a function of $k$

$$\int_0^\infty dx \frac{1}{\pi(1+x^2)}\sqrt{\frac{B(x-a)(x-b)}{x}} = k \tag{6.95}$$

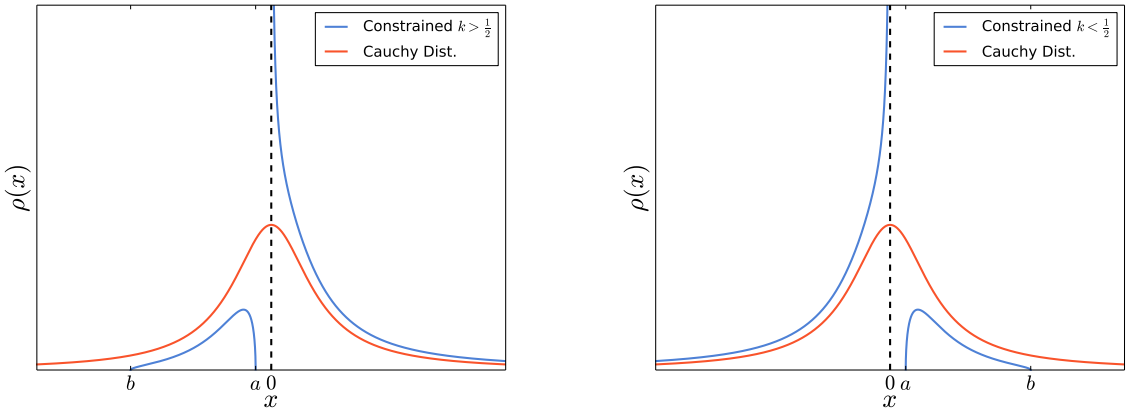


**(a)** **(b)**

**Figure 6.5** — Constrained average density (blue line) and comparison with Cauchy's distribution (orange line) for the index of the Cauchy ensemble in the cases (a) $k > \frac{1}{2}$ and (b) $k < \frac{1}{2}$ (equation (6.92)).

Note that, using $\sqrt{B}\sqrt{(x-a)(x-b)} \to \sqrt{x}$ for $B \to 0$, we have that $\rho^\star(x) \to \rho(x)$ the Cauchy distribution (see equation (6.91)) for $k \to 1/2$ as it should. This means that we recover the unconstrained Cauchy case if we impose a number of positive eigenvalues exactly equal to $N/2$, and this unconstrained case materializes when $B \to 0$. We have found the constrained average density, and we confirmed that one of the sides of the average density collapses into a compact support when there is an excess of eigenvalues in the other side.

### 6.3.3 Obtaining the rate function

We proceed to calculate the rate function $\psi(k)$. The procedure is extremely similar to the Gaussian case, and it is not hard to see that the only significant difference is the form of the potential $V(x)$. We take, without loss of generality, the case $k > 1/2$, described in figure (6.5a). We obtain

$$\psi(k) = S[\rho^\star] - S[\rho_{ca}(x)] \tag{6.96}$$

$$= \frac{1}{4}\int \rho^\star(x)\log(1+x^2)\mathrm{d}x - \frac{\mu k}{2} - \frac{\eta}{2} - S[\rho_{ca}(x)], \tag{6.97}$$

where

$$\mu = \int_0^a G(x)\mathrm{d}x - \frac{\log(1+a^2)}{2}, \tag{6.98}$$

and

$$\eta = \log|b| - \frac{\log(1+b^2)}{2} - \int_b^{-\infty}\left(G(x) - \frac{1}{x}\right)\mathrm{d}x. \tag{6.99}$$

We calculate the action on the Cauchy distribution, where we find $a = B = 0$ and $b \to \infty$. This implies $\mu = 0$ and $\eta = 0$, and the remaining integral is evaluated directly

$$\frac{1}{4\pi}\int \frac{\log(1+x^2)}{1+x^2}\mathrm{d}x = \frac{\log 2}{2}. \tag{6.100}$$

The rate function then reads

$$\psi(k) = \frac{1}{4}\int \rho^\star(x)\log(1+x^2)\mathrm{d}x - \frac{\mu k}{2} - \frac{\eta}{2} - \frac{\log 2}{2}. \tag{6.101}$$

And we obtain the decay of the probability of the index for large $N$ as

$$P(N_+ = kN) \approx e^{-\beta N^2 \psi(k)} \tag{6.102}$$

Again, we expressed the rate function as integrals of the resolvent. These integrals cannot be easily evaluated analytically, although numerically they represent no challenge. We plot the numerical evaluation of $\psi(k)$ in figure 6.6 and we confirm that $k = \frac{1}{2}$ is indeed its minimum.

### 6.3.4 Variance of the index

We perform a careful asymptotic analysis of the rate function $\psi(k)$ around its minimum $k = 1/2$. It turns out that this calculation is highly nontrivial, as several cancellations occur in the leading and next-to-leading terms of each contribution. The $a$, $b$ and $B$ parameters for the unconstrained Cauchy distribution are $a = B = 0$ and $b = -\infty$. We perturb $a$ by a small factor $\epsilon$, this yields

$$a = -\epsilon \quad b = -\frac{1}{\epsilon} \quad B = \epsilon. \tag{6.103}$$

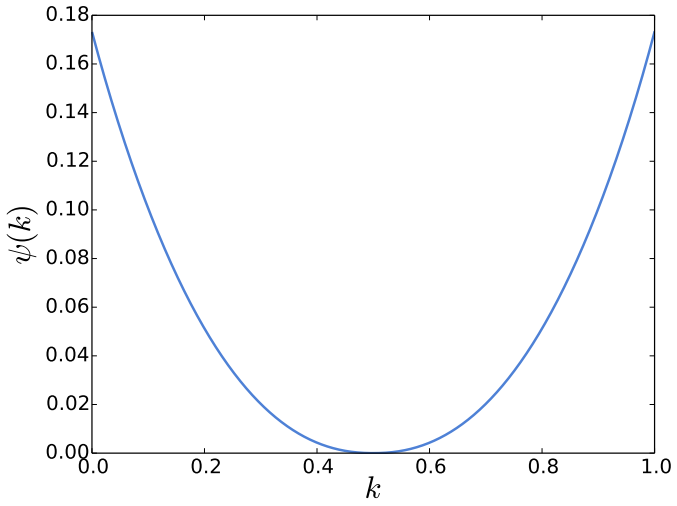


**Figure 6.6** — Rate function $\psi(k)$ for the index of the Cauchy ensemble (equation (6.101)).

The average density becomes

$$\rho^\star(x) = \frac{\sqrt{\epsilon}}{\pi(1+x^2)}\sqrt{\frac{(x+\epsilon)(x+1/\epsilon)}{x}} = \frac{1}{\pi}\frac{\sqrt{\epsilon(x^3+x)+x^2}}{x(x^2+1)}. \tag{6.104}$$

And we proceed to expand the integrals for the computation of the rate function to leading order of $\epsilon$.

### Integral for the potential

While in the Gaussian case we needed only to calculate the second moment of the average distribution, the first integral of the rate function is much more complicated. We want to integrate

$$I = \frac{1}{2}\int_{-\infty}^{+\infty}\rho^\star(x)\log(1+x^2)\mathrm{d}x. \tag{6.105}$$

This integral calculation represents a *tour de force* and we omit most of the tedious details of this long calculation.

First, we separate the integral as

$$I_1 = I_1^L + I_1^R \quad I_1^L = \frac{1}{2}\int_b^a \mathrm{d}x\rho^\star(x)\log(1+x^2) \quad I_1^R = \frac{1}{2}\int_0^{+\infty}\mathrm{d}x\rho^\star(x)\log(1+x^2). \tag{6.106}$$

Writing $I_1^R$ explicitly,

$$I_1^R = \frac{1}{2\pi}\int_0^{+\infty}\mathrm{d}x\frac{\sqrt{\epsilon(x^3+x)+x^2}}{x(x^2+1)}\log(1+x^2). \tag{6.107}$$

To compute the asymptotic behavior when $\epsilon \to 0$, we split this integral into two parts, one integral from 0 to $\epsilon$ and one from $\epsilon$ to $\infty$,

$$I_1^R = \frac{1}{2\pi}\left(\int_0^\epsilon \mathrm{d}x \frac{\sqrt{\epsilon(x^3+x)+x^2}}{x(x^2+1)}\log(1+x^2) + \int_\epsilon^\infty \mathrm{d}x \frac{\sqrt{\epsilon(x^3+x)+x^2}}{x(x^2+1)}\log(1+x^2)\right). \tag{6.108}$$

Now we can expand the integrands in series around $\epsilon = 0$ and integrate term by term to obtain (to order $\epsilon$)

$$I_1^R \xrightarrow[\epsilon\to 0]{} \frac{\log 2}{2} + \epsilon\frac{\log^2(\epsilon)}{4\pi} - \frac{\epsilon\log(\epsilon)}{2\pi}(1+\log 4) + \frac{\epsilon}{4\pi}\left(2 + 4\log 2(1+\log 2) + \frac{3\pi^2}{4}\right) + o(\epsilon). \tag{6.109}$$

We now turn our attention to $I_1^L$, calculating the asymptotic behavior when $\epsilon \to 0$ of the integral:

$$I_1^L = \frac{1}{2\pi}\int_b^a \mathrm{d}x \frac{\sqrt{\epsilon(x^3+x)+x^2}}{|x(x^2+1)|}\log(1+x^2). \tag{6.110}$$

To proceed, it is more convenient to express $I_1^L$ in terms of its edge points

$$I_1^L = \frac{\sqrt{\epsilon}}{2\pi}\int_b^a \mathrm{d}x \frac{\sqrt{(b-x)(x-a)}}{\sqrt{|x|}(x^2+1)}\log(1+x^2), \tag{6.111}$$

which is equivalent to (6.110). We proceed with the following change of variables: $y = \frac{b-x}{a-b}$, we have:

$$I_1^L = \frac{\sqrt{\epsilon}}{2\pi}\int_0^1 \frac{(a-b)\mathrm{d}y}{1+[(a-b)y+b]^2}\frac{(a-b)\sqrt{y(1-y)}}{\sqrt{|(a-b)y+b|}}\log\left[1+[(a-b)y+b]^2\right]. \tag{6.112}$$

We replace the asymptotic behaviors for $a$ and $b$ in (6.112), keeping only the leading orders for small $\epsilon$. The resulting integral can be computed explicitly and we can then extract its asymptotic behavior when $\epsilon \to 0$

$$I_1^L \xrightarrow[\epsilon\to 0]{} \frac{\log 2}{2} - \frac{\epsilon\log^2\epsilon}{4\pi} + \frac{(1+\log 4)(\epsilon\log\epsilon)}{2\pi} + \frac{\epsilon}{4\pi}\left(\frac{\pi^2}{4} - 2 - 4\log 2(1+\log 2)\right) + o(\epsilon). \tag{6.113}$$

Note an impressive series of cancellations in the sum $I_1^L + I_1^R$, resulting in

$$I_1 \xrightarrow[\epsilon\to 0]{} \log 2 + \frac{\pi}{4}\epsilon + o(\epsilon). \tag{6.114}$$

### Calculation of $\mu$

Fortunately, the calculation of $\mu$ is much simpler as the integral on the potential, as we were able to express it in terms of a single integral on the resolvent, which is an algebraic function.

Also, as in the Gaussian case, the integral necessary to calculate $\mu$ is performed in only a very short interval, so many approximations are available.

$$\mu = \int_a^0 G(x)\mathrm{d}x - \frac{\log(1+a^2)}{2} = \int_a^0 \frac{\sqrt{-\epsilon(x^3+x)-x^2}}{x(x^2+1)}\mathrm{d}x = \frac{\pi}{2}\epsilon + 0(\epsilon). \tag{6.115}$$

### Calculation of $\eta$

We begin by calculating the integral of the resolvent. Since the domain of integration are values of $x$ with very high absolute value, we have enough simplifications to evaluate the integral for leading order in $\epsilon$.

$$\int_b^\infty \left(G(x) - \frac{1}{x}\right)\mathrm{d}x = -\frac{\pi}{2}\epsilon + o(\epsilon). \tag{6.116}$$

The other terms of $\eta$ compensate each other: $\log b - \frac{1}{2}\log(1+b^2) \to 0$, so the value of $\eta$ is

$$\eta = -\frac{\pi}{2}\epsilon + o(\epsilon). \tag{6.117}$$

### Calculation of $k$

We recall that $\int_0^\infty \rho^\star(x)\mathrm{d}x = k = \frac{1}{2} + \delta$. As $k$ multiplies $\mu$ in the action and $\mu$ is of order $\epsilon$, we do not need to go deep into next-to-leading terms for the expansion of $k$. By applying similar techniques to those applied in the previous integrals we obtain

$$k = \int_0^\infty \rho^\star(x)\mathrm{d}x = \frac{1}{2} - \frac{\epsilon\log\epsilon}{\pi}. \tag{6.118}$$

Which yields $\delta = -\frac{\epsilon\log\epsilon}{\pi}$, whose inverse can be written to leading order in $\delta$ as

$$\epsilon \sim -\pi\frac{\delta}{\log\delta}. \tag{6.119}$$

### Calculation of the rate function

Adding all factors we obtain

$$\psi(k) = \frac{1}{4}\int \rho^\star(x)\log(1+x^2)\mathrm{d}x - \frac{\mu k}{2} - \frac{\eta}{2} - \psi\left(\frac{1}{2}\right) = -\frac{\pi}{4}\epsilon\delta + o(\epsilon\delta). \tag{6.120}$$

Using the inverse relation (6.119) we obtain

$$\psi(k) = \frac{\pi^2}{4}\frac{\delta^2}{\log\delta}. \tag{6.121}$$

We apply the saddle point in equation (6.65), we then have (for $N_+$ close to $N/2$)

$$P\left(N_+ = \left(\frac{1}{2}+\delta\right)N\right) \approx e^{\frac{\beta N^2}{2}\frac{\pi^2\delta^2}{2\log|\delta|}}. \tag{6.122}$$

Restoring $\delta = (N_+ - N/2)/N$ in the RHS of (6.122), we obtain the Gaussian behavior modulated by a logarithmic singularity

$$P(N_+) \approx e^{-\frac{(N_+ - N/2)^2}{2\,\mathrm{Var}(N_+)}} \text{ for } N_+ \to N/2, \tag{6.123}$$

with

$$\mathrm{Var}(N_+) \sim \frac{2}{\beta\pi^2} \log N + \mathcal{O}(1). \tag{6.124}$$

Remarkably, it scales twice as fast with the size of the matrix as the Cauchy ensemble. Since Cauchy and Gaussian ensembles have the same behavior in the bulk regime, this difference is emerging from the absence of compact support in the Cauchy case. Loosely speaking, the absence of edge allows for fluctuations to be larger, although the precise factor two could not be predicted from physical intuition.

### 6.3.5 Finite $N$ expansion

The Coulomb gas method is very powerful to explore large $N$ asymptotics of the index, but the orthogonal polynomial method is also available for Cauchy. We will briefly discuss how it could be applied, and we will use it for small values of $N$ to verify that, when $N$ increases, the slope of the variance indeed becomes close to the result calculated by the Coulomb gas (6.124).

In section 5.2, we derived a general formula for the variance of any linear statistics at finite $N$ and $\beta = 2$. Specializing it to the index case, we deduce that

$$\mathrm{Var}(N_+) = \frac{N}{2} - \iint_0^\infty \mathrm{d}x\mathrm{d}x' [K_N(x,x')]^2, \tag{6.125}$$

where $K_N(x,x')$ is the kernel of the ensemble, built upon suitable orthogonal polynomials. It turns out the in the Cauchy case, the orthogonal polynomials $\pi_n(x)$ satisfying

$$\int_{-\infty}^{\infty} \mathrm{d}x \frac{\pi_n(x)\pi_m(x)}{(1+x^2)^N} = \delta_{mn} \tag{6.126}$$

are

$$\pi_n(x) = \mathrm{i}^n 2^N \left[\frac{n!(N-n-\frac{1}{2})\Gamma^2(N-n)}{2\pi\Gamma(2N-n)}\right]^{1/2} P_n^{(-N,-N)}(\mathrm{i}x), \tag{6.127}$$

where $P_n^{(-N,-N)}(x)$ are Jacobi polynomials. The kernel then reads

$$K_N(x,x') = \frac{1}{(1+x^2)^{N/2}} \frac{1}{(1+x'^2)^{N/2}} \sum_{j=0}^{N-1} \pi_j(x)\pi_j(x') \tag{6.128}$$

and inserting (6.128) into (6.125) we obtain after simple algebra

$$\mathrm{Var}(N_+) = \frac{N}{2} - \sum_{n,m=0}^{N-1} \left(\int_0^\infty \mathrm{d}x \frac{\pi_n(x)\pi_m(x)}{(1+x^2)^N}\right)^2. \tag{6.129}$$

This integral form is suitable for numerical verifications for small values of $N$. We can continue the analysis of this formula to convince the reader of the power and limitations of the orthogonal polynomial method.

To simplify expression (6.129), we define:

$$I_{m,n,N} = \int_0^\infty \mathrm{d}x \frac{\pi_n(x)\pi_m(x)}{(1+x^2)^N}. \tag{6.130}$$

Using (6.127) we write:

$$I_{m,n,N} = \int_0^\infty \mathrm{d}x \frac{\pi_n(x)\pi_m(x)}{(1+x^2)^N} \tag{6.131}$$

$$= \mathrm{i}^{m+n} 2^{2N} \left[\frac{n!(N-n-\frac{1}{2})\Gamma^2(N-n)}{2\pi\Gamma(2N-n)}\right]^{\frac{1}{2}} \left[\frac{m!(N-m-\frac{1}{2})\Gamma^2(N-m)}{2\pi\Gamma(2N-m)}\right]^{\frac{1}{2}} \times \int_0^\infty \mathrm{d}x \frac{P_n^{(-N,-N)}(\mathrm{i}x) P_m^{(-N,-N)}(\mathrm{i}x)}{(1+x^2)^N}\,. \tag{6.132}$$

Next we use the definition of Jacobi polynomials as

$$P_n^{(-N,-N)}(\mathrm{i}x) = \sum_{k=0}^{n} c_{k,n}^{(N)} (1-\mathrm{i}x)^k \tag{6.133}$$

where

$$c_{l,\tau}^{(N)} = \frac{1}{\tau!} \frac{(-\tau)_l (-2N+\tau+1)_l (-N+l+1)_{\tau-l}}{l! 2^l}, \tag{6.134}$$

to write:

$$\int_0^\infty \mathrm{d}x \frac{P_n^{(-N,-N)}(\mathrm{i}x) P_m^{(-N,-N)}(\mathrm{i}x)}{(1+x^2)^N} = \sum_{k=0}^{m}\sum_{r=0}^{n} c_{k,m}^{(N)} c_{r,n}^{(N)} \sum_{s=0}^{k+r} \binom{k+r}{s} (-\mathrm{i})^s \frac{1}{2} B\left(\frac{1+s}{2}, N - \frac{1+s}{2}\right), \tag{6.135}$$

where

$$c_{l,\tau}^{(N)} = \frac{1}{\tau!} \frac{(-\tau)_l (-2N+\tau+1)_l (-N+l+1)_{\tau-l}}{l! 2^l}, \tag{6.136}$$

and $B(x,y)$ is Euler's Beta function.

Finally, we may write the variance of index for the Cauchy ensemble as:

$$\mathrm{Var}(N_+) = \frac{N}{2} - 2 \sum_{\substack{n<m \\ n+m \text{ odd}}}^{N-1} I_{m,n,N}^2, \tag{6.137}$$

where

$$I_{m,n,N} = \mathrm{i}^{m+n} 2^{2N} \left[\frac{n!(N-n-\frac{1}{2})\Gamma^2(N-n)}{2\pi\Gamma(2N-n)}\right]^{\frac{1}{2}} \left[\frac{m!(N-m-\frac{1}{2})\Gamma^2(N-m)}{2\pi\Gamma(2N-m)}\right]^{\frac{1}{2}} \times \sum_{k=0}^{m}\sum_{r=0}^{n}\sum_{s=0}^{k+r} c_{k,m}^{(N)} c_{r,n}^{(N)} \binom{k+r}{s} (-\mathrm{i})^s \frac{1}{2} B\left(\frac{1+s}{2}, N - \frac{1+s}{2}\right). \tag{6.138}$$

This expression can be numerically evaluated more easily than equation (6.129) and is ideal for more powerful and precise finite $N$ computations of the index.

### 6.3.6 Comparison with numerics

Since this is a new result, we are also interested in numerical confirmation of the constrained average density of eigenvalues, equation (6.92). In figure 6.7, we show a plot of the density (6.92) for $k = 0.7$ together with Monte-Carlo simulations for $N = 300$ and $10^6$ samples. We observe a nice agreement between our exact formula and the numerics.

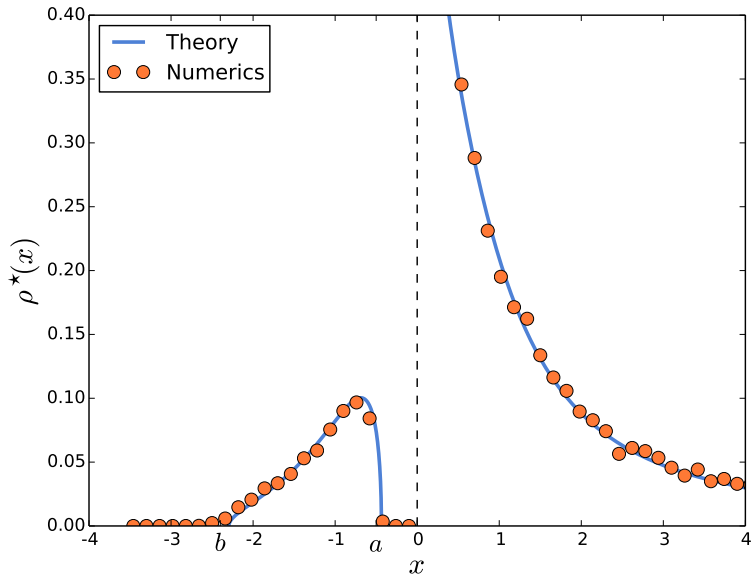


**Figure 6.7** — 1.000.000 Monte-Carlo iterations for a matrix with size $N = 300$ forcing 70% of the eigenvalues to be positive and the correspondent expected theoretical curve. Theory is equation (6.92).

To verify the variance of the index, we use formula (6.138) for various values of $N$ and we verify in figure 6.8 that the slope converges to the expected value, which implies a matching at leading order of $N$. We also plot the results for the Gaussian ensemble, obtaining the points by the same procedure described above with the use of Hermite polynomials. We verify that the variance of the Cauchy index grows twice as fast as the variance of the Gaussian index, confirming our prediction.

## 6.4 Summary of results

We conclude this chapter by recalling the results obtained on the subject. It was previously known [89, 90] that the variance of the number of positive eigenvalues of a Gaussian random matrix $N_+^G$ is given by

$$\mathrm{Var}(N_+^G) = \frac{1}{\beta\pi^2}\log N + O(1). \tag{6.139}$$

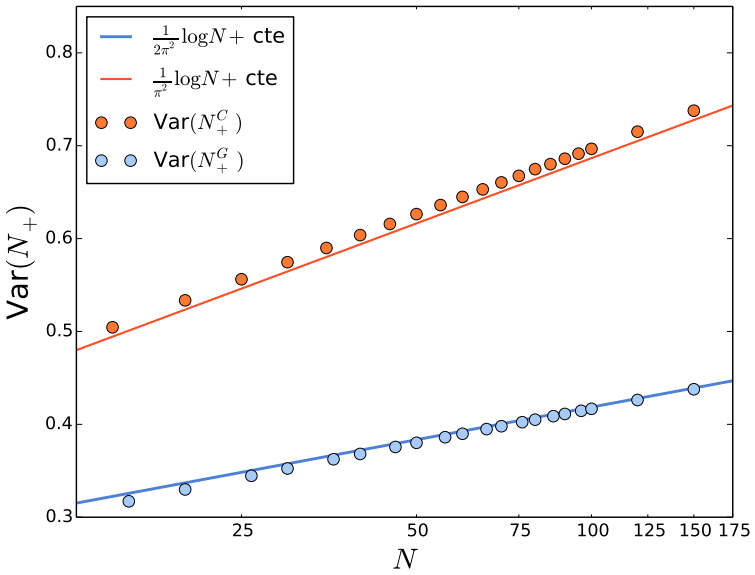


**Figure 6.8** — Numerical evaluation of the variance of the index using $\beta = 2$ for Cauchy ensemble (denoted $N_+^C$, top line and points) and the Gaussian ensemble (denoted $N_+^G$, bottom line and points).

Interested in the same question for the Cauchy ensemble, I was able to obtain the full probability distribution for the number of positive eigenvalues in the Cauchy ensemble $N_+^C$ and, in particular, derive the variance of this random variable

$$\mathrm{Var}(N_+^C) = \frac{2}{\beta\pi^2}\log N + O(1), \tag{6.140}$$

and we confirmed this behavior numerically comparing it with the finite $N$ calculation using orthogonal polynomials.

While we expected a larger value for the variance of the Cauchy ensemble, the precise factor two was not expected. As mentioned before, the reason for a larger variance is the absence of edge, and the role of the edge on the behavior of this variance should be explored to confirm this.

We performed some preliminary calculations for the Gaussian ensemble, to study how the edge affects the variance of the number of eigenvalues inside an interval, and the results were interesting enough to be explored fully. To see the effect of the edge on the variance, one should start analyzing the variance of the number statistics in an interval $[-L, L]$ and see how this variance evolves when $L$ increases. When $L$ approaches the edge, the behavior of the variance should change, and this study of the variance from small values of $L$ to values larger than the edge has not been performed.

In the domain of cold atoms, this variance is related to an important observable, the entanglement entropy of the system. This observable, and the behavior of the number variance for different sizes of interval, are discussed in the following chapter.

# — 7 —
# Number statistics of cold fermions

*It is as easy to count atomies as to resolve the propositions of a lover;*

`William Shakespeare` – As You Like It, III, ii.

## 7.1 Confined cold fermions and GUE

### 7.1.1 Correspondence with GUE

As mentioned in the introduction, at section 2.2, there is a direct correspondence between harmonically confined cold fermions and the eigenvalues of GUE. We argued that the number statistics of fermions, also called the full counting statistics, is a fundamental property of the system that yields information about fluctuations, correlations and other observables, such as the entanglement entropy. In this chapter, we shall explore this problem deeply, starting by explaining the connection between cold fermions and RMT.

Computing the full counting statistics was possible by using the connection between the statistics of one dimensional Fermi gases and random matrix theory [97]. Remarkably, as the presence of Wigner's semicircle indicated, the statistics of fermions trapped by a harmonic potential at zero temperature can be mapped to the statistics of eigenvalues of a certain random matrix ensemble [46]. The ground state many-body wave function of such system is given by the Slater determinant $\Psi(\vec{x}) = \det[\phi_i(x_j)]/\sqrt{N!}$, where $\phi_i(x_j)$ is the wave function of a single harmonic oscillator $\phi_n(x) \propto \mathrm{e}^{-x^2/2} H_n(x)$, and $H_n(x)$ are Hermite polynomials. By manipulating the determinant, we may cast the probability density of the ground state as

$$|\Psi(\vec{x})|^2 = \frac{1}{Z_N} \mathrm{e}^{-\sum_{i=1}^{N} x_i^2} \prod_{j<k} (x_k - x_j)^2, \tag{7.1}$$

where $Z_N$ is the normalization constant. Written in this form, we notice that the joint probability density function of the position of such fermions on their ground state is equivalent to the distribution of eigenvalues of an $N \times N$ Gaussian hermitian matrix. The statistics of a fundamental property of Fermi gases, the number of fermions inside an

interval at ground state, is, therefore, equivalent to counting eigenvalues from a Gaussian random matrix inside the interval.

Recent work has been done to generalize and expand this correspondence. In particular, we mention [36] for a generalization of the correspondence of random matrix and finite temperature fermions and [35] for a generalization of this correspondence for cold atoms in $d$-dimensional traps.

During my PhD, I was able to determine the full behavior of the number variance of such systems for all interval sizes by exploring this correspondence. We identify three regimes, highlighted in figures 7.3, 7.4 and 7.5: an *extended bulk* regime, an *edge* regime and a *tail* regime. The behavior of the variance changes drastically when the interval consider different regions, yields a rich behavior of this observable for such systems. In addition, this observable yields information about a fundamental physical quantity, the entanglement entropy, as we discuss it on the next section.

## 7.2 Calculating the number statistics

### 7.2.1 Coulomb gas

We define $N_{\mathcal{I}}$ as the number of eigenvalues inside the interval $\mathcal{I} = [a, b]$. The probability distribution of $N_L$ can be written as

$$P(N_{\mathcal{I}}) = \frac{1}{Z_{N,\beta}} \int \prod_{i=1}^{N} \mathrm{d}\lambda_i \mathrm{e}^{-\beta E[\boldsymbol{\lambda}]} \delta \left( N_{\mathcal{I}} - \sum_{i=1}^{N} \mathbb{1}_{[a,b]}(\lambda_i) \right) , \tag{7.2}$$

where $\mathbb{1}_{\mathcal{I}}(x)$ is the indicator function equal to 1 if $x \in \mathcal{I}$ and zero otherwise. Here we used the j.p.d.f. of the eigenvalues (3.17). Introducing now an integral representation for the delta function, we obtain

$$P(N_{\mathcal{I}}) \propto \int \prod_{i=1}^{N} \mathrm{d}\lambda_i \int \frac{\mathrm{d}\mu}{2\pi} \exp\left(-\beta E[\boldsymbol{\lambda}; \mu, N_{\mathcal{I}}]\right) , \tag{7.3}$$

where

$$E[\boldsymbol{\lambda}; \mu, N_{\mathcal{I}}] = E[\boldsymbol{\lambda}] + \frac{\mu}{2} \left( N_L - \sum_{i=1}^{N} \mathbb{1}_{[a,b]}(\lambda_i) \right) . \tag{7.4}$$

Following the recipe of passage from discrete to continuous described in section 4.1, we obtain that the probability of having a fraction $k_{\mathcal{I}} = N_{\mathcal{I}}/N$ of eigenvalues inside a box $[a, b]$ is given by

$$P(N_{\mathcal{I}}) \propto \int \mathcal{D}[\rho] \mathrm{d}\mu \mathrm{d}\eta \exp\left(-\beta N^2 S[\rho]\right) , \tag{7.5}$$

where we have neglected $\mathcal{O}(N)$ (entropic) contributions in the exponent and the action $S$ is given by

$$S[\rho] = \frac{1}{2} \int \mathrm{d}x x^2 \rho(x) - \frac{1}{2} \iint \mathrm{d}x \mathrm{d}x' \rho(x)\rho(x') \log|x - x'| \tag{7.6}$$

$$+ \eta \left( \int \mathrm{d}x \rho(x) - 1 \right) + \mu \left( \int_a^b \mathrm{d}x \rho(x) - k_L \right) . \tag{7.7}$$

### 7.2.2 Resolvent method

We apply the resolvent method to the action in order to calculate the average density of eigenvalues submitted to the condition that a fraction $k_{\mathcal{I}}$ of them should lie in the interval $\mathcal{I} = [a, b]$. Applying the saddle-point method into (7.7) yields the density $\rho^\star(x)$ that minimizes the action. We may write for large $N$

$$P(N_{\mathcal{I}} = k_{\mathcal{I}} N) = \frac{1}{Z_{N,\beta}} \int \mathcal{D}\rho \mathrm{d}\mu \mathrm{d}\eta \mathrm{e}^{-\beta N^2 S[\rho]} = \mathrm{e}^{-\beta N^2 (S[\rho^\star] - S[\rho_{sc}])} = \mathrm{e}^{-\beta N^2 \psi(k_{\mathcal{I}})} \ . \tag{7.8}$$

We note the rate function

$$\psi(k_{\mathcal{I}}) = S_{k_{\mathcal{I}}}[\rho^\star] - S_{k^\star_{\mathcal{I}}}[\rho_{sc}]. \tag{7.9}$$

$Z_{N,\beta}$ is a normalization constant, incorporated into the rate function when we subtract $S[\rho_{sc}]$, the action calculated when $k_{\mathcal{I}}$ is its average value $k^\star_{\mathcal{I}}$ and the average density is Wigner's semicircle. To obtain $\rho^\star(x)$, we differentiate $S[\rho]$ functionally with respect to $\rho$

$$\left.\frac{\delta S}{\delta \rho}\right|_{\rho^\star} = 0 = \frac{x^2}{2} - \int \mathrm{d}x' \rho^\star(x') \log|x - x'| + \mu \mathbb{1}_{\mathcal{I}}(x) + \eta, \quad x \in \text{supp } \rho^\star. \tag{7.10}$$

We differentiate it with respect to $x$ to obtain

$$x + \mu \left(\delta(x - b) - \delta(x - a)\right) = \fint \frac{\rho^\star(x')}{x - x'} \mathrm{d}x', \quad x \in \text{supp } \rho^\star, \tag{7.11}$$

which is the integral equation that, combined with the constraints $\int \rho^\star(x)\mathrm{d}x = 1$ and $\int_{\mathcal{I}} \rho^\star(x)\mathrm{d}x = k_{\mathcal{I}}$, defines $\rho^\star$.

Solving equation (7.11) is the main technical challenge of our problem. We can solve it adapting the standard resolvent (or Green's function) method. Let $G(z)$ be a holomorphic function, called the *resolvent*, defined as

$$G(z) = \int \frac{\rho^\star(x)}{z - x} \mathrm{d}x, \quad z \in \mathbb{C} \setminus \text{supp } \rho^\star. \tag{7.12}$$

Normalization of $\rho^\star$ to 1 implies that $G(z)$ behaves as $1/z$ when $|z|$ is large. Using the identity (4.39), the density $\rho^\star(x)$ can be reconstructed from the imaginary part of the resolvent

$$-\frac{1}{\pi} \lim_{\epsilon \to 0^+} \mathrm{Im} G(x + \mathrm{i}\epsilon) = \rho^\star(x) \ . \tag{7.13}$$

To find an equation for $G(z)$, we multiply equation (7.11) by $\frac{\rho^\star(x)}{z-x}$ and integrate over $x$. If either $a$ or $b$ are outside the support of $\rho^\star$, their contribution is zero. If $a$ and $b$ belong to the support of $\rho^\star$, this procedure yields

$$\int x \frac{\rho^\star(x)}{z - x} \mathrm{d}x + \frac{A}{z - a} + \frac{B}{z - b} = \iint \frac{\rho^\star(x)}{z - x} \frac{\rho^\star(y)}{x - y} \mathrm{d}y \mathrm{d}x, \tag{7.14}$$

where $A$ and $B$ are constants resulting from the integration of each delta function. Some regularization is required to perform the integrals on the deltas, as simply setting $x = a$

and $x = b$ in the two integrands is not possible. We set $x \to a - \varepsilon$ and $x \to b + \varepsilon$, and we take $\varepsilon \to 0$. This procedure converges, and the integrals are both finite and independent of the regularization used. More details can be found at the supplemental material of [97].

The RHS of equation (7.14) can be cast in terms of $G(z)$ with the following manipulation. We use the identity

$$\frac{1}{(z-x)(x-y)} = \left(\frac{1}{z-x} + \frac{1}{x-y}\right)\frac{1}{z-y}, \tag{7.15}$$

to write the RHS as

$$\iint \frac{\rho^\star(x)}{z-x}\frac{\rho^\star(y)}{x-y}\mathrm{d}x\mathrm{d}y = \iint \frac{\rho^\star(x)\rho^\star(y)}{(z-x)(z-y)}\mathrm{d}x\mathrm{d}y - \iint \frac{\rho^\star(x)}{z-x}\frac{\rho^\star(y)}{x-y}\mathrm{d}x\mathrm{d}y. \tag{7.16}$$

Since the first term of the RHS of equation (7.14) is $G^2(z)$ and the second is the original RHS of equation (7.14) with the sign changed, this implies that the original RHS of equation (7.14) is $(1/2)G^2(z)$.

The manipulations required to express the LHS in terms of $G(z)$ depend on the specific form of the potential, but are straightforward in the Gaussian case. The integral over the derivative of the potential in the LHS reads

$$\int x\frac{\rho^\star(x)}{z-x}\mathrm{d}x = \int (x - z + z)\frac{\rho^\star(x)}{z-x}\mathrm{d}x = -1 + zG(z). \tag{7.17}$$

The final equation for the resolvent thus reads

$$-1 + zG(z) + \frac{A}{z-a} + \frac{B}{z-b} = \frac{1}{2}G^2(z). \tag{7.18}$$

where $A$ and $B$ are constants that may be determined by the conditions $\int_{\mathcal{I}} \rho^\star(x)\mathrm{d}x = k_{\mathcal{I}}$ and by a supplementary condition we describe below. The solution to (7.18) reads

$$G_\pm(z) = z \pm \sqrt{z^2 - 2 + \frac{2A}{z-a} + \frac{2B}{z-b}} = z \pm \sqrt{\frac{(z-a_1)(z-a_2)(z-b_1)(z-b_2)}{(z-a)(z-b)}}, \tag{7.19}$$

where $a_1$, $a_2$, $b_1$ and $b_2$ are the roots of the polynomial $(z^2-2)(z-a)(z-b)+2A(z-b)+2B(z-a)$ (we chose $b_1 < a_1 < a_2 < b_2$) and the sign of the resolvent is chosen according to the normalization condition $G(z) \to 1/z$ when $|z| \to \infty$. We note that the resolvent is well defined on the real line outside on the support of $\rho^\star(x)$, and the sign choice for points in the real line is given by

$$G(x) = \begin{cases} G_-(x) \text{ for } x > b_2 \\ G_+(x) \text{ for } x < b_1 \\ G_+(x) \text{ for } k_{\mathcal{I}} > k_{\mathcal{I}}^\star \text{ and } b < x < a_2 \\ G_+(x) \text{ for } k_{\mathcal{I}} < k_{\mathcal{I}}^\star \text{ and } a < x < a_1 \\ G_-(x) \text{ otherwise }, \end{cases} \tag{7.20}$$

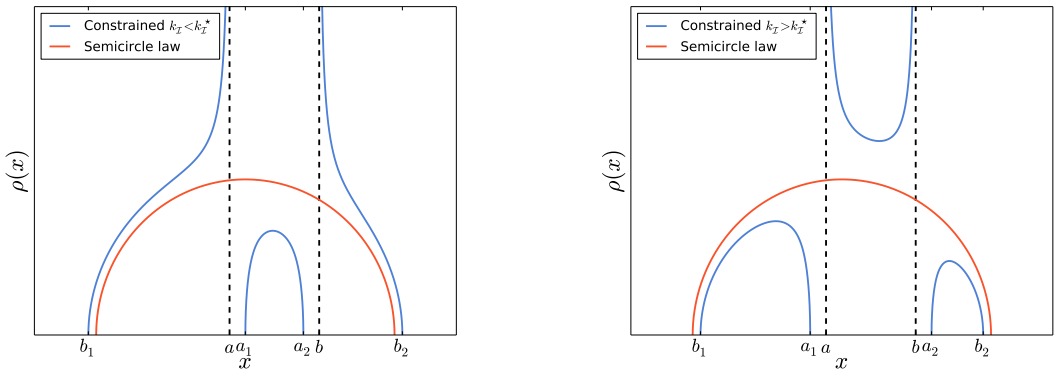


**(a)** $k_{\mathcal{I}} < k_{\mathcal{I}}^\star$. **(b)** $k_{\mathcal{I}} > k_{\mathcal{I}}^\star$.

**Figure 7.1** — Sketch of the expected behavior of $\rho^\star(x)$ for the Gaussian ensemble when $-\sqrt{2} < a < b < \sqrt{2}$, compared to the semicircle law ($k_L = k_L^\star$).

these regions are either "gaps" in the spectrum or the semi-lines $(-\infty, b_1]$, $[b_2, \infty)$. They become clear in figure 7.1.

The average density can then be extracted straightforwardly from the resolvent

$$\rho^\star(x) = -\frac{1}{\pi} \lim_{\epsilon \to 0^+} \mathrm{Im} G(x + \mathrm{i}\epsilon) = \frac{1}{\pi} \sqrt{\frac{(a_1 - x)(x - a_2)(x - b_1)(x - b_2)}{(x - a)(x - b)}}. \tag{7.21}$$

We note that the constants $a_1$, $a_2$, $b_1$ and $b_2$ define the edges of the support of $\rho^\star$ (see figure 7.1). They need four equations to be determined. Two equations are provided by the normalization constant, which is equivalent to identify the edges as the solutions of the polynomial $(z^2 - 2)(z - a)(z - b) + 2A(z - b) + 2B(z - a)$. A simple comparison on the coefficients of these polynomials yields

$$a_1 + a_2 + b_1 + b_2 = a + b \tag{7.22}$$

$$a_1 a_2 + a_1 b_1 + a_1 b_2 + a_2 b_1 + a_2 b_2 + b_1 b_2 = -2 + ab \tag{7.23}$$

The remaining two equations are given by the number of eigenvalues inside the interval, $\int_a^b \rho^\star(x)\mathrm{d}x = k_{\mathcal{I}}$, and a supplementary condition described below (equation (7.28)).

The average density of eigenvalues $\rho^\star(x)$ depends only on the fraction $k_{\mathcal{I}}$ of eigenvalues constrained to be inside the interval. We can see from figure 7.1 that $\rho^\star(x)$ changes drastically when $k_{\mathcal{I}} = k_{\mathcal{I}}^\star$, where $k_{\mathcal{I}}^\star = \int_a^b \rho_{sc}(x)\mathrm{d}x$ is the average number of eigenvalues inside $\mathcal{I}$ for the Gaussian ensemble.

The shape of the average density shown in figures 7.1 shows patterns of divergence at the edges of the interval in either case. As an example, let us take $k_{\mathcal{I}} > k_{\mathcal{I}}^\star$ (figure 7.1b). This means that the number of eigenvalues inside the interval $\mathcal{I}$ is larger than their expected value. Physically, since more charges are stacked *inside* the box than the expected value, they will tend to repel and accumulate towards the box walls, while the charges *outside* the box will be pushed further out by this excess of charge around the

walls. The reverse case, $k_{\mathcal{I}} < k_{\mathcal{I}}^{\star}$ (figure 7.1a), causes more charges to be outside the box than their expected value, and they accumulate towards the box walls on the other side, pushing those inside to a compact blob. When $k_{\mathcal{I}} = k_{\mathcal{I}}^{\star}$, there are no more divergences or convergences around the interval and the density is Wigner's semicircle (3.22).

### 7.2.3 Obtaining the rate function

Having obtained the average density $\rho^{\star}(x)$, we proceed to calculate the rate function $\psi(k_{\mathcal{I}})$. We must insert $\rho^{\star}$ into equation (7.7) and perform the necessary integrals to compute the full probability density of the random variable $N_{\mathcal{I}}$. There integrals are difficult, specially the double integral with the logarithm. We may rewrite the action in a more convenient form using equation (7.10).

We first insert $\rho^{\star}$ into (7.10), multiply the equation by $\rho^{\star}(x)$ and integrate it with respect to $x$ to obtain

$$\int \rho^{\star}(x)\frac{x^2}{2}\mathrm{d}x + \mu \underbrace{\int_a^b \rho^{\star}(x)\mathrm{d}x}_{=k_{\mathcal{I}}} + \eta \underbrace{\int \rho^{\star}(x)\mathrm{d}x}_{=1} = \iint \mathrm{d}x\mathrm{d}x' \rho^{\star}(x)\rho^{\star}(x')\log|x-x'|. \tag{7.24}$$

The RHS is exactly the double integral present in the original action (7.7). Therefore we can replace it with single integrals in the action evaluated at the saddle point $\rho^{\star}$, obtaining eventually

$$S[\rho^{\star}] = \frac{1}{2}\int \frac{x^2}{2}\rho^{\star}(x)\mathrm{d}x - \frac{\mu}{2}k_{\mathcal{I}} - \frac{\eta}{2}. \tag{7.25}$$

What remains to be determined are the multipliers $\mu$ and $\eta$. Equations for these parameters will arise from (7.10), once specialized to certain points within the domain of $\rho^{\star}(x)$.

Let us consider the case $k_{\mathcal{I}} > k_{\mathcal{I}}^{\star}$ (figure 7.1b). We call now $H(x) = \int \rho^{\star}(x')\log|x - x'|\mathrm{d}x'$. Evaluating (7.10) at $x = b$ and $x = a_2$ we obtain

$$H(a_2) = \frac{a_2^2}{2} + \eta \tag{7.26}$$

$$H(b) = \frac{b^2}{2} + \mu + \eta. \tag{7.27}$$

Which allows us to write $\mu = H(b) - H(a_2) + \frac{a_2^2}{2} - \frac{b^2}{2}$. Using the definition of the resolvent in equation (7.12), we note that $H(b) - H(a_2) = \int_{a_2}^{b} G(x)\mathrm{d}x$. The resolvent is well-defined between $a_2$ and $b$, since this interval does not belong to the support of $\rho^{\star}(x)$. This same reasoning may be applied to the other edge of the box, and we would obtain a similar equation with $a$ and $a_1$ (see figure 7.1b). These equalities allow us to calculate $\mu$ in terms of the edges and an integral on the resolvent.

$$\mu = -\int_b^{a_2} G(x)\mathrm{d}x + \frac{a_2^2}{2} - \frac{b^2}{2} = \int_{a_1}^{a} G(x)\mathrm{d}x + \frac{a_1^2}{2} - \frac{a^2}{2}. \tag{7.28}$$

Equation (7.28) is named the *chemical equilibrium condition*. Its physical interpretation in the context of the Coulomb gas is the following. The integral on the resolvent from $b$ to $a_2$ (see figure 7.1b) represents the variation of the intensity of the repulsion felt by a test charge at positions $b$ and $a_2$, while $\mu$ represents the balance between repulsion and potential, i.e. the amount of energy required to move one charge from inside the box to outside the box. The imposition of boundaries and constraints creates a pressure on the edges of the interval and equation (7.28) expresses the fact that such pressure is the same at both sides of the interval.

This equation is equivalent to apply equation (7.10) to a point in the support of the average density. When differentiating with respect to $x$ from equation (7.10) to (7.11), we lost some information, and we retrieve it by evaluating equation (7.10) at a point. Since the integral on the logarithm can be complicated, equation (7.28) is presented as a simpler alternative, since it involves only an integral on the resolvent.

To obtain $\eta$, we use (7.10) for values of $x$ inside the support of $\rho^\star$, but outside the box: $H(x) = \frac{x^2}{2} + \eta$. One can show that, if $b_2$ is the upper edge of the support $\rho^\star$ (see figure 7.1), we may expand $H(x)$ around $b_2$ to obtain

$$H(b_2) = \log b_2 - \int_{b_2}^{\infty} \left( G(x) - \frac{1}{x} \right) \mathrm{d}x = \frac{b_2^2}{2} + \eta. \tag{7.29}$$

We then obtain the following expression for $\eta$

$$\eta = \log b_2 - \frac{b_2^2}{2} - \int_{b_2}^{\infty} \left( G(x) - \frac{1}{x} \right) \mathrm{d}x. \tag{7.30}$$

It remains only to calculate the normalization constant, given by the action $S$ calculated on Wigner's semi circle (3.22). All integrals simplify greatly and we easily compute $S[\rho_{sc}] = \frac{3}{8} + \frac{\log 2}{4}$. The final formula for the rate function of the probability of finding $N_{\mathcal{I}} = N k_{\mathcal{I}}$ eigenvalues inside interval $\mathcal{I} = [a, b]$ is

$$\begin{aligned} \psi(k_{\mathcal{I}}) =& \frac{1}{2} \int \frac{x^2}{2} \rho^\star(x) \mathrm{d}x - \frac{\mu}{2} k_{\mathcal{I}} - \frac{\eta}{2} - S[\rho_{sc}] \\ =& \frac{1}{2} \int_{-\infty}^{+\infty} \rho^\star(x) \frac{x^2}{2} \mathrm{d}x - \frac{1}{2} \left( \int_b^{a_2} G(x) \mathrm{d}x - \frac{a_2^2}{2} + \frac{b^2}{2} \right) k_{\mathcal{I}} \\ & - \frac{1}{2} \left( \log b_2 - \frac{b_2^2}{2} - \int_{b_2}^{\infty} \left( G(x) - \frac{1}{x} \right) \mathrm{d}x \right) - \frac{3}{8} - \frac{\log 2}{4}. \end{aligned} \tag{7.31}$$

The resolvent $G(x)$ is given by equation (7.19), the average density $\rho^\star(x)$ given by equation (7.21) and the edges of its support are given by equations (7.22), (7.23), (7.28) and $\int_a^b \rho^\star(x) \mathrm{d}x = k_{\mathcal{I}}$.

### 7.2.4 Number variance

We turn our attention to a more specific problem: calculate the fluctuations of eigenvalues inside an interval, the number variance for the Gaussian ensemble. For simplicity, we take the interval $\mathcal{I} = [-L, L]$ and we determine the variance of the variable $N_{[-L,L]} = N_L$.

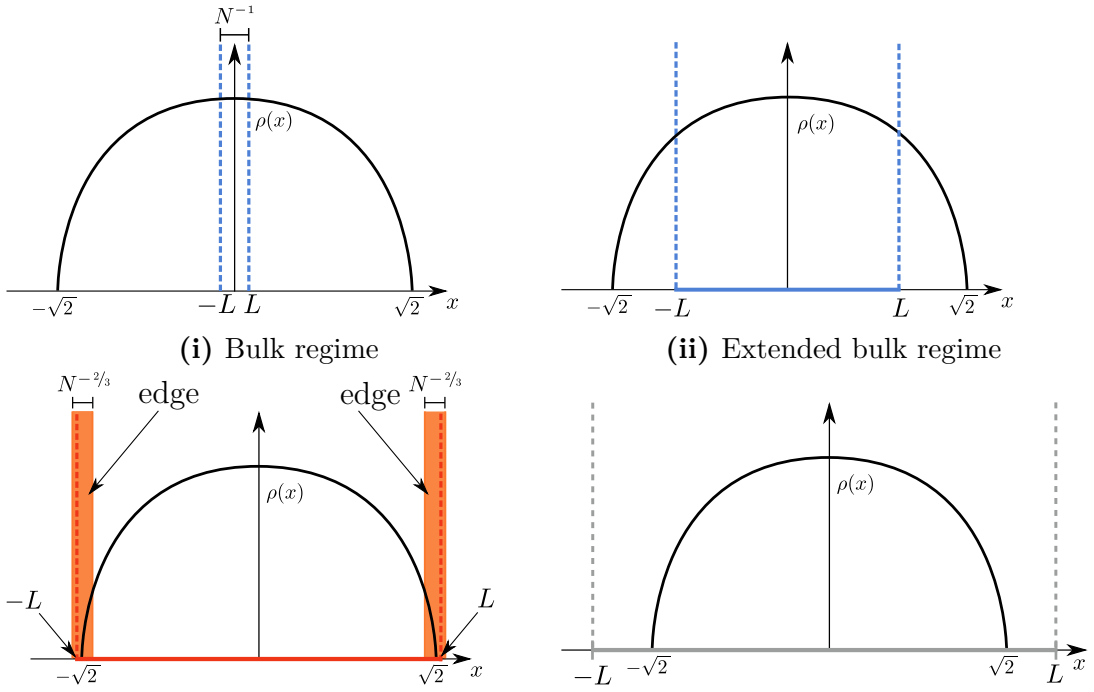


**(i)** Bulk regime **(ii)** Extended bulk regime

**(iii)** Edge regime **(iv)** Tail regime

**Figure 7.2** — Regimes of behavior of the number variance for the Gaussian ensemble.

Usually one can read off the variance of a random variable satisfying a large deviation principle directly from the quadratic behavior of the rate function around its minimum: this implies indeed that small fluctuations around the minimum are Gaussian (so mean and variance are automatically determined). In our case, though, the rate function is not simply quadratic around the minimum [90, 89] and so more effort is needed to extract the variance.

We shall perturb the parameters of (7.21) and expand perturbatively the rate function $\psi(k_{\mathcal{I}})$ around the unconstrained case $k_{[-L,L]} = k_L = k_L^\star + \delta$, where $k_L^\star$ represents its minimum, preserving only the leading terms in the perturbation and reading the variance from the quadratic term that remains. Depending on the value of $L$, however, we must consider three different regimes: (*i*) an extended bulk $N^{-1} < L < \sqrt{2} - N^{-2/3}$, (*ii*) an edge regime $|L - \sqrt{2}| \sim N^{-2/3}$ and (*iii*) a tail regime $L > \sqrt{2} + N^{-2/3}$ (see figure 7.2). There is a strong change in behavior when $L$ crosses the edge of the semicircle $\sqrt{2}$. We shall describe the analysis of each regime separately

### Extended bulk regime

The Gaussian potential and the interval $\mathcal{I} = [-L, L]$ are symmetrical, so all properties of the average density will be symmetrical: $a_1 = -a_2$ and $b_1 = -b_2$. This reduces the number of parameters that we must determine, and trivially satisfies the chemical equilibrium condition (7.28).

The unconstrained case, when $\mu = 0$ and the number of eigenvalues inside the interval

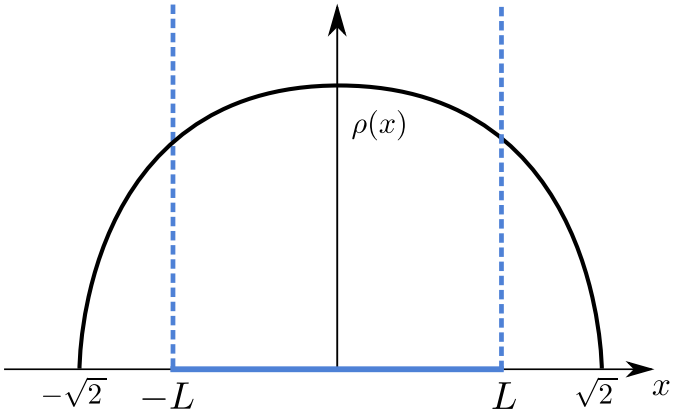


**Figure 7.3** — Extended bulk regime for the Gaussian ensemble. An interval is considered to be on the extended bulk regime when its endpoints lie inside the support, but sufficiently far from the edges.

is their expected value, is: $a_1 = -L$, $a_2 = L$, $b_1 = -\sqrt{2}$, $b_2 = \sqrt{2}$, which turns $\rho^\star$ into Wigner's semicircle. We perturb the parameter $a_1$ of a small shift $\epsilon$: $a_1 = -L - \epsilon$. The perturbation is negative because we expect a modification on the edges according to figure 7.1b, and we compute the consequent perturbation applied to the other parameters using equation (7.23).

We write

$$a_2 = L + \epsilon, \qquad b_1 = -\sqrt{2} + \epsilon_2, \qquad b_2 = \sqrt{2} - \epsilon_2 \ . \tag{7.32}$$

From the normalization condition (7.23) we find

$$\sqrt{2}\epsilon_2 = L\epsilon \tag{7.33}$$

Having calculated the perturbation on each parameter of the resolvent and average density, we proceed to expand the rate function (7.31) around its minimum by expanding each of the integrals involved in its calculation. This procedure is technical and we omit the details of calculations, as they are very similar to the previous integrals performed in the index case. We eventually obtain

$$\psi(k_L) = \frac{1}{4}\int x^2 \rho^\star(x)\mathrm{d}x - \frac{\eta}{2} - \frac{\mu}{2}k_I - \frac{3}{8} - \frac{\log 2}{4} = \frac{\pi}{4}\sqrt{2-L^2}\epsilon\delta + o(\epsilon^2 \log\epsilon), \tag{7.34}$$

where we denote $k_L = k_L^\star + \delta$. The value of $\delta$ as a function of $\epsilon$ is given by

$$\delta \approx \epsilon \frac{\sqrt{2-L^2}}{\pi}\left[\log\left(\left(2-L^2\right)L\right) - \log\epsilon\right] \ . \tag{7.35}$$

We now have to find $\epsilon$ as a function of $\delta$, inverting (7.35). We propose the following ansatz, correct to leading orders of $\delta$ and $\epsilon$

$$\epsilon \approx \frac{\pi}{\sqrt{2-L^2}} \frac{\delta}{\log\left((2-L^2)^{\frac{3}{2}}L\right) - \log\delta} \ . \tag{7.36}$$

We conclude that, for small fluctuations of $k_L$ around its average value $k_L^\star$ we have

$$\psi(k_L = k_L^\star + \delta) \approx \frac{\pi^2}{4} \frac{\delta^2}{\log\left((2-L^2)^{\frac{3}{2}} L\right) - \log\delta} \tag{7.37}$$

Replacing the asymptotic expansion of the rate function around its minimum we obtain, for small $\delta > 0$

$$P(N_L = (k_L^\star + \delta)N) \approx \exp\left[-\beta N^2 \frac{\pi^2}{4} \frac{\delta^2}{\log\left((2-L^2)^{\frac{3}{2}} L\right) - \log\delta}\right]. \tag{7.38}$$

We replace $\delta \to (N_L - N_L^\star)/N$, obtaining for small deviations of $N_L$ from $N_L^\star$

$$P(N_L) \approx \exp\left[-\beta \frac{\pi^2}{4} \frac{(N_L - N_L^\star)^2}{\log\left[(2-L^2)^{\frac{3}{2}} LN\right]}\right]. \tag{7.39}$$

Hence for small fluctuations around the average, $N_L$ has a Gaussian distribution modulated by a logarithmic dependence on $N$. From (7.39), we may directly read off the number variance $\mathrm{Var}(N_L)$

$$\mathrm{Var}(N_L) = \frac{2}{\beta\pi^2} \log\left[NL\left(2-L^2\right)^{3/2}\right] + \mathcal{O}(1). \tag{7.40}$$

The variance for the number of eigenvalues initially grows logarithmically with the size of the box, reaches a peak at $1/\sqrt{2}$ and decreases due to the presence of the edge of the semicircle at $\sqrt{2}$ (see fig 7.7). This is one of the main results of this work. This remarkably simple function describes the evolution of the number variance for very different interval sizes, from the bulk, where we retrieve the classical logarithmic dependence discovered by Dyson and Mehta, to the edge of the semicircle law. The critical value $L = 1/\sqrt{2}$ for the $[-L, L]$ box, where the fluctuations are maximal, is a new result found by this method.

### Edge regime

When the interval reaches the edge of the support, most of the approximations used in the last section are no longer valid and, as we mentioned before, the Coulomb gas method fails to provide a meaningful result at this regime. We then resort to the technique of orthogonal polynomials to investigate the scaling region around the semicircle edge. This calculation was performed in 5.3.2, and it applies fully to our case. We recall the main result. The variance of the number of eigenvalues inside the $L$-box is, in the edge regime for $\beta = 2$, given by

$$\mathrm{Var}(N_{[-L,L]}) = \tilde{V}_2(s), \quad \text{for } L = \sqrt{2} + \frac{s}{\sqrt{2}N^{2/3}}. \tag{7.41}$$

where the function $\tilde{V}_2(s)$ is

$$2\,\mathrm{Var}(N_{[L,\infty)}) = \tilde{V}_2(s) = 2\int_s^\infty \mathrm{d}u \int_{-\infty}^s \mathrm{d}v K_{\mathrm{Ai}}^2(u,v). \tag{7.42}$$

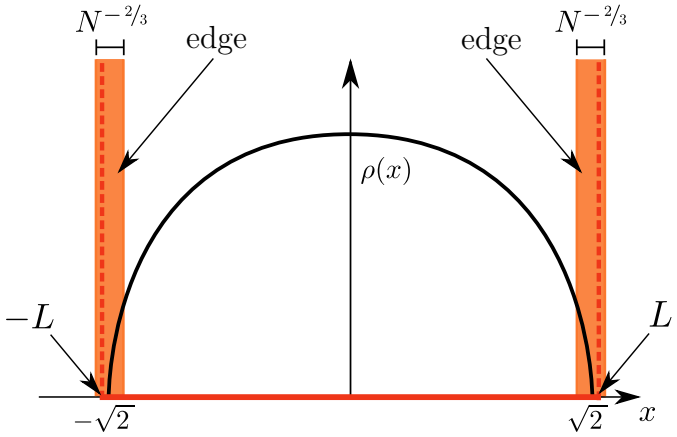


**Figure 7.4** — Edge regime for the normalized Gaussian ensemble. An interval is considered to be on the edge regime when its endpoints lie inside the colored area.

Asymptotics of $\tilde{V}_2(s)$ on the scaling variable $s$, studied by [62], are given in chapter 5 and we recall them

$$\tilde{V}_2(s) = \begin{cases} \frac{3}{2\pi^2}\log|s|, & \text{for } s \to -\infty \\ \frac{1}{8\pi s^{3/2}}\exp\left(-\frac{4}{3}s^{3/2}\right), & \text{for } s \to \infty \end{cases}. \tag{7.43}$$

We expect a matching between the limit $L \to \sqrt{2}$ from the extended bulk regime $N^{-1} < L < \sqrt{2}$ and the limit $s \to -\infty$ in the edge regime. Indeed, replacing $L = \sqrt{2} + \frac{s}{\sqrt{2}N^{2/3}}$ in equation (7.40) for $\beta = 2$ and taking the large $N$ limit yields

$$\frac{1}{\pi^2}\log\left(NL(2-L^2)^{3/2}\right) \overset{\text{large } N}{\longrightarrow} \frac{3}{2\pi^2}\log(-s), \quad \text{for } L = \sqrt{2} + \frac{s}{\sqrt{2}N^{2/3}}. \tag{7.44}$$

In agreement with the limit of equation (5.38) when $s \to -\infty$. Assuming this matching holds for all values of $\beta$, we expect the following asymptotic behaviors

$$\tilde{V}_\beta(s) = \begin{cases} \frac{3}{\beta\pi^2}\log|s|, & \text{for } s \to -\infty \\ \frac{1}{c_\beta s^{3/2}}\exp\left(-\frac{2\beta}{3}s^{3/2}\right), & \text{for } s \to \infty \end{cases}, \tag{7.45}$$

where $c_\beta$ is a constant that may depend on $\beta$.

### Tail regime

While it is certainly possible to use the Coulomb gas technique for the *tail* regime, where $L > \sqrt{2}$ (or $L < \sqrt{2}$) and $|L - \sqrt{2}| \gg N^{-2/3}$, it is more convenient to obtain its variance by recalling a few properties of the statistics of atypical fluctuations of the spectrum. We note that equation (5.36) may be also applied for any value of $L$ larger than $\sqrt{2}$, we need only only to determine $\mathrm{Var}(N_{[L,\infty)})$ when $L > \sqrt{2}$.

For values of $L$ larger than the edge of the semi-circle, the probability of finding one eigenvalue on the interval $[L, \infty)$ is equivalent to the probability of having the largest

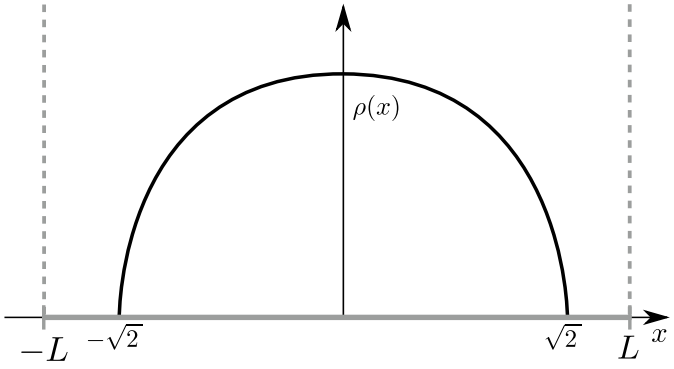


**Figure 7.5** — Tail regime for the normalized Gaussian ensemble. An interval is considered to be on the tail regime when its endpoints lie outside the support of the average distribution and far away from the edges.

eigenvalue at position $x \geq L$. This is an extreme atypical configuration whose statistics was first computed in [93]. Outside the edge regime, keeping only leading order terms for large $N$, the p.d.f. of the largest eigenvalue $\lambda_{\max}$ for the normalized Gaussian ensemble is given by $P(\lambda_{\max} = L) \approx \exp\left(-\beta N \phi(L)\right)$, where

$$\phi(L) = \frac{1}{2} L\sqrt{L^2 - 2} + \log\left[\frac{L - \sqrt{L^2 - 2}}{\sqrt{2}}\right]. \tag{7.46}$$

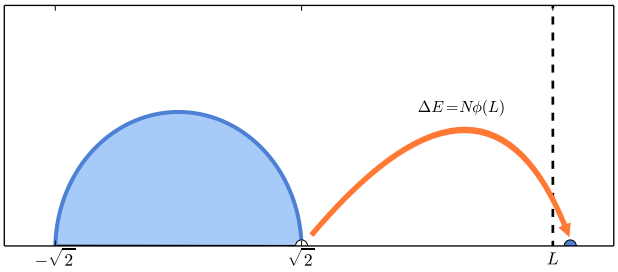


**Figure 7.6** — Energy required to take one eigenvalue from the semi-circle and place it at $L > \sqrt{2}$.

In the Coulomb gas framework, we identify $N\phi(L)$ as the energy required to pull one charge from the Wigner's sea and bring it to $L$ (see figure 7.6). For small values of $k$, the probability of finding $k$ eigenvalues in the interval $[L, \infty)$ becomes $P(k, L) = A \exp\left(-\beta N k \phi(L)\right)$, where $A$ is a normalization constant. For large values of $N$, $A$ may be approximated by $\left(\sum_{k=0}^{\infty} P(k, L)\right)^{-1} = 1 - \exp\left(-\beta N \phi(L)\right)$. The number variance on $[L, \infty)$ may then be calculated directly as

$$\mathrm{Var}(N_{[L,\infty)}) = \left\langle k^2 \right\rangle - \langle k \rangle^2 = \sum_{k=1}^{\infty} k^2 P(k, L) - \left(\sum_{k=1}^{\infty} k P(k, L)\right)^2 \approx \frac{\mathrm{e}^{-\beta N \phi(L)}}{\left(1 - \mathrm{e}^{-\beta N \phi(L)}\right)^2}, \tag{7.47}$$

to leading order in $N$. Therefore, the variance for the number of eigenvalues between $-L$ and $L$, when $L > \sqrt{2}$ and $N$ is large, reads

$$\mathrm{Var}(N_{[-L,L]}) = 2\,\mathrm{Var}(N_{[L,\infty)}) \approx \frac{\mathrm{e}^{-\beta N \phi(L)}}{(1-\mathrm{e}^{-\beta N \phi(L)})^2} \tag{7.48}$$

Replacing $L = \sqrt{2} + \frac{s}{\sqrt{2}N^{2/3}}$ and taking $s \to \infty$ on equation (7.47) will retrieve the leading order in $s$ of equation (7.43). We also note that $\mathrm{Var}(N_{[L,\infty)})$ decays exponentially with $L$, so we retrieve the expected result that fluctuations of eigenvalues inside an interval larger than their support are exponentially small as the interval increases.

### 7.2.5 Comparison with numerics

We are able to simulate eigenvalues from Gaussian random matrices with little computational effort using the equivalence between the spectrum of the Gaussian ensemble and the eigenvalues of a certain tri-diagonal matrix found by Dumitriu and Edelman [41]. Results for the extended bulk and edge regimes are found in figure 7.7. We are not able to perform simulations for the tail regime due to the extreme small probability of finding an eigenvalue above $\sqrt{2}$.

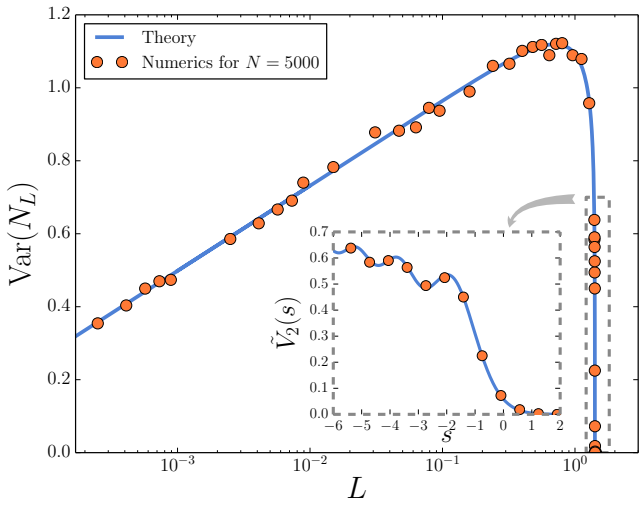


**Figure 7.7** — Results for the variance of $N_{\mathcal{I}}$ for the Gaussian ensemble when $\mathcal{I} = [-L, L]$ and $L < \sqrt{2}$. Theory is equation (7.40). Inset: results for the edge regime, where $s = (L - \sqrt{2})\sqrt{2}N^{2/3}$ and theory is equation (5.38).

Equation (7.31) is complicated to analyze directly, but represents no challenge numerically. Since the rate function depends on $k_L$ and $L$, we calculate this two variable function for two values of $L$ and we plot it in figure 7.8.

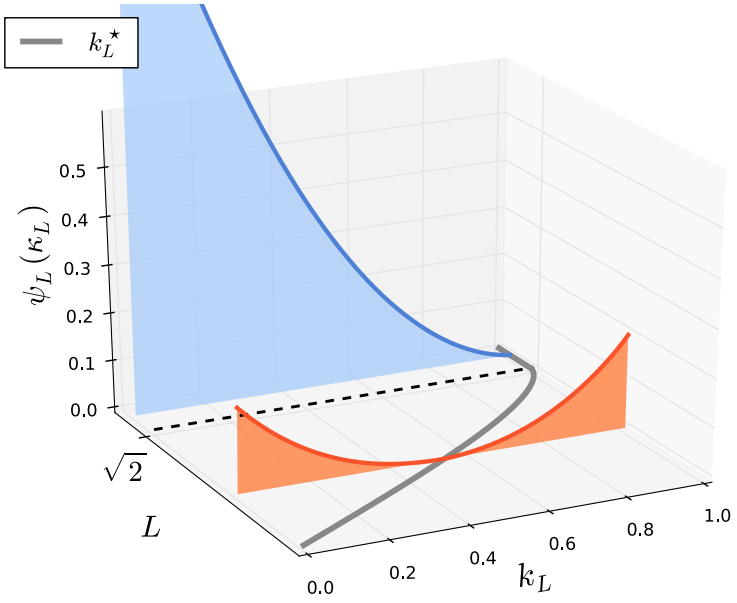


**Figure 7.8** — Behavior of the rate function $\psi(k_L)$ as a function of $k_L \in [0, 1]$ for two different values of $L$: $L = 0.6 < \sqrt{2}$ and $L = 1.6 > \sqrt{2}$. The solid gray line in the plane $(L, k_L)$ is the critical line $k_L^\star$, where $\psi(k_L)$ has a minimum (zero).

## 7.3 Entanglement entropy of confined fermions

The number of fermions $N_\mathcal{I}$ inside an interval $\mathcal{I}$ has a direct correspondence to the entanglement entropy of the sub-system $\mathcal{I}$. To explore this relation, we follow the account of [28]. We recall the definition of the entanglement entropy in terms of the reduced density matrix $\rho_\mathcal{I} = \mathrm{Tr}_{\mathcal{I}^C}\rho$ of a sub-system $\mathcal{I}$, where $\mathcal{I}^C$ is the complementary of $\mathcal{I}$

$$S_q = \frac{1}{1-q}\log \mathrm{Tr}\rho_\mathcal{I}^q. \tag{7.49}$$

The entanglement entropy can be calculated [30, 29] using the eigenvalues $\{a_i\}$ of the overlap matrix $A$, which coincide with the eigenvalues of the projected kernel $P_\mathcal{I} K P_\mathcal{I}$ (see section 5.4.2)

$$S_q = \frac{1}{1-q}\sum_{i=1}^{N}\log\left[a_i^q + (1-a_i)^q\right]. \tag{7.50}$$

Using the fact that the kernel $K$ is the same for cold fermions and GUE, we can apply results from random matrix directly to the calculation of the entanglement entropy of this quantum system. We define the the resolvent

$$G(z) = \mathrm{Tr}\frac{1}{z\mathbb{1} - A} = \sum_{i=1}^{N}\frac{1}{z - a_i}. \tag{7.51}$$

And it is clear that taking a path $C$ around the interval $]0,1[$, where lie the eigenvalues of $A$ (represented in figure 7.9), we may obtain the entanglement entropy by the following integral

$$S_q = \oint_C \frac{\mathrm{d}z}{2\pi i} \log\left[z^q + (1-z)^q\right] G(z). \tag{7.52}$$

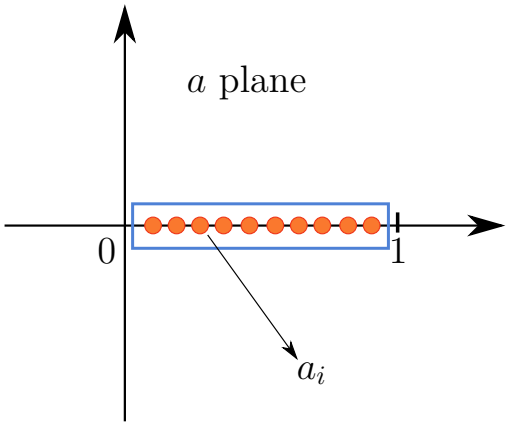


**Figure 7.9** — Representation of the integration path $C$

As shown in [28], the resolvent can be cast in terms of the number of fermions inside the interval $\mathcal{I}$

$$G(z) = \frac{N}{z} + \frac{1}{z(z-1)} \frac{\left\langle N_{\mathcal{I}} \left(1 - \frac{1}{z}\right)^{N_{\mathcal{I}}} \right\rangle}{\left(1 - \frac{1}{z}\right)^{N_{\mathcal{I}}}}. \tag{7.53}$$

Inserting this expression into (7.52) we obtain

$$S_q = \frac{1}{1-q} \frac{1}{2\pi i} \oint_C \frac{\mathrm{d}z}{z(z-1)} \log[z^q + (1-z)^q] \frac{\left\langle N_{\mathcal{I}} \left(1 - \frac{1}{z}\right)^{N_{\mathcal{I}}} \right\rangle}{\left(1 - \frac{1}{z}\right)^{N_{\mathcal{I}}}}, \tag{7.54}$$

which connects number statistics and entanglement entropy. This shows that, for cold fermions, the entanglement entropy is completely determined given the statistics of the number of particles inside the sub-system. For the particular case of a number statistics that is Gaussian distributed, integral (7.54) can be performed exactly and yields the result [28]

$$S_q = \frac{\pi^2}{6} \left(1 + \frac{1}{q}\right) \mathrm{Var}\left(N_{\mathcal{I}}\right), \qquad \text{for } N_{\mathcal{I}} \text{ Gaussian.} \tag{7.55}$$

In the case of cold fermions, in the bulk regime, for an interval of the order of the interparticle distance, the number statistics can be considered Gaussian (see section 5.3.1). For intervals larger than the interparticle distance, equation (7.55) is not necessarily true. The leading term, however, is correct; and we may obtain the leading behavior of the entanglement entropy of an interval of mesoscopic size from the number variance of the Gaussian unitary ensemble.

The entanglement entropy in the extended bulk regime for a symmetric interval was conjectured [137] to be approximated by

$$\mathrm{Var}\left(N_{[-L,L]}\right) \stackrel{?}{=} \frac{1}{\pi^2}\log\left[\sin\left(\frac{NL}{\sqrt{2}}\right)\right] + O(1), \tag{7.56}$$

which was obtained replacing the soft edge at $x = \sqrt{2}$ by a hard edge. As noted in [47], even though it is a numerically convincing approximation, this is not a very accurate one as the transition between hard edge and soft edge is, in some way, singular. During my PhD, I was able to show that the real function for the number variance for GUE of an interval of size $1/N < L < \sqrt{2} - N^{-2/3}$ is given in the large $N$ limit by

$$\mathrm{Var}\left(N_{[-L,L]}\right) = \frac{1}{\pi^2}\log\left[NL(2-L^2)^{3/2}\right] + O(1), \tag{7.57}$$

which yields the correct matching with bulk and edge regimes. This results yields the leading behavior for the entanglement entropy of cold fermions for interval of mesoscopic size, and it is one of the main results of this work.

## 7.4 Summary of results

In this chapter, I presented the correspondence between cold fermions on a line confined to a harmonic potential and eigenvalues of the Gaussian unitary ensemble. Using the Coulomb gas technique, I was able, during my PhD, to explore the macroscopic region of the spectrum and determine, for the first time, the number variance of the interval $[-L, L]$ as a function of $L$ for the whole spectrum, given by equation (7.58) for general $\beta$.

$$\mathrm{Var}(N_{[-L,L]}) \approx \begin{cases} \frac{2}{\beta\pi^2}\log\left(NL(2-L^2)^{3/2}\right), & N^{-1} < L < \sqrt{2} - N^{-2/3} \\ V_\beta(s), & L = \sqrt{2} + \frac{s}{\sqrt{2}}N^{-2/3} \\ \exp[-\beta N\phi(L)], & L > \sqrt{2} + N^{-2/3}, \end{cases} \tag{7.58}$$

and we confirmed it with numerical calculations of the variance of the number of Gaussian unitary eigenvalues inside an interval (figure 7.7).

Previous results [100, 43] pointed to a logarithmic dependence on $L$ of this variance in the interparticle distance scaling (equation (5.26)), and we obtain such results when applying the limit of small $L$ in our results. The matching between the three regions was verified, and has been studied previously in the context of cold fermions [46, 137]. This work, published in [97], reveals for the first time the full behavior of the number variance with system size, spanning values from the bulk to infinite, describing the sharp fall around the edge and the matching behavior between the identified regimes.

# — 8 —
# Number statistics of other ensembles

*Mathematicians are like Frenchmen: whatever you say to them they translate into their own language and then it is immediately something quite different.*

Johann Wolfgang von Goethe

The Coulomb gas method used to derive the number variance for the extended bulk and the tail regime is very general and changes little when applied to other invariant ensembles. Since their main difference is the potential $V(x)$, we may explore their number statistics and remark the differences in behavior between Gaussian, Wishart and Cauchy matrices.

The choice of these two ensembles is made based on their unique differences from the Gaussian case. We explored the symmetric interval on the Gaussian ensemble in the previous chapter, and the Wishart ensemble presents no evident symmetry. It is interesting to see the effects of this asymmetry in the behavior of the number variance for an interval of size $L$, and compare it to the Gaussian case. The Cauchy ensemble, on the other hand, presents no soft edge on its average density. Since the number variance changes dramatically when the interval crosses the edge, our natural interest is consider what happens to this quantity for the Cauchy case when the size of the considered interval grows.

## 8.1 Wishart ensemble

We begin by analyzing the number statistics of the Wishart ensemble. In the Gaussian case, we chose the symmetrical interval $[-L, L]$, but the Wishart case does not present the same symmetry. Instead, we decided to evaluate the interval $\mathcal{I} = [1, L]$, and we recall that 1 is the average value of the Wishart matrix when $M = N$. All this study does not depend on the values chosen for the interval $\mathcal{I}$, we take 1 as the lower bound for simplicity.

This study should yield a different result than the Gaussian case, because the limit when $L \to \infty$ is no longer zero. This distribution was originally studied in [94] in the context of Principal Component Analysis, and the techniques we use are similar.

### 8.1.1 The Coulomb gas

Using the Wishart potential neglecting the logarithm term $V(x) = x/2$, we write the p.d.f. of $N_{\mathcal{I}}$

$$P(N_{\mathcal{I}} = k_{\mathcal{I}}N) = \frac{1}{Z_{N,\beta}} \int \prod_{k=1}^{N} \mathrm{d}\lambda_k e^{-\beta N \sum_{k=1}^{N} \frac{\lambda_k}{2}} \prod_{i>j} |\lambda_i - \lambda_j|^{\beta} \delta \left( k_{\mathcal{I}} N - \sum_{l=1}^{N} \mathbb{1}_{\mathcal{I}}(\lambda_l) \right). \quad (8.1)$$

From (8.1), it is easy to see that most of the approach taken on the Gaussian case applies to the Wishart ensemble. We repeat the Coulomb gas method defining analogous functions to the Gaussian case. We write (8.1) as the Gibbs-Boltzmann weight of an associated thermodynamical system and we introduce the continuum density to convert multiple integrals into functional integrals over the densities. In the large-$N$ limit we find

$$P(N_{\mathcal{I}} = k_{\mathcal{I}}N) = \frac{1}{Z_N} \int \mathcal{D}\rho \mathrm{d}\mu \mathrm{d}\eta \mathrm{e}^{-\beta N^2 S[\rho]} = \mathrm{e}^{-\beta N^2 (S[\rho^\star] - S[\rho_{mp}])} = \mathrm{e}^{-\beta N^2 \psi(k_{\mathcal{I}})}, \quad (8.2)$$

where

$$\begin{aligned} S[\rho] = &\int \frac{x}{2} \rho(x) \mathrm{d}x - \frac{1}{2} \iint \mathrm{d}x \mathrm{d}x' \rho(x) \rho(x') \log |x - x'| \\ &+ \mu \left( \int_1^L \rho(x) - k_{\mathcal{I}} \right) + \eta \left( \int_0^\infty \rho(x) \mathrm{d}x - 1 \right), \end{aligned} \quad (8.3)$$

we note the extra Lagrange multiplier $\eta$ introduced to enforce normalization of the average density and positivity of the eigenvalues.

### 8.1.2 The resolvent method

Since $N$ is large, we may apply the saddle-point method to obtain the constrained average density of eigenvalues $\rho^\star(x)$. The functional derivative of the action reads

$$\left. \frac{\delta S}{\delta \rho} \right|_{\rho^\star} = 0 = \frac{x}{2} - \int \mathrm{d}x' \rho^\star(x') \log |x - x'| + \mu \mathbb{1}_{\mathcal{I}}(x) + \eta \mathbb{1}_{[0,\infty)}(x), \quad x \in \text{supp } \rho^\star. \quad (8.4)$$

And its derivative with respect to $x$ yields

$$\frac{1}{2} + \eta \delta(x) + \mu \left( \delta(x - L) - \delta(x - 1) \right) = \fint \frac{\rho^\star(x')}{x - x'} \mathrm{d}x', \quad x \in \text{supp } \rho^\star. \quad (8.5)$$

We note how the hard wall at 0 is responsible for an extra term on $\eta$ at the integral equation (8.5). Repeating the technique used for the Gaussian ensemble, we multiply both sides by $\frac{\rho^\star(x)}{z-x}$ and integrate over $x$. If $L$ is outside the support of $\rho^\star$, its contribution is zero. If $L$ belongs to the support of $\rho^\star$, this procedure yields

$$\frac{1}{2} \int \frac{\rho^\star(x)}{z - x} \mathrm{d}x + \frac{A}{z - 1} + \frac{B}{z - L} + \frac{C}{z} = \iint \frac{\rho^\star(x)}{z - x} \frac{\rho^\star(y)}{x - y} \mathrm{d}y \mathrm{d}x. \quad (8.6)$$

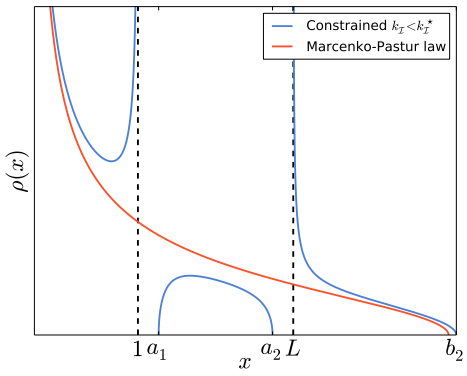


**(a)** Sketch of the expected behavior of $\rho^\star(x)$ for the Wishart ensemble when $k_L < k_L^\star$.

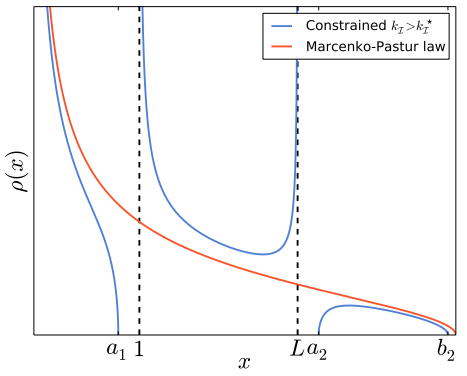


**(b)** Sketch of the expected behavior of $\rho^\star(x)$ for the Wishart ensemble when $k_L > k_L^\star$.

**Figure 8.1**

We define once again the resolvent function $G(z)$. The RHS of integral equation (8.6) is again $G(z)^2/2$, while the LHS can be trivially written in terms of $G(z)$. We obtain

$$\frac{1}{2}G(z) + \frac{A}{z-1} + \frac{B}{z-L} + \frac{C}{z} = \frac{1}{2}G^2(z). \tag{8.7}$$

with solution

$$G(z) = \frac{1}{2} \pm \sqrt{\frac{1}{4} + \frac{2A}{z-1} + \frac{2B}{z-L} + \frac{2C}{z}} = \frac{1}{2} \pm \frac{1}{2}\sqrt{\frac{(z-a_1)(z-a_2)(z-b_2)}{z(z-1)(z-L)}}\,. \tag{8.8}$$

The constrained spectral density (when a prescribed fraction of eigenvalues is assigned to the interval $\mathcal{I}$) can be directly read off from $G(z)$

$$\rho^\star(x) = \frac{1}{2\pi}\sqrt{\frac{(a_1-x)(a_2-x)(b_2-x)}{x(1-x)(L-x)}}, \tag{8.9}$$

where the constants $a_1$, $a_2$ and $b_2$ are the edges of the support (see figure 8.1) and should be determined by the normalization condition $|z| \to \infty \implies G(z) \to 1/z$ and the number of eigenvalues inside $\mathcal{I}$. Explicitly, these conditions are

$$a_1 + a_2 + b_2 = 5 + L, \qquad \int_1^L \rho^\star(x)\mathrm{d}x = k_{\mathcal{I}}. \tag{8.10}$$

We have two equations for three coordinates, we need one more equation to determine the remaining edge of the average distribution. This problem is particularly interesting and has not emerged in the previous studies, it is only present due to the asymmetry of the interval.

The root of this problem is the passage from the energy balance equation (8.4) to the force balance equation (8.5). When differentiating with respect to $x$, we lost some information, and the missing equation could be obtained by evaluating the energy balance equation in any point.

This equation, however, presents an integral of the average density multiplied by the logarithm, and we would rather deal with integrals without the logarithm. As we mentioned in the Gaussian case, the solution we propose is the use of the chemical equilibrium condition (7.28). For the Wishart case it reads

$$-\int_L^{a_2} G(x)\mathrm{d}x + \frac{a_2}{2} - \frac{L}{2} = \int_{a_1}^{1} G(x)\mathrm{d}x + \frac{a_1}{2} - \frac{1}{2} = \mu. \tag{8.11}$$

This condition was absent from previous cases because it is trivially satisfied when the interval is symmetrical. We mentioned it briefly when considering a general interval for the Gaussian case, but it was not needed to calculate the number variance of the symmetrical interval. This condition, together with the normalization and the imposition of a fraction $k_L$ of eigenvalues inside the interval (equation (8.10)), determines the edges $a_1$, $a_2$ and $b_2$ of the support (8.9).

### 8.1.3 Obtaining the rate function

To calculate the rate function, we notice that all steps taken in the Gaussian case may be applied if we replace the Gaussian potential by the Wishart potential. Using (8.4), we may write the action as

$$S[\rho^\star] = \frac{1}{2}\int \frac{x}{2}\rho^\star(x)\mathrm{d}x - \frac{\mu}{2}k_{\mathcal{I}} - \frac{\eta}{2}. \tag{8.12}$$

The Lagrange multipliers $\mu$ and $\eta$ will be calculated in precisely the same way as the Gaussian case, their formulas will only differ on the potential.

$$\mu = -\int_L^{a_2} G(x)\mathrm{d}x + \frac{a_2}{2} - \frac{L}{2}, \qquad \eta = \log b_2 - \frac{b_2}{2} - \int_{b_2}^{\infty}\left(G(x) - \frac{1}{x}\right)\mathrm{d}x. \tag{8.13}$$

And the action can be easily computed for the unconstrained case, when $k_{\mathcal{I}} = k_{\mathcal{I}}^\star$ and the average density is the Marčenko-Pastur distribution (3.24). We find $S[\rho_{mp}] = 3/4$.

The final formula for the rate function of $N_{\mathcal{I}}$ in the Wishart ensemble reads

$$\begin{aligned}\psi(k_{\mathcal{I}}) =& \frac{1}{2}\int_0^{\infty}\frac{x}{2}\rho^\star(x)\mathrm{d}x - \frac{\mu}{2}k_{\mathcal{I}} - \frac{\eta}{2} - S[\rho_{mp}] \\ =& \frac{1}{2}\int_0^{\infty}\frac{x}{2}\rho^\star(x)\mathrm{d}x - \frac{1}{2}\left(\int_L^{a_2} G(x)\mathrm{d}x - \frac{a_2^2}{2} + \frac{L^2}{2}\right)k_{\mathcal{I}} \\ & - \frac{1}{2}\left(\log b_2 - \frac{b_2^2}{2} - \int_{b_2}^{\infty}\left(G(x) - \frac{1}{x}\right)\mathrm{d}x\right) - \frac{3}{4},\end{aligned} \tag{8.14}$$

where $G(x)$ is equation (8.8) with the proper sign choice and $\rho^\star(x)$ is (8.9).

### 8.1.4 Number variance

As in the Gaussian case, equation (8.14) is too general to be analyzed directly. We turn our attention to a more specific case, the interval $[1, L]$. We choose the lower value as 1 for simplicity, we could have taken any value from the support and calculations would be similar. As we will see, the main variables for the number variance are the interval size and the edge of the Marčenko-Pastur distribution, not the starting point of the interval. We perturb the rate function around its minimum and we read the variance of $N_L$ from the quadratic term remaining.

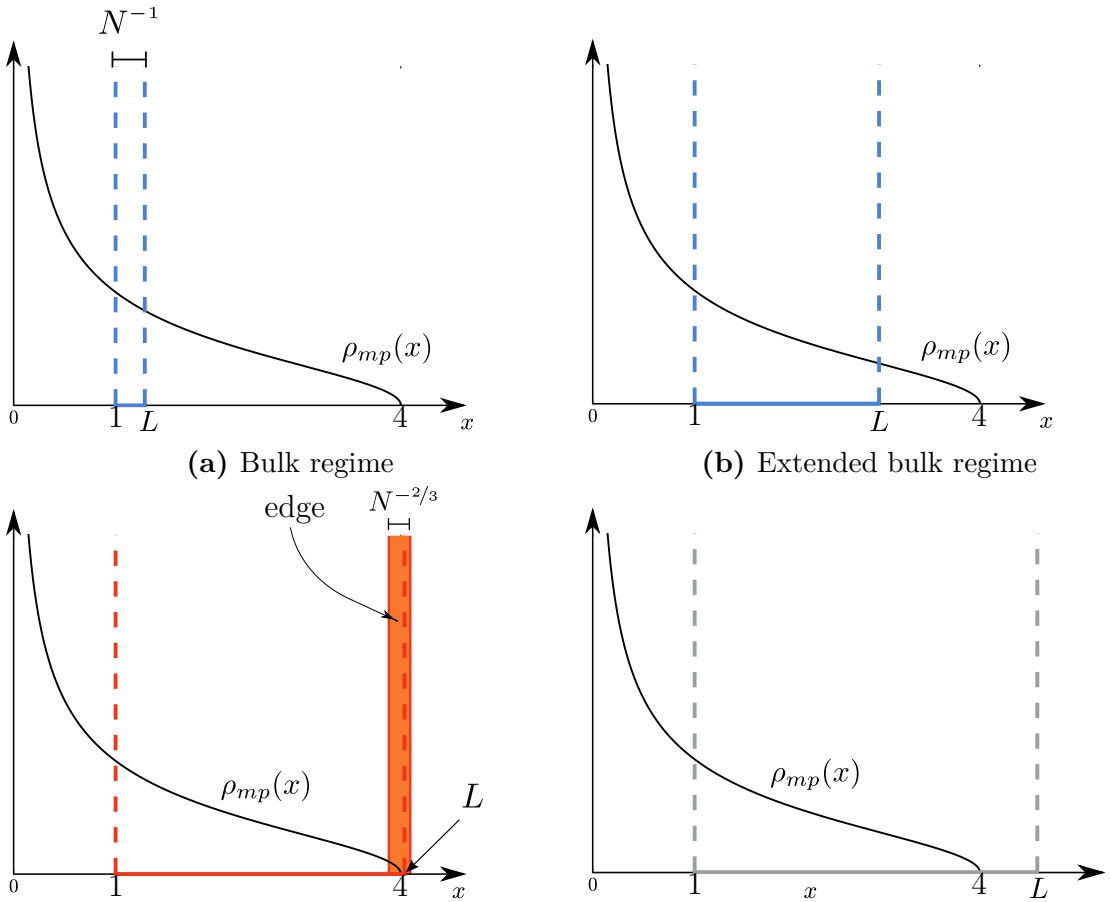


**(a)** Bulk regime **(b)** Extended bulk regime

**(c)** Edge regime **(d)** Tail regime

**Figure 8.2** — Regimes of behavior of the number variance for the Wishart ensemble.

The perturbative approach is similar, and we once more find three separate regimes for the number variance: an extended bulk, an edge and a tail regime, described in figure 8.2. We describe the calculation of the number variance in these regimes separately.

### Extended bulk regime

We define the variable $l = L - 1$ as the size of the interval, and perform very similar calculations to the Gaussian case. Integrals are performed in exactly the same way and we refer to the Gaussian ensemble (section 7.2.4) for the details of the calculations of $\mu$ and $\eta$. Denoting the number of eigenvalues inside $[1, 1 + l]$ as $N_l$, we obtain its variance, to leading orders of $N$ and for $1/N < l < 3$,

$$\operatorname{Var} N_l = \frac{2}{\beta\pi^2} \log\left(Nl(3-l)^{3/4}\right) + \mathcal{O}(1), \tag{8.15}$$

where $l = 3$ is a special point, corresponding to $L = 4$, the soft edge.

As expected, the behavior on the extended bulk is extremely similar to the Gaussian case. The variance reaches its maximum at a point, $l = \sqrt{6/5}$ for this ensemble, and decreases when the soft edge approaches.

### Edge regime

Results in the edge regime are similar to the Gaussian case, since both ensembles are governed by the Airy kernel near their soft edges. For the Wishart ensemble, we may write an equivalent of equation (5.36),

$$\operatorname{Var}(N_{[1,L]}) \overset{\text{large } N}{\sim} \operatorname{Var}(N_{[0,1]}) + \operatorname{Var}(N_{[L,\infty)}), \text{ for } L \sim 4\ . \tag{8.16}$$

Since $[0, 1]$ and $[1, \infty)$ are complementary sets on the positive semi-axis, $\operatorname{Var}(N_{[0,1]}) = \operatorname{Var}(N_{[1,\infty)})$ and the first term of the RHS of equation (8.16) is in fact the variance of the index of the Wishart ensemble. This result was obtained in [94].

$$\operatorname{Var}(N_{[0,1]}) = \operatorname{Var}(N_{[1,\infty)}) = \frac{1}{\beta\pi^2} \ln N. \tag{8.17}$$

To obtain $\operatorname{Var}(N_{[L,\infty)})$, we consider the $\beta = 2$ case. Equation (5.35) applies if we use the scaling $u = (N/4)^{2/3}(4 - x)$ [129, 75]

$$K_N\left(4 + \frac{u}{(N/4)^{2/3}}, 4 + \frac{v}{(N/4)^{2/3}}\right) \overset{N\gg 1}{\sim} (N/4)^{2/3} K_{\mathrm{Ai}}(u, v)\ , \tag{8.18}$$

$$K_{\mathrm{Ai}}(u, v) = \frac{\mathrm{Ai}(u)\mathrm{Ai}'(v) - \mathrm{Ai}(v)\mathrm{Ai}'(u)}{u - v}\ . \tag{8.19}$$

Using the scaling variable $s = (L - 4)(N/4)^{2/3}$, we find

$$\operatorname{Var}(N_{[L,\infty)}) = \frac{1}{2} V_2(s) = \int_s^\infty \mathrm{d}u \int_{-\infty}^s \mathrm{d}v K_{\mathrm{Ai}}^2(u, v). \tag{8.20}$$

The variance becomes, for $\beta = 2$

$$\operatorname{Var}(N_{[1,L]}) = \frac{1}{2\pi^2} \ln N + \frac{1}{2} V_2(s), \text{ for } L = 4 + \frac{s}{(N/4)^{2/3}}. \tag{8.21}$$

Asymptotics of $V_2(s)$ for $s \to \pm\infty$ were studied by [62] and are given by equation (7.43). We notice a fundamental difference between this case and the Gaussian case, the presence of the $\ln N$ term. This contribution arises from fluctuations on the left side on the interval, on the $x = 1$ point. The other contribution, $V_2(s)$, represents fluctuations on the right side on the interval, and increasing $L$ decreases the probability of having an eigenvalues to the right of the interval and hence decreases fluctuations on this side.

We notice that, as in the Gaussian case, we can explore the limits $s \to \pm\infty$ to obtain the matching between the edge regime and the extended bulk and tail regimes. For $\beta = 2$ we confirm that this matching holds, and we can conjecture that it holds for all values of $\beta$. If we take $L = 4 + \frac{s}{(N/4)^{2/3}}$ in equation (8.15), we obtain, for large values of $N$:

$$\frac{2}{\beta\pi^2} \ln\left[Nl(3-l)^{3/4}\right] \xrightarrow{N\gg 1} \frac{1}{\beta\pi^2} \ln N + \frac{3}{2\beta\pi^2} \ln|s| + \mathcal{O}(1), \text{ for } L = 4 + \frac{s}{(N/4)^{2/3}}. \quad (8.22)$$

If we assume that this matching holds for all values of $\beta$, we can write a general expression for the variance of the edge regime

$$\mathrm{Var}(N_{[1,L]}) = \frac{1}{\beta\pi^2} \ln N + \frac{1}{2} V_\beta(s), \text{ for } L = 4 + \frac{s}{(N/4)^{2/3}}. \quad (8.23)$$

and its asymptotic behavior, to match its neighboring regions, should be

$$V_\beta(s) \sim \begin{cases} \frac{3}{\beta\pi^2} \ln|s|, & \text{for } s \to -\infty \\ \frac{1}{C_\beta(s)} \exp\left(-\frac{2\beta}{3} s^{3/2}\right), & \text{for } s \to \infty \end{cases}, \quad (8.24)$$

where $C_\beta(s)$ is a power of $s$ dependent on $\beta$ whose value for $\beta = 2$ is given by $C_2(s) = 8\pi s^{3/2}$. The asymptotic behavior for $s \to \infty$ for general $\beta$ is obtained using the matching with the tail regime, presented in the next section.

### Tail regime

As the kernel $K_N(x, y)$ of both Gaussian and Wishart ensembles is described by the Airy kernel (5.33) on the correct scaling limit, the statistics of their largest eigenvalue is equally described by the Tracy-Widom distribution. This implies that the probability of finding the largest eigenvalue far away from the support edge can be derived in an equivalent way for both ensembles, and we find a similar result for the variance of $N_{\mathcal{I}}$ when $L$ is larger than the soft edge $x = 4$. The only difference is the form of the large deviation function $\phi$. For the Wishart ensemble [93, 109], the probability of finding the largest eigenvalue to be much larger than its average value is given by

$$P(\lambda_{\max} > w) \sim \mathrm{e}^{-\beta N \Phi(w)}, \quad w > 4, \quad (8.25)$$

where

$$\Phi(w) = \sqrt{\frac{w(w-4)}{4}} + \ln\left[\frac{w - 2 - \sqrt{w(w-4)}}{2}\right]. \quad (8.26)$$

We denote by $P(k, L)$ the probability of finding $k$ eigenvalues at positions larger than $L$, and $L > 4$. Since the energy required to move one eigenvalue to position $L$ is $N\Phi(L)$, we obtain

$$\mathrm{Var}(N_{[L,\infty)}) = \left\langle k^2 \right\rangle - \langle k \rangle^2 = \sum_{k=1}^{\infty} k^2 P(k, L) - \left( \sum_{k=1}^{\infty} k P(k, L) \right)^2 \approx \mathrm{e}^{-\beta N \Phi(L)} \,, \tag{8.27}$$

to leading order in $N$. Since equation (5.36) applies also to the Wishart ensemble, we find, for $L > 4$

$$\mathrm{Var}(N_{[1,L]}) = \frac{1}{\beta \pi^2} \ln N + T_\beta(L), \tag{8.28}$$

where $T_\beta(L) \approx \mathrm{e}^{-\beta N \Phi(L)}$.

As above, replacing $L = 4 + \frac{s}{(N/4)^{2/3}}$ and taking the leading order in $N$ on equation (8.27) will retrieve

$$T_\beta \left( 4 + \frac{s}{(N/4)^{2/3}} \right) = \mathrm{e}^{-\beta N \Phi\left(4 + \frac{s}{(N/4)^{2/3}}\right)} \xrightarrow{N \gg 1} \mathrm{e}^{-\frac{2\beta}{3} s^{3/2}}, \tag{8.29}$$

which is the leading order in $s$ of equation (8.23) for $s \to \infty$. This confirms, as in the Gaussian case, the matching between the right limit of the edge regime and the tail regime.

### 8.1.5 Comparison with numerics

Numerical calculations in the Wishart ensemble are similar to the Gaussian ensemble. A tridiagonal ensemble with equivalent statistics was also found by Dumitriu and Edelman [41] and its diagonalization is less costly than taking Gaussian matrices, multiplying them by their conjugate and diagonalizing the Wishart matrix. Results obtained are in figure 8.3.

## 8.2 Cauchy ensemble

### 8.2.1 The Coulomb gas

We consider the case of the Cauchy ensemble. We note that the average density is already $N$-independent, so no rescaling is needed. Since the potential is of the same order as the repulsion between charges in the Coulomb gas, $V(x)$ is not strong enough to confine the eigenvalues into a compact region and the average density extends to infinity. We define the interval $\mathcal{I} = [a, b]$ and we repeat the previous derivation of the Coulomb gas method.

The Cauchy potential is given by

$$V_c(x) = \beta \left( \frac{N-1}{2} + \frac{1}{\beta} \right) \log(1 + x^2). \tag{8.30}$$

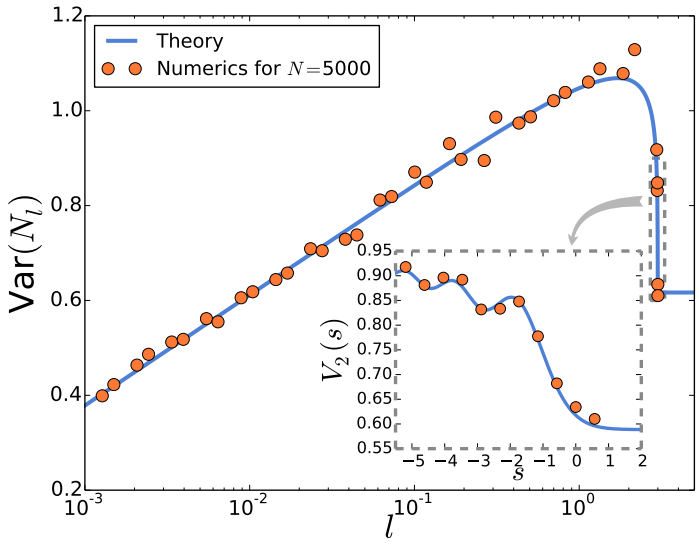


**Figure 8.3** — Results for the variance of $N_{\mathcal{I}}$ for the Wishart Unitary ensemble when $\mathcal{I} = [1, 1+l]$ and $l < 3$. Theory is equation (8.15). Inset: results for the edge regime, where $s = (l-3)(N/4)^{2/3}$ and theory is equation (5.38).

When taken in the large-$N$ limit, this potential can be written as simply $\beta N \log(1+x^2)/2$. Using this potential, we write the p.d.f. of $N_{\mathcal{I}}$

$$P(N_{\mathcal{I}} = k_{\mathcal{I}} N) = \frac{1}{Z_{N,\beta}} \int \prod_{k=1}^{N} \mathrm{d}\lambda_k e^{-\beta N \sum_{k=1}^{N} \frac{1}{2}\log(1+\lambda_i^2)} \prod_{i>j} |\lambda_i - \lambda_j|^\beta \delta\left(k_{\mathcal{I}} N - \sum_{l=1}^{N} \mathbb{1}_{\mathcal{I}}(\lambda_l)\right). \tag{8.31}$$

Again, we apply the Coulomb-gas method using the continuum approximation to the average density and the saddle-point approximation to probability (8.31).

$$P(N_{\mathcal{I}} = k_{\mathcal{I}} N) = \frac{1}{Z_N} \int \mathcal{D}\rho \mathrm{d}\mu \mathrm{d}\eta \mathrm{e}^{-\beta N^2 S[\rho]} = \mathrm{e}^{-\beta N^2 (S[\rho^\star] - S[\rho_{mp}])} = \mathrm{e}^{-\beta N^2 \psi(k_{\mathcal{I}})}, \tag{8.32}$$

where

$$\begin{aligned} S[\rho] =& \frac{1}{2}\int_{-\infty}^{+\infty} \log(1+x^2)\rho(x)\mathrm{d}x - \frac{1}{2}\iint_{-\infty}^{+\infty} \mathrm{d}x\mathrm{d}x' \rho(x)\rho(x')\log|x-x'| \\ &+ \mu\left(\int_a^b \rho(x) - k_{\mathcal{I}}\right) + \eta\left(\int_{-\infty}^{+\infty} \rho(x)\mathrm{d}x - 1\right). \end{aligned} \tag{8.33}$$

### 8.2.2 The resolvent method

We obtain the average density $\rho^\star(x)$ by differentiating (8.33) functionally with respect to $\rho$

$$\left.\frac{\delta S}{\delta \rho}\right|_{\rho^\star} = 0 = \frac{\log(1+x^2)}{2} - \int \mathrm{d}x' \rho^\star(x') \log|x-x'| + \mu \mathbb{1}_{\mathcal{I}}(x) + \eta, \quad x \in \mathrm{supp}\ \rho^\star. \tag{8.34}$$

And its derivative with respect to $x$ yields

$$\frac{x}{1+x^2} + \mu\left(\delta(x-b) - \delta(x-a)\right) = \fint \frac{\rho^\star(y)}{x-y} dy. \tag{8.35}$$

Once again, we multiply both sides of equation (8.35) by $\rho^\star(x)/(z-x)$ and we integrate both sides with respect to $x$. We wish to express both sides as algebraic expressions of the resolvent function $G(z)$, equation (7.12), and while the RHS is the same as the previous examples, the LHS is not polynomial and the technique used in the Gaussian and Wishart ensembles needs to be modified. This procedure is analogous to the case described in [96]. The algebraic equation for the resolvent is

$$aA + bB - \frac{1}{2} + z(A+B) + zG(z) = (1+z^2)\left(\frac{1}{2}G^2(z) + \frac{A}{z-a} + \frac{B}{z-b}\right), \tag{8.36}$$

where $A$ and $B$ are constants to be determined by the chemical equilibrium condition and the fraction of eigenvalues inside $[a,b]$. The solution of (8.36) is lengthy, but straightforward

$$G(z) = \frac{z}{1+z^2} \pm \frac{1}{1+z^2}\sqrt{\frac{P(A,B,a,b,z)}{(z-a)(z-b)}}, \tag{8.37}$$

where $P(A,B,a,b,z) = ab - 2Ab - 2a^2Ab - 2aB - 2ab^2B + (-a + 2A + 2a^2A + 2B + b(-1+2bB))z + (1 - 2Ab - 2a^2Ab - 2aB - 2ab^2B)z^2 + (2A(1+a^2) + 2(1+b^2)B)z^3$ is a third-degree polynomial in $z$. As it has three roots, the edges of the support of $\rho^\star(x)$, we write an alternate form for the Cauchy resolvent

$$G(z) = \frac{z}{1+z^2} \pm \frac{1}{1+z^2}\sqrt{\frac{(z-a_1)(z-a_2)(z-b_2)}{K(z-a)(z-b)}}, \tag{8.38}$$

where $K$, $a_1$, $a_2$ and $b_2$ are determined by equating $(z-a_1)(z-a_2)(z-b_2)/K = P(A,B,a,b,z)$. The average density is obtained directly

$$\rho^\star(x) = \frac{1}{\pi}\frac{1}{1+x^2}\sqrt{\frac{(a_1-x)(x-a_2)(x-b_2)}{K(x-a)(x-b)}}. \tag{8.39}$$

### 8.2.3 Analysis for $[-L, L]$

We write $\mathcal{I} = [-L, L]$. Equation (8.36) simplifies greatly due to the symmetries of this case, we find $a = -b = L$ and $A = -B$. The resolvent becomes

$$G(z) = \frac{z}{1+z^2} - \frac{1}{1+z^2}\sqrt{\frac{a_1^2 - z^2}{z^2 - L^2}}. \tag{8.40}$$

We may read directly the average density $\rho^\star(x)$ (see figure 8.4)

$$\rho^\star(x) = \frac{1}{\pi}\frac{1}{1+x^2}\sqrt{\frac{x^2 - a_1^2}{x^2 - L^2}}, \tag{8.41}$$

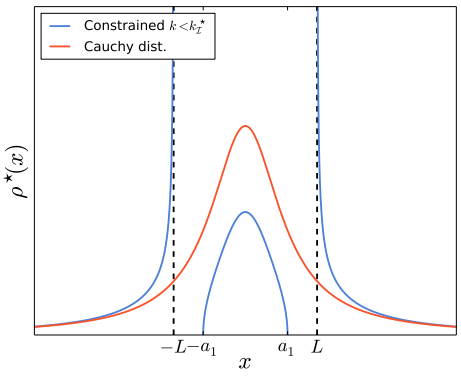


**(a)** Sketch of the expected behavior of $\rho^\star(x)$ for the Cauchy ensemble when $\mathcal{I} = [-L, L]$ and $k_L < k_L^\star$.

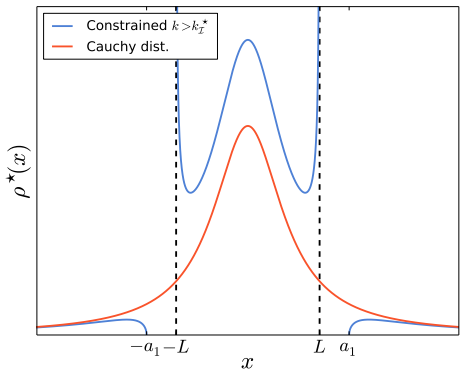


**(b)** Sketch of the expected behavior of $\rho^\star(x)$ for the Cauchy ensemble when $\mathcal{I} = [-L, L]$ and $k_L > k_L^\star$.

**Figure 8.4**

where the only variable to determine is $a_1$, which is found by imposing $\int_{-L}^{L} \rho^\star = k_L$.

We recall once more our simplified equation for the action (7.25)

$$S[\rho^\star] = \frac{1}{2}\int \log(1+x^2)\rho^\star(x)\mathrm{d}x - \frac{\mu}{2}k_{\mathcal{I}} - \frac{\eta}{2}. \tag{8.42}$$

The Lagrange multipliers are obtained in a similar way as the other two cases, with a small difference. The formula for $\mu$ is precisely the same, changing the potential to the Cauchy potential, but for $\eta$ we cannot apply the simplification (7.29), as there is no "upper bound" on the Cauchy regime. This forces us to write $\eta$ as a slightly more complicated integral as previous cases. Applying equation (8.34) in a point $p$ inside the support of $\rho^\star$ but outside the interval $[-L, L]$ yields an expression for $\eta$ in terms of integrals of $\rho^\star$. For the Lagrange multipliers we find

$$\mu = -\int_L^{a_1} G(x)\mathrm{d}x + \frac{1}{2}\log\left(\frac{1+a_1^2}{1+L^2}\right), \quad \eta = \int \rho^\star(x)\log|p-x|\mathrm{d}x - \log(1+p^2), \tag{8.43}$$

where $p$ is a point inside the support of $\rho^\star$ but outside the interval $[-L, L]$.

Calculating the action for the unconstrained case is, once again, straightforward and yields $S[\rho_{ca}] = \log 2$. The final formula for the rate function for the number statistics of the Cauchy ensemble when the interval is symmetrical is

$$\begin{aligned}\psi^c(k_{\mathcal{I}}) = &\frac{1}{2}\int_{-\infty}^{+\infty}\rho^\star(x)\frac{\log(1+x^2)}{2}\mathrm{d}x - \frac{1}{2}\left(\int_L^{a_1} G(x)\mathrm{d}x - \frac{1}{2}\log\left(\frac{1+a_1^2}{1+L^2}\right)\right)k_{\mathcal{I}} \\ &- \frac{1}{2}\left(H(p) - \frac{\log(1+p^2)}{2}\right) - \frac{\log 2}{2},\end{aligned} \tag{8.44}$$

where $H(x) = \int \rho^\star(x')\log|x-x'|\mathrm{d}x'$ and $p \in \operatorname{supp}\rho^\star \setminus \mathcal{I}$.

### 8.2.4 Number variance

To obtain the variance of $N_{[-L,L]} = N_L$ for typical fluctuations, we repeat the asymptotic method applied above for Gaussian and Wishart ensembles. Since the Cauchy distribution has no edge, we expect no sharp decline on the variance. However, our method is not capable of describing the variance for the full range of $L$. Again, we find three different regimes: an *extended bulk* regime $1/N < L < N$, an *effective edge* regime $L \sim N$ and a *tail* regime $L > N$, represented in figure 8.5. This is surprising, since the Cauchy distribution has no edge, but indeed in terms of the behavior of the variance we find that the average position of the largest eigenvalue (see [92] and equation (6.127)), which is of order $N$, behaves as an effective edge for the Cauchy distribution.

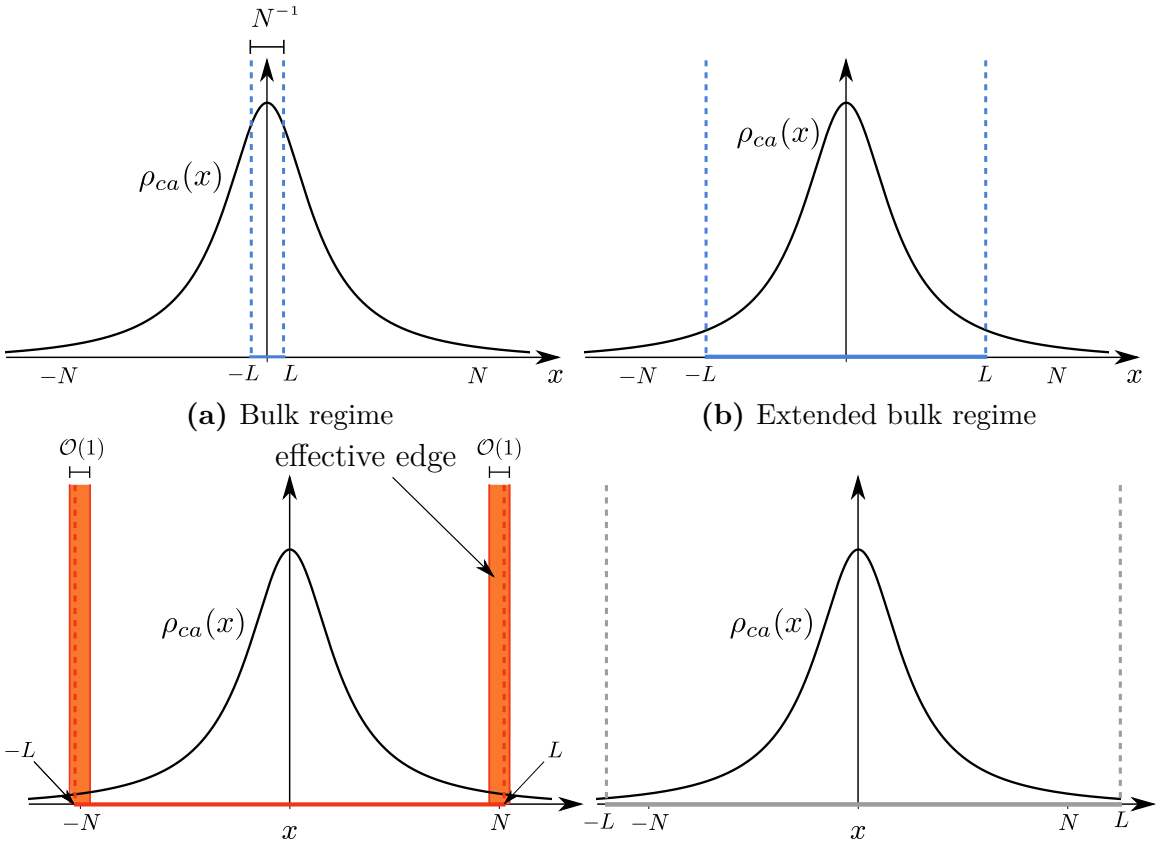


**(a)** Bulk regime **(b)** Extended bulk regime

**(c)** Effective edge regime **(d)** Tail regime

**Figure 8.5** — Regimes of behavior of the number variance for the Cauchy ensemble.

Even in this simplified symmetric case, the number variance for the Cauchy regime is extremely difficult to obtain for all identified regimes, and we are only able to compute it for the extended bulk regime. The edge regime is problematic because our orthogonal polynomial technique has no simple asymptotics for the Cauchy case, the polynomials involved in the treatment of this ensemble are complicated (see [92]) and their analysis represents a challenge we leave for future work. The tail regime also presents problems,

since calculations for a finite number of eigenvalues beyond the effective edge $N$, similar to (7.47) and (8.27), have divergences in $\langle k^2 \rangle$ and $\langle k \rangle^2$. Although their difference is finite, we are not able to compute the tail number variance using this method.

#### Extended bulk regime

Once again, we want to calculate the asymptotics for small $\delta$ for the action (8.42). Calculations are performed in a very similar way to the previous ensembles, and we omit them for brevity. For values of $L$ such as $1/N < L < N$ we find

$$\mathrm{Var}(N_L) = \frac{2}{\beta\pi^2} \log\left(\frac{NL}{1+L^2}\right) + \mathcal{O}(1). \tag{8.45}$$

We notice how the value $L \sim N$ behaves just as $L \sim \sqrt{2}$ for the Gaussian ensemble or $L \sim 4$ for the Wishart ensemble.

### 8.2.5 Comparison with numerics

We are able to simulate Cauchy eigenvalues by using the correspondence between the Cauchy ensemble and the circular ensemble [96]. Comparing our prediction for the extended bulk regime in the Cauchy ensemble with numerical results for three different values of $N$, figure 8.6, we see perfect agreement within the prescribed bounds, which reinforces the idea of the presence of an effective edge at the average position of the highest eigenvalue.

Note in figure 8.6 how our calculations for the extended bulk no longer correspond to the numerical result when $L > N$ for three different values of $N$. Even though we always assume a large $N$ limit, this result is fairly accurate when $N = 10$ and we can see how formula (8.45) is only valid for $10^{-1} < L < 10$.

## 8.3 Summary of results

In this chapter, I applied the Coulomb gas method to obtain the full probability density function of the number of eigenvalues inside an interval $\mathcal{I}$ for the Wishart and Cauchy regime. The choice of ensemble was given by their particular properties: Wishart presents a natural asymmetry and Cauchy has no soft edge on its average eigenvalue density.

The asymmetry in the Wishart ensemble brought a new technical difficulty, an extra equation is needed to set the edges of the constrained density. The equation used (8.11) was inspired in the thermodynamical interpretation of the Coulomb gas, and named the chemical equilibrium condition, as it imposes that the Lagrange multiplier of the condition on the number of eigenvalues inside the interval is the same when calculated on different edges of the interval.

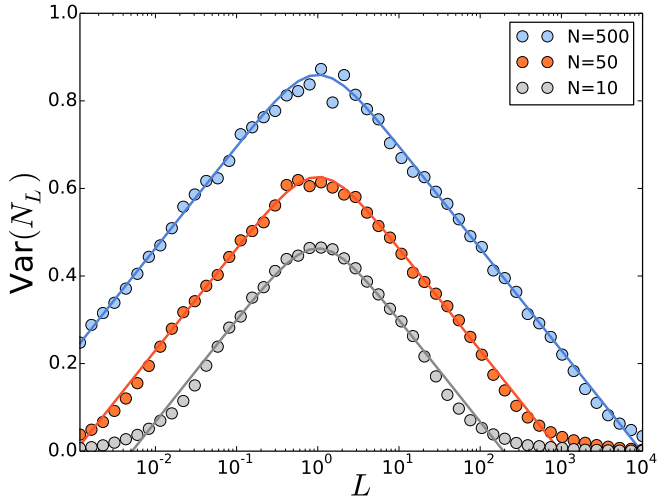


**Figure 8.6** — Results for the variance of $N_{\mathcal{I}}$ for the Cauchy ensemble when $\mathcal{I} = [-L, L]$. Solid lines are equation (8.45) for values of $N = 10, 50, 500$.

The interval studied for the Wishart ensemble was $[1, 1+l]$, and $l$ is the interval size. The value for the number variance obtained for large $N$ was

$$\mathrm{Var}(N_{[1,1+l]}) \approx \begin{cases} \frac{2}{\beta\pi^2}\ln\left(Nl(3-l)^{3/4}\right), & N^{-1} < l < 3 - N^{-2/3}, \\ \frac{1}{\beta\pi^2}\ln N + \frac{1}{2}V_\beta(s), & l = 3 + \frac{s}{4}N^{-2/3}, \\ \frac{1}{\beta\pi^2}\ln N + T_\beta(l), & l > 3, \end{cases} \tag{8.46}$$

where $T_\beta(l) \propto e^{-\beta N\Phi(l-3)}$, $\Phi(x)$ is given by (8.26) and $V_\beta(s)$ is determined for $\beta = 2$ in equation (8.21).

As expected, this variance converges to the variance of the index obtained in [94] when $l > 3$. Since the Wishart ensemble is also described by the sine kernel in the bulk regime, for distances of the order of $1/N$, we expect to retrieve Dyson and Mehta's result for the number variance (section 5.3.1) when $l \to 0$, and indeed we recover it taking this limit in the first case of equation (8.46).

The absence of edge in the Cauchy ensemble revealed interesting aspects of this set of matrices. While the average density does not have an edge, we found that the average position of the largest eigenvalue, at position $N$, behaves as an effective edge for the purpose of calculating the number variance. The Coulomb gas technique cannot provide the full behavior of the number variance for the interval $[-L, L]$ for all values of $L$, and we still obtain the structure of extended bulk – edge – tail regimes; the edge is an interval or the order of unity around $N$. Our method does not allow for calculations of edge and tail regimes, and we present the number variance for the extended bulk

$$\mathrm{Var}\left(N_{[-L,L]}\right) \approx \frac{2}{\beta\pi^2}\log\left(\frac{NL}{1+L^2}\right), \quad -N < L < N. \tag{8.47}$$

The results presented in this chapters were not yet published, and are part of a longer paper in final stages of preparation.

# — 9 —
# Quantum transport of electrons in weakly non-ideal chaotic cavities.

*I find the great thing in this world is not so much where we stand, as in what direction we are moving.*

Oliver Wendell Holmes

## 9.1 Introduction to quantum chaotic cavities

### 9.1.1 Ideal chaotic cavities

Another fundamental application of random matrix theory I explored during my PhD is quantum transport of electrons. Random matrix theory has proven very successful in describing the universal regime of electronic transport in mesoscopic cavities exhibiting chaotic classical dynamics [14]. The cavities have electronic channels, leads, in the left and right side; we refer to the number of left (right) leads as $n_L$ ($n_R$), and $N = n_R + n_L$ is the total number of channels, as represented by figure 9.1.

At low temperatures and applied voltage, provided that the average electron dwell time is well in excess of the Ehrenfest time, statistical universality emerges upon a suitable energy or ensemble averaging procedure. A stochastic approach to the problem, pioneered by Imry [69], Büttiker [25, 26] and Landauer [84], models the single-electron Hamiltonian $\mathcal{H}$ as a $M \times M$ ($M \to \infty$) random matrix with appropriate symmetries.

Classical scattering theory [3] allows to connect the scattering matrix of the cavity to the Hamiltonian and the couplings to the leads. The distribution of the scattering matrix $S$ within the unitary group is given in full generality by the so-called Poisson kernel [22, 101]:

$$P_\beta(S) \propto \left[\det(\mathbb{1}_N - \bar{S}S^\dagger)\det(\mathbb{1}_N - S\bar{S}^\dagger)\right]^{\beta/2-1-\beta N/2} \tag{9.1}$$

where $\beta = 1, 2, 4$ is the Dyson index and encodes system symmetries: $S$ is unitary and symmetric for $\beta = 1$, just unitary for $\beta = 2$ and unitary self-dual for $\beta = 4$. The

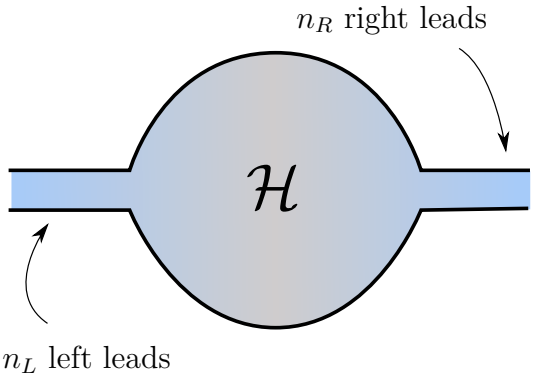


**Figure 9.1** — Visual representation of a chaotic cavity.

microscopic details of the coupling between the cavity and the leads are all contained in a single (sub-unitary) average scattering matrix $\bar{S}$, whose singular values $\gamma_i$ $(i = 1, \ldots, N)$ will be called *opacities* as they are related via $\gamma_i = \sqrt{1 - \Gamma_i}$ to the tunnel probabilities $\Gamma_i$ in the leads. The *ideal* limit corresponding to $\Gamma_i \to 1$ $(\gamma_i \to 0)$ implies that $P_\beta(S) = \text{const.}$ in the unitary group, a simplification that turns out to be crucial for most analytical developments of the theory. Indeed, the scattering matrix can be written in the block form

$$S = \begin{pmatrix} r & t \\ t' & r' \end{pmatrix}, \tag{9.2}$$

where $r$ $(n_L \times n_L)$ and $r'$ $(n_R \times n_R)$ are reflection blocks connecting wave function coefficients of electrons that come in and exit from the same lead, while $t$ $(n_L \times n_R)$ and $t'$ $(n_R \times n_L)$ are transmission blocks across the leads.

Landauer-Büttiker theory [83, 52, 27] expresses most physical observables as linear statistics on the eigenvalues $\{T_1, \ldots, T_n\}$ (if $n = \min\{n_R, n_L\}$) of the hermitian transmission matrix $tt^\dagger$, for example the conductance

$$\frac{G(\mathbf{T})}{G_0} = \sum_{i=i}^{n} T_i, \tag{9.3}$$

where $G_0 = 2e^2/h$, the shot-noise (the time average of current fluctuations at zero temperature)

$$\frac{P(\mathbf{T})}{P_0} = \sum_{i=i}^{n} T_i(1 - T_i), \tag{9.4}$$

where $P_0 = 2eVG_0$ ($V$ being the voltage difference between the two leads), or again the moments $\tau_m = \sum_i T_i^m$, relevant for the statistics of transmitted charge.

Note that unitarity of $S$ implies that $T_j = 1 - R_j$, where $R_j$ are the eigenvalues of $rr^\dagger$. The assumption that $S$ is a random unitary matrix implies that the $T_j$'s (or equivalently the $R_j$'s) are strongly correlated random variables characterized by a certain joint probability density function (j.p.d.f) $P_\beta(T_1, \ldots, T_n)$. In the case of *ideal* leads, this

j.p.d.f. is given [11, 55, 70] by the Jacobi ensemble of random matrices:

$$P^{(0)}(\mathbf{T}) \propto |\Delta(\mathbf{T})|^{\beta} \prod_{j=1}^{n} T_j^{\beta/2-1+\beta|n_L-n_R|/2} \tag{9.5}$$

where $\Delta(\mathbf{T}) = \prod_{j<k}(T_j - T_k)$.

Using the rather explicit expression (9.5), a number of analytical results on the statistics of conductance and shot noise have been derived. In [11, 13, 68, 71] it was established that the variance of conductance and shot noise (hereafter measured in dimensionless units) become independent of $n$ as $n \to \infty$, and depend only on the presence or absence of time-reversal symmetry, i.e.

$$\lim_{n\to\infty} \mathrm{Var}(G) = \frac{1}{8\beta} \qquad \lim_{n\to\infty} \mathrm{Var}(P) = \frac{1}{64\beta}, \tag{9.6}$$

for symmetric cavities ($n_L = n_R$), a phenomenon that has been dubbed *universal conductance fluctuations*.

A semiclassical derivation of the average and variance of $G$ as well as of the average of $P$ to all orders in $1/n$ was put forward [19, 65]. A fruitful approach to the same quantities based on the theory of Selberg integral was first developed in [123] and afterwards extended [126, 124] to compute the variance of $P$ and the first four cumulants of $G$ non-perturbatively. The full distributions of $G$ and $P$, known to be strongly non-Gaussian for a small number of channels [81, 126, 79], were studied for any $n$ and $\beta = 2$ using integrability arguments and the machinery of Painlevé functions in [112, 113], while the large $n$ behavior for all $\beta$ (including large deviation tails) was investigated in [141, 142]. Statistics of moments $\tau_m$ was studied in [110, 111, 143, 86] by RMT tools using semiclassical methods. Conductance cumulants and their asymptotics were thoroughly investigated in [111, 79] and more general results have been discovered in [102, 103, 104]. The full distribution of another quantum observable, such as Wigner's time delay, has also been recently computed[133].

### 9.1.2 Non-ideal chaotic cavities

Due to the complicated expression of the Poisson kernel (9.1), a systematic theoretical investigation into the domain of *non-ideal* cavities has been undertaken only very recently, whilst a tunable opacity in the leads is by now an established experimental protocol [63]. Vidal and Kanzieper [138] were eventually able to evaluate the j.p.d.f. of reflection eigenvalues for cavities with broken time-reversal symmetries ($\beta = 2$) in the case of ideal leads on the right side and non-ideal leads (characterized by a set of opacities $\{\gamma_i\}$, $i = 1, \ldots, n_L$) on the left side ($n = n_L \leq n_R$).

The exact j.p.d.f. of reflection eigenvalues in this case reads

$$P^{(\boldsymbol{\gamma})}(R_1, \ldots, R_{n_L}) = C_{n_R,n_L} \det(\mathbb{1} - \boldsymbol{\gamma})^N \frac{\Delta(\mathbf{R})}{\Delta(\boldsymbol{\gamma})} \det\left[{}_2F_1(n_R+1, n_R+1; 1; \gamma_i R_j)\right]$$

$$\times \prod_{i=1}^{n_L} (1-R_i)^{n_R-n_L}, \tag{9.7}$$

the matrix $\boldsymbol{\gamma}$ being $\boldsymbol{\gamma} = \mathrm{diag}(\gamma_1, \ldots, \gamma_{n_L})$, ${}_2F_1$ a standard hypergeometric function and $C_{n_R,n_L}$ a normalization constant

$$C_{n_R,n_L} = \prod_{j=0}^{n-1} \frac{(n_R-n_L+n+j)!}{(n_R-n_L+j)!} \frac{1}{j!(j+1)!}. \tag{9.8}$$

Note that in the non-ideal case the eigenvalue repulsion is no longer logarithmic, and (9.5) is recovered for $\gamma_i \to 0$ (with $R_j = 1 - T_j$) where the ratio $\frac{\det F}{\Delta(\boldsymbol{\gamma})}$ ingeniously restores the standard Vandermonde determinant (see next section).

The expression (9.7) is however hardly operational, even though for $n_L = n_R = 2$ has already proven effective in the context of entanglement production [139]. The purpose of this study is to make two simplifying assumptions, $\iota$) all opacities are the same $\gamma_1 = \gamma_2 = \cdots = \gamma$, and $\iota\iota$) they are small, $\gamma \ll 1$. We develop the expression (9.7) to first order in $\gamma$ and compute (as an example) moments of conductance and its variance to the same accuracy. In principle, the simple approximate formula we derive (see (9.20)) allows to compute the first correction in $\gamma$ for any linear or nonlinear statistics, such as pure or mixed moments (see below). We find that the variance for symmetric cavities with a large number of channels ($n = n_L = n_R \gg 1$) becomes asymptotically independent of $n$ even at first order in $\gamma$. The persistence of universal conductance fluctuations in the weakly non-ideal case is a phenomenon that may be within reach of current experimental capabilities. In general, we find that (at least for not too high moments of the conductance) the approximate formulas for the cumulants are excellent approximations of the exact results whenever available (see figure 9.2).

Following this study, we generalize our findings to higher orders in $\gamma$ using Schur polynomials. The results are less explicit, but provide a systematic method to obtain the contributions of all orders of $\gamma$.

## 9.2 Small $\gamma$ expansion

### 9.2.1 Expansion in first order

The crucial point is that in the limit when all $\gamma_i$'s are the same, the quantity $\frac{\det F}{\Delta(\boldsymbol{\gamma})}$ in (9.31) reduces to a single determinant,

$$\frac{\det F}{\Delta(\boldsymbol{\gamma})} \to \det M, \tag{9.9}$$

whose elements are obtained from L'Hôpital's rule and are given by

$$M_{ij} = \frac{d^{i-1}}{dx^{i-1}} \, {}_2F_1(n_R+1, n_R+1; 1; xR_j)\Big|_{x=\gamma}. \tag{9.10}$$

We shall expand each element of $M$ up to first order in $\gamma$. Let

$$ {}_2F_1(n_R+1, n_R+1; 1; \gamma R) = \sum_{n=0}^{\infty} C_n \frac{(\gamma R)^n}{n!} \tag{9.11} $$

be the expansion of the hypergeometric function. We know that

$$ C_n = \frac{(n_R+1)_n^2}{n!} = \frac{(n_R+n)^2}{n} C_{n-1}. \tag{9.12} $$

We must use (9.11) up to order $i$ in $\gamma$ to compute line $i$ of matrix $M$. In the end, we have $M \approx A + \gamma B$ where the elements of $A$ are given by

$$ A_{ij} = C_{i-1} R_j^{i-1} \tag{9.13} $$

and the elements of $B$ are given by

$$ B_{ij} = C_i R_j^i. \tag{9.14} $$

Using the relation $\log\det = \mathrm{Tr}\log$, we have

$$ \det(A+\gamma B) \approx [\det A]\,(1+\gamma \mathrm{Tr}[A^{-1}B]). \tag{9.15} $$

We can show the relation

$$ \mathrm{Tr}[A^{-1}B] = \frac{(n_R+n_L)^2}{n_L} \left[\sum_{i=1}^{n_L} R_i\right]. \tag{9.16} $$

Moreover, it is easy to see that

$$ \det A \propto \Delta(\mathbf{R}). \tag{9.17} $$

The final result is that, when all $\gamma$'s are the same and small, the joint probability density of transmission eigenvalues $T_i = 1 - R_i$ is approximately given by

$$ P^{(\gamma \ll 1)}(\mathbf{T}) \simeq C_{n_R,n_L} \det(\mathbb{1} - \boldsymbol{\gamma})^N \Delta(\mathbf{T})^2 \prod_{i=1}^{n_L} (T_i)^{n_R - n_L} \left[1 + \gamma \frac{(n_R+n_L)^2}{n_L} \left(\sum_{i=1}^{n_L} (1-T_i)\right)\right]. \tag{9.18} $$

This can be viewed as the sum of two contributions, namely the standard j.p.d.f. (9.5) valid for the ideal case, and

$$ P^{(0)}(\mathbf{T}) G(\mathbf{T}) = C_{n_R,n_L} \Delta(\mathbf{T})^2 \prod_{i=1}^{n_L} (T_i)^{n_R - n_L} \sum_{j=1}^{n_L} T_j, \tag{9.19} $$

where the notation $G(\mathbf{T})$ is consistent with the standard definition (9.3) of dimensionless conductance in quantum transport. Expanding $\det^{n_R+n_L}(\mathbb{1} - \boldsymbol{\gamma})$ for small values of $\gamma$ we get up to first order in $\gamma$

$$ P^{(\gamma \ll 1)}(\mathbf{T}) \simeq P^{(0)}(\mathbf{T}) + \gamma \left( n_R(n_R+n_L) P^{(0)}(\mathbf{T}) - \frac{(n_R+n_L)^2}{n_L} P^{(0)}(\mathbf{T}) G(\mathbf{T}) \right). \tag{9.20} $$

Equation (9.20) is the first of our main results. We note that the correction term is simply a linear combination of the probability density for the ideal case $\gamma = 0$ and a product of this probability and the conductance itself. Hereafter, we denote the average taken with respect to $P^{(0)}$ as $\langle\cdot\rangle_{(0)}$, while averages with respect to the total truncated probability (9.20) as $\langle\cdot\rangle_{(\gamma\ll1)}$.

The simplicity of our approximate expression (9.20) makes it now possible to explore analytically (to first order in $\gamma$) the statistics of $\iota$) conductance fluctuations, and $\iota\iota$) *any* linear or nonlinear statistics of the transmission eigenvalues, to first order in $\gamma$ (weakly non-ideal case). The former task is tackled in the next section. About the latter, we observe the following formula for e.g. a general nonlinear statistics on the transmission eigenvalues in the non-ideal case

$$\begin{aligned}\langle T_1^{\lambda_1}\cdots T_n^{\lambda_n}\rangle_{(\gamma\ll1)} \simeq &\langle T_1^{\lambda_1}\cdots T_n^{\lambda_n}\rangle_{(0)} \\ &+\gamma\left(n_R(n_R+n)\langle T_1^{\lambda_1}\cdots T_n^{\lambda_n}\rangle_{(0)} - (n_R+n)^2\langle T_1^{\lambda_1+1}\cdots T_n^{\lambda_n}\rangle_{(0)}\right)\end{aligned} \tag{9.21}$$

if $n = n_L \leq n_R$. Equation (9.21) efficiently generates nonlinear statistics for the weakly non-ideal case exploiting the known results in the ideal case [87, 124]. This is the second main result of our paper.

### 9.2.2 Universal conductance fluctuations

Let us first consider the first two moments of the conductance through the cavity. In the ideal case, they are given by [14, 110, 79]

$$\langle G\rangle_{(0)} = \frac{n_L n_R}{n_R+n_L} \tag{9.22}$$

$$\left\langle G^2\right\rangle_{(0)} = \frac{n_L^2 n_R^2}{(n_L+n_R-1)(n_L+n_R+1)}. \tag{9.23}$$

while higher moments in the ideal case have been derived using a variety of analytical methods (see e.g. [102, 103, 104]). Equation (9.20) directly yields the first-order correction in $\gamma$ for the $n$-th moment of the conductance: it suffices to multiply (9.20) by $\left(\sum_i T_i\right)^n$ and integrate over the $T_i$'s.

This yields

$$\langle G^n\rangle_{(\gamma\ll1)} \simeq \langle G^n\rangle_{(0)} + \gamma\left[n_R(n_R+n_L)\,\langle G^n\rangle_{(0)} - \frac{(n_R+n_L)^2}{n_L}\left\langle G^{n+1}\right\rangle_{(0)}\right], \tag{9.24}$$

namely a general formula that expresses the $n$-th moment of conductance in the weakly non-ideal case as a combination of the $n$-th and $(n+1)$th moments in the ideal case. Applied to the case of the average conductance itself, using (9.22) and (9.23), it produces

$$\langle G\rangle_{(\gamma\ll1)} \simeq \frac{n_L n_R}{n_R+n_L}$$

$$-\gamma\left[\frac{n_L n_R^2}{(n_L+n_R-1)(n_L+n_R+1)}\right] \tag{9.25}$$

We note that the correction term is always negative, which implies that a larger opacity $\gamma$ lets the conductance decrease, as expected.

In figure 9.2 we compare the exact results for $\langle G\rangle_{(\gamma)}$ for the case $n_L = 1$ (obtained by multiplying equation (11) on [138] by $G$ and integrating over $G$ between 0 and $n_L = 1$) with our approximate formula (9.24) for $n = 1$. The approximation for small $\gamma$ proves to be excellent, with relative errors of the order of $10-15\%$ for $\gamma$ as large as $0.5-0.6$. However, the accuracy gets worse as one considers higher and higher moments.

Our general formula (9.24) eventually allows to compute the first correction in $\gamma$ to the variance of $G$,

$$\mathrm{Var}(G)_{(\gamma\ll 1)} = \left\langle G^2\right\rangle_{(\gamma\ll 1)} - \langle G\rangle^2_{(\gamma\ll 1)} \tag{9.26}$$

for any $n_L, n_R$ and afterwards for a large number of propagating channels, where for $\gamma\to 0$ we expect to recover the universal conductance fluctuation result (9.6) for $\beta = 2$.

In order to make the asymptotic limit more transparent, we set $n_L = n$ and $n_R = \kappa n$. This gives

$$\mathrm{Var}(G)_{(\gamma\ll 1)} \simeq \frac{\kappa^2 n^2}{(\kappa+1)^2\left(\kappa^2 n^2+2\kappa n^2+n^2-1\right)} \tag{9.27}$$

$$+\left(\frac{2\left(\kappa^4-2\kappa^3+\kappa^2\right)n^4}{(\kappa+1)\left(\kappa^2 n^2+2\kappa n^2+n^2-4\right)\left(\kappa^2 n^2+2\kappa n^2+n^2-1\right)}\right)\gamma \tag{9.28}$$

Setting $n\to\infty$ and $\kappa = 1$ (symmetric cavities), the first term in (9.28) correctly reproduces $1/16$ from (9.6). It is interesting to notice that the correction term also attains a finite limit $\frac{2(\kappa-1)^2\kappa^2}{(\kappa+1)^5}$ for $n\to\infty$, and that this correction vanishes for symmetric cavities ($\kappa = 1$). The persistence of universal conductance fluctuations even in the case of weakly non-ideal cavities is a new effect that may be within reach of current experimental capabilities.

## 9.3 Higher orders of $\gamma$

### 9.3.1 Expansion in Schur polynomials

The previous argument can be generalized to obtain the following orders of $\gamma$. This generalization is not straightforward, and it was one of the main results of the work I did during my PhD on this subject [121].

Let $(a)_n = a(a+1)\cdots(a+n-1)$ be the rising factorial and let

$${}_2F_1(a,b;c;x) = \sum_{n\geq 0}\frac{(a)_n(b)_n}{(c)_n n!}x^n \tag{9.29}$$

be the hypergeometric function. Let $\mathcal{F}$ be the $N_1\times N_1$ matrix whose elements are

$$\mathcal{F}_{ij} = {}_2F_1(N_2+1, N_2+1; 1; \gamma_i R_j). \tag{9.30}$$

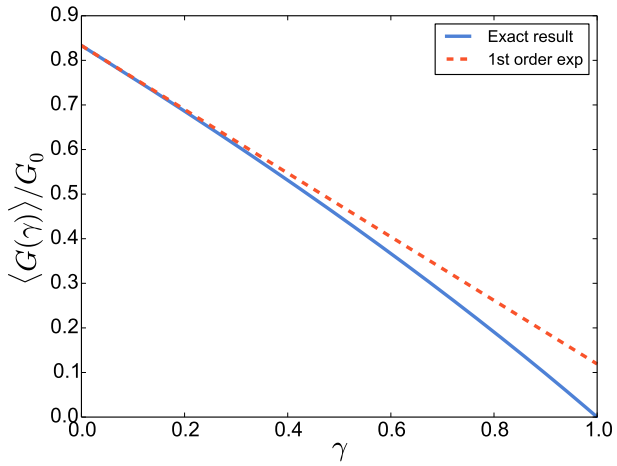


**Figure 9.2** — Comparison between $\langle G\rangle$ in the general $\gamma$ case and the linear approximation in $\gamma$, for $n_L = 1$ and $n_R = 5$.

We recall that when the non-ideal lead supports $N_1$ channels, the j.p.d.f. of reflection eigenvalues is given by [138]

$$P_2^{(\gamma)}(R) = Z\,\det{}^N(1-\gamma)\frac{\Delta(R)}{\Delta(\gamma)}\det(\mathcal{F})\prod_{i=1}^{N_1}(1-R_i)^{N_2-N_1}, \tag{9.31}$$

where $Z$ is a normalization constant,

$$Z = \frac{N!}{N_1!N_2!}\prod_{i=1}^{N_1}\frac{(N_2)!^2}{(N_2+i)!(N_2-i)!}. \tag{9.32}$$

Again, the expression (9.31) is hardly operational. We therefore start by writing it in a perturbative way, i.e. as an infinite series in $\gamma$. This is the same procedure as before, but we no longer assume that all values of $\gamma_i$ are the same.

Let a non-increasing sequence of positive integers $\lambda_1, \lambda_2, \ldots$ be called a partition of $n$ if $\sum_i \lambda_i = n$ and let this be denoted by $\lambda \vdash n$. The number of parts in $\lambda$ is $\ell(\lambda)$ and we assume $\lambda_m = 0$ if $m > \ell(\lambda)$. Partitions can be used to label a very important set of symmetric polynomials known as Schur polynomials, which are denoted by $s_\lambda$. Assuming $N_1$ variables, they are defined by

$$s_\lambda(x) = \frac{1}{\Delta(x)}\det\left(x_j^{\lambda_i - i + N_1}\right). \tag{9.33}$$

For example, the first few such polynomials are given by

$$s_0(x) = 1, \quad s_1(x) = \sum_{i=1}^{N_1} x_i, \tag{9.34}$$

$$s_{11}(x) = \sum_{i<j}^{N_1} x_i x_j, \quad s_2(x) = s_{11}(x) + \sum_{i=1}^{N_1} x_i^2. \tag{9.35}$$

If we define

$$\alpha_\lambda = \prod_{i=1}^{N_1} \binom{N + \lambda_i - i}{N_2}^2, \tag{9.36}$$

the following expansion can be established:

$$\det(\mathcal{F}) = \Delta(\gamma)\Delta(R) \sum_\lambda \alpha_\lambda s_\lambda(\gamma) s_\lambda(R), \tag{9.37}$$

where the infinite sum is over all possible partitions. This follows from the nice structure of $\mathcal{F}_{ij}$, which depends on the indexes $ij$ only through the combination $\gamma_i R_j$. An account of this and similar identities can be found for example in the book by Hua [67].

In order to use (9.37) to express the j.p.d.f. of reflection eigenvalues, it is useful to factor out the $\alpha_0$ term and notice that

$$\frac{\alpha_\lambda}{\alpha_0} = \frac{[N]_\lambda^2}{[N_1]_\lambda^2}, \tag{9.38}$$

where

$$[N]_\lambda = \prod_{i=1}^{\ell(\lambda)} \frac{(N + \lambda_i - i)!}{(N-i)!} \tag{9.39}$$

is a generalization of the rising factorial. The normalization constant then simplifies as

$$Z' = Z\ \alpha_0 = \prod_{i=1}^{N_1} \frac{(N-i)!}{(N_1 - i)!(N_2 - i)! i!}. \tag{9.40}$$

This is precisely the normalization constant missing from (9.5). Finally, combining (9.5), (9.31), (9.37) and (9.38) we get the final result,

$$\frac{P_2^{(\gamma)}(R)}{P_2^{(0)}(R)} = Z' \det(1-\gamma)^N \sum_\lambda \frac{[N]_\lambda^2}{[N_1]_\lambda^2} s_\lambda(\gamma) s_\lambda(R). \tag{9.41}$$

This equation generalizes the fact that the j.p.d.f. (9.41) equals the j.p.d.f. of the ideal case times a correction which can be systematically expanded in powers of $\gamma$.

### 9.3.2 Computing observables

Since any observable is a symmetric function of the reflection eigenvalues, it must be expressible as a linear combination of Schur polynomials; hence it suffices to obtain the average value of $s_\mu(R)$ for an arbitrary partition $\mu$. In this way we are led to consider the multiple integral

$$\int_0^1 \Delta^2(R) s_\lambda(R) s_\mu(R) \prod_{i=1}^{N_1} (1 - R_i)^{N_2 - N_1} dR, \tag{9.42}$$

(where $dR \equiv \prod_j dR_j$) which is a generalization of Selberg's integral [57]. However, this is difficult to evaluate directly. One way to proceed is to express the product of two Schur polynomials again as a linear combination of Schur polynomials,

$$s_\lambda(R)s_\mu(R) = \sum_\nu C^\nu_{\lambda\mu} s_\nu(R), \tag{9.43}$$

where the constants $C^\nu_{\lambda\mu}$ are known as Littlewood-Richardson coefficients [122]. There is no explicit formula for them, but they can be computed using some recursive algorithms and there are tables for the first ones. For instance, the coefficients with $\nu$ up to 4 are given by

$$\begin{aligned} s_0 s_\lambda &= s_\lambda, & s_1 s_1 &= s_2 + s_{11}, \\ s_2 s_1 &= s_3 + s_{21}, & s_{11} s_1 &= s_{111} + s_{21}, \\ s_3 s_1 &= s_4 + s_{31}, & s_{21} s_1 &= s_{31} + s_{22} + s_{211}, \\ s_2 s_2 &= s_4 + s_{31} + s_{22}, & s_2 s_{11} &= s_{31} + s_{211}, \\ s_{111} s_1 &= s_{1111} + s_{211}, & s_{11} s_{11} &= s_{1111} + s_{211} + s_{22}. \end{aligned}$$

By means of the Littlewood-Richardson coefficients, we only need to consider the simpler integral

$$\mathcal{I}_\nu = \int_0^1 \Delta^2(R) s_\nu(R) \prod_{i=1}^{N_1} (1-R_i)^{N_2-N_1} dR, \tag{9.44}$$

which is known to be given by [77, 76]

$$\mathcal{I}_\nu = s_\nu(1^{N_1}) \prod_{i=1}^{N_1} \frac{i!(N_1+\nu_i-i)!(N_2-i)!}{(N+\nu_i-i)!}, \tag{9.45}$$

where $s_\nu(1^{N_1})$ is the value of a Schur polynomial when all its arguments are equal to unity.

If we combine the above result with $Z'$ we get a substantial simplification, which is manifestly a rational function of $N_1$ and $N_2$, i.e. the variable $N_1$ no longer appears as the limit to products. The result is

$$Z'\mathcal{I}_\nu = \frac{[N_1]^2_\nu \chi_\nu(1)}{[N]_\nu |\nu|!}, \tag{9.46}$$

where $\nu \vdash |\nu|$ and $\chi$ is the character function in the permutation group, so $\chi_\nu(1)$ is the dimension of the irreducible representation of that group associated with partition $\nu$ (to arrive at this result we have used that $s_\nu(1^{N_1}) = \chi_\nu(1)[N_1]_\nu/n!$). The final result is that the average value of $s_\mu(R)$, with respect to the j.p.d.f. (9.41), is given by

$$\langle s_\mu(R)\rangle_\gamma = \det{}^N(1-\gamma) \sum_\lambda D_{\mu\lambda} s_\lambda(\gamma), \tag{9.47}$$

with

$$D_{\mu\lambda} = \frac{[N]^2_\lambda}{[N_1]^2_\lambda} \sum_\nu C^\nu_{\lambda,\mu} \frac{[N_1]^2_\nu \chi_\nu(1)}{[N]_\nu |\nu|!}. \tag{9.48}$$

### 9.3.3 The leading order

In this way any observable in the finite-$\gamma$ regime can be expressed in terms of observables computed in the ideal regime. For example, to leading order we have

$$\frac{P_2^{(\gamma)}(R)}{P_2^{(0)}(R)} \propto \left[1 + \frac{N}{N_1}\left(\frac{N}{N_1}s_1(R) - N_1\right)\mathrm{Tr}\gamma\right]. \tag{9.49}$$

As a first application, let $\langle G^n\rangle_\gamma$ be the average value of the $n$-th moment of the conductance in the non-ideal case. Using (9.49) and the fact that $s_1(R) = N_1 - G$, it is easy to see that the difference between the weakly non-ideal case and the ideal case is given to leading order by

$$\langle G^n\rangle_\gamma - \langle G^n\rangle_0 \approx \frac{N}{N_1}\mathrm{Tr}\gamma\left[N_2\langle G^n\rangle_0 - \frac{N}{N_1}\left\langle G^{n+1}\right\rangle_0\right]. \tag{9.50}$$

A similar estimate holds for other transport statistics.

## 9.4 Summary of results

In summary, combining the theory of symmetric functions and generalized Selberg integrals we presented a systematic perturbation theory in the opacity matrix $\gamma$ for the jpd of reflection eigenvalues in chaotic cavities with $\beta = 2$ and supporting one ideal and one non-ideal leads. This jpd is found to be given by the standard Jacobi ensemble (9.5), valid for the ideal case, times a correction that can be systematically expanded in $\gamma$ (see (9.41)). Using this result, we computed the average and variance of conductance, as well as average shot-noise, up to the second order in $\gamma$ and moments of conductance to leading order.

Our results are valid for arbitrary $N_1, N_2$, in contrast with previously available results which are exact in $\gamma$ but perturbative in $N_1, N_2$ and often limited to the leading order term as $N \to \infty$. Comparison with numerics for $N_1 = 1$ showed that our perturbative expressions are generally rather accurate for moderate $\gamma$, and have the advantage of a complete analytical tractability. The formula obtained is then employed to find a general expression connecting the moments of the conductance in the weakly non-ideal case with those pertinent to the completely ideal case, and in particular to probe universal conductance fluctuations even to first order in $\gamma$ in the limit $N \to \infty$. This is a new effect that might be within reach of current experimental capabilities.

# — 10 —
# Conclusions

*When the flush of a newborn sun fell first on Eden's green and gold,*
*Our father Adam sat under the Tree and scratched with a stick in the mold;*
*And the first rude sketch that the world had seen was joy to his mighty heart,*
*Till the Devil whispered behind the leaves: "It's pretty, but is it Art?"*

`Rudyard Kipling.` – The Conundrum of the Workshops

This thesis puts together three years of work in random matrix theory, and it focuses in one particular aspect of it: the counting of eigenvalues inside a given interval. While this problem has been treated in the past in many occasions [43, 128, 54, 33], there were very few results for number statistics outside of the classical bulk and edge regimes.

The beginning of my work was not on this exact subject. I started working in applications of random matrix theory to quantum transport, which is described in chapter 9. We were able to show that the effects of impurities in channels of a quantum dot can be obtained in terms of quantities calculated in the ideal case, and we provided the tools to perform this calculation. The full general case, although not trivial, was obtained in terms of Schur polynomials, a natural setting for symmetric variables such as transmission eigenvalues of a quantum transport.

From this interest we shifted to more general considerations about the Cauchy ensemble, a class of matrices that emerges naturally from quantum transport whose average density of eigenvalues has the remarkable property of being supported on the whole real line. The statistics of the number of positive eigenvalues of a Gaussian matrix was obtained in [89, 90], and we wanted to know if the same technique could be applied to a different case, the Cauchy ensemble, where the average density of eigenvalues presents no edge. To our surprise, the fluctuations of positive eigenvalues of the Cauchy ensemble were precisely twice the size of the fluctuations of the Gaussian ensemble, as shown in figure 10.1. For the variance of the index of the Cauchy ensemble we find

$$\mathrm{Var}(N_+^C) = \frac{2}{\beta\pi^2}\log N + O(1), \tag{10.1}$$

This result lead us to consider the role of the edge in fluctuations. Previous results for fluctuations of Gaussian eigenvalues [43, 100] showed that, for small intervals, the number variance grows logarithmically with the interval size. Taking a symmetric interval $[-L, L]$,

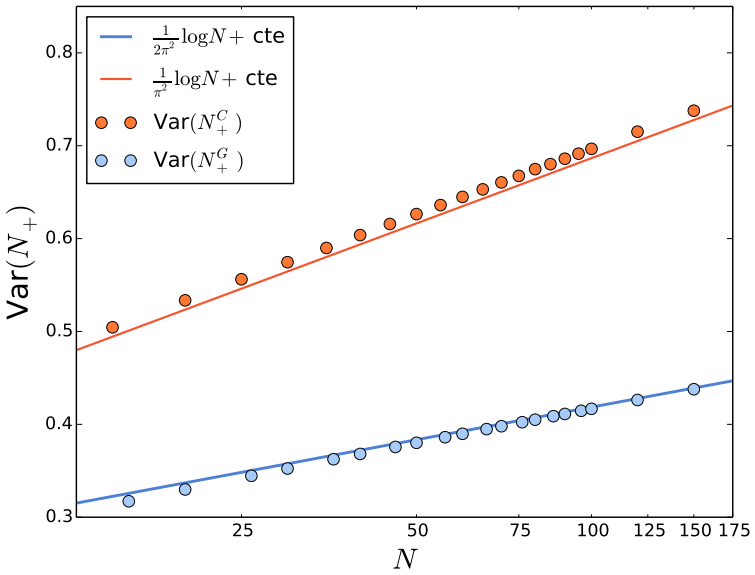


**Figure 10.1** — Numerical evaluation of the variance of the index using $\beta = 2$ for Cauchy unitary ensemble (denoted $N_+^C$, top line and points) and the Gaussian unitary ensemble (denoted $N_+^G$, bottom line and points). See reference [96].

it is clear that this variance should go to zero if the interval contains the entire support of the average distribution, as exponentially few eigenvalues would fall outside the interval and fluctuations would not be produced. From logarithmic growth to zero a matching function is required, and this change in behavior would happen in the mesoscopic scale.

Information about mesoscopic scales, when the interval considered was of the order of the system size, were almost inexistent, and in collaboration with Majumdar, Schehr and Vivo I obtained, for the first time, the full picture of the number statistics of GUE [97], as we discussed in chapter 7. The results for the number variance matched numerical simulations remarkably well, as shown in figure 10.2.

The method to obtain this result, the Coulomb gas method, proved to be very general and yields results for a large class of random matrices, those whose eigenvalue distribution can be written as equation (4.1). We explored this results for Wishart matrices and Cauchy matrices in chapter 8, but the same study can be applied for the Circular ensemble or the Jacobi ensemble, as they share the same structure for their eigenvalue distribution.

Applying this method to other ensembles showed interesting similarities for these very different types of matrices. In particular, the structure of the number variance for the so called extended bulk regime is similar. We find, for large values of $N$,

$$\mathrm{Var}(N_{\mathcal{I}}) \approx \begin{cases} \frac{2}{\beta\pi^2}\log\left(NL(2-L^2)^{\frac{3}{2}}\right), & \text{Gaussian and } \mathcal{I}=[-L,L] \\ \frac{2}{\beta\pi^2}\log\left(Nl(3-l)^{\frac{3}{4}}\right), & \text{Wishart and } \mathcal{I}=[1,1+l] \\ \frac{2}{\beta\pi^2}\log\left(\frac{NL}{1+L^2}\right), & \text{Cauchy and } \mathcal{I}=[-L,L] \end{cases} \tag{10.2}$$

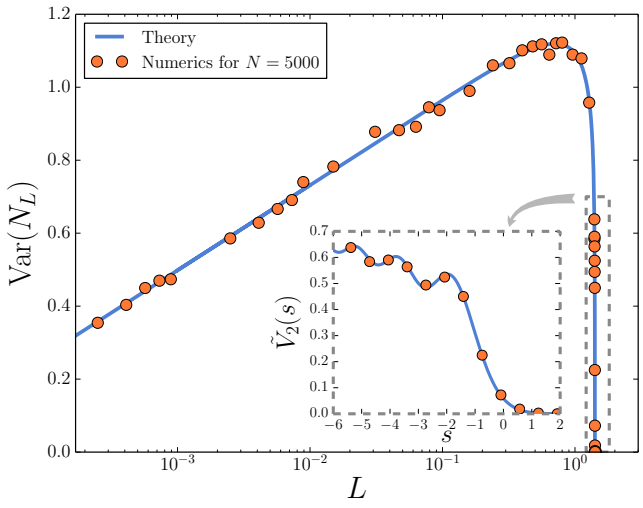


**Figure 10.2** — Results for the variance of $N_{\mathcal{I}}$ for the Gaussian ensemble when $\mathcal{I} = [-L, L]$ and $L < \sqrt{2}$. Theory is equation (7.40). Inset: results for the edge regime, where $s = (L - \sqrt{2})\sqrt{2}N^{2/3}$ and theory is equation (5.38). See reference [97].

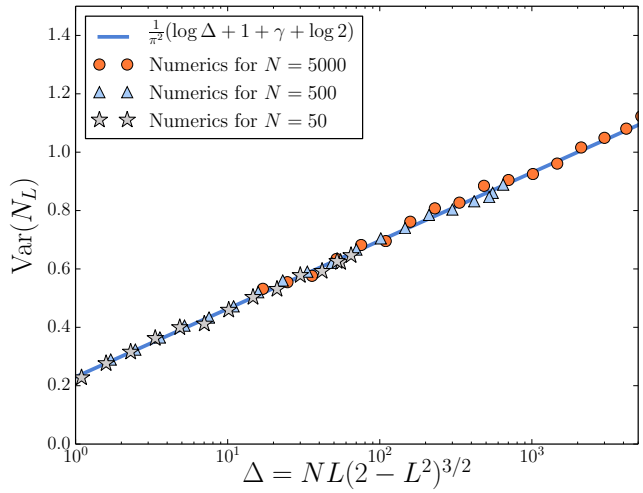


**Figure 10.3** — Numerical simulations of the number variance for GUE for different matrix sizes.

This structure $\mathrm{Var}(N_{\mathcal{I}}) \approx \frac{2}{\beta\pi^2}\log\Delta$, where $\Delta$ is a scaling variable, hints for a connection between $\Delta$, the potential of the ensemble $V(x)$ and the interval $\mathcal{I}$, which still eludes us. Numerical simulations, as displayed in figure 10.3, show that this variable seems to be the correct scaling variable for the number variance. As noted in [28], this number variance has most likely the expansion

$$\mathrm{Var}(N_L) = \frac{2}{\beta\pi^2}\log\Delta + \mathrm{cte} + O\left(\frac{1}{\Delta}\right). \tag{10.3}$$

This clarifies the "extended bulk regime" as the region in which $\Delta$ is large, and we notice that $\Delta$ becomes small either when we approach the bulk regime ($L \to \frac{1}{N}$ for GUE) or when we approach the edge regime ($L \to \sqrt{2}$ for GUE). Not surprisingly, $\Delta$ matches, in these regimes, their respective scaling variables.

Another important question raised by this scaling variable is its maximum. The result we obtained for the number variance of GUE shows that the interval $\mathcal{I} = [-1/\sqrt{2}, 1/\sqrt{2}]$ has the largest fluctuation of eigenvalues of all possible symmetrical intervals. This number $L = 1/\sqrt{2}$, which represents halfway through the semicircle, has no particular significance in random matrix and its interpretation is not yet clear. This maximum is certainly not universal, as the Cauchy ensemble, also considering a symmetric interval, reaches its maximum variance at $L = 1$.

The method presented to tackle the number statistics problems can be easily adapted to solve other types of linear statistics. The inclusion of Lagrange multipliers to force constrains and their interpretation in the electrostatic context are very general tools that can be applied to other observables of a random matrix ensemble.

We summarize the main new results presented in this work

- The imposition of a hard wall in $\zeta$ in the spectrum of invariant random matrix can be calculated by adding a $\delta(x-\zeta)$ contribution to the integral equation used to obtain the average density. This result is used extensively in the problems
  - The index problem, placing a hard wall in zero, for Gaussian and Cauchy ensemble in chapter 6.
  - In the calculation of fluctuations in the number of eigenvalues of the Gaussian ensemble inside an interval $\mathcal{I} = [-L, L]$ by placing hard walls in $L$ and $-L$ in chapter 7.
  - In the calculation of fluctuations in the number of eigenvalues in the Wishart and Cauchy ensembles for intervals $[1, L]$ and $[-L, L]$ respectively in chapter 8.
- The variance of the number of positive eigenvalues in the Cauchy ensemble is twice as large as the variance for positive eigenvalues of the Gaussian ensemble. This difference is caused by the absence of a compact average distribution of eigenvalues for the Cauchy ensemble, and is presented in chapter 6.

- The average density of eigenvalues for the Cauchy ensemble is supported on the whole real line, but the constrained average density, obtained when we impose a fraction $k$ of eigenvalues to be positive and $k \neq 1/2$, is supported in two disjoint intervals, one of which is compact (see figure 6.7).

- The variance of the number $N_L$ of eigenvalues of a Gaussian matrix inside an interval $\mathcal{I} = [-L, L]$ depends strongly on $L$. Previous results were only able to provide results for $L \sim \frac{1}{N}$ or $L \sim \sqrt{2}$, bulk and edge regime. We provided in chapter 7 the full probability density function of $N_L$ for large $N$ and we obtained the asymptotic behavior of its variance for all values of $L$. The new results we obtained are for values of $L$ in the "extended bulk" regime, which are values of $L$ inside the support, and "tail" regime, which are values of $L$ far away from the support. This matching function of the variance from bulk to edge regime has remarkable importance in the context of cold atoms, and previous studies tried without success to obtain its leading behavior for large $N$ [137].

- The same calculation of the statistics of the number of eigenvalues inside an interval was performed for Wishart and Cauchy ensembles, and these results are discussed in chapter 8.

  - The asymmetric nature of the average density of Wishart eigenvalues brought a new difficulty to calculations, we needed an extra equation to determine parameters that, in the symmetric case, would be determined by the symmetries of the problem. We used an insight in the electrostatic equivalent problem, the fact that the chemical potential of two disjoint parts of the spectrum should be the same, to obtain the extra equation and calculate the number variance for the Wishart case.

  - The absence of edge in the Cauchy average density of eigenvalues generates an interesting discussion on the asymptotic behavior of the number variance. When we consider the symmetric interval $[-L, L]$ for the number variance, the Coulomb gas method can only provide results when $1/N < L < N$, where $N$ is the matrix size. This indicates the presence of an effective edge at the average position of the largest eigenvalue in the Cauchy matrix, and our classification of extended bulk, edge and tail, surprisingly, also applies to the Cauchy ensemble.

- The j.p.d.f. of transmission eigenvalues in a quantum chaotic cavity with non-deal leads can be written as an asymptotic expansion in the impurities $\gamma$ whose coefficients are related to the j.p.d.f. of the ideal case. This allows us to write the moments of many interesting quantities of this problem, such as conductance and shot noise, as expansions in $\gamma$ whose coefficients are determined using the statistics of the much simples ideal case, when $\gamma = 0$. These results are described in chapter 9.

The results presented in this thesis yielded 3 publications, and there are non published results in this thesis spanning results from two articles in final stages of preparation.

- Rodríguez-Pérez, S., Marino, R., Novaes, M., and Vivo, P. Statistics of quantum transport in weakly nonideal chaotic cavities. Phys. Rev. E **88** (2013), 052912.
- Marino, R., Majumdar, S. N., Schehr, G., and Vivo, P. Index distribution of Cauchy random matrices. J. Phys. A: Math. Theor. **47** (2014), 055001.
- Marino, R., Majumdar, S. N., Schehr, G., and Vivo, P. Phase transitions and edge scaling of number variance in gaussian random matrices. Phys. Rev. Lett. **112** (2014), 254101.

# Bibliography


[1] Aazami, A., and Easther, R. Cosmology from random multifield potentials. *J. Cosmol. Astro. Phys. 03* (2006), 013.

[2] Akemann, G., Jinho, B., and Francesco, P. D. *The Oxford Handbook of Random Matrix Theory.* Oxford University Press, Oxford, 2011.

[3] Alhassid, Y. The statistical theory of quantum dots. *Rev. Mod. Phys. 72* (2000), 895.

[4] Allez, R., Bouchaud, J.-P., and Guionnet, A. Invariant $\beta$-ensembles and the Gauss-Wigner crossover. *Phys. Rev. Lett. 109* (2012), 094102.

[5] Allez, R., Bouchaud, J.-P., Majumdar, S. N., and Vivo, P. Invariant $\beta$-wishart ensembles, crossover densities and asymptotic corrections to the Marchenko-Pastur law. *J. Phys. A: Math. Theor. 46* (2013), 015001.

[6] Anderson, M. H., Ensher, J. R., Matthews, M. R., Wieman, C. E., and Cornell, E. A. Observation of Bose-Einstein condensation in a dilute atomic vapor. *Science 269* (1995), 198.

[7] Andréief, I. C. Note sur une relation les integrates definies des produits des fonctions. *Mem. de la Soc. Sci., Bordeaux 2* (1883), 1.

[8] Angelone, A., Campostrini, M., and Vicari, E. Universal quantum behavior of interacting fermions in one-dimensional traps: From few particles to the trap thermodynamic limit. *Phys. Rev. A 89* (2014), 023635.

[9] Aurich, R., Bolte, J., and Steiner, F. Universal signatures of quantum chaos. *Phys. Rev. Lett. 73* (1994), 1356.

[10] Bai, Z. D. Convergence rate of expected spectral distributions of large random matrices. *Ann. Probab. 21* (1993), P625.

[11] Baranger, H. U., and Mello, P. A. Mesoscopic transport through ballistic cavities: A random S-matrix theory approach. *Phys. Rev. Lett. 73* (1994), 142.

[12] Bateman, H. In *Higher Transcendental Functions*, A. Erdélyi, W. Magnus, F. Oberhettinger, and F. G. Tricomi, Eds., vol. 2. MacGraw Hill, New York, 1953.

[13] Beenakker, C. W. J. Universality in the random-matrix theory of quantum transport. *Phys. Rev. Lett. 70* (1993), 1155.

[14] Beenakker, C. W. J. Random-matrix theory of quantum transport. *Rev. Mod. Phys. 69* (1997), 731.

[15] Biroli1, G., Bouchaud, J.-P., and Potters, M. Extreme value problems in random matrix theory and other disordered systems. *J. Stat. Mech.* (2007), P07019.

[16] Bloch, I., Dalibard, J., and Zwerger, W. Many-body physics with ultracold gases. *Rev. Mod. Phys. 80* (2008), 885.

[17] Bohigas, O., Giannoni, M. J., and Schmit, C. Characterization of chaotic quantum spectra and universality of level fluctuation laws. *Phys. Rev. Lett. 52* (1984), 1.

[18] Bradley, C. C., Sackett, C. A., Tollett, J. J., and Hulet, R. G. Evidence of Bose-Einstein condensation in an atomic gas with attractive interactions. *Phys. Rev. Lett. 75* (1995), 1687.

[19] Braun, P., Heusler, S., Müller, S., and Haake, F. Semiclassical prediction for shot noise in chaotic cavities. *J. Phys. A: Math. Gen. 39* (2006), L159.

[20] Brézin, E., and Zee, A. Universality of the correlations between eigenvalues of large random matrices. *Nucl. Phys. [FS] B402* (1993), 613.

[21] Brézin, E., and Zinn-Justin, J. Renormalization group approach to matrix models. *Phys. Lett. B288* (1992), 54.

[22] Brouwer, P. W. Generalized circular ensemble of scattering matrices for a chaotic cavity with nonideal leads. *Phys. Rev. B 51* (1995), 16878.

[23] Burda, Z., Janik, R. A., Jurkiewicz, J., Nowak, M. A., Papp, G., and Zahed, I. Free random Lévy matrices. *Phys. Rev. E 65* (2002), 021106.

[24] Burda, Z., and Jurkiewicz, J. Heavy tailed random matrices. In *The Oxford Handbook of Random Matrix Theory*, G. Akemann, J. Baik, and P. D. Francesco, Eds. Oxford University Press, Oxford, 2011.

[25] Büttiker, M. Four-terminal phase-coherent conductance. *Phys. Rev. Lett. 57* (1986), 1761.

[26] Büttiker, M. Symmetry of electrical conduction. *IBM J. Res. Dev. 32* (1988), 317.

[27] Büttiker, M. Scattering theory of thermal and excess noise in open conductors. *Phys. Rev. Lett. 65* (1990), 2901.

[28] Calabrese, P., Doussal, P. L., and Majumdar, S. N. Random matrices and entanglement entropy of trapped Fermi gases. *Phys. Rev. A 91* (2015), 012303.

[29] Calabrese, P., Mintchev, M., and Vicari, E. The entanglement entropy of 1d systems in continuous and homogenous space. *J.Stat.Mech.*.

[30] Calabrese, P., Mintchev, M., and Vicari, E. Entanglement entropy of one-dimensional gases. *Phys. Rev. Lett. 107* (2011), 020601.

[31] Campostrini, M., and Vicari, E. Equilibrium and off-equilibrium trap-size scaling in one-dimensional ultracold bosonic gases. *Phys. Rev. A 82* (2010), 063636.

[32] Cavagna, A., Garrahan, J. P., and Giardina, I. Index distribution of random matrices with an application to disordered systems. *Phys. Rev. B 61* (2000), 3960.

[33] Costin, O., and Lebowitz, J. L. Gaussian fluctuation in random matrices. *Phys. Rev. Lett. 75* (1995), 69.

[34] Davies, K. B., Mewes, M.-O., Andrews, M. R., van Druten, N. J., Durfee, D. S., Kurn, D. M., and Keterlee, W. Bose-Einstein condensation in a gas of sodium atoms. *Phys. Rev. Lett. 75* (1995), 3969.

[35] Dean, D. S., Doussal, P. L., Majumdar, S. N., and Schehr, G. Universal ground state properties of free fermions in a d-dimensional trap.

[36] Dean, D. S., Doussal, P. L., Majumdar, S. N., and Schehr, G. Finite temperature free fermions and the Kardar-Parisi-Zhang equation at finite time. *Phys. Rev. Lett. 114* (2014), 110402.

[37] Dean, D. S., and Majumdar, S. N. Large deviations of extreme eigenvalues of random matrices. *Phys. Rev. Lett. 97* (2006), 160201.

[38] Dean, D. S., and Majumdar, S. N. Extreme value statistics of eigenvalues of Gaussian random matrices. *Phys. Rev. E 77* (2008), 041108.

[39] Diaconis, P., and Shahshahani, M. On the eigenvalues of random matrices. *J. Appl. Probab. 31A* (1994), 49.

[40] Douglas, M. R., Shiffman, B., and Zelditch, S. Critical points and supersymmetric vacua. *Commun. Math. Phys. 252* (2004), 325.

[41] Dumitriu, I., and Edelman, A. Matrix models for beta ensembles. *J. Math. Phys. 43* (2002), 5830.

[42] Dyson, F. Preface. In *The Oxford Handbook of Random Matrix Theory*, G. Akemann, J. Baik, and P. D. Francesco, Eds. Oxford University Press, Oxford, 2011.

[43] Dyson, F. J. Statistical theory of the energy levels of complex systems. i–iii. *J. Math. Phys. 3* (1962), 140.

[44] Dyson, F. J. The Threefold Way. Algebraic Structure of Symmetry Groups and Ensembles in Quantum Mechanics. *J. Math. Phys. 3* (1962), 1199.

[45] Dyson, F. J., and Mehta, M. L. Statistical theory of the energy levels of complex systems. iv. *J. Math. Phys. (N.Y.) 4* (1963), 701.

[46] Eisler, V. Universality in the full counting statistics of trapped fermions. *Phys. Rev. Lett. 111* (2013), 080402.

[47] Eisler, V., and Peschel, I. Surface and bulk entanglement in free-fermion chains. *J. Stat. Mech.* (2014), P04005.

[48] Eisler, V., and Rácz, Z. Full counting statistics in a propagating quantum front and random matrix spectra. *Phys. Rev. Lett. 110* (2013), 060602.

[49] Erdos, L. Universality of Wigner random matrices: a survey of recent results. *Russ. Math. Surv. 66* (2010), 507.

[50] Eynard, B. Lecture notes in random matrices, 2015. Available at http://eynard.bertrand.voila.net/.

[51] Facchi, P., Marzolino, U., Parisi, G., Pascazio, S., and Scardicchio, A. Phase transitions of bipartite entanglement. *Phys. Rev. Lett. 101* (2008), 050502.

[52] Fisher, D. S., and Lee, P. A. Relation between conductivity and transmission matrix. *Phys. Rev. B 23* (1981), R6851.

[53] Fisher, R. A. The sampling distribution of some statistics obtained from non-linear equations. *The Annals of Eugenics 9* (1939), 238.

[54] Fogler, M. M., and Shklovskii, B. I. Probability of an eigenvalue number fluctuation in an interval of a random matrix spectrum. *Phys. Rev. Lett. 74* (1995), 3312.

[55] Forrester, P. J. Quantum conductance problems and the Jacobi ensemble. *J. Phys. A: Math. Gen. 39* (2006), 6861.

[56] Forrester, P. J. *Log-Gases and Random Matrices*. London Mathematical Society monographs, London, 2010.

[57] Forrester, P. J., and Warnaar, S. O. The importance of the Selberg integral. *Bull. Am. Math. Soc. 45* (2008), 489.

[58] Fyodorov, Y. V. Introduction to the random matrix theory: Gaussian unitary ensemble and beyond. In *Recent Perspectives in Random Matrix Theory and Number Theory*, F. Mezzadri and N. C. Snaith, Eds. Cambridge University Press, 2005, pp. 31–78.

[59] Fyodorov, Y. V., Khoruzhenko, B. A., and Nock, A. Universal K-matrix distribution in $\beta = 2$ ensembles of random matrices. *J. Phys. A: Math. Theor. 46* (2013), 262001.

[60] Giorgini, S., Pitaevski, L. P., and Stringari, S. Theory of ultracold atomic Fermi gases. *Rev. Mod. Phys. 80* (2008), 1215.

[61] Grabsch, A., and Texier, C. Capacitance and charge relaxation resistance of chaotic cavities – joint distribution of two linear statistics in the Laguerre ensemble of random matrices. *Europhys. Lett. 109* (2015), 50004.

[62] Gustavsson, J. Gaussian fluctuations of eigenvalues in the gue. *Ann. Inst. H. Poincaré Probab. Statist. 41* (2005), 151.

[63] Gustavsson, S., Leturcq, R., Simovič, B., Schleser, R., Ihn, T., Studerus, P., Ensslin, K., Driscoll, D. C., and Gossard, A. C. Counting statistics of single-electron transport in a quantum dot. *Phys. Rev. Lett. 96* (2006), 076605.

[64] Heinzner, P., Huckleberry, A., and Zirnbauer, M. Symmetry classes of disordered fermions. *Commun. in Math. Phys. 257* (2005), 725.

[65] Heusler, S., Müller, S., Braun, P., and Haake, F. Semiclassical theory of chaotic conductors. *Phys. Rev. Lett. 96* (2006), 066804.

[66] Hsu, P. L. On the distribution of roots of certain determinantal equations. *The Annals of Eugenics 9* (1939), 250.

[67] Hua, L. *Harmonic Analysis of Functions of Several Complex Variables in the Classical Domains*, vol. 6 of *Translations of mathematical monographs*. American Mathematical Soc., 1963.

[68] Iida, S., Weidenmüller, H. A., and Zuk, J. A. Wave propagation through disordered media and universal conductance fluctuations. *Phys. Rev. Lett. 64* (1990), 583.

[69] Imry, Y. *Directions in Condensed Matter Physics*. World Scientific, 1986, p. 101.

[70] Jalabert, R. A., and Pichard, J. L. Quantum mesoscopic scattering: Disordered systems and Dyson circular ensembles. *J. Phys. I France 5* (1995), 287.

[71] Jalabert, R. A., Pichard, J. L., and Beenakker, C. W. J. Universal quantum signatures of chaos in ballistic transport. *Europhys. Lett. 27* (1994), 255.

[72] James, A. T. Distributions of matrix variates and latent roots derived from normal samples. *Ann. Math. Statist. 35* (1964), 475.

[73] Johansson, K. On random matrices from the compact classical groups. *Ann. of Math. 145* (1997), 519.

[74] Johansson, K. On fluctuations of eigenvalues of random Hermitian matrices. *Duke Math. J. 91* (1998), 151.

[75] Johnstone, I. M. On the distribution of the largest eigenvalue in principal components analysis. *Ann. Statist. 29*, 2 (04 2001), 295.

[76] Kadell, K. W. J. The Selberg–Jack symmetric functions. *Adv. Math. 130* (1997), 33.

[77] Kaneko, J. Selberg integrals and hypergeometric functions associated with Jack polynomials. *SIAM J. Math. Anal. 24* (1993), 1086.

[78] Kazakopoulos, P., Mertikopoulos, P., Moustakas, A. L., and Caire, G. Living at the edge: A large deviations approach to the outage MIMO capacity. *IEEE Transactions on Information Theory 57* (2011), 1984.

[79] Khoruzhenko, B. A., Savin, D. V., and Sommers, H. J. Systematic approach to statistics of conductance and shot-noise in chaotic cavities. *Phys. Rev. B 80* (2009), 125301.

[80] Kinoshita, T., Wenger, T., and Weiss, D. S. Observation of a one-dimensional tonks-girardeau gas. *Science 305* (2004), 1125.

[81] Kumar, S., and Pandey, A. Conductance distributions in chaotic mesoscopic cavities. *J. Phys. A: Math. Theor. 43* (2010), 285101.

[82] Laloux, L., Cizeau, P., Bouchaud, J.-P., and Potters, M. Noise dressing of financial correlation matrices. *Phys. Rev. Lett. 83* (1999), 1467.

[83] Landauer, R. Spatial variation of currents and fields due to localized scatterers in metallic conduction. *IBM J. Res. Dev. 1* (1957), 223.

[84] Landauer, R. Electrical transport in open and closed systems. *Z. Phys. B 68* (1987), 217.

[85] Liou, H. I., Camarda, H. S., Wynchank, S., Slagowitz, M., Hacken, G., Rahn, F., and Rainwater, J. Neutron-resonance spectroscopy. viii. the separated isotopes of erbium: Evidence for dyson's theory concerning level spacings. *Phys. Rev. C 5* (1972), 974.

[86] Livan, G., and Vivo, P. Moments of Wishart-Laguerre and Jacobi ensembles of random matrices: application to the quantum transport problem in chaotic cavities. *Acta Phys. Pol. B 42* (2011), 1081.

[87] Luque, J.-G., and Vivo, P. Nonlinear random matrix statistics, symmetric functions and hyperdeterminants. *J. Phys. A: Math. Theor. 43* (2010), 085213.

[88] Lytova, A., and Pastur, L. Central limit theorem for linear eigenvalue statistics of random matrices with independent entries. *Ann. Probab. 37* (2009), 1778.

[89] Majumdar, S. N., Nadal, C., Scardicchio, A., and Vivo, P. Index distribution of Gaussian random matrices. *Phys. Rev. Lett. 103* (2009), 220603.

[90] Majumdar, S. N., Nadal, C., Scardicchio, A., and Vivo, P. How many eigenvalues of a Gaussian random matrix are positive? *Phys. Rev. E 83* (2011), 041105.

[91] Majumdar, S. N., and Schehr, G. Top eigenvalue of a random matrix: large deviations and third order phase transition. *J. Stat. Mech.* (2014), P01012.

[92] Majumdar, S. N., Schehr, G., Villamaina, D., and Vivo, P. Large deviations of the top eigenvalue of large Cauchy random matrices. *J. Phys. A: Math. Theor. 46* (2013), 022001.

[93] Majumdar, S. N., and Vergassola, M. Large deviations of the maximum eigenvalue for Wishart and Gaussian random matrices. *Phys. Rev. Lett. 102* (2009), 060601.

[94] Majumdar, S. N., and Vivo, P. Number of relevant directions in principal component analysis and Wishart random matrices. *Phys. Rev. Lett. 108* (2012), 200601.

[95] Marco, B. D., and Jin, D. S. Onset of Fermi degeneracy in a trapped atomic gas. *Science 285* (1999), 1703.

[96] Marino, R., Majumdar, S. N., Schehr, G., and Vivo, P. Index distribution of Cauchy random matrices. *J. Phys. A: Math. Theor. 47* (2014), 055001.

[97] Marino, R., Majumdar, S. N., Schehr, G., and Vivo, P. Phase transitions and edge scaling of number variance in Gaussian random matrices. *Phys. Rev. Lett. 112* (2014), 254101.

[98] Marčenko, V. A., and Pastur, L. A. Distribution of eigenvalues for some sets of random matrices. *Mat. Sbornik 72* (1967), 507.

[99] May, R. M. Will a large complex system be stable? *Nature 238* (1972), 413.

[100] Mehta, M. L. *Random Matrices.* Academic Press, Boston, 1991.

[101] Mello, P. A., and Baranger, H. U. Interference phenomena in electronic transport through chaotic cavities: An information-theoretic approach. *Waves In Random Media 9* (1999), 105.

[102] Mezzadri, F., and Simm, N. J. Moments of the transmission eigenvalues, proper delay times and random matrix theory I. *J. Math. Phys. 52* (2011), 103511.

[103] Mezzadri, F., and Simm, N. J. Moments of the transmission eigenvalues, proper delay times and random matrix theory II. *J. Math. Phys. 53* (2012), 053504.

[104] Mezzadri, F., and Simm, N. J. Tau-function theory of quantum chaotic transport with beta=1,2,4. *Commun. Math. Phys. 324* (2013), 465.

[105] Montgomery, H. L. The pair correlation of zeros of the zeta function. In *Analytic number theory (Proc. Sympos. Pure Math., Vol. XXIV, St. Louis Univ., St. Louis, Mo., 1972)*. Amer. Math. Soc., Providence, R.I., 1973, p. 181.

[106] Montgomery, H. L. Distribution of the zeros of the Riemann zeta function. In *Proceedings of the International Congress of Mathematicians (Vancouver, B. C., 1974), Vol. 1* (1975), Canad. Math. Congress, Montreal, Que., p. 379.

[107] Nadal, C. *Matrices aléatoires et leurs applications à la physique statistique et la physique quantique*. PhD thesis, Université Paris-Sud, Orsay, 2011. In French.

[108] Nadal, C., Majumdar, S. N., and Vergassola, M. Phase transitions in the distribution of bipartite entanglement of a random pure state. *Phys. Rev. Lett. 104* (2010), 110501.

[109] Nadal, C., Majumdar, S. N., and Vergassola, M. Statistical distribution of quantum entanglement for a random bipartite state. *J. Stat. Phys. 142* (2011), 403.

[110] Novaes, M. Full counting statistics of chaotic cavities with many open channels. *Phys. Rev. B 75* (2007), 073304.

[111] Novaes, M. Statistics of quantum transport in chaotic cavities with broken time-reversal symmetry. *Phys. Rev. B 78* (2008), 035337.

[112] Osipov, V. A., and Kanzieper, E. Integrable theory of quantum transport in chaotic cavities. *Phys. Rev. Lett. 101* (2008), 176804.

[113] Osipov, V. A., and Kanzieper, E. Statistics of thermal to shot noise crossover in chaotic cavities. *J. Phys. A: Math. Theor. 42* (2009), 475101.

[114] Paredes, B., Widera, A., Murg, V., Mandel, O., Fölling, S., Cirac, I., Shlyapnikov, G. V., Hänsch, T. W., and Bloch, I. Tonks–girardeau gas of ultracold atoms in an optical lattice. *Nature 429*, 6989 (2004), 277–281.

[115] P.Forrester. The sprectrum edge of random matrix ensembles. *Nucl. Phys. B B402 [FS]* (1993), 709.

[116] Pitaevskii, L., and Stringari, S. *Bose-Einstein Condensation*. Clarendon Press, Oxford, 2003.

[117] Plerou, V., Gopikrishnan, P., Rosenow, B., Nunes Amaral, L. A., and Stanley, H. E. Universal and nonuniversal properties of cross correlations in financial time series. *Phys. Rev. Lett. 83* (1999), 1471.

[118] Porter, C. E. *Statistical Theories of Spectra: Fluctuations*. Academic, New York, 1965.

[119] Porter, C. E., and Rosenzweig, N. Statistical properties of atomic and nuclear spectra. *Ann. Acad. Sci. Fennicae, Ser. A, VI Physica 44* (1960), 1.

[120] Rambeau, J., and Schehr, G. Distribution of the time at which $n$ vicious walkers reach their maximal height. *Phys. Rev. E 83* (2011), 061146.

[121] Rodríguez-Pérez, S., Marino, R., Novaes, M., and Vivo, P. Statistics of quantum transport in weakly nonideal chaotic cavities. *Phys. Rev. E 88* (2013), 052912.

[122] Sagan, B. E. *The symmetric group: representations, combinatorial algorithms, and symmetric functions*. Graduate Studies in Mathematics. Springer, 2001.

[123] Savin, D. V., and Sommers, H. J. Shot noise in chaotic cavities with an arbitrary number of open channels. *Phys. Rev. B. 73* (2006), 081307.

[124] Savin, D. V., Sommers, H. J., and Wieczorek, W. Nonlinear statistics of quantum transport in chaotic cavities. *Phys. Rev. B 77* (2008), 125332.

[125] Sinaĭ, Y. G., and Soshnikov, A. Central limit theorem for linear eigenvalue statistics of random matrices with independent entries. *Bol. Soc. Brasil. Mat. (N.S.) 29* (1998), 1778.

[126] Sommers, H. J., Wieczorek, W., and Savin, D. V. Statistics of conductance and shot-noise power for chaotic cavities. *Acta Phys. Pol. A 112* (2007), 691.

[127] Soshnikov, A. Level spacings distribution for large random matrices: Gaussian fluctuations. *Ann. of Math. 148* (1998), 573.

[128] Soshnikov, A. Gaussian fluctuation for the number of particles in Airy, Bessel, sine, and other determinantal random point fields. *J. Stat. Phys. 100* (2000), 491.

[129] Soshnikov, A. A note on universality of the distribution of the largest eigenvalues in certain sample covariance matrices. *J. Stat. Phys. 108*, 6 (2002), 1033.

[130] Stöferle, T., Moritz, H., Schori, C., Köhl, M., and Esslinger, T. Transition from a strongly interacting 1d superfluid to a mott insulator. *Phys. Rev. Lett. 92* (2004), 130403.

[131] Susskind, L. *The Anthropic Landscape of String Theory*, 2003.

[132] Tao, T. *Topics in random matrix theory*, vol. 132 of *Graduate Studies in Mathematics*. American Mathematical Society, Providence, RI, 2012.

[133] Texier, C., and Majumdar, S. N. Wigner time-delay distribution in chaotic cavities and freezing transition. *Phys. Rev. Lett. 110* (2013), 250662.

[134] Tracy, C. A., and Widom, H. Level-spacing distributions and the Airy kernel. *Commun. Math. Phys. 159* (1994), 151.

[135] Tracy, C. A., and Widom, H. On orthogonal and symplectic matrix ensembles. *Commun. Math. Phys. 177* (1996), 727.

[136] Tricomi, F. G. *Integral Equations*. Pure and Applied Mathematics, Vol. V. Interscience, London, 1957.

[137] Vicari, E. Entanglement and particle correlations of Fermi gases in harmonic traps. *Phys. Rev. A 85* (2012), 062104.

[138] Vidal, P., and Kanzieper, E. Statistics of reflection eigenvalues in chaotic cavities with non-ideal leads. *Phys. Rev. Lett. 108* (2012), 206806.

[139] Villamaina, D., and Vivo, P. Entanglement production in non-ideal cavities and optimal opacity. *Phys. Rev. B 88*, 041301.

[140] Vivo, P., Majumdar, S. N., and Bohigas, O. Large deviations of the maximum eigenvalue in Wishart random matrices. *J. Phys. A: Math. Theor. 40* (2007), 4317.

[141] Vivo, P., Majumdar, S. N., and Bohigas, O. Distributions of conductance and shot noise and associated phase transitions. *Phys. Rev. Lett. 101* (2008), 216809.

[142] Vivo, P., Majumdar, S. N., and Bohigas, O. Probability distributions of linear statistics in chaotic cavities and associated phase transitions. *Phys. Rev. B. 81* (2010), 104202.

[143] Vivo, P., and Vivo, E. Transmission eigenvalue densities and moments in chaotic cavities from random matrix theory. *J. Phys. A: Math. Theor. 41* (2008), 122004.

[144] Wales, D. J. *Energy Landscapes: Applications to Clusters, Biomolecules and Glasses*. Cambridge University Press, Cambridge, 2004.

[145] Weyl, H. *Classical Groups*. Princeton Univ. Press, Princeton, 1946.

[146] Wigner, E. P. On a class of analytic functions from the quantum theory of collisions. *Ann. of Math. 53* (1951), 36.

[147] Wigner, E. P. Characteristic vectors of bordered matrices with infinite dimensions. *Ann. of Math. 62* (1955), 548.

[148] Wigner, E. P. Distribution of neutron resonance level spacing. In *Proceedings of the International Conference on the Neutron Interactions with the Nucleus* (1957), United States Atomic Energy Commission, p. 223.

[149] Wigner, E. P. On the distribution of the roots of certain symmetric matrices. *Ann. of Math. 67* (1958), 325.

[150] Wigner, E. P., and Eisenbud, L. Higher angular momenta and long range interaction in resonance reactions. *Phys. Rev. 72* (1947), 29.

[151] Wilks, S. S. *Mathematical statistics*. A Wiley Publication in Mathematical Statistics. John Wiley & Sons, Inc., New York-London, 1962.

[152] Wishart, J. The generalised product moment distribution in samples from a normal multivariate population. *Biometrika 20A* (1928), 32.

[153] Zirnbauer, M. R. Symmetry classes. In *The Oxford Handbook of Random Matrix Theory*, G. Akemann, J. Baik, and P. D. Francesco, Eds. Oxford University Press, Oxford, 2011.

ÉCOLE DOCTORALE
Physique en île-de-France (EDPIF)

**Titre :** Statistique de comptage de valeurs propres de matrices aléatoires et applications en mécanique quantique.

**Mots clés :** matrices aléatoires, statistiques de comptage, large deviations

**Résumé :** L'objectif principal de cette thèse est de répondre à la question: étant donné une matrice aléatoire avec spectre réel, combien de valeurs propres tomber entre A et B? Ceci est une question fondamentale dans la théorie des matrices aléatoires et toutes ses applications, autant de problèmes peuvent être traduits en comptant les valeurs propres à l'intérieur des régions du spectre. Nous appliquons la méthode de gaz Coulomb à ce problème général dans le cadre de différents ensembles de matrice aléatoire et l'on obtient de résultats pour intervalles générales [a, b]. Ces résultats sont particulièrement intéressants dans l'étude des variations des systèmes fermioniques unidimensionnelles de particules confinées non-interaction à la température zéro.

**Title :** Number statistics in random matrices and applications to quantum systems.

**Keywords :** random matrices, full counting statistics, cold fermions

**Abstract :** The main goal of this thesis is to answer the question: given a random matrix with real spectrum, how many eigenvalues fall between a and b? This is a fundamental question in random matrix theory and all of its applications, as many problems can be translated into counting eigenvalues inside regions of the spectrum. We apply the Coulomb gas method to this general problem in the context of different random matrix ensembles and we obtain many results for general intervals [a,b]. These results are particularly interesting in the study of fermionic fluctuations for one-dimensional systems of confined non-interacting particles at zero temperature.

**Université Paris-Saclay**
Espace Technologique / Immeuble Discovery
Route de l'Orme aux Merisiers RD 128 / 91190 Saint-Aubin, France